DEVELOPMENT OF NANO DELIVERY SYSTEM FOR TOPICAL THERAPY OF PSORIASIS

A thesis submitted to the

UPES

For the Award of

Doctor of Philosophy

in

Pharmaceutical Sciences

by

Siddharth Singh

August 2024

Supervisor

Dr. Rajendra Awasthi

Department of Pharmaceutical Sciences

School of Health Sciences and Technology (SoHST)

UPES

Dehradun - 248007: Uttarakhand

DEVELOPMENT OF NANO DELIVERY SYSTEM FOR TOPICAL THERAPY OF PSORIASIS

A thesis submitted to the

UPES

For the Award of

Doctor of Philosophy

in

Pharmaceutical Sciences

by

Siddharth Singh

(SAP ID: 500090012)

August 2024

Supervisor

Dr. Rajendra Awasthi

Associate Professor

Department of Pharmaceutical Sciences

School of Health Sciences and Technology, UPES

Department of Pharmaceutical Sciences

School of Health Sciences and Technology (SoHST)

UPES

Dehradun - 248007: Uttarakhand

DECLARATION

I hereby declare that the submission, being presented in the abstract entitled "Development of nano delivery system for topical therapy of psoriasis" in partial fulfillment of the award of the degree of Doctor of Philosophy submitted to the Department of Pharmaceutical Sciences, School of Health Sciences and Technology, UPES, Dehradun, Uttarakhand, India is a verified and authentic record of my own research conducted out under the supervision of Dr. Rajendra Awasthi, Associate Professor, Department of Pharmaceutical Sciences, School of Health Sciences and Technology, UPES, Dehradun, India.

I declare that this work has not been submitted anywhere else for any part-time or full-time award for a diploma or degree program to the best of my knowledge. Additionally, this work doesn't contain any previously published results or material by any person except where the due acknowledgment and references have been mentioned in the text.

Siddharth Singh

Junior Research Fellow, PhD Scholar

Department of Pharmaceutical Sciences, School of Health Sciences and Technology

UPES, Bidholi, Dehradun-248007, Uttarakhand

CERTIFICATE

UPES
UNIVERSITY OF TOMORROW

Great Place To Work. Certified FEB 2024-FEB 2025 INDIA

August 21, 2024

CERTIFICATE

I certify that **Siddharth Singh** has prepared his thesis entitled "Development of nano delivery System for topical therapy of Psoriasis", for the award of Ph.D. degree in Pharmaceutical Sciences from UPES, under my guidance. He has carried out his research work at the School of Health Sciences and Technology, UPES.

Dr. Rajendra Awasthi
Associate Professor
Department of Pharmaceutical Sciences,
School of Health Sciences and Technology
UPES, Dehradun – 248007, Uttarakhand, India

ABSTRACT

Background: Psoriasis is an autoimmune disease characterized by excessive proliferation of keratinocytes, and it affects almost 2–3% of the total world population. It is a multifactorial disease that can be transferred from generation to generation. These factors are genetic background, oxidative pressure, lifestyle, drugs, epigenetic, and environmental factors. Several current therapies are available for psoriasis treatment, but their undesirable side effects and issues cannot be accepted. Conventional dosage forms typically result in suboptimal therapeutic outcomes due to inadequate penetration to the site of action. In systemic therapy, high doses of drug moieties cause many side effects, such as Ustekinumab, etc., which may lead to malignancy. Psoralen plus UVA radiation (PUVA) and UVB have been documented for their unacceptable side effects, such as cellular mechanism alterations, burning sensation, pain, cost, and discomfort. **Aims:** The study aimed to develop a topical delivery of berberine HCl and diacerein-loaded transferosomal hydrogel for psoriasis treatment, ensuring a sustained release of loaded bioactives at the disease site. **Methods:** The optimization of transferosomes was performed by a Box-Behnken design that offered 13 runs comprised of different combinations of independent factors. Independent factors strongly influenced dependent factors and provided optimized transferosome formulation with significant results at *in vitro* and *in vivo* studies. The developed mathematical model was validated using a nonlinear quadratic polynomial model. This model can be utilized to produce dual delivery transferosomes with desired features. **Results:** Formulation BDT-10 had an optimized transferosome formulation of 110.90 ± 2.8 particle size and 0.296 PDI with 12.44 ± 0.39% deformability. Formulation BDT-10 exhibited high encapsulation efficiency of berberine HCl 89.05 ± 1.5 and diacerein 91.23 ± 1.8% with a remarkable drug release profile (at 24 h, diacerein 98.73 ± 3.21% and berberine HCl 90.546 ± 0.21%). Optimized formulation showed transdermal flux of 0.0224 μg cm^{-2} h^{-1} and 0.0462 μg cm^{-2} h^{-1}, respectively, for diacerein and berberine HCl. The formulation effectively permeated pig ear skin, as confirmed by Raman analysis because of its deformable property. The optimized formulation (formulation BDT-10) showed antioxidant activity with an IC_{50} value of 36.42 μg mL^{-1} in the DPPH assay and was found non-toxic in

the HaCaT cell line cytotoxicity test that was performed by the MTT assay. The formulation did not cause any skin irritation and was found stable at 4°C and 25 ± 2°C/60 ± 5% RH for 3 months. The optimized transferosome formulation (formulation BDT-10) was loaded into a 1% hyaluronic acid gel base (formulation BDTG). The optimized transferosomal hydrogel formulation was found to be homogenous with a pH of 5.4 ± 0.4, which is acceptable for topical delivery. The transferosomal hydrogel exhibited pseudoplastic behavior that is acceptable for dermatological therapy with 9.8 g cm sec-1 spreadability. It was found that diacerein released 88.44 ± 2.11 % and berberine HCl released 81.56 ± 0.11 % over the course of 24 hours, showing a sustained release profile. The hydrogel formulation (BDTG transferosomal gel) showed a reduction in erythema and scaling in the psoriatic BALB/c mice model. The skin histology depicted an alleviation of epidermal thickness and reduced acanthosis. ELISA assay confirmed that the hydrogel formulation reduced inflammation by minimizing TNF-α and IL-17A levels. **Conclusion:** co-delivery of diacerein and berberine HCl in lipid-based nanocarriers has effective therapeutic outcomes in psoriatic animals due to the improved skin penetration and prolonged local residence time. **Future prospects:** the future scope necessitates clinical studies of the developed formulation to prove its anti-psoriatic activity.

GRAPHICAL ABSTRACT

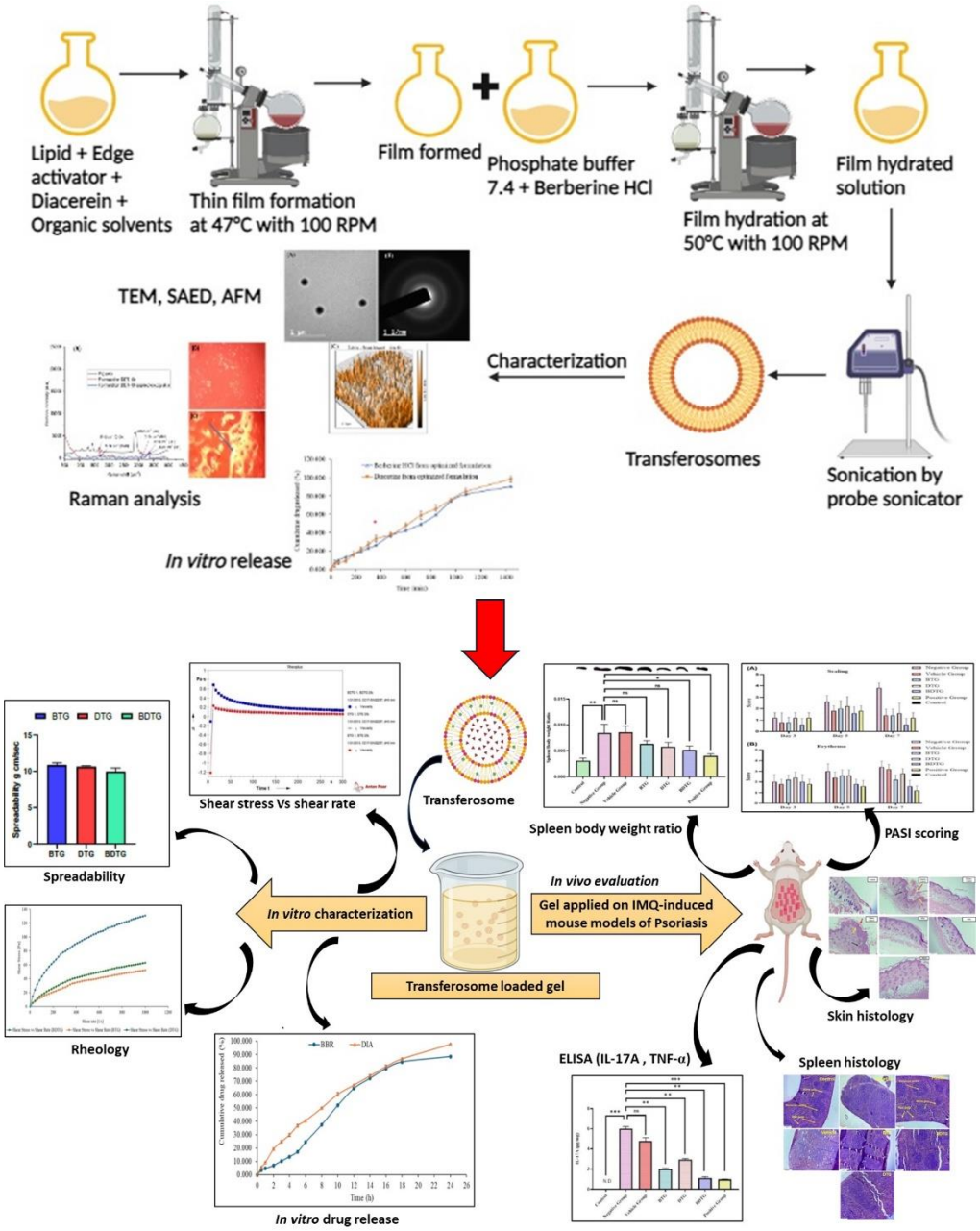

ACKNOWLEDGMENT

First and foremost, I would like to thank my **Shri Ji** and my **Kanha Ji** who have been the driving force behind all of my endeavors to finish my PhD journey and continuously helping me to accomplish the last goal of my life *सत्य, प्रेम, शान्तिः*

I feel immense pleasure in expressing my sincere and profound gratitude to my thesis supervisor **Dr. Rajendra Awasthi** whose guidance helped me to carry out my research work. His valuable and immense support towards my PhD journey was truly exceptional. His guidance in achieving all objectives of this study was valuable and cannot be described in words. I will be grateful throughout my life for his great support towards achieving this PhD.

I would also like to express my sincere gratitude to the **late Dr. Manish Gupta** with whom I started my PhD journey. His support and guidance always boosted me. I would like to thank **Dr. Shraddha Manish Gupta** for her valuable support in this study wherever possible.

I would like to express my gratitude to **Mrs. Richa Bahuguna** for her valuable technical conversation and assistance in accomplishing the primary goal of this work. I have always been grateful for her valuable support.

I would like to express my gratitude to **Mr. Prashant AnilKumar Singh** for his remarkable teachings during *in vivo* studies and immeasurable support in my PhD. His motivational and technical help will always be valuable and meant to me.

I would like to thank **Dr. Pankaj Thakur** for his great support and guidance for providing facility smoothly during experimental studies. I am also thankful to **Dr. Anand Gaurav** for his contribution to smooth non-technical processes.

I am thankful to **Dr. Deepanmol Singh**, **Ms. Vaishali Joshi**, **Mrs. Taranjot Kaur**, **Mr. Piyush Verma**, **Ms. Smriti Mishra, Ms. Tanu, Mr. Ankur, Mr. Vaibhav Pandey, Mr. Anshul, Dr. Iram Khan, Ms. Pratibha, and Ms. Moulika** for providing necessary help during this study.

I would like to thank the **Vice Chancellor**, **Dean R & D**, **Dean SoHST**, and **Cluster Heads of SoHST, UPES** for providing me with the required infrastructure and best resources to complete my research work. I am also thankful to the security staff and housekeeping staff of UPES for their support during night work.

I would like to thank my DRC members, **Dr. Prashant Shukla, Dr. Sandhya, and Dr. Ravindra Kaushik,** for their constructive feedback throughout the study. I am also thankful to lab staff **Mr. Ganesh Saini, Ms. Tripti, Mr. Heera Singh, Ms. Dhatri, Mr. Pradeep, and Ms. Bhagyashri** for their great help in experimental studies.

Next, I extend my gratitude to my parents and sisters, **Mrs. Karishma Singh, Mrs. Deepti Singh, and Mrs. Jyoti Singh,** for their unconditional emotional support throughout my PhD journey. Without their motivation and consistent belief in me, it would not have been possible to complete this research within the prescribed time. I am extremely thankful to **Dr. Deepika Sharma**, **Professor (Dr.) N V Satheesh Madhav**, **Dr. Deepika Raina, Ms. Shweta Paliwal, Dr. Sitabja Mukherjee, Dr. Ansab Akhtar, Dr. Divya Rawat, Dr. Shammy Jindal, Mr. Deepankar Bahuguna, Ar. Swapnil Gupta and Ar. Rohan Rathore** for their help in this PhD journey.

The blessings of my mentors, teachers, and colleagues at SoHST have been crucial for me in achieving the goal of this study.

Siddharth Singh

Junior Research Fellow, PhD Scholar

Department of Pharmaceutical Sciences, School of Health Sciences and Technology, UPES, Bidholi, Dehradun-248007, Uttarakhand

TABLE OF CONTENTS

LIST OF FIGURES

LIST OF TABLES

LIST OF ABBREVIATIONS

S. No.	Abbreviations	Complete Name
1	Ab	Antibody
2	AFM	Atomic Force Microscope
3	ANOVA	Analysis of Variance
4	BDT	Berberine Diacerein Transferosomes
5	BDTG	Berberine Diacerein Transferosomal Gel
6	BTG	Berberine Transferosomal Gel
7	DCs	Dendritic cells
8	DTG	Diacerein Transferosomal Gel
9	FT-IR	Fourier Transfer Infrared
10	HaCaT	Human epidermal keratinocytes
11	HRTEM	High-resolution transmission electron microscopy
12	IMQ	Imiquimod
13	IFN-γ	Interferon-gamma
14	IL-8	Interleukin-8
15	IL-12	Interleukin-12
16	IL-17A	Interleukin-17A
17	IL-20	Interleukin-20
18	IL-23	Interleukin-23
19	MDCs	Myeloid dendritic cells
20	NF-kB	Nuclear factor kappa B
21	NLCs	Nanostructured Lipid Carriers
22	NKT	Natural killer T cells
23	PASI	Psoriasis Area and Severity Index (PASI)

24	PBS	Phosphate buffer solution
25	PDCs	Plasma cell-like dendritic cells
26	PDI	Polydispersity index
27	PUVA	Psoralen ultraviolet A
28	ROS	Reactive Oxygen Species
29	SEM	Scanning Electron Microscope
30	SLN	Solid Lipid Nanoparticles
31	TGF-β	Transforming Growth Factor
32	TNF-α	Tumor necrosis factor-alpha
33	TWEAK	TNF-like weak inducer of apoptosis
34	UV	Ultraviolet

LIST OF SYMBOLS

S. No	Symbol	Name
1	µg	Microgram
2	µL	Microliter
3	Ng	Nanogram
4	^{o}C	Degree celsius
5	%	Percent
6	N	Scan rate
7	pg	Picogram
8	cm^{-1}	Centimeter inverse
9	M	Molar
10	Mm	Millimolar
11	Nm	Nanometer
12	Ppm	Parts per million
13	pg/mL	Picogram/milliliter
14	r^2	Coefficient of Determination
15	Tc	Phase transition temperature

CHAPTER 1

INTRODUCTION

1.1. INTRODUCTION

Skin is the most complicated and largest organ in the body that separates the exterior and interior. The main purpose of the skin is to maintain a stable body temperature and prevent the loss of fluids. Additionally, it serves as a defense against physical injuries, chemicals, viruses, and ultraviolet (UV) radiation (Mohamed *et al.*, 2021). The skin exhibits significant variations in both its function and structure across different regions, rendering it a remarkably intricate organ or tissue. Skin, the biggest organ in an adult (6% of body weight), covers two square meters and is 2.5 mm thick. Figure 1.1 illustrates cross-sectional structure of the skin. The epidermal appendages that penetrate deeply into the subcutaneous fat layer consist of hair follicles, mammary glands, sebaceous glands, apocrine glands, and fingernails (Bragazzi *et al.*, 2019; Mohamed *et al.*, 2021; McKnight *et al.*, 2022).

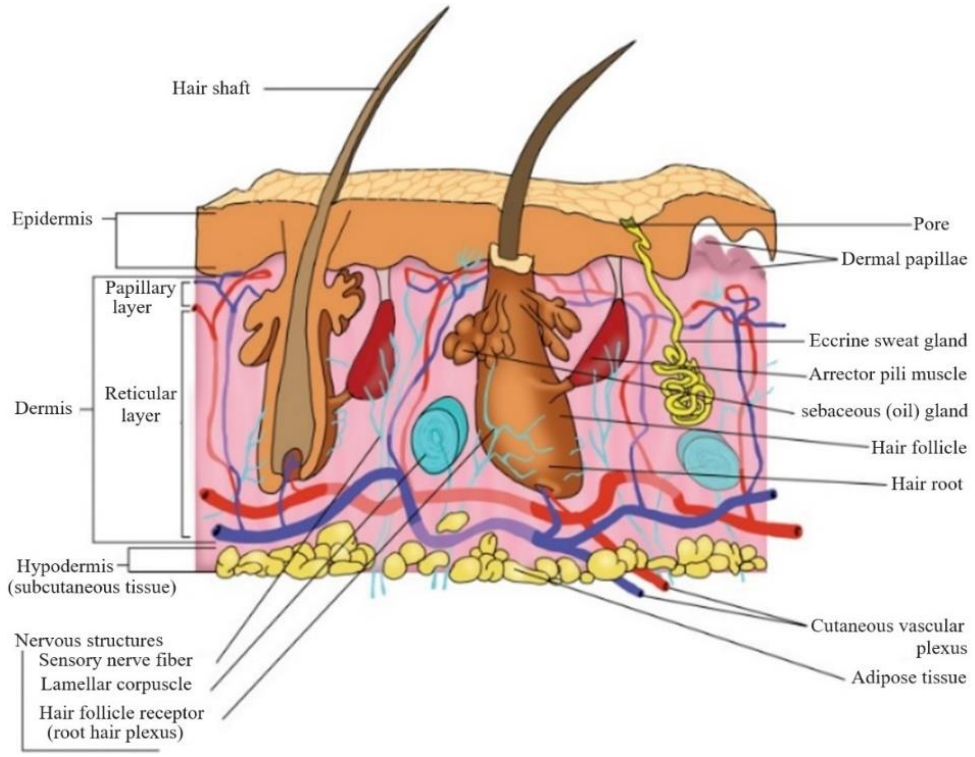

Figure 1.1. Cross-sectional view of skin layers: Hypodermis, dermis, epidermis (Reproduced with permission. Yousef *et al.*, 2017).

It has three layers, each with its own structure and functions: the outermost layer, called as epidermis, the layer underneath it known as the connective tissue or dermis, and the deepest layer called hypodermis. The skin's intricate barrier system shields the body from viruses and other exterior hazards such as poisons and pollution, and also internal trauma such as exhaustion and stress. The barrier's exceptional mechanical characteristics arise from the interconnection of bigger proteins such as cystatin, desmoplakin, and filaggrin and small proline-rich proteins during its formation. Skin plays a crucial role in maintaining homeostasis through its exocrine and endocrine processes, and its regulation of perspiration and temperature.

Keratinocytes, which are cells found in the outer layer of the skin called the epidermis, play a role in the endocrine system by producing vitamin D when exposed to UV light from the sun. The sebaceous and sweat glands regulate the skin's exocrine functions. Nociceptors are essential for detecting and transmitting signals related to touch, pain, and temperature (Slominski *et al.,* 2015). The epidermis is a type of squamous epithelium that undergoes continuous keratinization or cornification and ends at the mucocutaneous junctions. Along with the stem cell-like keratinocytes, the basal layer of the epidermis contains melanocytes and Merkel cells, which produce melanin at a ratio of 1:36 with keratinocytes. Langerhans cells, derived from the bone marrow, can be located in the stratum spinosum, specifically 8-10 layers of keratinocytes above the suprabasal layer (Hoath *et al.*, 2003). The subcutaneous layer is a keratinized layer that plays a vital role in maintaining the protective function of the epidermis. The cells are connected by corneodesmosomes and are covered with lipids. The physical barrier functions to prevent water loss and protect against microbial invasion (Elias *et al.,* 2005; Slominski *et al.,* 2012).

The mucocutaneous junctions is a stratified squamous epithelium undergoing continuous keratinization or cornification. Merkel cells and melanocytes, which produce melanin, are found in the basal layer of the epidermis, but in considerably less quantities compared to the keratinocytes, which resemble

stem cells (Mohamed *et al.,* 2021; Slominski *et al.,* 2012; Slominski *et al.,* 2012). The stratum corneum is major hurdle in the skin permeation for topical and transdermal delivery. It is composed of proteins and lipids and act as a barrier. The drug can pass through the skin either by transepidermal route and transappendageal route. In transepidermal route, drugs can further pass through either by transcellular or intercellular route. In transappendageal route, drug can pass through follicular route, sweat glands, and sebaceous glands. The diameter of sweat glands pores is 60-80 µm and diameter of sebaceous pores if 10-70 µm. It has been reported that the transcellular route offers strongly transport for hydrophilic molecules while the lipophilic molecules can pass through the intercellular route (Zeb *et al.,* 2019; Raszewska-Famielec *et al.,* 2022).

The basement membrane serves as a barrier between the dermis and epidermis, and its main function is to establish the polarity of the squamous epithelium, which is constantly renewing and differentiating. Fibrocytes and fibroblasts are crucial mesenchymal cell populations that are present in the dermis. These structures all enter the outer layer of the skin and the small cavities where hair grows to serve as nerve receptors that detect sensations of touch, mechanical stimuli, and pressure (Slominski *et al.,* 2012; Stenn *et al.,* 2018; Bragazzi *et al.,* 2019; Mohamed *et al.,* 2021; McKnight *et al.,* 2022).

The dermis and hypodermis are widely recognized for their mechanical and thermoregulatory roles. The hypodermis is composed of fat lobules that are separated by fibrous septa. These septa are rich in blood vessels and have a role in the skin's functions of insulation, energy storage, and cushioning. The dermis and hypodermis get oxygen, nutrients, and regulatory elements from both deep and superficial vascular beds. The comprehensive neural network collects the information from all skin components and sends it to various coordinating centers, including the local, spinal cord, para- and sympathetic centers, and the brain (Slominski *et al.,* 2000; Paus *et al.,* 2007; Slominski *et al.,* 2012).

1.2. PSORIASIS, DEPRESSION AND SUICIDALITY

Psoriasis is characterized by a loss of regulation of the epidermal physical barrier. The development of skin lesions is caused by the hyperproliferation of keratinocytes and the aberrant differentiation of these cells, which ultimately leads to the destruction of the epidermal barrier and injury to the epidermis. But unlimited cell differentiation led to plaque formation. To be more specific, plaques have a cell density that is two to five times higher than regular skin, and their transit time via programmed differentiation is at least five to seven times faster than normal skin. These lesions are made up of dead skin and reduced the effectiveness of treatment because of the poor drug delivery (Orsmond *et al.,* 2021). Psoriasis leads to excessive cell growth and abnormal skin development on the outer regions of the elbows, knees, area between the buttocks, belly button, scalp, and nails. This chronic inflammatory skin disorder is characterized by painful white or red itchy scales or plaques (Thomas *et al.,* 2016). Skin scalps occur due to excessive growth of the outer layer of the skin, accelerated development of skin cells, and insufficient formation of the protective layer of the skin. Mild psoriasis results in the development of scaly skin and rashes. In severe instances, individuals may experience the emergence of erythematous and pruritic dermal patches (Li *et al.,* 2012).

There are six distinct classifications of psoriasis, which include guttate psoriasis, plaque psoriasis, erythrodermic psoriasis, inverse psoriasis, and pustular psoriasis. Plaque psoriasis is the predominant form of psoriasis characterized by the presence of silver patch scales, itching, and dryness. The prevalent anatomical sites are the scalp, knee, elbow, and lower back. Pustular psoriasis is characterized by the accumulation of fluid within scaly skin, resulting in the formation of pustules. Pustular psoriasis manifests specifically on the fingertips and toes. Erythrodermic psoriasis is a disorder characterized by inflammation and redness affecting 90% of the body's surface area. Inverse psoriasis is characterized by inflammation of the skin in a smooth patchwork pattern (Rendon *et al.,* 2019; Ahmad *et al.,* 2022; Dhabale *et al.,* 2022). Figure 1.2 illustrates various types of psoriasis.

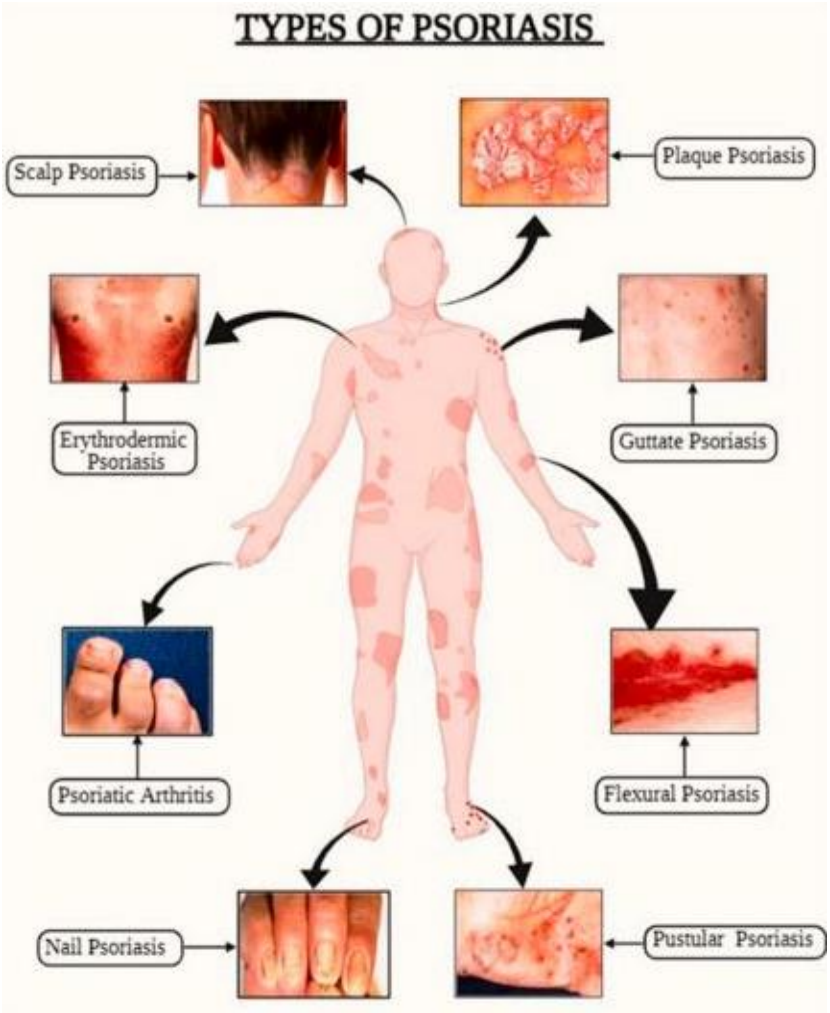

Figure 1.2. Schematic presentation of various types of psoriasis (Reproduced with permission Tambe *et al.,* 2021).

The development of suicidal behavior and thoughts is impacted by external factors and the specific circumstances in which they arise (Case *et al.*, 2015). Psoriasis can cause severe symptoms and skin stigma, leading to social isolation. Psoriasis patients frequently experience comorbidities such as anxiety, depression, and suicidal tendency (Koo *et al.,* 2017). The interplay between depression, stress, and psoriasis is elucidated in Figure 1.3 (Alesci *et al.,* 2022), illustrating the cyclic mechanism underlying their association. Case *et al.,* 2015 found that middle-aged white males in the US have a higher likelihood of engaging in suicide compared to other demographic groups. The

limitations imposed by the disease on social and psychological aspects of life result in a significant number, up to 50%, of individuals with psoriasis experiencing feelings of despair and isolation. Suicidality include the ideas of suicide, actual suicide attempts, and completed suicides. Suicidal behavior includes the activities of devising a plan, coordinating the necessary steps, and making an actual attempt to end one's life (Ring *et al.*, 2007; Bewkey *et al.*, 2014)

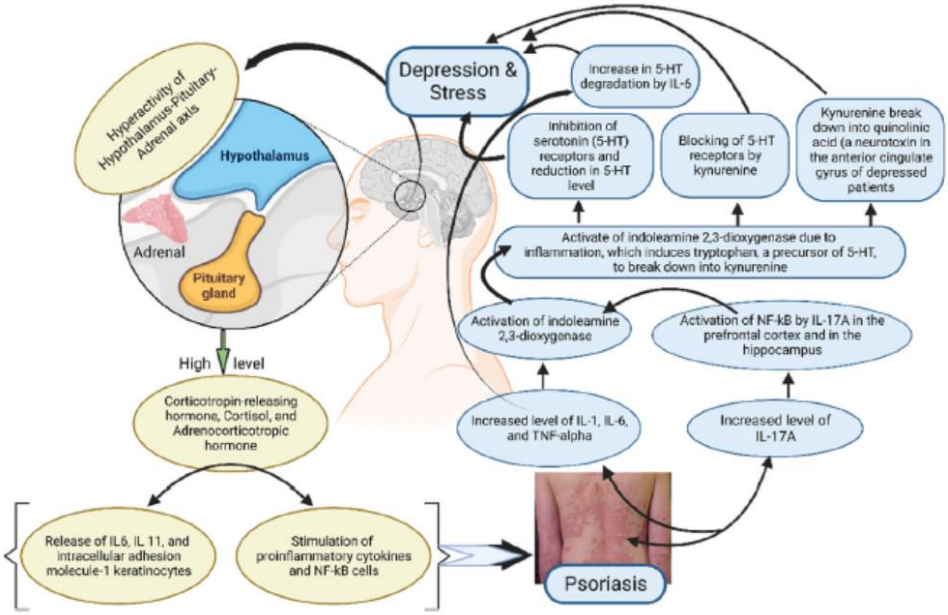

Figure 1.3. Mechanism explaining relationship between depression stress, and psoriasis (Reproduced with permission. Singh and Awasthi 2023).

Poor mental health, characterized by symptoms of anxiety or sadness, is closely linked to the patient quality of life. The social and psychological ramifications of psoriasis are significant as individuals with psoriasis are more susceptible to mental health issues and stressful occurrences, which can increase the likelihood of developing psoriasis (Martínez-Ortega *et al.*, 2019). Psoriasis can manifest at any age, although it predominantly affects those under the age of 40, with 75% of sufferers falling into this age group. Additionally, 50% of cases occur in individuals under the age of 30. During this period of high maturity, the act of stigmatizing causes individuals to experience a loss of confidence

when interacting with others, resulting in mental impairment and a struggle to achieve a stable life. A higher susceptibility to suicidal tendencies has been documented in individuals with more severe psoriasis and younger age groups (Singh *et al.*, 2017).

Psoriasis may attenuate the correlation between age and suicidality by introducing an extra vulnerability for younger persons. There is a correlation between the severity of a condition and a decline in the quality of life due to illness. This decline has been found to be correlated with an increase in suicidal ideation. People who have severe illnesses are significantly more likely to engage in self-harm and attempt suicide, especially when compared to individuals with intermediate disorders (Egeberg *et al.*, 2016). Individuals diagnosed with psoriasis demonstrated a notable increase in depressive symptoms, and they are at least 1.5-fold more prone to developing depression and utilizing a greater quantity of antidepressant medications (Dowlatshahi *et al.*, 2014).

The Patient Health Questionnaire-9 (PHQ-9) was developed by Mental Health Research Network specialists to assess depression based on recognized and validated criteria (Lamb *et al.*, 2017; Wu *et al.*, 2017; Koo *et al.*, 2019). According to a study by Olivier *et al.*, 2010, severe psoriatic patients are at higher risk of depression, with a hazard ratio of 1.72. In comparison, individuals with mild psoriasis have a hazard ratio of 1.38. Assessing the detrimental repercussions of depression using COX regression is challenging since there are just a few instances available for analysis (Strober *et al.*, 2018). Therefore, it is imperative to closely monitor the correlation, since successful therapy has the capacity to diminish the intensity of the illness and the likelihood of suicide.

1.3. EPIDEMIOLOGY AND ETIOLOGY OF PSORIASIS

Psoriasis is an autoimmune disease characterized by excessive proliferation of keratinocytes and it affects almost 2 – 3 % of the total world population.

Although both men and women are susceptible to psoriasis, females and those with a genetic predisposition tend to experience an earlier onset. Recently, it has been documented that high-income countries such as central and western Europe, North America, and Australasia show the highest prevalence rate of psoriasis. Moreover, countries like India, the United States, China, Brazil, France, Germany, and the United Kingdom with a high adult population depicted psoriasis cases also, because this disease is strongly influenced by an age factor. The age at which it often begins displays a bimodal distribution, with the highest occurrences observed between the ages of 30 and 39, and between 60 and 69, in men and in women, the commencement tends to occur approximately 10 years earlier.

The incidence rates of psoriasis range from 0.09 percent to 11.4 percent, making it an important illness condition on a global scale. In India, it affects people at the age of 30-50 years with a prevalence of 0.44 - 2.8%. Moreover, the chance of males being impacted is twice that of females. Countries that are geographically closer to the equator tend to have a lower disease prevalence rate. The disparity in incidence among nations can be linked to multiple variables, encompassing genetic disparities, environmental exposures, healthcare availability, and cultural perspectives on skin-related problems.

Psoriasis is a multifactorial disease that can be transferred from generation to generation. These factors are genetic background, oxidative pressure, lifestyle, drugs, epigenetic and environmental factors. The majority of the twelve unique PSORS (Psoriasis Susceptibility (PSORS)1-9) loci were found by linkage analysis of families with multiple cases of psoriasis. One of the earliest and most common genetic susceptibility regions discovered in psoriasis was located on the short arm of chromosome 6. The first loci associated with psoriasis susceptibility, known as PSORS 1, were found to be located on the human leukocyte antigen (HLA)- Cw6 gene, specifically positioned at chromosomal location 6p21.3.

There are several genes related to pathways that play several major functions in psoriasis. The HLA-C*0602 and ERAP1 genes associated with antigen pathway and that's responsible for the anti-presentation and MHC-1 binding peptides modification. The ZC3H12C, STAT5A/B, IL12B, and ILF3 genes associated with Th1 signalling pathway while TYK2, JAK2, STAT3, IL22, KLF4, IL17RD, ETS1, and SOCS1 are linked with Th17 signalling pathway. Moreover, innate immunity and skin barrier function pathway are directly depended on C-REL, TNFAIP3, NFKBIA, DDX58, MICA and DEFB4, LCE3B/C, and GJB2 genes (Capon *et al.,* 2017; Pradhan *et al.,* 2018; Parisi *et al.,* 2020; Mateu-Arrom *et al.,* 2023).

Epigenetic mechanisms cause changes in gene expression by modifying DNA and histones, without affecting the DNA sequence. These alterations affect chromatin structure and activate transcription factors, leading to changes at both the transcriptional and post-transcriptional levels. Through non-coding RNAs can interact with gene transcription, including DNA methylation and histone changes, or translation. In addition, it has been reported that methotrexate is used to reverse the methylation. Alcohol consumption for a long period directly contributes to the keratinocytes overgrowth and also enhances TNF-α level. This factor directly affects the immune system and enhances the risk of psoriasis development. Besides alcohol consumption, UV exposure, smoking, and medication also contribute in the release of TNF-α levels and cause epigenetic condition that responsible for the psoriasis development (Berna-Rico *et al.,* 2023; Mateu-Arrom *et al.,* 2023; Olejnik-Wojciechowska *et al.,* 2024).

1.4. PATHOPHYSIOLOGY OF PSORIASIS

The exact cause of psoriasis is still unknown. However, there are two main factors that can lead to the proliferation of keratinocytes. The interactions of IL-17, TNF-α, and IFN-γ, lead to inflammation and excessive growth of the outer layer of the skin. Additionally, the genetic material and LL37 complexation

produce an increase in the synthesis of type 1 IFN, which in turn leads to the development of chemokines. The chemokines mentioned play a crucial role in causing inflammation and promoting the growth of keratinocytes. Dendritic cells (DCs) can be distinguished based on their spatial distribution, source of origin, and biological role (Wu *et al.,* 2020; Ben *et al.,* 2021).

Cytokines produced by dendritic cells have an impact on T cells and are significant in the cause and progression of psoriasis. Toll-like receptor 9 is triggered by pDCs because of the release of LL-37 (an antimicrobial peptide released by wounded and stressed keratinocytes) and the formation of complexes with cell-free DNA. The activation of toll-like receptor 9 leads to the release of IFN-α, which in turn contributes to the creation of MDC and affects the activation of T-cells, specifically Th-1 and Th-17 cells. T cells secrete IFN-γ, TNF-α, IL-22, and IL-17 in response to antigens.

Myeloid dendritic cells relocate to lymph nodes because of heightened production of IL-12 and IL-23, and TNF-α. In addition, IFN-α stimulates the synthesis of IL-22R and hinders the differentiation of keratinocytes, hence contributing to the thickening of the epidermis (Kopfnagel *et al.,* 2018; Xie *et al.,* 2021; Kadagothy *et al.,* 2023). T-cells have a crucial function in the development of psoriasis. Activated dendritic cells (DCs) travel to the lymph node that drains the skin and stimulate the transformation of CD8+ and CD4+ T cells into Th17 cells, induced by IL-23, and Th1 cells, induced by IL-12, respectively. Th17 cells have a significant impact on immune control by releasing IL-17, IL-22, and TNF-α. In addition, IL-22 stimulates the STAT pathway, which in turn boosts the growth and specialization of keratinocytes. Additionally, it is accountable for the secretion of chemokines from keratinocytes.

Therefore, Th17 cells and dendritic cells (DCs) migrate within the epidermis. These chemokines sustain the influx of neutrophils into the epidermis, hence contributing to the development of psoriasis. Keratinocytes secrete angiogenic

growth factors such as VEGF, FGF, and angiopoietin 2. Transforming Growth Factor-β (TGF-β), IL-6, IL-1α, IL-20, IL-8, and IL-21 when stimulated by these ligands, stimulate the growth of the outer layer of the skin, hinder the process of specialization, and cause the formation and reorganization of the material surrounding the cells. Memory CD8+ T lymphocytes adhere to collagen IV to penetrate the epidermis and induce inflammation. Chemokines attract natural killer T (NKT) or T cells, which are activated by glycolipid-CD1d complexes, resulting in the development of harmful inflammation. Cytokines produced by keratinocytes influence the growth of stromal cells and blood vessels, facilitating the entry of inflammatory cells into the microenvironment. During the occurrence of psoriasis, nearby fibroblasts, leukocytes, and keratinocytes, engage in communication to enhance and maintain inflammation. Figure 1.4 illustrates the pathways by which leucocytes activate type 1 inflammatory genes that control the last stage of inflammation in the skin and contribute to the onset of psoriasis (Volari´c *et al.*, 2019; Gr¨an *et al.*, 2020; Hu *et al.*, 2021; Xie *et al.*, 2021).

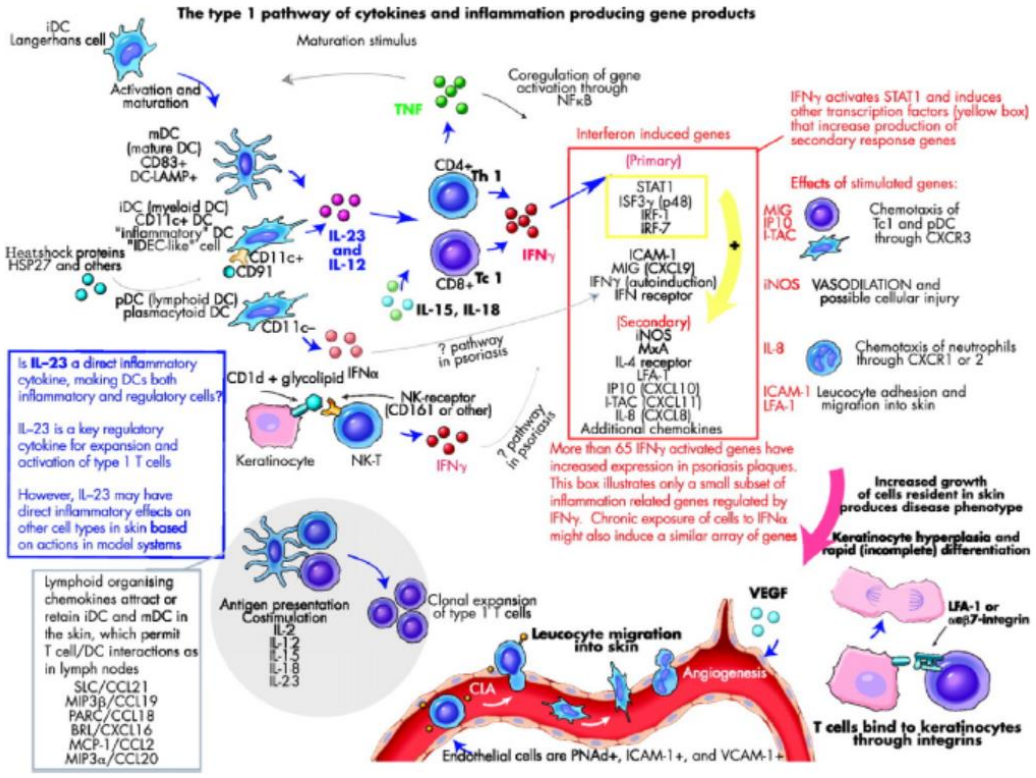

Figure 1.4: Pathogenesis of psoriasis (Reproduced with permission. Krueger *et al.*, 2005).

1.5. EXISTING THERAPIES

Despite there is no cure for psoriasis, the symptoms can be treated with a variety of treatment methods. The therapy choices available are influenced by the severity of a disease. Topical therapy is used to treat mild to moderate cases, while combining topical therapy with systemic therapy, biological agents, or phototherapy may be beneficial for moderate to severe cases. The treatments mentioned are currently accessible in diverse formats (Miyagaki *et al.,* 2015; Armstrong *et al.,* 2018; Rapalli *et al.,* 2018).

1.5.1. Topical therapy

1.5.1.1. Calcineurin inhibitors

Calcineurin is a cytoplasmic protein that binds to calcium and can stimulate the activation of T lymphocytes. Additionally, its ability to activate itself relies on cyclophilins and immunophilins. Tacrolimus and pimecrolimus are the predominant calcineurin inhibitors in clinical practice. They form complexes with immunophilins and cyclophilins, thereby inhibiting the activation of calcineurin. This suppresses the production of cytokines and relieves the symptoms of psoriasis. There are three commercially available formulations for the treatment of psoriasis: a 0.03% tacrolimus ointment, and 1% and 0.1% pimecrolimus creams. These formulations can partially decrease psoriasis lesions (Wollina *et al.,* 2007; Zhang *et al.,* 2015; Dattola *et al.,* 2018).

1.5.1.2. Corticosteroids

Corticosteroids suppress and hinder the generation of cytokines and diminish inflammatory mediators. They are recommended for mild to moderate instances that involve 10% of the entire body surface area. They made clear marks on DNA and stopped the recurrence of phospholipase A2. Additionally, it enhanced the expression of genes related to anti-inflammatory cytokines. Studies have shown that combining corticosteroids with additional topical treatments such as vitamin D analogs, salicylic acid, and retinoids has produced significant outcomes. For children and newborns, it is recommended to use a

corticosteroid with low potency. Adults are advised to use mid-potency corticosteroids. Highly powerful corticosteroids are utilized to treat skin plaques and lesions on the scalp (Menter *et al.,* 2010; Chiricozzi *et al.,* 2017; Torseker *et al.,* 2017; Gabros *et al.,* 2021).

1.5.1.3. Vitamin D analogous

Analogues of Vitamin D3 were initially introduced in the early 1990s. Vitamin D deficiency is linked to psoriasis due to its ability to hinder the generation of potent cytokine molecules that promote inflammation and impede cytotoxicity. They disrupt the process of dendritic cell development and hinder the activation of T-cells. These analogs possess non-irritating capabilities towards the skin, demonstrate anti-proliferative and anti-inflammatory characteristics, and have an affinity for binding to vitamin D receptors. The combination of betamethasone dipropionate and calcipotriol exhibits a synergistic effect in reducing inflammation. Vitamin D3 analogues are comparatively safe alternatives as they do not induce erythema or irritation (Tremezaygues *et al.,* 2011; Chiricozzi *et al.,* 2017; Al-Dhubaibi *et al.,* 2018; Filoni *et al.,* 2018).

1.5.1.4. Anthralin

Anthralin is widely recognized as a highly effective topical therapy for stable psoriasis vulgaris. Dithranol, also referred to as anthralin, possesses the capacity to inhibit the growth of keratinocytes and the activation of T-cells. It has also been utilized for the treatment of scalp psoriasis and plaque psoriasis. However, the therapeutic effectiveness of this substance is hindered by its limited solubility, permeability, and stability (Mendonca *et al.,* 2003; Hollywood *et al.,* 2015; Torseker *et al.,* 2017; Benezeder *et al.,* 2020).

1.5.1.5. Topical retinoids

Tazarotene and acitretin are two vitamin A derivatives that have been approved by the USFDA for the treatment of psoriasis. Tazarotene is available in cream

and gel forms with concentrations of 0.1% and 0.05%, while acitretin is taken orally. The retinoid X receptors (RXR α, β, and γ) and retinoic acid receptors (RAR α, β, and γ) on keratinocyte cells form bonds with each other. This interaction leads to the modification of inflammatory genes and reduces the excessive growth of keratinocyte cells. In addition, studies have shown that when used in conjunction with topical corticosteroid therapy, they have demonstrated significant results (Heath *et al.,* 2018; Erol *et al.,* 2020; Roux *et al.,* 2020; Brozyna *et al*., 2022).

1.5.1.6. Coal tar

Coal tar was extensively employed for prolonged durations to cure psoriasis, particularly on the scalp. However, its usage has diminished in the past few decades. However, only approximately 400 out of the estimated 10,000 constituents of coal tar have been recognized. They consist of polycyclic aromatic hydrocarbons, water, and carbon. They can decrease inflammation and scaling associated with psoriasis. However, the issue of patient noncompliance poses a significant difficulty due to the inherent limitations of present coal tar formulations, including their toxicity, tendency to color the skin, and the carcinogenic activities of polycyclic aromatic hydrocarbons. Due to these problems, the utilization of coal tar for psoriasis treatment has become less frequent (Sekhon *et al.,* 2018; Heymann et al., 2019 Avalos-Viveros *et al.,* 2022). The PLGA nanoparticles loaded with coal tar exhibited reduced toxicity in human dermal fibroblasts and demonstrated significant accumulation in the stratum corneum with minimal penetration. The results indicate the inclusion of coal tar in the competition for psoriasis treatment and propose investigating other lipid-based nanocarriers for improved results (Sunoqrot *et al.*, 2022).

1.5.1.7. Salicylic acid

It is advisable to apply salicylic acid topically along with calcineurin inhibitors and corticosteroids. The simultaneous administration of calcineurin inhibitors with salicylic acid demonstrates its exceptional penetration into psoriatic skin.

When used to treat scalp psoriasis, salicylic acid alone can cause temporary hair loss in the telogen phase. However, ceasing its use may resolve this issue. Salicylic acid, when used in quantities greater than 10%, can result in oral mucosal burn, frontal headache, and nausea. Salicylic acid can improve the penetration of substances into the skin when combined with a corticosteroid, calcineurin inhibitor, and vitamin D analogue (Nordin *et al.,* 2021).

1.5.2. Systemic therapies

Psoriasis can be described as moderate to severe if it affects more than 10% of the body's total surface area, and mild to moderate if it affects less than 10% of the total surface area. For psoriasis that is moderate to severe, treatment typically requires the use of systemic medication, which can be taken orally or administered by injections. Treating psoriasis can be particularly difficult when it manifests in areas such as the ear, pelvic region, scalp, and other locations where topical therapies and phototherapy are not helpful. In certain severe situations, it is advisable to combine all three therapies for psoriasis (phototherapy, systemic, and topical) (Kornhauser et al., 2010; Gisondi *et al.*, 2017; Yan et al., 2021).

1.5.2.1. Oral therapies

Anti-psoriatic drugs can distribute throughout the body after they enter the systemic circulation. Oral therapy is the preferred method for eliminating psoriasis. Acitretin, methotrexate, and cyclosporin A are among the medications recommended for oral administration. In certain countries, fumaric acid esters are also licensed. Methotrexate hinders the activity of dihydrofolate reductase, which in turn prevents the growth of keratinocytes and immune cells. TWEAK, also known as TNF-like weak inducer of apoptosis, has been discovered to exhibit a strong association with the PASI, which stands for psoriasis area and severity index. Further research is necessary to ascertain its manifestation and association with psoriasis. Methotrexate reduces the Psoriasis Area and Severity

Index (PASI) score and enhances the expression and levels of TWEAK in psoriatic patients (El-Esawy *et al.,* 2022).

Increased serum levels of TWEAK have been reported in individuals who received conventional dosages of acritetin, cyclosporin, and methotrexate, (Engin *et al.,* 2020). Additional scientific information is necessary to ascertain the behavior of TWEAK in psoriasis. While cyclosporin effectively hinders T-cell activation, calcineurin phosphatase activity, and keratinocyte proliferation, it also carries inevitable adverse effects, including the potential for liver damage, cardiovascular complications, and gastrointestinal problems. These side effects pose challenges for the long-term use of the medication (Frusic-Zlotkin *et al.,* 2012; Kim et al., 2018; Zhao *et al.,* 2020).

1.5.3. Parenteral therapies/ biological therapies

The American Academy of Dermatology (AAD) and the National Psoriasis Foundation define biologics as "recombinant monoclonal antibodies and fusion proteins that exhibit their therapeutic effects by inhibiting certain cytokines or cytokine receptors that cause psoriatic inflammation." Biologic proteins, as compared to other common therapies, exhibit a substantial molecular weight and provide notable efficacy in suppressing the immune system. The USFDA has granted approval for eleven biologic medicines, including etanercept, adalimumab, brodalumab, certolizumab, guselkumab, ixekinumab, infliximab, Risankizumab, secukinumab, tidrakizumab, and ustekinumab, which target specific cytokines. Despite the specificity of these medicines, their high cost and difficulty in penetrating biological membranes due to their huge size pose a significant obstacle to the ongoing use of the therapy. In general, traditional treatments cannot match the superiority and significant effectiveness of biological therapies. This therapy has revolutionized the management of psoriasis (Hawkeys *et al.,* 2018; Mala *et al.,* 2019; Menter *et al.,* 2019; Nordin *et al.,* 2021).

1.5.4. Phototherapy

Phototherapy is a frequently employed method for treating psoriasis that ranges from moderate to severe. Phototherapy, a treatment for psoriasis, has been developed and widely used since the 1920s. Psoriasis treatment often involves the use of three specific phototherapies: excimer laser or lamp (targeted phototherapy), narrowband ultraviolet B (NB-UVB), and psoralen (PSR) plus ultraviolet A (PUVA). Therapeutic radiation has been found to occur within the wavelength range of 290 to 400 nm, namely in the form of UV radiation. Narrowband ultraviolet B (NB-UVB) light is the primary treatment modality and is administered at a wavelength of 311 nm for patients with stable plaque psoriasis. It triggered programmed cell death in T lymphocytes and keratinocytes as a treatment for psoriatic skin. However, immunological contraindications frequently occur in individuals with AIDS, photosensitive diseases, cancer, and during pregnancy.

Psoriasis can be effectively treated using excimer laser treatment, also known as lamp therapy, which operates at a wavelength of 308 nm. The AAD suggests utilizing excimer laser therapy for superior therapeutic results compared to excimer lamps when used over an extended period (Morita *et al.,* 2018; Ardeleanu *et al.,* 2020; Zheng *et al.,* 2021). PSR is a phytoconstituent derived from the Psoralea corylifolia (Babchi) plant. It is composed of light-sensitive molecules and has medicinal qualities. PUVA therapy, which involves the combination of UVA and PSR, is regarded as a second-line treatment strategy for psoriasis. The action of PUVA can be elucidated by two theories: (i) PUVA generates unstable molecules in the outer layer of the skin, which then cause damage to the cell's cytoplasm, nucleus, and cell membrane, so impeding cell growth, (ii) an alternative hypothesis proposes that PUVA hinders the process of DNA replication by creating connections between molecules and obstructs excessive growth of the outer layer of the skin. Additionally, it interferes with many proteins and chemical structures that result in a decrease in the growth of epidermal cells. UVB phototherapy has been determined to be a safer option for pregnant patients when compared to PUVA therapy. Nanoparticle-mediated

drug delivery methods provide a feasible approach to address the issues associated with PSR, such as toxicity and rapid degradation (Gisondi *et al.*, 2017; Ren *et al.,* 2020; Bhat *et al.,* 2021).

1.6. CHALLENGES OF EXISTING THERAPIES

Although there have been improvements in the management of psoriasis, there are still notable deficiencies in treatment that have a negative effect on the quality of life of patients (Ryan *et al.,* 2014). A notable deficiency in the management of psoriasis is the absence of efficacious therapies for individuals with moderate to severe psoriasis. Topical therapy is the initial therapeutic method commonly employed for managing psoriasis. Individuals with moderate psoriasis, which is characterized by psoriasis affecting less than 10% of their body surface area, may find this treatment beneficial. These treatments are disagreeable and require an excessive amount of time to demonstrate their therapeutic results. These traditional compositions have several additional constraints, including the tendency to leave behind a sticky or greasy residue with an unpleasant smell. Ointments, sprays, Creams, foams, lotions, oils, tapes, shampoos, and gels are many kinds of medication used for topical treatment (Sala *et al.,* 2016; Aldredge *et al.,* 2018; Kui *et al.,* 2018).

The extended application of corticosteroids and vitamin D analogs is constrained by unfavorable consequences, so complicating the management of mild to severe forms of the condition. The commercially available tacrolimus ointment and pimecrolimus cream face challenges in penetrating the skin affected by psoriasis, which restricts their effectiveness as treatments. In addition to these, topical therapies can cause various other side effects, including folliculitis in coal tar-based treatment, peeling, burning, skin irritation, dryness, staining in anthralin delivery, adrenal axis suppression in corticosteroid topical delivery, and erythema, skin atrophy (Wollina *et al.*, 2007; Menter *et al.,* 2009; Bakshi *et al.*, 2020; Chat *et al.,* 2022; Le *et al.,* 2022).

Systemic therapy is essential for addressing the inevitable challenges associated with topical treatment. Topical treatment becomes ineffective when the size and severity of lesions rise, causing discomfort to the patient. Medications such as methotrexate, cyclosporin A, fumaric acid ester, and acitretin are employed for systemic therapy. However, the systemic side effects and infrequent unfavorable consequences that come with them are not sustainable in the long term. Acicutan® (acitretin), Sandimmun®, Immunosporin® (cyclosporine A), Metex® (methotrexate), Fumaderm® (fumaric esters), Neotigason®, and Lantarel® may cause side effects including dry skin, gingival hyperplasia, hyperlipidemia, hair loss, tremor, nephropathy, leukopenia, and lymphopenia. These medications also include inherent undesirable effects, such as the potential for skin cancer, convulsions, and hepatotoxicity. Acitretin and methotrexate are contraindicated during pregnancy because they have the potential to cause birth defects. Biologic medications such as secukinumab (Cosentyx®), etanercept (Enbrel®), adalimumab (Humira®), ustekinumab (Stelara®), and infliximab (Inflectra®, Remicade®, and Remsima®) have the potential to induce anaphylaxis, paradoxical psoriasis, pruritus, facial nerve paralysis, malignant tumors, and other adverse effects (Rozenblit *et al.,* 2009; Dogra *et al.,* 2013; Volc *et al.,* 2016; Bakshi *et al.,* 2020; Jappe *et al.,* 2021). For moderate to severe psoriasis, more intensive therapies such phototherapy or biologic medicines are necessary (Gelfand *et al.,* 2012). However, these treatments do not yield positive results for every patient, and certain individuals may encounter notable adverse reactions, such as heightened susceptibility to infection or the development of cancer (Gisondi *et al.,* 2017). Although, PSR with UVA radiation (PUVA) and UVB are commonly used, they have various adverse effects. These therapies can change cellular systems and cause burning feeling, pain, and discomfort. Therefore, the urgent need for new therapeutic alternatives with less bad effects and improved outcomes, such as techniques based on nanotechnology, has emerged (Cestari *et al.,* 2007; Borgia *et al.,* 2018; Mascarenhas-Melo *et al.,* 2022; Makuch *et al.,* 2022).

One such limitation in the therapy of psoriasis is the lack of individualized therapeutic choices. Psoriasis is a highly complex disease, with significant variations in severity and treatment response among people. Hence, a uniform therapeutic approach may not be optimal for all patients. Personalized treatment choices that consider the patient's specific disease characteristics and treatment objectives are necessary (Ryan *et al.,* 2014). Moreover, there is a dearth of comprehension regarding the fundamental mechanics of psoriasis. Psoriasis is classified as an autoimmune disease, although the precise triggers and pathways that contribute to its development are not yet comprehensively understood. Gaining a more comprehensive comprehension of the fundamental mechanisms of psoriasis has the potential to facilitate the creation of more precise and efficacious treatments (Meng *et al.,* 2018). To address these deficiencies, promising strategies involve employing lipid-based nanocarriers for precise and targeted delivery of medications to the desired location on the skin. Additionally, improved genetic research can aid in the identification of additional genetic markers linked to psoriasis, which might be utilized to create an appropriate method of drug administration. Moreover, the utilization of artificial intelligence and machine learning can discern patterns in patient data, enabling the prediction of treatment results and the identification of novel treatment approaches (Huang *et al.,* 2023). Another potentially effective strategy is the creation of innovative biological substances that specifically target the pathways responsible for the development of psoriasis. For instance, clinical trials have demonstrated the potential efficacy of biologics that specifically target interleukin-17 (IL-17). These treatments may be a viable option for individuals who do not experience positive outcomes with existing therapies (Ariza *et al.,* 2013).

1.7. TRANSFEROSOMES AS A NOVEL DRUG DELIVERY SYSTEM

The term "transferosome" is claimed owned by the German company IDEA AG. The Latin term transferre means "to transport across," while the Greek word soma means "body." Since Cevc and Blume first described it in the 1990s, this technology has been the subject of an abundance of patents and academic

articles for the last 30 years (Opatha *et al.,* 2020). Transfersosmes are composed of a phospholipid bilayer and edge activator with an aqueous core. These are double-bilayer vesicular structures with ultra-deformable and flexible properties.

The various phospholipids such as dimyristoyl phosphatidylcholine-DMPC, dipalmitoyl phosphatidylcholine-DPPC, dipalmitoyl phosphatidylglycerol-DPPG, soybean phosphatidylcholine, and egg phosphatidylcholine. The phosphatidylcholine is most broadly available in the eukaryotic cell membrane and is highly compatible with skin without adverse effects like hypersensitive reactions (Thomas *et al.,* 2016; Fernandez-García *et al.,* 2020).

The transferosomes have deformability and flexibility features due to the presence of a single-chain edge activator that makes the lipid bilayer destabilize. These vesicular structures are elastic and can penetrate the skin without rupturing. Therefore, transferosomes possess the capacity to pass through pores that surpass their own size. They can be stable in an aqueous solution for up to three months without any aggregation in contrast to liposomes and niosomes. These transferosomes systems can cross the skin barrier and deliver the drugs into the bloodstream (Rai *et al.,* 2017; Fernandez-García *et al.,* 2020; Opatha *et al.,* 2020). The size, shape and property of the particles strongly affects the drug delivery and cellular uptake. The conventional liposomes also get affects by many factors such as surface charge, lipid bilayers thermodynamic state, lipid composition, and liposomal charge. To overcome from these problems, deformable liposomes were developed by using edge activator that provides deformable property to them. They can easily deliver the molecules in the stressful environment via osmotic gradient (Zeb *et al.,* 2019). Free flow properties of transferosomes are regulated by two main aspects, one is vesicle deformability, and another is trans-epidermal osmotic gradient. The transferosome permeation and penetration are governed by the principles of hydrotaxis and electromechanics. A transdermal water activity differential is created by a natural transdermal gradient, which applies force to the skin

through transferosome vesicles. This force is responsible for the intercellular junctions widening and transferosomes can pass easily through transcutaneous channels (Figure 1.5).

Proper ratio between surfactant and phospholipids serves flexibility to the transferosomes while an improper ratio leads to the transferosomes movement hindrance from the skin barrier. This flexibility of transferosomes reduces the vesicle rupturing and provides deformability properties to them in the skin. The resulting highly flexible particles can enter and then effectively transit through the pores because the membrane can be deformed at a much lower energy cost. The properties such as ultra deformability and softness of transferosomes make them unique in contrast to liposomes. The self-regulating and self-optimizing properties of transferosomes allow them to pass through any barrier in the body. Moreover, permeation enhancers such as propylene alcohol and ethanol can also be used for lipid polar head region modification. Therefore, it is vital to conduct precisely customized research methodologies for each therapeutic agent to create the most viable carriers with drug-carrying capacity, excellent deformability, and stability (Myschik *et al.*, 2009; Rai *et al.*, 2017; Opatha *et al.*, 2020).

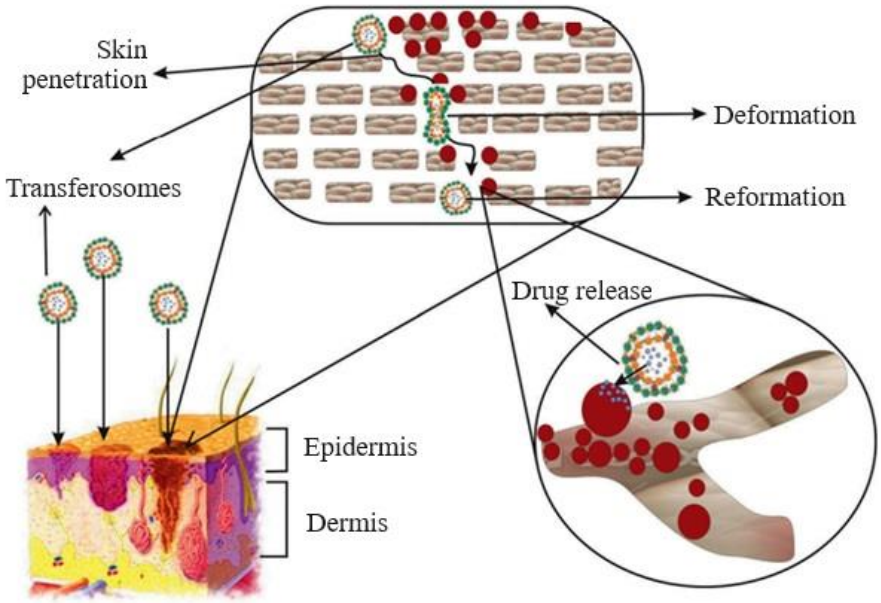

Figure 1.5. Schematic illustration of transferosomes permeation via skin (Reproduced with permission. Opatha *et al.*, 2020).

1.8. DRUG PROFILE

1.8.1. Berberine

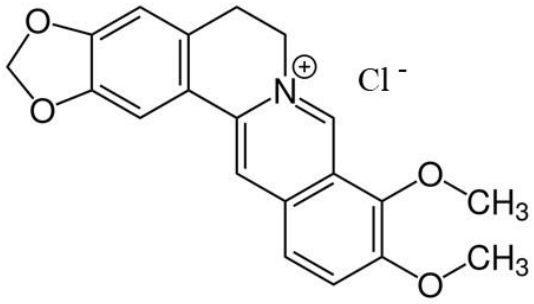

Figure 1.6. Structure of berberine HCl.

Berberine (Figure 1.6) is a crystal bright yellow color isoquinoline alkaloid mostly found in the medicinal herbs of the Berberis genus. It is hydrophobic and has poor bioavailability. It has several pharmacological activities such as anti-inflammatory, antioxidant, anti-hyperglycemic, and anti-cancer. Berberine also can potentially suppress cytokines such as TNF-α, IL-17, IL-1β, IL-6, and IL-8. Moreover, it enhances the CAT, SOD, and GP× activity and can reduce the factors such as MDA, protein carbonyl content, and nobles that are responsible for the antioxidant activity.

In ancient times, it was used as a raw material in Ayurveda and Traditional Chinese medicine systems for wound healing, hemorrhoids, infection, and uterine treatment. It has been reported that berberine also has antidote activity against snake bites and scorpion stings. It is also effective in eliminating toxins, damp heat syndrome, purging fire, and clearing heat in the liver. It can up-regulate the insulin receptor substrate-2 and down-regulate UCP-2 (uncoupling protein-2) which leads to the improvision of insulin resistance that regulates lipid metabolism. Berberine is also reported for promoting AMPK phosphorylation, apoptosis and autophagy regulation, and elevation of LDR mRNA expression.

In addition, berberine also has been reported to block the synthesis of cholesterol and triglycerides synthesis in HepG2 and primary hepatocyte cell lines. It also shows cardio protective effect by modulating AMPK activity, AKT phosphorylation, and JAK/STAT pathway. In 2019, berberine has been reported for anti-psoriatic activity by inhibiting JAK-STAT3 signaling in keratinocytes that inhibit the proliferation of cells (Sun *et al.,* 2019; Suadoni *et al.,* 2021; Khan *et al.,* 2022; Shams *et al.,* 2024).

1.8.2. Diacerein

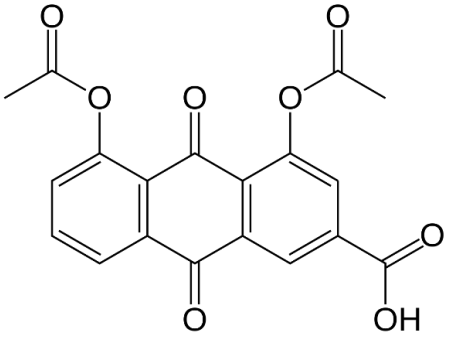

Figure 1.7. Structure of diacerein.

Diacerein (Figure 1.7) is a slow-acting non-steroidal anti-inflammatory drug and has shown excellent efficacy and safety. It is a USFDA and EMA-approved drug for rheumatoid arthritis in 2008. However, due to its severe gastrointestinal side effects, EMA issued new guidelines in 2014 for its oral administration. It is an anthraquinone derivative that developed from aloin, and its deacetylation leads to the formation of rhein. It is a hydrophobic drug with a yellow colour appearance. It has several properties such as anti-inflammatory, anti-pyretic, and analgesic.

Being an NSAIDs, it has a unique mechanism of action, it targets the IL-1β related pathways instead of PGE2 (prostaglandin E2) and COX2 (cyclooxygenase 2) regulations. It has been reported that diacerein can inhibit caspase-1 secretion and minimize the maturation of IL-1β. The poor IL-1β maturation alleviates the AP-1 and NFκB activity and also reduces the

expression of TNF-α and IL-6. Moreover, it has been documented as an immunomodulatory agent in rheumatoid arthritis for neutrophil phagocytic activity, chemotaxis, superoxide anion production, and macrophage migration.

Diacerein reduced the effects of IL-1α and IL-1β in keratinocytes, suppressing the expression of pro-inflammatory genes. It also has the potential to alleviate psoriasis skin inflammation and psoriasis-related splenomegaly by reducing $CD11c^{+}$ dendritic cells in the skin. DCN inhibits the binding of transcription factors NF-κB and AP-1, affecting the expression of pro-inflammatory genes in chondrocytes. In addition, diacerein also exhibited therapeutic effects towards epidermolysis bullosa, thyroid function, testicular injury, acute kidney injury, and cancer (Kaur *et al.*, 2019; Almezgagi *et al.*, 2022; Baxi *et al.*, 2022; Brunner *et al.*, 2023).

AIM AND OBJECTIVES

Aim: Development of nano delivery system for topical therapy of psoriasis

Objectives

- To develop and optimize lipid-based topical transferosomal nanocarriers of berberine and diacerein.
- *In vitro* characterization of drug-loaded transferosomal formulations.
- Loading of selected transferosomes formulation into hydrogel.
- *In vivo* characterization of optimized lipid-based topical transferosomal hydrogel.

CHAPTER SCHEMES

Chapter 1 (ongoing chapter) elaborated on psoriasis, its epidemiology, and etiology. The current existing therapies and challenges related to their use were also discussed. In addition, drug profile, transferosomes information, and objective of the study were documented properly.

Chapter 2 showcases a literature review of vesicular structures like liposomes, transferosomes, niosomes, ethosomes, transethosomes, phytosomes, cerosomes, and glycerosomes. The other lipid nanoparticles like solid lipid nanoparticles, nanostructured lipid carrier, spanlastics, and liquid crystals that were developed for psoriasis management.

Chapter 3 briefly explain methodology that was used for development of berberine HCl and diacerein loaded transferosomes. The pre-formulation studies were carried out to examine physiochemical properties of drug molecules. The transferosomes were formulated and optimized by Box-Behnken design. The optimized formulation was subjected for FTIR, XRD, TGA, TEM, AFM, zeta potential, particle size, deformability, *in vitro* release studies, *ex vivo* studies, Raman, anti-oxidant activity, cytotoxicity studies. Furthermore, the transferosomal hydrogel was developed by loaded with optimized transferosomes formulation into 1 % hyaluronic acid and subjected to determination of pH, rheological study, spreadability, *in vitro* release, and psoriatic Balb/c mice model.

Chapter 4 discussed results of pre-formulation studies and formulation studies. The FTIR revealed functional groups of drugs and showed compatibility between drug-drug interaction. The XRD confirmed crystallinity and TGA showed weight loss of drugs and excipients at specific temperature. The optimization was done successfully, and quadratic equations were developed and provided optimized formulation with significant ANOVA table. The particle and PDI was found in acceptable range for topical delivery and formulation was stable with desirable zeta potential. The optimized formulation showed sustained release profile, skin penetration and its confirmation in pig skin was depicted in *ex vivo* and Raman analysis. Moreover, the developed optimized transferosomes loaded hydrogel showed pseudoplastic behaviour.

The formulated hydrogel also exhibited anti-psoriatic activity in psoriasis induced BALB/c mice model.

Chapter 5 briefly elaborated conclusion of key findings, results integration, and suggested future work requirements for better clinical therapeutic outcomes.

CHAPTER 2
LITERATURE REVIEW

2. LITERATURE REVIEW

Psoriasis is a multifactorial autoimmune disease characterized by excessive proliferation of keratinocytes, inflammatory infiltration, and abnormal epidermis growth. These abnormal features of psoriasis bring it into a hall of fame in the research world. The demand for effective treatment is attracting the interest of both formulation scientists and medical professionals. The improper penetration and skin retardation of the conventional topical dosage form hinder psoriasis treatment (Jindal *et al.,* 2021). To avoid the unforeseen outcomes and significant adverse effects associated with conventional treatment, researchers have created numerous nanomedicines (Singh *et al.,* 2023). The nanoparticle can address many issues related to conventional dosage forms by offering enhanced hydrophobic drug solubility, sustained release, and a desirable drug payload at the disease site (Pandey *et al.,* 2020). Despite numerous studies on the efficacy of nanomedicines, the precision of targeting these nanocarriers remains a limitation (Mishra *et al.,* 2022).

Scientists frequently develop lipid nanocarriers to transport drugs via the skin, either topically or through a transdermal approach. Day by day, scientists are now investigating novel technologies to deliver the drug effectively through the skin barrier without disturbing it and improvising drug absorption via a dermal delivery approach. Lipid-based vesicular drug delivery systems have established significant therapeutic efficacy in treating a wide range of disorders over the last thirty years. These nanoparticles are comprised of aqueous and lipid layers. They can efficiently encapsulate hydrophobic and lipophobic drugs and easily deliver them to the desired location. Moreover, these structures enhance drug bioavailability and improve its half-life, followed by alleviating side effects (Pandey *et al.,* 2020).

The stratum corneum is the major obstacle to topical and transdermal delivery systems. Chemical penetration enhancers and physical procedures like iontophoresis, sonophoresis, microdermabrasion, and electroporation may

lessen the therapeutic effects of the dose regimen, reduce skin irritation, and help with problems caused by patients not following the instructions. These vesicular structures, unlike physical and chemical methods, can penetrate skin barriers by addressing the limitations of physical and chemical approaches (Figure 2.1) (Kapoor *et al.*, 2019; Chacko *et al.*, 2020; Dhiman *et al.*, 2021).

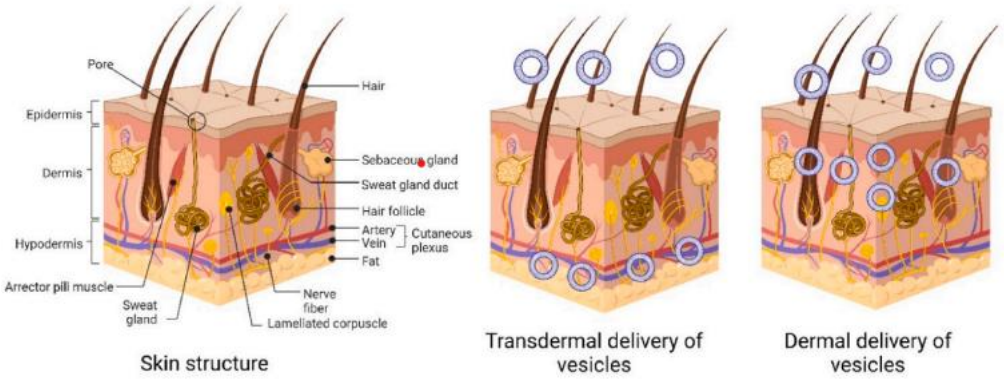

Figure 2.1 Dermal and transdermal drug delivery using vesicular structures (Singh and Awasthi 2023).

2.1 LIPOSOMES

In 1965, Bingham first presented liposomes, which are small concentric rings composed of lipid bilayers consisting of phospholipids and cholesterol. These circles have a spherical shape and contain an aqueous center, with a size ranging from 50 to 500 nm. These vesicles are both biocompatible and biodegradable, making them highly advantageous for drug administration due to their ability to carry a large amount of medication, simplicity of modification, reduction of toxicity, and suitability for large-scale production. The US Food and Drug Administration (USFDA) has granted approval for numerous nanotherapeutics utilizing liposomes, which are used in the treatment of various diseases. The FDA and the EMA both issued licenses for Doxil®/Caelyx®, Abraxane®, Lipodox®, and Lipusu®. Liposomes can be classified based on the number of lamellar layers they have, such as unilamellar, multilamellar, and multivesicular liposomes. Another factor that differentiates liposomes is their surface charge. The liposomes with positive and negative charges have the

capacity for gene delivery and reduced cytotoxicity, respectively (Hare *et al.,* 2017; He *et al.,* 2022; Nsairat *et al.,* 2022; Nel *et al.,* 2023;).

Eukaryotic outer cell membranes are made up of phosphatidylcholine lipids that have a negative charge on their head and a positive charge on the choline part. Phosphatidylcholine is zwitterionic and overall charge neutral across a broad pH range because phosphate has a pKa below 2 and choline is a quaternary ammonium cation. The phase transition temperature (Tc) also controls how fluid lipid bilayers are. When temperatures are above Tc, the lipid part of the membrane has a liquid-crystalline phase and moves around easily. When temperatures are below Tc, the lipid part moves around slowly because the lipid tails expand, and the membrane looks like gel. Increment in the carbon chain and double bond leads to enhancement and alleviation of Tc. The cell membrane has a negative charge, whereas lipids such as 1,2-dioleoyl-3-trimethylammonium-propane (DOTAP) have a positive charge, and electrostatic interaction develops between them. Cationic liposomes loaded with negative charge genetic material can cause cytotoxicity, immunological reactions, and signaling pathway changes (Liu *et al.,* 2021).

Haghiralsadat *et al.,* developed liposomes loaded with doxorubicin made up of 20% DOTAP in combination with 3% DSPE-mPEG (2000). The formulation demonstrated six months of stability and 89% encapsulation efficiency, followed by a positive charge with a 71 nm diameter. The optimized formulation and siRNA were incubated for 30 minutes to develop cationic gene liposomal complex formation and examined for cytotoxic studies on MG-63 cell lines. In cell line studies, it was found that functionalized siRNA-doxorubicin-loaded liposomes displayed high toxicity in contrast to free doxorubicin and doxorubicin liposomes and achieved gene co-delivery with cationic lipids (Haghiralsadat *et al.,* 2018).

In order to achieve skin delivery, researchers investigated liposomes with varying surface charges and levels of flexibility. They prepared four different liposomes with DOTAP lipid and DOPS lipid (1,2-dioleoyl-sn-glycero-3-phospho-L-serine, a negative charge) and DOPC lipid (neutral charge) with cholesterol in different ratios, followed by DOPE/CHEMS liposomes separately. It was found that DOPE/CHEMS had -52.4 ± 0.5 mV zeta potential, a particle size of 50.7 ± 12.0 nm, and a fast transmembrane permeation time as compared to other liposomal formulations. The anionic and neutral-charge liposomes cause less skin irritation and penetration in comparison to the cationic-charge DOTAP liposomes due to skin collapse and charge interaction. The RAW 264.7 macrophage cell lines play a significant role in skin problems because they regulate inflammatory and allergic reactions. It was found that cationic liposomes have more cellular uptake as compared to other surface charge liposomes and exhibit more cytotoxicity to RAW 264.7 cell lines as compared to anionic and neutral charge-based liposomes (Ibaraki *et al.,* 2019).

The US FDA has authorized PUVA therapy for treating severe cases of psoriasis. PUVA therapy combines PSR with UV A radiation. Conventional topical PSR has limited therapeutic promise and safety, despite its permeability and skin deposition capabilities. Cationic and anionic liposomal gels have been developed to address this issue. Using thin film hydration approach, cationic liposomes and anionic liposomes (L-α-Egg lecithin (EL), cholesterol, and 1, 1′, 2, 2′-tetramyristoyl cardiolipin (CL)) were synthesized and then loaded into HPMC gel. Phenotypic imaging showed that the PSR-CL-gel and PSR-AL-gel treated group showed the most improvement in psoriasis symptoms when compared to the PSR-solution treated group. *Ex-vivo* permeation studies showed 9.18 ± 0.07% and 9.28 ± 0.65% permeation by the PSR-CL-Gel and PSR-AL-gel, respectively. When compared to the negative control group, the levels of IL-17 and IL-22 were 2.07-fold lower and 2.20-fold lower after using PSR-CL-gel. The results with PSR-AL-gel were also quite similar with the values of IL-17 and IL-22 of 2.08-fold lower and IL-22 2.05-fold lower,

respectively. PUVA potency and skin penetration were enhanced by both cationic or anionic nanocarriers (Doppalapudi *et al.,* 2017).

Dendritic cells (DCs) establish intricate relationships with keratinocytes and other immune cells to trigger the development of psoriasis. Dendritic cells secrete cytokines such as IL-12 and IL-23, which are subsequently followed by TNF-α, leading to the development of keratinocytes. The study conducted by Xi *et al.,* considered target-specific administration of liposomes by specifically targeting mannose receptors that are expressed on dendritic cells. Liposomes containing Celastrol were created, and their surface was modified using mannose for specific distribution. The efficacy of celastrol liposomes and celastrol solution was evaluated both *in vitro* and *in vivo* using the formulation of mannose-modified celastrol liposomes. CEL-MAN-LPs exhibited superior cellular absorption rates in JAW II cell lines as compared to celastrol liposomes and celastrol solution. In addition, modified liposomes were administered to the animals using microneedles. It was observed that the levels of IL-17 and IL-23 were decreased compared to the levels detected in celastrol liposomes and celastrol solution. Overall, the utilization of mannosylated modified celastrol liposomes exhibited remarkable efficacy and safety in treating psoriasis (Xi *et al.,* 2022). The omiganan-loaded liposomes were prepared using reverse phase evaporation technique and transformed into a liposomal gel using Carbopol 943P. The liposomal gel exhibited enhanced permeability and superior cellular absorption compared to the commercially available formulation. The liposomes reduced the levels of inflammatory cytokines IL-4, IL-6, and TNF-α *in vivo*, as compared to the conventional gel (Javia *et al.,* 2022).

Dual drug-loaded liposomes containing curcumin and ibrutinib were developed and loaded into a 1% Carbopol gel base and examined for anti-psoriatic activity in the imiquimod-induced psoriasis mice model. The optimized dual drug-loaded liposomal gel reduced PASI scoring, ear, and epidermal skin thickness. Histopathology revealed that liposomal gel reduced hyperplasia and acanthosis. Liposomal gel also reduced IL-17 and TNF-α (Jain *et al.,* 2022).

Methotrexate is a known immunomodulator and anti-proliferative therapeutic molecule recommended *via* systemic route for psoriasis treatment. However, patient compliance due to its side effects hinders its long-term treatment use. Bahramizadeh *et al.,* prepared methotrexate loaded liposomes and further incorporated them into a gel for topical treatment of psoriasis. The optimal gel formulation containing 0.05% methotrexate was found to have minimal methotrexate penetration through healthy skin and significant penetration through IMQ-induced psoriatic skin in BALB/c mice (Bahramizadeh *et al.,* 2019). Wang *et al.,* examined the combined use of TRA (all-trans retinoic acid) and BT (betamethasone) in psoriasis treatment following a multi-target approach by addressing the solubility issue and high dose-associated side effects. The thin film hydration method was used for the preparation of liposomes loaded with TRA and BT. The cytotoxicity and cellular uptake studies were performed using HaCaT cell lines. Anti-psoriatic activity of liposomes was performed on an IMQ-induced psoriasis mice model. The results showed that the liposomal gel reduced levels of TNF-α and IL-6. Cellular uptake properties were dependent on the passage of time (Wang *et al.,* 2020).

Several pathways contribute strongly to the psoriasis progression and lead to the production of inflammatory cytokines. JAK/STAT pathway also gets activated and strongly contributes to keratinocyte differentiation. There is evidence that the natural bioactive ginsenoside Rg3 inhibits STAT3 pathway activation due to its anti-inflammatory and immunological modulatory properties. Hung *et al.,* formulated ginsenoside Rg3 loaded liposomes by film hydration method. These liposomes were loaded into microneedles for topical delivery. Microneedles were fabricated using polydimethylsiloxane and sodium hyaluronate materials by a two-step centrifugation micro-molding technique. The pyramidal shape with pointed ends and force-holding potential of 0.59 N/needle allowed these microneedles to penetrate the epidermis layer. Results showed that the points of microneedles dissolved after 10 min and reduced skin thickness in an IMQ psoriatic mouse model. The Rg3 microneedles patch enhances drug retardation in psoriatic skin by inhibiting the JAK/STAT-3

pathway and reducing IL-17, TNF-α, and IL-23 cytokines as per immunohistochemical microscopy (Huang *et al.,* 2022).

Walunj *et al.,* formulated calcineurin inhibitors cyclosporine-loaded liposomes for the inhibition of T-cells activation to treat psoriasis. The optimized cationic liposomes were incorporated into a liposomal gel. The IMQ plaque psoriatic model was used to test the optimized liposomal gel. Gel exhibited shear thinning properties and reduced IL-17, TNF-α, and IL-22 cytokines storms and reduced inflammation (Walunj *et al.,* 2020). Also, a lipid-based vesicular nanocarrier is recommended for the topical delivery of tacrolimus in the treatment of psoriasis. This approach is being suggested since it is safe and the potential side effects are minimal (Jindal *et al.,* 2020).

An improved understanding of molecular mechanisms underlying skin diseases can develop targeted systems. In preclinical studies, oligonucleotide liposomal topical delivery has shown to alleviate psoriasis inflammation by blocking IL-17 receptors and reducing IL-17 cytokine storm (Korkmaz *et al.,* 2020). IL-17 is an important factor in the development of psoriasis and its inhibition can be achieved by target-specific therapy and contributes significantly to the success of treatments for the disease. The IL-17A receptors were targeted in the mice model by formulating liposomal spherical nucleic acids. The prepared liposomes reduced IL-17 and other cytokines such as, TNF-α, S100a7, Pi3, Defb4, and Krt16. Overall, it was concluded that (Liu *et al.,* 2020).

Bexarotene is an agonist of retinoid X receptor. It has the potential to induce apoptosis that would be beneficial for psoriasis treatment. Topical delivery of bexarotene does not permeate keratinocytes easily because of poor water solubility and high log P value. In this context, Saka *et al.,* formulated bexarotene liposomes for their better permeability. The optimized liposomal gel formulation applied to the IMQ-induced psoriatic BALB/c mice. The optimized formulation alleviated IL-17, 23, 22, and TNF-α cytokines storm followed by a

decline in scaling and inflammation (Saka *et al.,* 2020). For transcellular distribution by the paper patch technique, researchers created the recombinant therapeutic moiety AP-rPTP (Astrotactin 1-derived peptide-recombinant protein tyrosine phosphate) to treat psoriasis. This protein controlled the rate of proliferation in an IMQ-induced model by inhibiting STAT1, STAT3, and STAT6 (Kim *et al.,* 2018).

Yu *et al.,* formulated curcumin-loaded liposomes with peptide modification (CRC-TD-Lip) and curcumin-loaded liposomes (CRC-Lip) analysis were performed for both *in vivo and in vitro* studies. HaCaT cell lines used for *in vitro* analysis. Higher cellular uptake and potential proliferation inhibition were depicted by CRC-TD-Lip than the CRC-Lip. CRC-TD-Lip alleviated skin inflammation and epidermis thickness in comparison to the CRC-Lip. CRC-TD-Lip reduced TNF-α, IL-17A, and IL-17F levels and achieved anti-psoriatic activity due to peptide binding with Na+/K+- ATPase beta subunit (Yu *et al.,* 2021).

2.2. TRANSFEROSOMES

Transferosomes are ultra-flexible and ultra-deformable vesicular structures that are composed of phosphatidylcholine and edge activators with an aqueous core. Eukaryotic cell membranes are rich in phosphatidylcholine and show a high level of skin tolerance with a low risk of adverse reactions (Fernandez García *et al.,* 2020; Opatha *et al.,* 2020). These vesicles do not break skin structure because of the edge activator, which destabilizes phospholipids in the transferosomes. Transferosomes can pass via pores that are smaller in size than their own (Rai *et al.,* 2017; Fernandez García *et al.,* 2020; Opatha *et al.,* 2020). Transferosomes penetrate and permeate due to hydrotaxis and elastromechanics principle. The surfactant ratio determines the flexibility of transferosomes, which protects the vesicle from rupturing and drug leakage. Moreover, some penetration enhancers, such as ethanol and propylene alcohol, have been used

in the development of transferosomes (Myschik and Rades 2009; Rai *et al.,* 2017; Opatha *et al.,* 2020).

Triamcinolone acetonide is the most common corticosteroid for the treatment of psoriasis due to its multiple pharmacological activities such as anti-proliferative, anti-inflammatory, vasoconstrictive and immunosuppressive activities. Triamcinolone acetonide-loaded transferosomes were developed and loaded into the Carbopol gel base. The triamcinolone acetonide transferosomal gel penetrated up to 165 μm depth and 145 AU fluoresce intensity while the triamcinolone acetonide liposomes loaded gel exhibited 140 μm depth and 80 AU fluoresce intensity. Transferosomal gel alleviated erythema and inflammation by reducing inflammatory cytokines IL-10, IL-23 and IL-17 levels (Yadav *et al.,* 2021).

Parkash *et al.,* synthesized tacrolimus-loaded liposomes and transferosomes using the thin-film hydration method. Transferosomes reduce ear thickness and enhance transdermal flux. Compared to liposomes, transferosomes had a much longer residence time (52.58 ± 3.62 h). The penetration of transferosomes in rat skin was significantly higher (15.44 ± 1.79 h) compared to liposomes (Parkash *et al.,* 2018). Fluocinolone acetonide can alleviate psoriatic skin irritation and itching. Fluocinolone acetonide-loaded transferosomes prepared by the thin-film hydration method showed antiproliferative activity against imiquimod-stimulated HaCaT cells and high transdermal flow. Transferosomes enhanced cellular absorption and decreased levels of TNF-α and IL-6 (Dhavale *et al.,* 2021).

Resveratrol has been documented for its well-known anti-inflammatory properties and can effectively reduce psoriasis inflammation. In this regard, investigators developed transresveratrol-loaded transferosomes that alleviated lipid peroxidation and ROS species in HaCaT cell lines (Scognamiglio *et al.,* 2013). RNA interferon-loaded transferosomes formulated by the solvent

evaporation method alleviated psoriatic pathological problems effectively without any adverse effect (Desmet *et al.,* 2016).

2.3. NIOSOMES

In 1989, L'Oréal filed invention disclosures (US Patent 8430857) after being the first cosmetic firm to produce niosomes in 1987. These double-layer vesicular structures are made up of non-ionic surfactants, are stable in nature, and are osmotically active in comparison to liposomes. They can also entrap water-soluble and water-insoluble drugs and deliver them effectively to the target site. It has been reported that niosome characteristics can be tunable by changing the vesicle composition and that attracting and repulsive van der Waals forces act within the vesicles. The hydrophilic part of the niosomoes offers surface modification, but leakage and aggregation issues due to hydrolysis directly affect their stability.

The lipidic membranes' reverse disruption can help niosomes to penetrate the dermal layers of skin. Transdermally, they can create a pathway between stratum corneum cells and alter the properties of skin occlusion. Endocytosis and drug release into the cytoplasm are outcomes of lysozyme-mediated vesicular destruction of niosomes. Three different factors need to be carefully considered when choosing a surfactant: CPP (critical packing parameter), HLB value, and gel-liquid transition temperature. These factors directly affect vesicle type formation and entrapment efficiency. A surfactant's alkyl chain length and vesicle size are both affected by its HLB score. Niosome preparation is hindered by surfactants with HLB values between 14 and 17, while HLB 8 provides the most effective trapping performance (Abdelkader *et al.,* 2014; Awasthi *et al.,* 2014; Kumar *et al.,* 2015; Singh and Sharma 2016; Chen *et al.,* 2019; Bhardwaj *et al.,* 2020; Purohit *et al.,* 2022).

The US FDA has approved acitretin, also known as all-trans-acitretin, for treating severe resistance psoriasis through a systemic route. Hepatic toxicity,

teratogenicity, and hyperlipidemia are unavoidable side effects of oral administration of acitretin, necessitating the development of a novel drug delivery system. In this regard, acitretin loaded niosomes were developed by the film hydration method and further converted into niosomal gel. The L929 and HaCaT cell lines have been investigated for MTT assay. A retinol-loaded niosomal gel stopped cell growth in the lab and reduced epidermal thickness in a mouse model that had been given imiquimod (Hashim *et al.,* 2018).

Celastrol has been reported for its suppression activity of the NF-kB pathway, followed by its anti-inflammatory property and Th17 cell development inhibition. Celastrol-loaded niosomes were formulated by using the thin film hydration method and converted into niosomal gel by using a Carbopol 974 gelling agent. It was found that niosomes loaded with hydrogel alleviated inflammatory cytokines like IL-22, IL-23, and IL-17 levels in the psoriasis mice model. The reduction in cytokine levels directly improved the animals' PASI score, erythema, and spleen weight. The study concluded that celastrol-loaded niosomes can effectively treat the psoriatic-like symptoms in the imiquimod-induced mouse model (Meng *et al.,* 2019). Film hydration method was used for the preparation of niosomes loaded with pentoxifylline for the psoriasis treatment. The prepared niosomes were subjected to an imiquimod-induced mice model. Pentoxifylline-loaded niosomes effectively reduced PASI score, epidermal thickness, and inflammation. Moreover, the developed niosome formulation was found stable at 4 °C for 3 months (Bhardwaj *et al.*, 2022).

2.4. ETHOSOMES

Touitou coined the term "ethosomes" in 2000. These vesicular structures consist of co-centric lipid layers that contain 20–50% ethanol. The ethanol has deformable properties for the ethosomes and acts as a permeation enhancer. The addition of ethanol directly makes the ethosomes more flexible, which could make them very useful for delivering drugs to cells that are resistant to water and fat. They can easily penetrate the toughest layer of skin, i.e., the stratum corneum. They are biodegradable and biocompatible and pass into the skin via

a follicular route. High ethanol concentration gives ethosomes a negative charge, which promotes steric stabilization and deeper drug penetration through transdermal flux. Ethosomes release the drug slowly into the skin due to the bursting of vesicles, and phospholipids stay on the skin surface (Khampieng *et al.,* 2018; Mahmood *et al.,* 2018; Kapoor *et al.,* 2019; Jafari *et al.,* 2022).

Ethosomes can easily deliver lipophilic drugs into deeper layers of skin than liposomes. The addition of ethanol reduces the lipid layer size of liposomes, leading to an unfavorable response. Because of the electrostatic interaction between the cell membrane and surface charge vesicles, even cationic ethosomes were better at taking in cells and encasing them than regular ethosomes. There are several ethosomal marketed products: Nanominox, Noicellex, Supravir, Cellutight EF, Decorin, and Skin Genuity (Nagadevi *et al.,* 2014; Yang *et al.,* 2017; Mancuso *et al.,* 2021; Chauhan *et al.,* 2022).

The combination of methotrexate and salicylic acid results in methotrexate unionization, which leads to deeper skin penetration than a formulation containing just methotrexate. The ethosomes were prepared and loaded with methotrexate and salicylic acid by the cold method and loaded into a gel base. Optimized ethosomes demonstrated a particle size of 376.04 ± 3.47 nm and 91.77 ± 0.02% encapsulation efficiency. In animal studies, the optimized ethosome-loaded gel reduced PASI scoring, epidermal thickness, and inflammation in comparison to plain drug solution. The above outcomes led to the conclusion that topical delivery of methotrexate and salicylic acid serves as a prominent and effective treatment therapy for psoriasis (Chandra *et al.,* 2019). Because of its binding capability, the CD44 protein expression is highly expressive on psoriatic cells and could be a potential target for targeted-based delivery systems using hyaluronic acid. In this research framework, curcumin-loaded ethosomes were prepared and coated with hyaluronic acid. It was found that surface-modified ethosomes accumulated in psoriatic mice skin and effectively alleviated the inflammatory cytokines TNF-α, IL-17F, and IL-17A levels and reduced inflammation (Zhang *et al.,* 2019).

Psoralen ultraviolet A (PUVA) is a successful therapy for psoriatic skin. However, the inadequate penetration via the stratum corneum hindered the treatment approach. The comparison between PSR ethosomes and liposomes revealed that PSR ethosomes demonstrated superior transdermal flux, skin penetration, and skin retention compared to liposomes. However, both formulations exhibited safety and toxicity in *in vivo* level. Zhang *et al.,* 2014 concluded that ethosomes proved to be more effective delivery nanocarriers than liposomes for topical application. GA-TPGS (glycyrrhetinic acid-D-α-tocopherol acid polyethylene glycol succinate)-decorated curcumin-loaded ethosomes reduce IL-6-induced inflammation in HaCaT cell lines synergistically. Curcumin and GA-TPGS successfully inhibit HaCaT growth by inhibiting 11β-hydroxysteroid dehydrogenase activity. The anti-psoriatic activity of decorated ethosomes was evaluated in the imiquimod-induced mice model, and it inhibited STAT and NF-κB pathways and decreased IL-17 and IL-23 cytokine levels. This smart functionalized delivery method may offer a novel psoriasis therapy strategy because of its incredible anti-psoriatic effectiveness (Guo *et al.,* 2021).

2.5. TRANSETHOSOMES

The latest liposome technology has elasticity and deformability properties, making them special for topical delivery systems for skin diseases. The combination of transferosome and ethosome features led to the development of transethosomes. They are comprised of phospholipids, edge activators, and permeation enhancers. Their fluid membranes distinguish them from liposomes and ethosomes, and they exhibit greater flexibility and deformability compared to ethosomes and transferosomes. They also offer high drug entrapment and penetration capabilities. Studies have documented that transethosomes demonstrate higher drug deposition in skin layers compared to other vesicular structures like liposomes, transferosomes, and ethosomes (Abdulbaqi et al., 2018; Verma *et al.,* 2019; Wadhwa *et al.,* 2019).

Rosmarinic acid, a water-insoluble drug, has low permeability and chemical instability. It has remarkable anti-inflammatory and antioxidant properties. Rosmarinic acid-loaded transethosomes have been formulated using a rotatory evaporator and further incorporated into a gel. The prepared transethosomal gel was subjected to anti-psoriatic activity in a mouse model. It was discovered that the transethosomal gel effectively lowered levels of the cytokines TNF-α and IL-6 compared to plain rosmarinic acid gel. This was due to its superior ability to penetrate psoriatic skin (Rodriguez Luna *et al.,* 2021). Apremilast is an anti-inflammatory drug that can inhibit PDE-4. Apremilast-loaded transethosomes containing gel effectively permeated rat skin and released drug in a sustained pattern in 24 h. The above results suggest that the apremilast transethosomal gel could serve as an effective therapeutic approach for treating psoriasis (Rahangdale *et al.,* 2021).

The shed snake skin is arranged into three layers, named beta, meso, and alpha layers. The snake skin is naturally formed into scales and hinges. The scales are stiff, and the hinges are soft. The transethosomes were prepared and subjected to *ex-vivo* permeation studies via shed snake-skin. The transethosome vesicular structure allowed 1519.68 ± 363.84 μg/cm^2 of drug to pass through, which is 12.27 times higher than transferosomes, which only allowed 621.25 ± 12.89 μg/cm^2 of drug to pass through, which is 5.01 times higher. Overall, research concludes that transethosomes exhibit superior permeability compared to transferosomes and shed snake-skin presents a viable alternative to rodent skin for permeability studies (Albash *et al.,* 2019).

2.6. PHYTOSOMES

Many plants, found in both aquatic and terrestrial habitats, contain a variety of therapeutic molecules that can be used for various acute and chronic diseases. These molecules have been used for decades in a traditional approach. However, their oral administration bioavailability directly affects therapeutic outcomes at a clinical level. To resolve this issue, phytosomes were invented for the delivery

of bioactives that can also address solubility and bioavailability issues. "Phyto" refers to plants, while "some" describes a cell-like shape. These are known as herbosomes. Because of their lipophobic properties, several compounds have been delivered as phytosomes. These compounds include phenolics, flavonoids, carotenoids, glycosides, terpenoids, and tannins. They also absorb through the skin and exhibit hepatoprotective effects. They are superior to liposomes for the delivery of nutraceuticals and herbal remedies due to their increased stability and less leakage problems (Deshpande *et al.,* 2014; Lu *et al.,* 2019; Barani *et al.,* 2021).

Boswellic acid has therapeutic potential to treat inflammatory issues like asthma, osteoarthritis, and arthritis. Topical treatments for psoriasis have been the subject of a randomized, placebo-controlled, and double-blind trial. The clinical study registered psoriasis patients (36 men and 26 females) and treated them for 30 days, twice a day, with vaccinium myrtillus seed oil, boswellic phytosomes (Bosexil®), and blank phytosomes. Compared to the vaccinium myrtillus seed oil group, the boswellic phytosomes group had a lower PASI score and better erythema, which was followed by scaling. Overall, boswellic acid-loaded phytosomes can effectively treat psoriasis at the clinical level (Togni *et al.,* 2014).

2.7. SOLID LIPID NANOPARTICLES

In 1991, Muller developed solid lipid nanoparticles in the research domain with the goal of increasing the bioavailability and solubility of medications. Emulsifiers combine with solid lipids in an aqueous medium to form solid lipid nanoparticles (SLNs). The solid lipid nanoparticle shows a particle size range of 40–1000 nm. Because of this particle size range, these nanoparticles offer a huge surface area that facilitates high drug absorption. They are unique nanoparticles because they show a solid phase at body temperature and degrade slowly, offering a controlled and sustained drug release profile. They can deliver both types of hydrophilic and hydrophobic drugs and protect the drug from

protuberance by hindering particle coalescence. Compared to liposomes, they are more cost-effective and easier to scale up (Lauterbach *et al.,* 2015; Katopodi *et al.,* 2021; Mirchandani *et al*., 2021; Yaghmur *et al.,* 2021; Sheoran *et al.,* 2022).

The immunosuppressive effects and suppression of T-cell activity of cyclosporin-A have made it a potential candidate for psoriasis treatment. But their long-term use may also lead to side effects such as hyperlipidemia, nephrotoxicity, granulomatous, hepatitis, paresthesia, etc. Cyclosporin-A has a high molecular weight that hinders its topical delivery. SLNs developed by loading cyclosporin-A using trehalose and oleic acid showed permeation in rabbit ear skin of about 150.89 ± 4.0 μg/cm^2. SLNs penetrate the skin via the transfollicular channel and treat psoriasis without causing systemic toxicity (Trombino *et al.,* 2019).

The FDA has approved acitretin as a highly effective drug for treating psoriasis. SLNs loaded with acitretin were formulated by using the solvent injection method. The prepared nanoparticles were further loaded into a Carbopol 934 gel base. Moreover, it was found that acitretin SLNs depicted better drug penetration and drug deposition in comparison to acitretin-marketed formulation (Mahajan *et al.,* 2022). Halobetasol propionate-loaded SLNs were formulated and further loaded into the gel base. Halobetasol propionate SLNs-loaded gel showed sustained release delivery for 12 h. Moreover, the prepared SLNs have better drug accumulation in comparison to the marketed formulation on human cadaver skins (Bikkad *et al.,* 2014).

Fluocinolone acetonide-loaded SLNs were developed for topical delivery by using the emulsification sonication method. The prepared SLNs showed high skin retention and drug accumulation. Overall, this study concluded that these lipid-based nanoparticle colloidal systems offer new platforms for treating psoriasis (Pradhan *et al.,* 2015). To increase solubility and prevent oral adverse

effects, SLNs of tazarotene were produced using a heated homogenization process followed by sonication (Sharma *et al.,* 2022). This research formulated tretinoin-loaded liposomes, SLNs, NLCs (nanostructured lipidic carriers), and niosomes, finding that SLNs and NLCs demonstrated better anti-psoriatic activity with better topical delivery (Raza *et al.,* 2013).

Aland *et al*., prepared tazarotene-loaded SLNs using hot homogenization and sonication methods. They then loaded the prepared SLNs into the gel base. The SLNs-loaded gel had a higher drug concentration in the skin than the Tazret® gel-marketed formulation. However, there was no skin irritation, and the redness went down afterward (Aland *et al.,* 2019). The methotrexate and etanercept-loaded SLNs were developed by using the hot ultrasonication method for psoriasis treatment. The toxicity studies revealed sustained drug release patterns and safety in the prepared SLNs (Ferreira *et al.,* 2017).

2.8. CEROSOMES

The stratum corneum is composed of a multilamellar bilayer arrangement consisting of cholesterol, ceramides, and fatty acids. Ceramides are inherent sphingolipid constituents that make up around 45-50% of the overall composition of the stratum corneum. Ceramides are essential because they regulate the skin's immune response, strengthen the epidermis's ability to self-renew, and maintain the integrity of the epidermal barrier. Reports suggest that ceramide can effectively treat psoriasis and lower the PASI score. Moreover, ceramide has a beneficial effect on the skin and can be applied topically (Thaci *et al.,* 2015; Li *et al.,* 2020; Vovesna *et al.,* 2021).

The US FDA approved methotrexate for psoriasis treatment because of its anti-inflammatory properties. It hinders psoriasis cell DNA synthesis and depicts anti-psoriatic activity. Cerosomes loaded with methotrexate and nicotinamide were formulated by the ethanol injection method for psoriasis treatment in an imiquimod-induced mouse model. In skin permeation and retention studies, the

prepared cerosomes demonstrated remarkable permeation and drug retention. Also, the prepared cerosomes lowered the PASI score and the spleen index. They also lowered the levels of IL-23, IL-1, IL-17A, IL-6, and IL-22, which are inflammatory cytokines (Yang *et al.,* 2021).

Abdelgawad *et al*., synthesized cerosomes loaded with tazarotene using the film hydration method. The prepared cerosomes were examined for skin permeation and anti-psoriatic activities. The tazarotene cerosomes were retained in the skin at 69.62 ± 2.3% for 72 h, which also reduced the PASI score. This research concludes that cerosomes provide new therapeutic platforms for psoriatic treatment (Abdelgawad *et al.,* 2017).

2.9. GLYCEROETHOSOMES

These vesicular structures are made up of glycerol, phospholipids, and ethanol. Glycerosol provides vesicular structures with co-solvency and a moisturizing environment, whereas ethanol is a penetration enhancer. Despite its anti-inflammatory and antioxidant characteristics, the low absorption of mangiferin hinders its topical application. An alternative delivery system is required for naturally occurring therapeutic compounds (Angelova-Fischer *et al.,* 2018). The glyceroethosomes were developed loaded with mangiferin and subjected to therapeutic evaluation against psoriasis in mouse models. The prepared glyceroethosomes possessed good penetration features and entrapment efficiency. In 3T3 cell lines, the prepared formulation demonstrated up to 70% cell viability. Moreover, they also alleviated odema and myeloperoxidase activity. From the above result, it has been concluded that glyceroethosomes effectively deliver mangiferin for psoriasis treatment and open new research venues for other topical diseases (Pleguezuelos-Villa *et al.,* 2020).

Glycyrrhetinic glyceroethosomes were developed through an ethanol injection sonication method for improving skin penetration. The formulation was made up of glycerol 50% and ethanol 25% and showed enhancement in skin

permeation, followed by stability studies. Glyceroethosomes facilitate a prolonged absorption of the payload into the dermal layer. Glyceroethosomes also promote an increase in transdermal permeability by enhancing lipid fluidity in the stratum corneum (Kowalska *et al.,* 2019; Zhang *et al.,* 2022).

In another research framework, Baicalin-loaded modified vesicular structures were formulated by the hydration and sonication method. The formulation was comprised of ethanol, glycerol, propylene, glycol, water, and phospholipids. In the inflammation model, the glyceroethosomes stopped myeloperoxidase activity and reduced swelling because they accumulated in the skin (Manconi *et al.,* 2019). The mometasone furoate glyceroethohyalurosomes that contained hyaluronic acid showed 15% better anti-inflammatory and oxidative stress protection in CD-1 female mice than the commercially available cream (Elocom®) (Tal'ens-Visconti *et al.,* 2022).

2.10. SPANLASTICS

Kakkar and Kaur have developed a modified niosomal vesicular system. It is composed of ethanol, a nonionic surfactant (Span 60, Span 65, Tween 20, Tween 80, Tween 40, Brij 35, Span 80, Brij 97), and an edge activator. They can deliver hydrophilic and lipophilic molecules. They are non-immunogenic and biodegradable and can pass through any biological barrier because of an edge activator. They also provide stability for the drug molecules. Spanlastics were formulated by loading ascorbic acid and topically delivered through UVB-damaged skin treatment. They also showed remarkable permeability and stability. Similarly, spanlastics loaded with boswellic acid showed good penetration and good topical delivery (Badria *et al.,* 2020; Elhabak *et al.,* 2021; Alharbi *et al.,* 2022; Ansari *et al.,* 2022). Researchers have recorded promising results when using these vesicles to treat acne with topical retinoic spanlastics and arthritis through transdermal administration (Shamma *et al.,* 2019; Sharma *et al.,* 2020; Alaaeldin *et al.,* 2021).

The quercetin-loaded spanlastic was developed by ethanol injection, and an optimized formulation was further loaded into the gel base. A gel containing 0.02% quercetin was topically applied once daily to 10 patients who were suffering from persistent plaque psoriasis. It was found that PASI score was reduced from a baseline of 5.19 ± 1.14 to 2.26 ± 1.1. Moreover, quercetin spanlastics improved permeability and alleviated caspase-9 and livin expression. Overall, the study concluded that the spanlastics offer new treatment strategies for mild to moderate psoriasis (Ali *et al.,* 2022). Resveratrol-loaded spanlastics developed by ethanol injection alleviated erythema and scaling, followed by cytokine storms, in a psoriatic mouse model induced by imiquimod (Elgewelly *et al.,* 2022).

The tazarotene fluidized spanlastics have been formulated for the treatment of psoriasis via the topical route. The prepared spanlastic showed excellent skin retardation and deposition. The clinical assessment was conducted with the patient's consent and with the approval of the ethical committee. Plaque psoriasis affected eight females and twelve males within the age range of 20 to 50 years. Patients have received instructions to apply the commercially available Acnitaz® gel and the formulated spanlastic to lesion A and lesion B, respectively. Lesion A experienced a PASI score reduction from 13 to 8.9, while lesion B saw a reduction from 13.2 to 3.6. Similarly, epidermal thickness reduction was more evident in lesion B in comparison to lesion A. In conclusion, top-notch skin-layer fluidized spanlastic retardants effectively alleviate psoriasis and serve as platforms for further drugs (Elmowafy *et al.,* 2019).

2.11. NANOSTRUCTURED-LIPID CARRIERS

NLCs, referred to as "second-generation lipid-based nanocarriers," were created in the late 1990s to address the constraints of traditional treatments. These nanocarriers consist of a combination of solid and liquid lipids. Their occlusion function forms a single layer of lipid film that inhibits the loss of water through the skin and enhances skin hydration. They have a high affinity for

encapsulating hydrophobic pharmaceuticals; however, they face challenges while encapsulating hydrophilic drugs. They can minimize the drug melting point and keep NLCs stable and solid. They are safe, biocompatible, biodegradable, and non-toxic (Dudhipala *et al.,* 2018; Khosa *et al.,* 2018; Khan *et al.,* 2019; Agrawal *et al.,* 2020; Van *et al.,* 2022; Patil *et al.,* 2023).

Dithranol inhibits keratinocyte proliferation and has anti-psoriatic activity, but it also causes irritation and a burning sensation in the skin. In this context, dithranol-loaded NLCs were developed by the hot melt homogenization method and optimized formulation loaded into methylcellulose gel base. The prepared gel formulation was subjected to anti-psoriatic activity examination in the plaque-psoriatic mouse model. NLC gels significantly reduced erythema and PSAI scores. It also reduced inflammation and alleviated cytokines like IL-17, IL-22, IL-23, and TNF-α. Overall, dithranol NLC gel was found to be a suitable topical delivery system for psoriasis (Sathe *et al.,* 2019). In *ex vivo* studies, mometasone furoate NLCs loaded with hydrogel demonstrated prolonged drug release patterns and high drug deposition. Furthermore, the formulated NLC hydrogel proved to be non-irritating to the skin and enhanced the skin condition of psoriatic mice. The formulated nano-delivery system was found effective in topical therapy for psoriasis treatment (Kaur *et al.,* 2018).

Pentoxifylline is a therapeutic molecule that is lyophobic and has anti-psoriatic activity. However, it is hard to get to psoriatic skin because it permeates so easily. Pentoxifylline NLCs were formulated by the thin-film microwave-assisted method and examined in an IMQ-induced psoriatic model for their anti-psoriatic potential. In *ex vivo* permeation, prepared NLCs depicted 13.97% drug release and skin retention of 84.63 ± 3.95 % with a 4.84 ± 0.45 $\mu g/cm^2$/ h permeation flux. Histopathological studies showed that the drug-loaded NLCs-treated group had low epidermis and stratum corneum thickness. Overall, pentoxifylline NLCs showed a sustained release pattern of seven hours and reduced inflammation in psoriatic skin (Ghate *et al.,* 2019).

Methotrexate (MTX)-loaded NLCs loaded into carbomer gel showed 28.8% drug deposition and prolonged drug release. The methotrexate NLCs gel reduced erythema and could be an effective topical therapy for psoriasis treatment (Tripathi *et al.,* 2018). In another study, MTX NLCs gel was found to be higher in drug deposition in contrast to MTX-plain gel in the cadaver of human skin. The MTX NLC-loaded gel alleviated cytokines Il-1β, IL-6, and TNF-α storm and reduced inflammation, followed by PSAI score and ROS level (Agrawal *et al.,* 2020).

Fluocinolone acetonide (FA) NLCs were prepared by a microemulsion method and loaded into a gel with plain salicylic acid psoriasis treatment (FSG). Simultaneously, the conventional gel was also prepared and loaded with FA and salicylic acid for comparison analysis (PFSG). The nanoformulation FSG demonstrated a prolonged release lasting up to 24 h, and an r^2 value of 0.9679 indicated that Higuchi's diffusion model provided the best fit. In studies of pharmacokinetics in the skin, FSG-release FA retardation was much higher than PFSG-release FA retardation. The confocal microscopy results showed that the FSG formulation reached deep layers of skin, while the PFSG formulation did not even reach the stratum corneum skin layer. The FSG formulation lowered the levels of the cytokines IL-22, IL-17, and TNF-α in living things. As a result, the prepared delivery system was more effective at treating psoriasis than the conventional dose (Pradhan *et al.,* 2021).

Raza *et al*., developed fluocinolone acetonide (FLU) and acitretin (ACT) loaded NLCs to address the treatment of psoriasis while reducing their adverse effects, including skin irritation, burning, teratogenicity, and xeropthalmia. ACT-FLU NLCs were developed and optimized by a modified microemulsion and the Box-Behnken model, respectively. In both *in vitro* and *ex vivo* studies, the optimized ACT-FLU NLC formulation loaded into the gel base, demonstrating drug permeation and a sustained release pattern, which contrasted with the ACT-FLU suspension and conventional gel. Therefore, this co-delivery could be explored in *in vivo* level to determine clinical therapeutic efficacy (Raza *et*

al., 2022). In an IMQ-induced psoriatic mouse model, Viegas *et al*., co-delivered tacrolimus and siRNA loaded in NLCs and showed a reduction of TNF-α cytokines levels by about 7-fold. Hence, this co-delivery strategy treated psoriasis with a synergistic effect and offered the possibility for other nano-carrier systems (Viegas *et al.,* 2020).

Calcipotriol-loaded NLC containing nanogel has been reported to treat psoriatic skin *via* topical delivery. The calcipotriol NLC-loaded nanogels demonstrated a high drug retention rate and did not cause irritation or drug penetration into the skin. Moreover, animal studies observed orthokeratosis enhancement and drug activity. Overall, this study demonstrated that psoriasis treatment based on the newly developed formulation has a high chance of success (Pradhan *et al.,* 2021). A combination of curcumin and ibrutinib-loaded NLCs gel was examined to determine its anti-psoriatic synergistic potential in comparison to plain drug gel. It was found that NLCs-loaded gel alleviated such IL-23, IL-6, IL-22, and, TNF-α cytokines levels and psoriatic scores with great potential in BALB/c psoriatic mice. Therefore, the repurposing attempt for psoriasis treatment was found beneficial with no inflammation (Jain *et al.,* 2022).

2.12. LIPID-BASED LIQUID CRYSTALS

Liquid crystals are mesophases that represent an intermediate state between the solid and liquid phases. The investigation of liquid crystals commenced in 1888 by Friedrich Reinitzer, who identified two distinct liquid phases in cholesteryl benzoate. Vsevolod Fredericksz, a Russian physicist, subsequently made the significant discovery that an electric field can synchronize liquid crystals. The drug delivery field explores these nanoparticles for their solid and liquid orientations. They have several properties like solids, such as electrical, optical, mechanical, fluidity, and, magnetic.

Liquid crystals are highly adaptable systems characterized by their diverse polarities, different characteristics, and stability. There are two types of liquid

crystals, *i.e*., lyotropic and thermotropic. The addition of a solvent induces the lyotropic effect, while temperature changes trigger the thermotropic effect. Drug delivery systems commonly use lyotropic liquid crystals, which exhibit liquid crystallinity as a function of solute concentration. Lyotropic liquid crystals offer protection for the drugs from oxidation and hydrolysis. They can penetrate the stratum corneum and hydrate the skin by enhancing water retardation (Bisoyi *et al.,* 2021; Kawai *et al.,* 2021; Chavda *et al.,* 2022; Prado *et al.,* 2022; Blanco-Fernandez *et al.,* 2023).

Apremilast is a USFDA-approved molecule that can inhibit the PDE-4 enzyme and alleviate inflammatory cytokine levels. However, due to its unavoidable oral administration side effects, apremilast topical delivery is a good choice for psoriasis treatment. In this research framework, apremilast-loaded lyotropic liquid crystals were formulated by the hot emulsification method in addition to a high-shear homogenizer. The Box-Behnken design was used for formulation optimization, and optimized formulations were subjected to various examinations. The formulation, which was made up of 100 mg of lipid and 0.75% surfactant, had a prolonged release profile that lasted 18 h. Free apremilast released within 6 hours. The cytotoxicity studies were performed on HaCaT cell lines and found no toxicity in cell viability studies. An *in vitro* psoriatic model was used to test the expression of TNF-α. The LCNPs had cycle threshold values that were 3.73 times higher than the positive control. The Swiss albino mouse model revealed that the formulated liquid crystals exhibited superior permeability coefficient, retention time, and transdermal flux compared to plain gel. Researchers concluded that lyotropic liquid crystal-loaded gels provide a new avenue for lipophilic molecules to treat psoriasis through topical delivery systems (Rapalli *et al.,* 2023).

Methotrexate-loaded isopropyl myristate-based liquid crystals containing hydrogel formulations demonstrated superior elasticity and bio-adhesion on pig skin compared to lamellar and hexagonal liquid crystals. Compared to the liquid crystal formulation, the alkylated carbomer hydrogel reduced epidermal

thickness and cytokines TNF-α and IFN-γ levels (Bernardes *et al.*, 2021). Small interfering RNA (siRNA) has limitations because it hinders administration and body distribution. siRNA-loaded liquid crystal nanodispersions were developed and subjected to various evaluation parameters, such as cellular uptake, cell viability, skin irritation, and the *in vitro* psoriasis skin model. The nanodispersions were safe, with a cellular viability of 92.1 ± 4.7% and no skin irritation. They were able to take up 89.13 ± 1.40% of the cells that were tested. Furthermore, the reconstructed human skin model showed a 3.3-fold alleviation of the IL-6 level compared to the control group. Hence, gene therapy opens new platforms for topical delivery for psoriasis treatment (Depieri *et al.*, 2016).

Tacrolimus-loaded monoolein-based liquid crystals have been developed to improve their bioavailability and examined for their anti-psoriatic activity in an imiquimod-induced mouse model. The prepared liquid crystals showed 65% skin retardation, while the drug solution with propylene glycol showed 25%. Moreover, the prepared liquid crystals showed a reduction in PASI score, erythema thickness, and inflammatory cells. It is proposed that liquid crystals could serve as a nanocarrier for an alternative therapeutic approach for psoriasis (Thapa *et al.*, 2014).

CHAPTER 3 MATERIALS & METHODS

3. MATERIALS & METHODS

3.1. PRE-FORMULATION STUDIES

The pre-formulation studies primarily examine the physical and chemical properties of materials, which can impact drug activity and the production of an effective dosage form. These studies offer a conceptual understanding of the physical and chemical properties of materials, providing an empirical basis for formulation development. During this phase, drug and excipient identification tests were carried out to offer valuable assistance in formulating dosage forms.

3.2. PHYSICAL CHARACTERIZATION OF DRUGS

The physical characteristics like color, appearance, and odor of diacerein and berberine HCl were observed and analyzed with the review literature (Fan *et al.,* 2019; Bansal *et al.,* 2022)

3.3. DETERMINATION OF MELTING POINT

The melting points of diacerein and berberine HCl were determined by capillary fusion method. The required amount of drug was placed into the one-sided capillary and then placed into a melting point apparatus (Remi, Mumbai, India). The temperature was observed at which the solid drug converted into liquid. The recorded temperature was compared with the literature value (Javed *et al.,* 2021).

3.4. PREPARATION OF CALIBRATION CURVES

3.4.1. Berberine HCl

3.4.1.1. Determination of HCl λmax (absorption maxima) for berberine HCl

Berberine HCl (100 mg) was weighed and placed into a 100 mL volumetric flask and dissolved into phosphate buffer (7.4 pH). The flask containing berberine HCl in phosphate buffer was subjected to sonication for 15 min and the volume of buffer solution was adjusted to the mark. Ten millilitres of the

stock solution was collected using a pipette and placed into another 100 mL volumetric flask and the volume was made up to the mark for obtaining 100 µg/mL stock solution. In the next step, 5 µg/mL concentration of solution was obtained by diluting the stock solution and subjected to a scanning process within the range of 200 – 800 nm in UV spectrophotometer spectrum mode.

3.4.1.2. Preparation of calibration curve of berberine HCl

Calibration curve helps in the quantification of drug during the formulation development stages. The calibration curve was prepared in phosphate buffer (pH 7.4) as per USP. Berberine HCl (100 mg) was weighed and placed into a 100 mL volumetric flask and dissolved into the minimum amount of phosphate buffer (pH 7.4). Berberine HCl was dissolved properly in phosphate buffer and the volume was made up to the mark for the preparation of standard stock solution. Different volumes (2, 4, 6, 8, 10, 12, 14, and 16 µg/mL) of stock solution were pipetted and transferred into 10 mL volumetric flasks and filled with phosphate buffer (pH 7.4) up to the mark. The prepared dilutions were subjected to the determination of absorbance values using a UV spectrophotometer and graph was plotted using PCP Disso-software (Gupta *et al.*, 2009).

3.4.2. Diacerein

3.4.2.1. Determination of λmax (absorption maxima) for diacerein

Diacerein (100 mg) was weighed and placed into a 100 mL volumetric flask and dissolved in DMSO and then into phosphate buffer (7.4 pH) at 3:7 ratio. The flask containing diacerein solution was subjected to sonication for 15 min and the volume of buffer solution was adjusted to the mark. Ten millilitres of the stock solution was collected using a pipette and placed into another 100 mL volumetric flask and the volume was made up to the mark for obtaining 100 µg/mL stock solution. In the next step, 5 µg/mL concentration of solution was

obtained by diluting the stock solution and subjected to a scanning process within the range of 200 – 800 nm in UV spectrophotometer spectrum mode.

3.4.2.2. Preparation of calibration curve of diacerein

The calibration curve was prepared in a 10 mL mixture of DMSO and phosphate buffer (pH 7.4) at 3:7 ratio. Diacerein (100 mg) was weighed and placed into a 100 mL volumetric flask and dissolved into the minimum amount of phosphate buffer (pH 7.4). Diacerein was dissolved properly in phosphate buffer and the volume was made up to the mark for the preparation of standard stock solution. Different volumes (1, 2, 3, 4, 5, 6, 7, and 8 µg/mL) of stock solution were pipetted and transferred into 10 mL volumetric flasks and filled with phosphate buffer (pH 7.4) up to the mark. The prepared dilutions were subjected to the determination of absorbance values using a UV spectrophotometer and the graph was plotted using PCP Disso-software (Patel *et al.,* 2014).

3.5. PREPARATION OF DIACEREIN-BERBERINE HCL LOADED DUAL DELIVERY TRANSFEROSOMOES

The diacerein and berberine HCl loaded transferosomes were prepared by thin film hydration approach using a rotatory evaporator (DLAB-RE Pro 100, Thermo Life Sciences, Mumbai, India). Sodium deoxycholate (edge activator), phosphatidylcholine (phospholipid), and diacerein were properly mixed in organic solvent (chloroform and methanol at 2:1 ratio) in a round bottom flask for film formation at 47°C and 100 rpm for 30 min. The film-formed flask was placed for 24 h in a desiccator. Berberine HCl was dissolved in phosphate buffer, pH of 7.4. This solution was then hydrated for 1 h to form a film at 37 °C (Table 3.1). Transferosomes loaded with bioactives were obtained by subjecting the hydrating solution to sonication using a probe sonicator for 1, 3, and 5 minutes with a 20-second pulse on/off. This process resulted in the formation of diacerein-berberine HCl-loaded transferosomes (Figure 3.1) (Balata *et al.,* 2020). The formulated transferosomes were stored at -20 °C in a deep freezer (ULT-185, REMI, India). The formulated transferosomes

underwent lyophilization for 24 h under vacuum (Alpha 2-4 LSCplus, Christ, Germany) at -45 °C (Singh *et al.*, 2021).

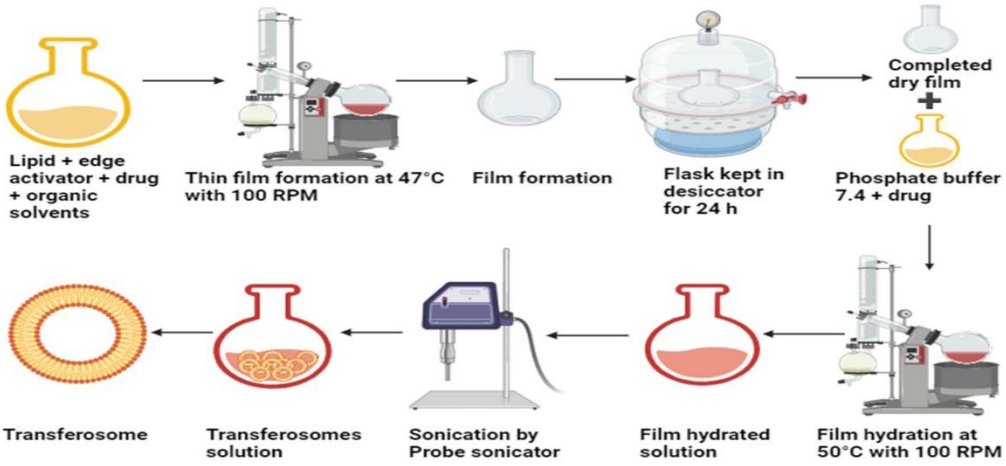

Figure 3.1. Illustration of preparation method of diacerein-berberine HCl loaded dual delivery transferosomes

3.6. OPTIMIZATION STUDIES

The optimization of transferosomes was performed by using the Box-Behnken design in the DOE software. There were three different independent variables, and three dependent variables were pondered. Independent variables were the phosphatidylcholine amount (A), sodium deoxycholate (B), and sonication cycles (C) and the dependent variables were particle size, and percentage entrapment efficiency. We optimized the effect of independent variables on dependent variables using a 3-level factorial design. Statistical tests, including regression coefficient (R^2), goodness-of-fit, and analysis of variance (ANOVA) tests were used to ascertain the relevance of the developed model.

3.6.1. Mathematical model

Design Expert v23.0.0 64-bit software (Stat-Ease, Inc. Minneapolis, MN) was used to precisely investigate the effects of independent variables on dependent variables. This software facilitated the creation of a nonlinear quadratic polynomial model. Points placed on the multidimensional cube's midpoint and replicated center points were taken into account during the experimental design.

To optimize the transferosomes formulations using the quadratic model (Eq. 3.1), when evaluating the main impacts of the formulation factors, the significance of the center point region of the three-dimensional cube was determined.

$$Y_i = \beta_0 + \beta_1 A + \beta_2 B + \beta_3 C + \beta_4 AB + \beta_5 AC + \beta_6 BC + \beta_7 A^2 + \beta_8 B^2 + \beta_9 C^2 \quad (3.1)$$

Where Yi = dependent variables related to each factor, A = concentration of the phosphatidylcholine, B = concentration of the sodium deoxycholate, and C = sonication cycles period. The above-mentioned independent variables consider low (-1), median (0), and high (+1) values. The phosphatidylcholine was weighed into three levels as low level was 75 mg, the median was 85 mg, and the high level was 95 mg while sodium deoxycholate was 5, 15, and 25 mg as low, median, and high levels respectively. In addition, the last independent variable was the sonication cycles that were considered 1, 3, and 5 min from low to high values (Table 3.1).

Table 3.1. Box-Behnken design for optimization

Formulation code	**Independent variables***		
	A: Phosphatidylcholine (mg)	**B: Sodium deoxycholate (mg)**	**C: Sonication cycles (min)**
BDT-1	1 (95)	-1 (5)	0
BDT-2	0 (85)	-1 (5)	-1 (1)
BDT-3	0 (85)	1 (25)	1 (5)
BDT-4	0 (85)	-1 (5)	1 (5)
BDT-5	-1 (75)	1 (25)	0 (3)
BDT-6	1 (95)	1 (25)	0 (3)
BDT-7	1 (95)	0 (15)	-1 (1)
BDT-8	-1 (75)	0 (15)	-1 (1)
BDT-9	0 (85)	1 (25)	-1 (1)
BDT-10	0 (85)	0 (15)	0 (3)
BDT-11	-1 (75)	0 (15)	1 (5)

BDT-12	1 (95)	0 (15)	1 (5)
BDT-13	-1 (75)	-1 (5)	0 (3)

*Values in bracket indicate the real values.

The impact of the independent variables was assessed on the dependent factors Y_1 = particle size (minimum), Y_2 = berberine HCl entrapment efficiency (maximum), and Y_3 = diacerein entrapment efficiency (maximum). The statistical design was confirmed by the significant responses shown by the polynomial equations. Model optimization and validation were assessed by calculating the ANOVA, with an F-Value, and ensuring that the P-value was less than 0.05 (Prakash *et al.*, 2018).

The interaction and relationship between the response and variables were shown by counterplots and 3D response surfaces. The optimized additional checkpoints of the formulation were used to determine the difference between the predicted value and the actual value. The formulations were created and evaluated according to the number of obtained from Box-Behnken design.

3.7. CHARACTERIZATION OF TRANSFEROSOMES

3.7.1. Fourier transform infrared analysis

The purity and structure of diacerein, berberine HCl, sodium deoxycholate, phosphatidylcholine, and optimized formulation was determined by Fourier Transform Infrared (FTIR) spectroscopy using KBr disk method (Frontier FT-IR/FIR, PerkinElmer, USA). The drug-drug interaction studies were also performed and recorded. Sample mixed KBr pellets were prepared in 1:10 ratio and pressed at 10 tons for 2 minutes. The prepared pellets were placed in the sample holder and analyzed between 4000 to 400 cm^{-1} (Arora *et al.,* 2019).

3.7.2. X-ray diffraction analysis

The X-ray diffractometer (D8-Advance-Eco, Bruker, USA) was used to determine the lattice structure of diacerein, berberine HCl, sodium deoxycholate, phosphatidylcholine, and optimized formulation. The specified

quantity of the sample was positioned on the sample stage and subjected to scanning in the 2-theta range of 0-90°, with a step size of 0.02°. This scanning was carried out using Cu Kα radiation, with a wavelength of 15.4 nm, a voltage of 40 kV, and a current of 200 mA (Dahiya *et al.,* 2023).

3.7.3. Thermogravimetric analysis

The thermal degradation of diacerein, berberine HCl, sodium deoxycholate, phosphatidylcholine, and optimized transferosomes was examined by thermal gravimetric analysis (TGA-50, Shimadzu, Japan). The 5 mg of sample was placed on the crucible under insert conditions between 30 to 900 °C under insert conditions (Mishra *et al.,* 2022).

3.7.4. Determination of polydispersity index, zeta potential, and vesicle size

The average vesicle size and polydispersity index (PDI) of prepared formulation were examined via dynamic light scattering technique at room temperature through Malvern particle analyzer EN1690, Malvern Instruments, United Kingdom. The sample was diluted with phosphate buffer (pH 7.4) in 1:10 and triplicate readings were taken at a dissipating angle 90°. The optimized formulation was examined to determine zeta potential in triplicates using a Zetasizer (Litesizer 500, AntonPaar, Austria) (Singh *et al.,* 2021).

3.7.5. Determination of drug loading and encapsulation efficiency

The determination of drug loading and entrapment efficiency was performed by UV spectroscopy. The formulation (5 mL) was dispersed in 5 mL of phosphate buffer (pH 7.4) solution and dispersed properly and subjected to centrifugation at 10000 rpm for 30 minutes at 4°C in REMI C-24 PLUS, Mumbai, India. The supernatant was collected and free drugs (diacerein at 258 nm and berberine HCl at 340 nm) were analyzed by UV-VIS spectrophotometer UV-1900 Shimadzu, Japan. In the next step, the drug loading and entrapment efficiency were determined using equation 3.2 and 3.3, respectively (Mishra *et al.,* 2022).

$$\text{Drug Loading, \%} = \frac{\text{Amount of drug taken– free drug}}{\text{Amount of drug loaded transferosomes}} \text{ X } 100 \qquad (3.2)$$

$$\text{Entrapment Efficiency, \%} = \frac{\text{Amount of drug taken – free drug}}{\text{Amount of drug taken}} \text{ X } 100 \qquad (3.3)$$

3.7.6. Determination of deformability

The degree of deformability of the transferosomes formulation was examined by using extrusion methodology. The formulations vesicle size was determined through DLS before and after passing through an extruder that has pore size 100 nm polycarbonate membrane filter. Transferosome deformability was determined and reported by using equation 3.4 (Varia *et al.*, 2023).

$$\text{Deformability} = J \left(\frac{\text{rv}}{rp}\right)^2 \qquad (3.4)$$

3.7.7. Morphological characterization

The morphological analysis of the optimized formulation was done using HR-TEM (high-resolution transmission electron microscopy) at 80 kV (JEM 2100 Plus, JOEL, Japan). The formulation was diluted with solvent and a single drop of it was placed on the carbon-coated copper grid. The sample containing grid was dried properly and unwanted liquid was cleaned through tissue paper. The stained sample was dried properly and subjected to morphological analysis (Dahiya *et al.*, 2023).

Surface roughness was analyzed by atomic force microscopy (AFM) (NANOSURF NG, Liestal, Switzerland). A single drop of the diluted sample was dispersed on a thin glass slide by spin-coater. The film was formed and subjected to image capturing at 256×256-pixel resolution using a 300 kHz cantilever frequency, and 48 N/m of nominal force constant at 25 °C.

3.7.8. *In vitro* drug release

USP dissolution apparatus (type II) (model, Mumbai, India) was used to carry out dissolution studies. Dialysis membrane was placed in a sodium bicarbonate solution for 15 minutes to activate it. The activated membrane was washed with double distilled water. The activated membrane was filled with transferosomes equivalent to 5 mg of diacerein and 5 mg of berberine HCl. Transferosome containing membrane was placed in the dissolution medium, PBS (pH 7.4) at 37 ± 0.5 °C. The paddle was rotated at 100 rpm. At 0, 1, 2, 3, 4, 5, 6, 8, 10, 12, 16, and 24 hours intervals, 5 mL samples were withdrawn. Sink conditions were maintained by adding a similar volume of fresh buffer maintained at the same temperature. The samples were filtered and subjected to analysis using a UV spectrophotometer (UV-1900, Shimadzu, Japan). Berberine HCl was analysed at 340 nm, while diacerein was analyzed at 258 nm (Dhavale *et al.,* 2021).

The release kinetics of diacerein and berberine HCl from dual delivery transferosomes was assessed as first-order and zero-order. The drug release kinetics was accessed following Higuchi's model. To determine the drug diffusion mechanism, whether it is non-Fickian or Fickian, dissolution data was examined using Korsmeyer-Peppas' model. This model plots the logarithm of the percent drug release (cumulative) against the logarithm of time. The Hixson-Crowell model was utilized to analyze the drug release data obtained from *in vitro* experiments. The analysis involved plotting the cube root of the residual drug amount in the matrix against time. Regression coefficient values were calculated to predict the release mechanism (Balata *et al.*, 2020). The PCP Disso V3 program (developed by PCP, BVDU, Pune, India) was utilized to perform kinetic modeling.

3.7.9. Antioxidant assay of transferosomes

2,2-diphenyl-1-picrylhydrazyl (DPPH) assay technique was used for the determination of the antioxidant activity of optimized transferosomes. DPPH agent can develop free radical formation and depicts its absorption band at 517

nm. The standard sample (ascorbic acid) (0.004% w/v) and optimized formulation were mixed with DPPH solution at 3.9, 7.8, 15.6, 31.25, 62.5, 125, 250, and 500 µg/mL concentrations. The solution was subjected to incubation for a duration of 15 minutes in a dark setting at a temperature of 25 °C. The solution underwent a color transformation from purple to yellow during the incubation period. A UV spectrophotometer (UV-1900, Shimadzu, Japan) was used to record the absorbance at 517 nm. Antioxidant activity was calculated using equation 3.5. The optimized transferosome's half maximal inhibitory concentration (IC_{50}) was determined and compared with ascorbic acid (Abd-Allah *et al.*, 2023).

$$\text{Antioxidant activity, \%} = \frac{\text{Absorbance of DPPH}}{\text{Absorbance of DPPH}} \text{ X } 100 \qquad (3.5)$$

3.7.10. *Ex vivo* permeation studies

The hairless pig ear skin was collected from a slaughterhouse (Premnagar, Dehradun, India) for *ex vivo* permeation studies. The collected pig ear skin was washed with phosphate buffer (7.4 pH) and stored in a freezer at -8 °C. The ex-vivo permeation studies were performed using the Franz diffusion apparatus. The optimized formulation was applied uniformly to the pig ear skin. The formulation applied to the pig ear skin was placed between the receiver and donor compartments. The epidermis was oriented towards the donor compartment, while the dermis was oriented towards the receiver compartment filled with PBS (pH 7.4). At different intervals of 0, 1, 2, 3, 4, 5, and 6 hours, the 2 mL samples were withdrawn in triplicates and after each sampling, the sink conditions were balanced by adding 2 mL of fresh solvent into the receiver compartment. The collected sample solution was subjected to absorbance analysis (258 nm for diacerein and 340 nm for berberine HCl) by using a UV spectrophotometer (UV-1900, Shimadzu, Japan). The cumulative drug permeation was determined by evaluating the skin surface area over time to estimate the permeability coefficient and flux Jss (µg cm^{-2} h^{-1}) (Arora *et al.*, 2019).

3.7.11. Raman analysis

The blank pig skin, optimized formulation, and pig skin directly collected from *in vitro* permeation studies were subjected to Raman analysis. This analysis examines the permeation level of the optimized formulation applied to pig ear skin by using a "direct-coupled universal modular Raman spectrometer with imaging" (RIMS-U-DC, Rinztech Nz Ltd., New Zealand). Samples were examined under a magnification of 20 x at a wavelength of 785 nm and a laser power of 300 mW, with a subsequent laser stability of 1%. The data was observed, analyzed, and reported (Gómez *et al.*, 2023).

3.7.12. Skin irritation test

The skin safety study used male BALB/c mice, aged 10 weeks and weighing 20 to 22 g. The "Institutional Animal Ethics Committee of the Central Animal House Facility, UPES, Dehradun, India" approved (UPES/IAEC/2023/3/07, dated 20/12/2023). The dorsal back skin of mice was shaved by 2 cm × 2 cm, and hair was removed by using hair removal cream. After that, the mice were kept under observation for 24 h. Imiquimod cream (5 %) "Imiquad® cream, Glenmark Pharmaceuticals, Mumbai, India" was applied consecutively for 6 days to the mice skin for psoriasis induction. The optimized diacerein and berberine HCl-loaded transferosomes and saline solution were topically applied once a day to the mice psoriatic skin from 3rd day to 6th day (Bhardwaj *et al.*, 2022). By using the modified Draize approach, the skin was visually scored on day 7 for any noticeable alteration. A score of 0 to 4 criteria was used to assign erythema as: 0 - no redness, 1 - hardly seeming light pink (trial erythema), 2 - dusky pink (moderate erythema), 3 - bright red (moderate to high erythema), and 4 - dark red (high levels of erythema) (Yadav *et al.*, 2021).

3.7.13. Stability studies

Stability study of the optimized formulation was conducted at two different temperatures, such as 25 ± 2 °C / 60 ± 5 % and 4 ± 1 °C / 60 ± 5 % of RH (relative humidity) for 3 months as per the ICH guidelines (Dahiya *et al.*, 2023).

In the next step, the optimized transferosomes was evaluated for zeta potential, physical appearance, vesicle size, and morphology.

3.7.14. *In vitro* cytotoxicity evaluation of transferosomes

3.7.14.1. Cell line and cell culture medium

The immortalized human keratinocyte cell lines (HaCaT) were obtained from the "National Center for Cell Science, Pune, Maharashtra, India". The cell lines were grown in DMEM medium. The media included 100 IU/mL penicillin, 10% inactivated fetal bovine serum (FBS), 5 µg/mL amphotericin B, and 100 µg/mL streptomycin. It was incubated at 37 °C in a humid environment with 5% CO_2. The cell detachment process was carried out with TPVG (Trypsin Phosphate Versene Glucose) solution, which contained 0.05% glucose, 0.02% EDTA, and 0.2% trypsin in PBS. Following detachment, the fluid was neutralized with DMEM, and the cells were reseeded in a T25 cm^2 culture flask.

3.7.14.2. Cytotoxicity studies

The cytotoxicity analysis were performed by using an MTT assay. The optimized formulation was exposed to HaCaT cell lines for cytotoxic studies by using an MTT assay. In this assay, initially, the HaCaT cells were trypsinized by using a TPVG solution. The cells were counted using a hemocytometer. The “cells were seeded at a density of 10,000 cells per well in a 96-well plate” and allowed to adhere by incubating at 37 °C in a humid 5% CO_2 environment. Different dilutions of the optimized formulations were added to a 96-well plate that contained adherent cells and subjected to incubation for 24 h. The cells that were not treated were referred to as the control group. The MTT solution was prepared at a concentration of 5 mg/mL in PBS. In each well, 25 µL of the above-prepared solution was added. Again, the plate was subjected to incubation for 2 h at 37 °C. DMSO (100 µL) was added to the plate after removing the medium from the wells. Gently, the plates were shaken for the solubilization of formazan crystals. The plates were subjected to absorbance

measurements at 540 nm and 660 nm by using an ELISA plate reader. The IC_{50} value (concentration of optimized formulation that reduced cell viability by 50%) was determined by using the software Graph Pad Prism and reported (Yao *et al.,* 2023).

3.8. PREPARATION OF TRANSFEROSOMES-LOADED GEL

Formulation and initial characterization of berberine-diacerein loaded dual delivery transferosomes were described in detail in our previous publication (Singh and Awasthi, 2024). Berberine-loaded transferosomes and diacerein-loaded transferosomes were developed using similar protocol to investigate the effect of single bioactive loaded transferosomes and compare their *in vivo* effectiveness with dual delivery transferosomes. Gel formulation containing berberine, diacerein, and berberine-diacerein loaded transferosomes are coded as formulation BTG, DTG, and BDTG, respectively. Briefly, optimized transferosomes were loaded into a hyaluronic acid gel-base formulation. The double-distilled water was taken in a dry beaker and 1% hyaluronic acid, ethanol, methylparaben, and propylparaben were added to it. The optimized transferosomes and Tween 80 were added to the homogenous gel system and mixed using a magnetic stirrer. The prepared gel system was kept for swelling at room temperature for 24 h, and after that, propylene glycol and glycerine were added to the transferosome gel system (Jain *et al.,* 2022; Li *et al.,* 2023).

3.9. *IN VITRO* EVALUATION OF OPTIMIZED TRANSFEROSOMES LOADED GEL

3.9.1. Determination of pH of optimized transferosomes loaded gel

Drug loaded transferosomes containing gel (10% w/v) was dispersed in double-distilled water. The pH was determined in triplicates using a calibrated digital pH meter.

3.9.2. Rheological study

Rheological properties of the gel were analyzed using a phase-shear pressure test using a rheometer (C-LTD80/QC, Anton Paar GMBH, Austria). At 50 different points, shear rate (1/s) and viscosity were measured as a function of shear pressure (Pa). Shear pressure was varied between 80–250 Pa and 250–80 Pa, with each point being equilibrated for 10 seconds (Yadav *et al.*, 2021).

3.9.3. Spreadability

Transferosomal gel (100 mg) was placed on a glass plate. Another glass plate was placed over the gel containing plate with. Initially, the gel diameter was measured and weights ranging from 5 to 100 g were applied to the gel. The weights were added at set intervals of 30 s. After each addition, the diameter was measured. The spreadability factor was calculated using equation 3.6 (Jain *et al.*, 2021).

$$\text{Sreadability factor } (\text{cm}^2.\text{g}^{-1}) = \frac{\text{Final spread area in cm}^2}{\text{Total weight applied on the gel in gram}} \qquad (3.6)$$

3.9.4. *In vitro* drug release studies

USP type II dissolution apparatus was used to determine release profiles of the payload from formulated transferosomal gel. The dialysis membrane was placed in sodium bicarbonate solution for 15 minutes to activate it and washed with double distilled water. The activated membrane was filled with transferosomes equivalent to 5 mg of diacerein and 5 mg of berberine HCl. Transferosomal gel containing dialysis membrane was immersed in the dissolution medium, PBS (pH 7.4), maintained at 37 ± 0.5 °C. The paddle was rotated at 100 rpm. Five millilitres of the samples were withdrawn at 0, 1, 2, 3, 4, 5, 6, 8, 10, 12, 16, and, 24 hours intervals. The sink condition was maintained by adding an equivalent amount of phosphate buffer (pH 7.4) after each sampling. The samples were filtered and subjected to analysis using a UV spectrophotometer (UV-1900, Shimadzu, Japan). Sampling was done in triplicate. The samples were analyzed at 340 nm and 258 nm, respectively, for Berberine HCl diacerein (Dhavale *et al.*, 2021).

3.10. *IN VIVO* EVALUATION OF OPTIMIZED TRANSFEROSOMES LOADED GEL

3.10.3. Determination of anti-psoriatic activity

Anti-psoriatic activity was accessed in the imiquimod-induced psoriatic BALB/c mice model at 8–10 weeks of age and a weight of 20–22 g. Protocol was approved by the IAEC of UPES, Dehradun, India (UPES/IAEC/2023/3/07 dated December 20, 2023. The animals were placed in controlled environment (25 ± 1°C, 55 ± 5% RH, and 12 h of dark and light cycles) with food and water ad libitum.

The animals were divided into seven groups (n = 5). Group I was the control group, receiving no treatment. Group II, the positive control, was treated with imiquimod cream and betamethasone valerate cream (0.01%, Betnovate cream, Glaxo SmithKline Pharm. Ltd., Bangalore, India). Group III, the negative control, was treated with only imiquimod cream. Group IV, the vehicle control, was treated with imiquimod cream and a gel base without active drugs. Group V was treated with imiquimod cream and berberine HCl transferosomal hydrogel. Group VI received imiquimod cream and diacerein transferosomal hydrogel. Group VII was treated with imiquimod cream and a combination of berberine HCl and diacerein transferosomal hydrogel (Yadav *et al.,* 2021; Jain *et al.*, 2022;). The dorsal skin of mice, measuring 2 cm by 2 cm, was shaved and observed for 24 h. Imiquimod cream (62.5 mg/day) (Imiquad®, Glenmark Pharm., Mumbai, India) was applied to the shaved skin of mice for 6 days for the induction of psoriasis. The treatment was initiated on the third day of the induction of disease and continued until the sixth day of the study (Figure 3.3).

3.10.2. Evaluation of Severity Index and Psoriasis Area

The evaluation of psoriasis area and severity index (PASI) scheme was used to determine the inflammation level by observing scaling and erythema on the dorsal skin. The extent of scaling and erythema was assessed using a rating scale

ranging from 0 to 4, where 0 indicates no, 1 indicates mild, 2 indicates moderate, 3 indicates significant, and 4 indicates severe. The scoring was done each day for seven consecutive days (Yadav *et al.*, 2021; Jain *et al.*, 2022).

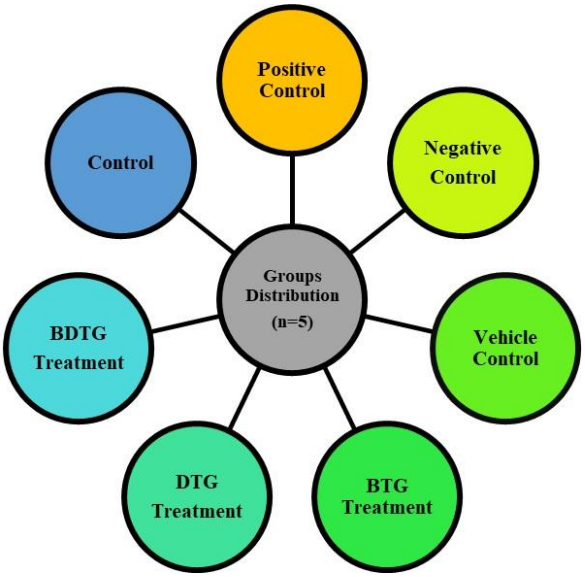

Figure 3.2. Groups distribution of mice model for anti-psoriatic assessment.

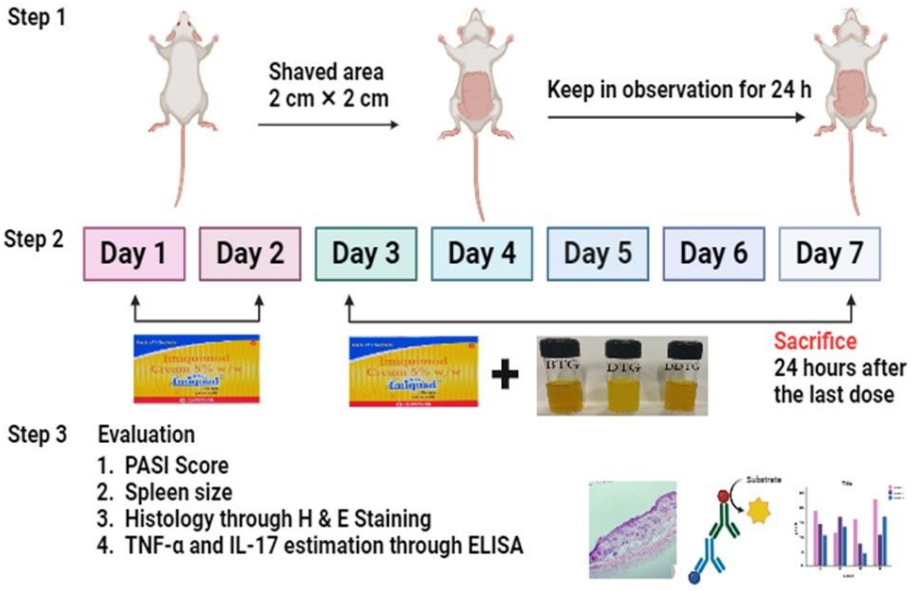

Figure 3.3. Graphical illustration of assessment of anti-psoriatic efficacy in mice model.

3.10.3. Histopathology of dorsal skin lesion and spleen

Following a painless decapitation, the animals underwent cervical dislocation on the 7th day. Histopathology of dorsal skin and spleen was done. Skin and spleen samples were preserved in 10% v/v formalin. The skin and spleen samples were stained using hematoxylin and eosin for 12 h at 25 °C, and a digital microscope (BT-E Cilika microscope by Medprime Technologies Pvt. Ltd., Maharashtra, India) was used for image capturing. The severity of disease progression was studied carefully. Each animal underwent separate evaluation for its cornified epidermis and dermal layer, followed by pathological alterations such as hyperkeratosis, acanthosis, and inflammatory infiltrates (Yadav *et al.,* 2021; Jain *et al.,* 2022).

3.10.4. Determination of cytokines using ELISA

Disease incidence directly correlates with an increase in cytokine levels. It is necessary to quantify the level of cytokines that helps to determine the effect of treatment therapy. Inflammatory cytokine levels (TNF-α and IL-17A) were examined by the ELISA method. The skin tissue sections were homogenized at 3000 rpm for 5 min in extraction buffer (150 mM NaCl, 10 mM Tris pH 7.4, and 1% Triton X-100) using a tissue homogenizer (REMI Electro Kinetic Ltd., India). The homogenates were centrifuged (Remi C-24 Plus, Mumbai, India) at 4 °C with 10,000 rpm for 5 min. The supernatant was collected and subjected to cytokine (TNF-α and IL-17A) analysis using the standard protocol mentioned on the ELISA kit. The kit provided instructions for performing experiment. The plates were coated with a 50 µL capture antibody, and the appropriate wells were filled with 100 µL of standards and sample. The plates were incubated for 2 h at 25 °C. The incubated plate was further washed three times with a wash buffer. The washed plates were filled with 100 µL of a diluted detection antibody (Biotin Conjugated Detection Antibody) solution. The plates were incubated for 1 h at 25 °C. After incubation, the plates were washed three times with wash buffer. The plates were further incubated with 100 µL of streptavidin-HRP solution for 1 h. The incubated plates were washed with wash buffer and incubated with 100 µL of 3,3’,5,5’-tetramethylbenzidine solution for 30 min in the dark. For the termination of the

reaction, 100 µL of stop solution was added to each well and examined for absorbance at 450 nm (Jain *et al.*, 2022).

3.10.5. Statistical analysis

The statistics were analysed by using 8.0.2 trial version of GraphPad Prism software. The one-way ANOVA by using an Unpaired two-tailed t-test was used to determine the level of statistical significance at p-values of < 0.01 (**), < 0.05 (*), or < 0.005 (***).

CHAPTER 4

RESULTS AND DISCUSSION

RESULTS AND DISCUSSION

4.1. Pre-formulation studies

4.1.1. Physical characterization of bioactives

Diacerein was a fine, yellow powder with no odour. The findings were consistent with the existing literature (Patel *et al.,* 2020; Bansal *et al.,* 2022). Berberine HCl was a yellow, odorless powder. The findings were consistent with the existing literature (Singh *et al.,* 2018; Fan *et al.,* 2019).

4.1.2. Melting point

Melting point of diacerein was determined by the capillary method (255 ± 1.2 °C). We found the observed value to be closest to the reported value of 255.2 °C (Patel *et al.,* 2020). The melting point of berberine HCl was found to be 145 ± 1.44 °C. We found it to be closest to the reported value of 145.1–146.7 °C (Ai *et al.,* 2021; Javed *et al.,* 2021).

4.1.3. λ_{max} (absorption maxima) and calibration curve of berberine HCl

The λ_{max} of berberine HCl was determined in phosphate buffer (pH 7.4) using a UV spectrophotometer. The λ_{max} of berberine HCl was found at 340 nm (Figure 4.1). The berberine HCl calibration curve was prepared in phosphate buffer pH 7.4 nm (Figure 4.2) and methanol with 340 nm (Figure 4.3) and showed r^2 0.9977 and 0.9985, respectively. In phosphate buffer (pH 7.4)**,** berberine HCl showed linearity between 2-16 µg/mL concentration with a R^2 value of 0.9977.

4.1.4. λ_{max} (absorption maxima) and calibration curve of diacerein

The λ_{max} of diacerein was identified in DMSO and phosphate buffer (pH 7.4) ratio (3:7) by using a UV spectrophotometer and scanned from 200 to 800 nm. The λ_{max} of diacerein was found at 258 nm (Figure 4.4). The diacerein calibration curve was prepared in DMSO and phosphate buffer, pH 7.4 (at a

ratio of 3:7) (Figure 4.4) and showed r^2 value 0.9965. Diacerein, in phosphate buffer (pH 7.4) containing DMSO**,** showed linearity between 1-8 µg/mL concentration range with a R^2 value of 0.9977.

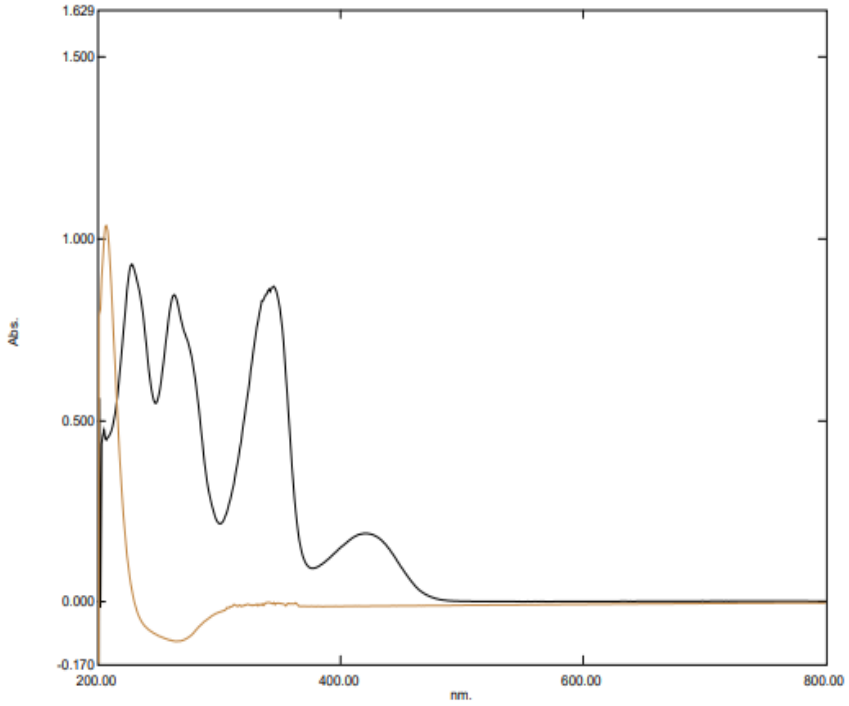

Figure 4.1. UV scan of berberine HCl in phosphate buffer, pH 7.4 (black line); and UV scan of diacerein in DMSO and phosphate buffer, pH 7.4 (yellow line).

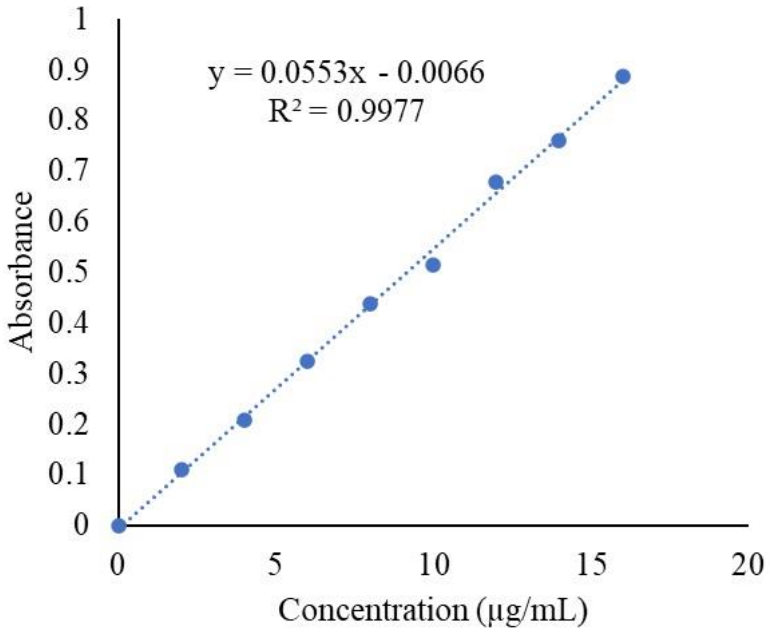

Figure 4.2. Calibration curve of berberine HCl in phosphate buffer (pH 7.4)**.**

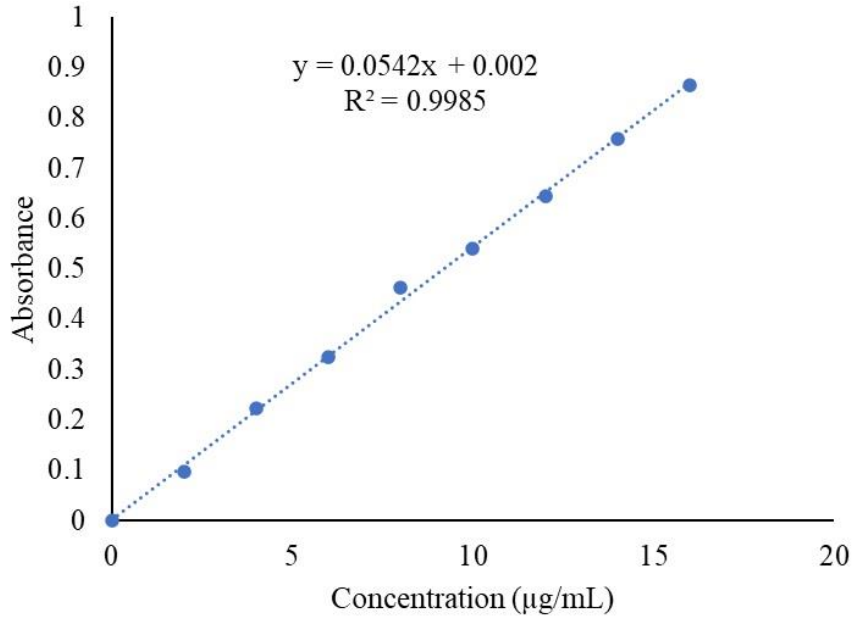

Figure 4.3. Calibration curve of berberine HCl in methanol.

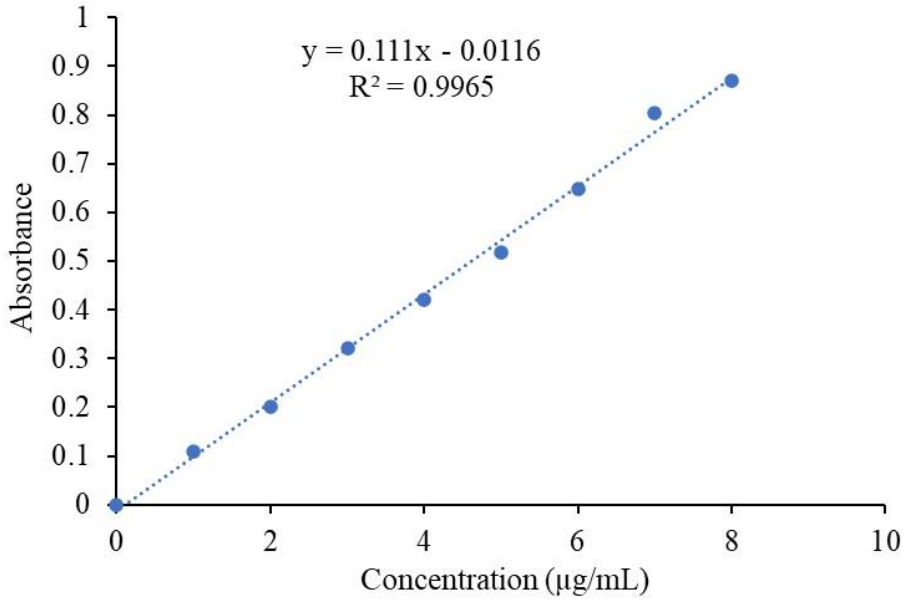

Figure 4.4. Calibration curve of diacerein in DMSO and phosphate buffer, pH 7.4 (3:7 ratio).

4.2. OPTIMIZATION STUDIES

Diacerein and berberine HCl-loaded transferosomes were optimized by using Box-Behnken design. Here, three independent variables were used to develop the

significant model: A-concentration of phosphatidylcholine, B-concentration of sodium deoxycholate, and C-sonication time. We used a three-level factorial design to optimize the interactions between the individual variables and their influence on the experimental responses, specifically vesicle size and entrapment efficiency of diacerein and berberine HCl (Tables 4.1 and 4.2). The statistical measures used to determine model significance include the analysis of variance (ANOVA) and regression coefficient (R^2) tests. The results revealed that the BDT-10 formulation, with an 85:15 ratio of phosphatidylcholine (A) and sodium deoxycholate (B) and a 3-minute sonication time (C), was an optimized formulation (Tables 1 and 2).

Table 4.1. Results of diacerein and berberine HCl loaded dual delivery transferosomes

Formulatio code	Particle size (nm)	Entrapment efficiency (%)		Drug loading (%)		Deformability (%)
		Berberine HCl	Diacerein	Diacerein	Berberine HCl	
BDT-1	95.93±2.5	69.14±1.4	71.32±2.2	15.03±0.65	12.94±0.03	8.47±0.02
BDT-2	118.45±1.4	65.30±1.7	72.34±1.4	15.09±0.39	12.70±0.24	13.11±0.09
BDT-3	103.00±1.2	62.11±1.4	66.61±1.5	14.59±0.02	12.35±0.11	10.79±0.19
BDT-4	114.60±3.5	59.24±1.5	64.87±1.6	14.47±0.20	12.04±0.02	12.97±0.02
BDT-5	104.50±2.2	85.73±1.5	88.22±1.8	19.37±0.36	17.05±0.07	11.47±0.36
BDT-6	90.80±2.7	68.32±2.4	65.51±1.2	14.51±0.14	12.90±0.07	8.35±0.18
BDT-7	99.90±1.6	64.51±1.6	69.11±2.1	15.07±0.05	12.50±0.04	9.78±0.12
BDT-8	119.00±2.8	72.11±2.1	84.09±1.4	18.96±0.16	15.7±0.19	14.51±0.12
BDT-9	106.90±2.6	60.27±1.4	61.15±1.4	14.40±0.07	12.16±0.09	10.80±0.11

BDT-10	110.90±2.8	89.50±1.5	91.23±1.8	21.91±0.05	19.41±0.47	12.44±0.39
BDT-11	115.00±1.6	75.42±1.2	74.42±1.5	15.90±0.65	16.17±0.06	13.34±0.25
BDT-12	86.98±2.4	66.16±2.4	68.61±2.3	14.98±0.28	12.77±0.02	7.43±0.04
BDT-13	121.45±2.5	76.00±1.2	82.32±1.5	18.22±0.07	16.70±0.21	14.15±0.08

The study examined the effect of three independent variables (A- concentration of phosphatidylcholine, B- concentration of sodium deoxycholate, and C- sonication cycles) on the dependent factors (particle size, entrapment efficiency of transferosomes for diacerein, and berberine HCl) of the dual drug-loaded transferosomes (Table 4.1). 3D response surface and contour plots of parameters as a function of formulation variables such as particle size (Figures 4.5, 4.6, and 4.7) percentage entrapment efficiency of berberine HCl (Figures 4.8, 4.9, and 4.10), and percentage entrapment efficiency of diacerein (Figures 4.11, 4.12, and 4.13) were plotted. The correlation between the dependent and independent variables are represented by following quadratic equations (Eq. 4.1 – 4.3).

$$Y_1 = 110 - 10.79A - 5.65B - 3.08C + 2.96AB - 2.23AC - 0.0125BC - 6.62A^2 - 1.11B^2 + 0.9437C^2 \quad (4.1)$$

$$Y_2 = 89 - 5.13A + 0.7500B + 0.1250C - 2.50AB - 0.2500AC + 2.00BC - 3.37A^2 - 11.12B^2 - 16.38C^2 \quad (4.2)$$

$$Y_3 = 90.85 - 6.88A - 1.13B - 1.75C - 3.00AB + 2.25AC + 3.25BC - 3.17A^2 - 11.17B^2 - 13.93C^2 \quad (4.3)$$

In this equation, A represents the quantity of phospholipid, B represents the quantity of edge activator, C represents the duration of the sonication cycle, AB

represents the effect of phospholipid and edge activator, AC represents the effect of phospholipid and the duration of the sonication cycle, and BC represents the effect of edge activator and the duration of the sonication cycle.

Equation 4.1 demonstrated a negative correlation between the amount of phosphatidylcholine (phospholipid) and the size of the transferosome particle. Research indicates that an increase in phospholipid concentration leads to a decrease in vesicle size (Qushawy *et al.,* 2018; Vasanth *et al.,* 2020). Similarly, the amount of sodium deoxycholate, an edge activator, also had a negative effect on the size of the vesicle. So, to make transferosomes with smaller particles, it would be better to use more phosphatidylcholine (a phospholipid) and sodium deoxycholate (an edge activator). It is because the edge activator destabilizes the phospholipids and increases the flexibility of the lipid bilayer. The utilization of response surface plots further elucidated the correlation between the dependent and independent variables. Figure 4.5 depicts an increase in the amount of phosphatidylcholine (phospholipid), which causes a decrease in the mean vesicle size. In addition, a higher sonication cycle level is responsible for less particle aggregation and smaller vesicles (Figure 4.6); hence, the duration of the sonication cycle suppresses the vesicle size.

It is possible that the drugs' low solubility in water is responsible for their high percentage of encapsulation efficiency and drug loading. For berberine HCl, the percentage entrapment efficiency was 59.24 ± 1.5 to 89.50 ± 1.5%, and the percentage drug loading was 12.04 ± 0.02 to 19.41 ± 0.47%. For diacerein, the percentage entrapment efficiency was 61.15 ± 1.4 to 91.23 ± 1.8%, and the percentage drug loading was 14.40 ± 0.07 to 21.91 ± 0.05%. Equations 4.2 and 4.3 clearly show a negative correlation between phospholipid (phosphatidylcholine) and the encapsulation of diacerein and berberine HCl. That means that when there is more phosphatidylcholine, there is less diacerein and berberine HCl encapsulated in the transferosomes (Shaji *et al.,* 2014). Therefore, it has been suggested that the use of lower amount of phosphatidylcholine lead to high drug encapsulation efficiency.

However, sodium deoxycholate (edge activator) had a positive correlation with the encapsulation efficiency of berberine HCl (equation 4.2), Figures 4.8, 4.9, and 4.10) and a negative correlation with the encapsulation efficiency of diacerein (equation 4.3), Figures 4.11, 4.12, and 4.13). Ahad *et al.*, 2012 reported a negative effect of edge activator level on drug entrapment efficiency. Similarly, an increased concentration of surfactant can result in a reduction in entrapment efficiency (Jain *et al.*, 2003; Patel *et al.*, 2009). The potential explanation is that the arrangement of edge activator molecules within the lipid bilayer structure of the vesicle is responsible for the elevation of phospholipid layer permeability. The arrangement of the edge activator may create vesicle membrane openings, leading to increase in fluidity and leaking out of the loaded drugs (Bnyan *et al*., 2018; Opatha *et al.*, 2020).

We found that the entrapment efficiency of diacerein was higher than that of berberine HCl. The increase in the number of vesicles is dependent on the higher concentration of the edge activator. Furthermore, this creates a larger hydrophobic bilayer area that allows for hydrophobic drug encapsulation (Opatha *et al.,* 2020). Table 4.2 shows that the observed and predicted values revealed a substantial degree of agreement, which suggests that the constructed model is valid. We systematically examined the possible interaction between all independent factors shown in Figure 4.14, 4.15, and 4.16 and their effects on dependent factors, such as particle size (A), entrapment efficiency of berberine HCl (B), and diacerein (C). This model depicted higher drug encapsulation and loading, surpassing the findings of a previously reported study (Mishra *et al.*, 2022).

Phosphatidylcholine (A) had a substantial impact on the size of the vesicles (Y1) (F value 151.47), with a p-value less than 0.05, in comparison to sodium deoxycholate (B) (F value 41.57) and the sonication cycle time (C) (F value 12.37). The duration of sonication reduced the size of the vesicles. The size of the vesicles was considerably affected by the combination of phosphatidylcholine and sodium deoxycholate (AB), as indicated by the

statistical analysis (p value 0.0974, F value 5.68). The squared form of phosphatidylcholine quantity (A^2) had a significantly stronger impact on vesicle size compared to the combination of variables, as indicated by the F value of 16.30 (Table 4.3).

The independent factors A (phosphatidylcholine), B (sodium deoxycholate), and C (sonication time) showed significant effects on the entrapment efficiency of diacerein and berberine HCl at $p < 0.05$. Factor A (phosphatidylcholine) showed a relatively greater influence on the entrapment efficiency of diacerein and berberine HCl than the factor B (sodium deoxycholate) and factor C sonication cycle time, as indicated by measured F values (21.93 and 28.90, respectively, for diacerein and berberine HCl).

There was a suppressive effect of sonication time on entrapment efficiency. The berberine HCl entrapment efficiency was significantly (F value 2.61 and p value 0.2047) influenced by the combination of phosphatidylcholine and sodium deoxycholate (AB). Similarly, the diacerein entrapment efficiency was significantly (F value 3.23 and p value 0.1702) influenced by the combination of sodium deoxycholate and sonication time (BC). Moreover, the combination of phospholipid (phosphatidylcholine) and sonication time (AC) did not show any interaction on the entrapment efficiency of berberine HCl. The squared form of sodium deoxycholate amount (B^2) and sonication duration (C^2) had a greater impact on berberine HCl (F value 29.52 and 63.95, respectively) and diacerein (F value 21.82 and 33.88, respectively) entrapment than the combined effect of the variables (Table 4).

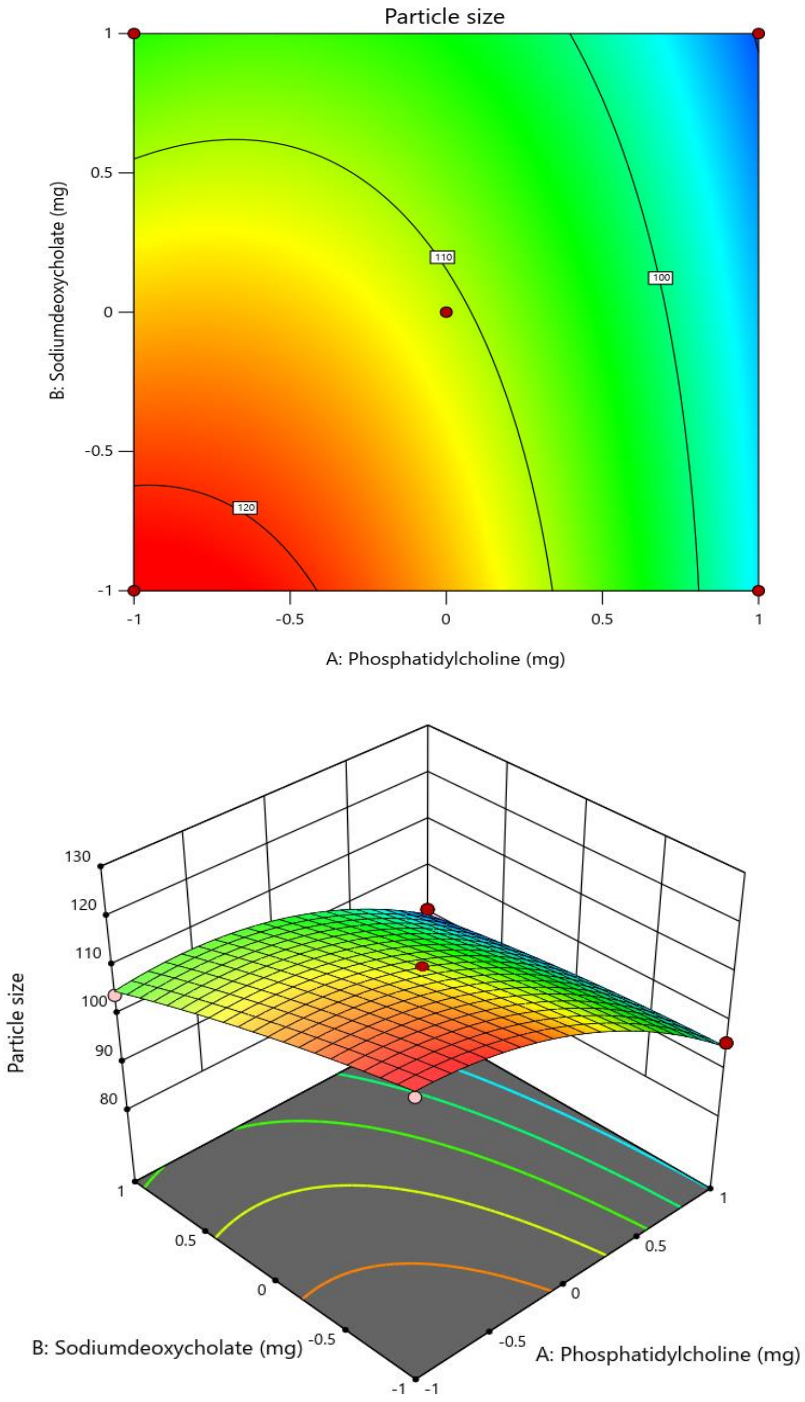

Figure 4.5. 3D response surface and contour plots illustrating the relationship between formulation variables (phosphatidylcholine concentration and sodium deoxycholate concentration) on particle size.

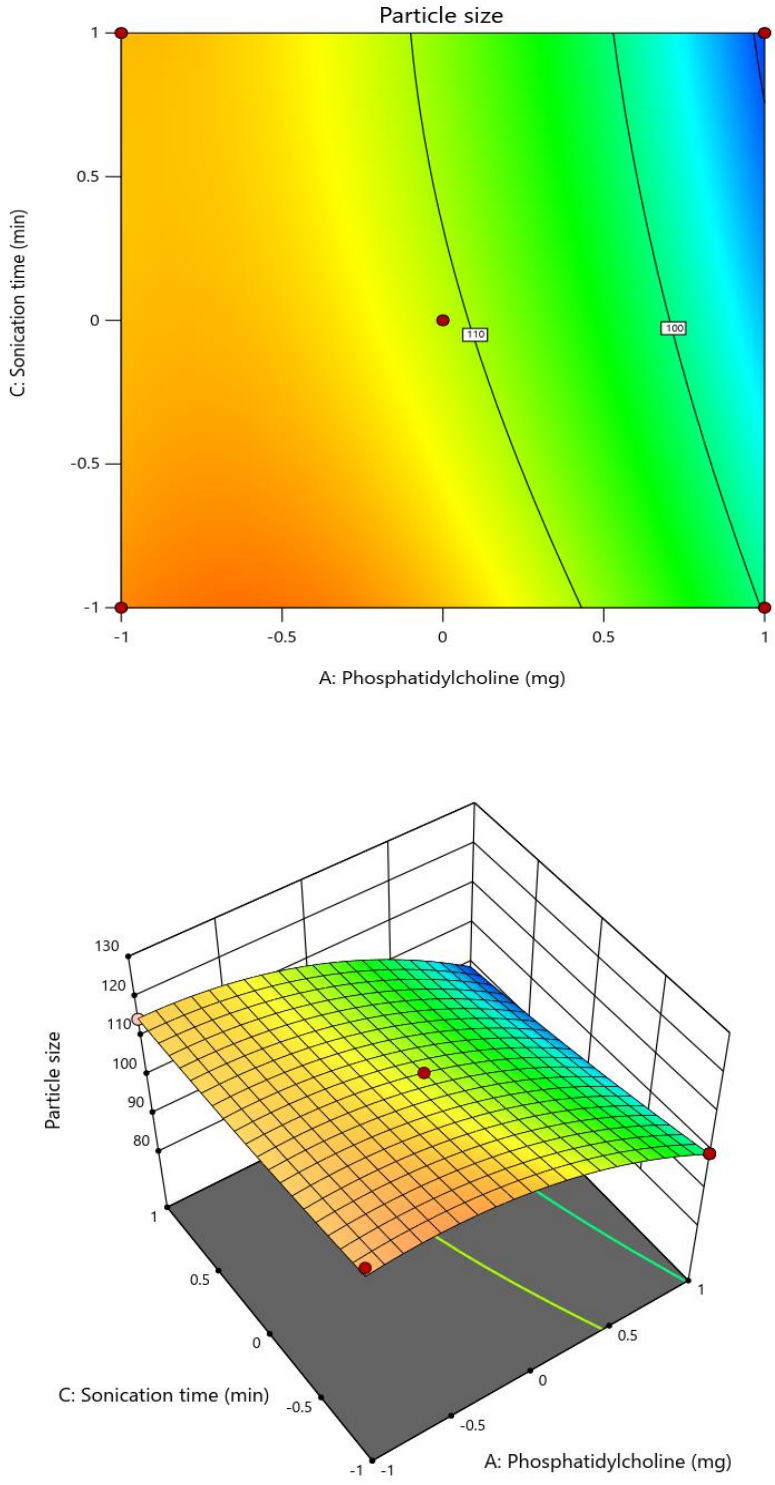

Figure 4.6. 3D response surface and contour plots illustrating the relationship between formulation variables (sonication cycles and phosphatidylcholine concentration) on particle size.

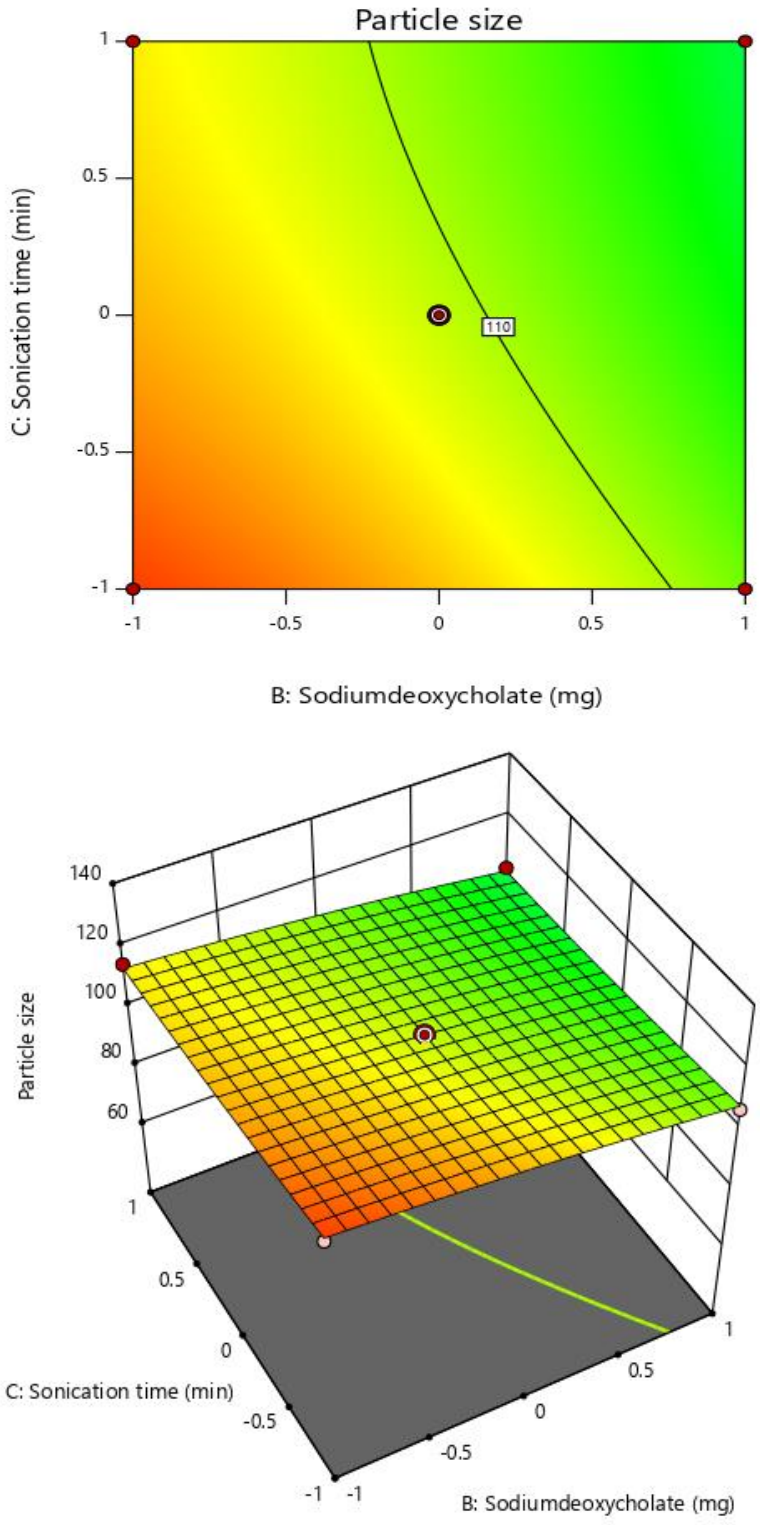

Figure 4.7. 3D response surface and contour plots illustrating the relationship between formulation variables (sonication cycles and sodiumdeoxycholate concentration) on particle size.

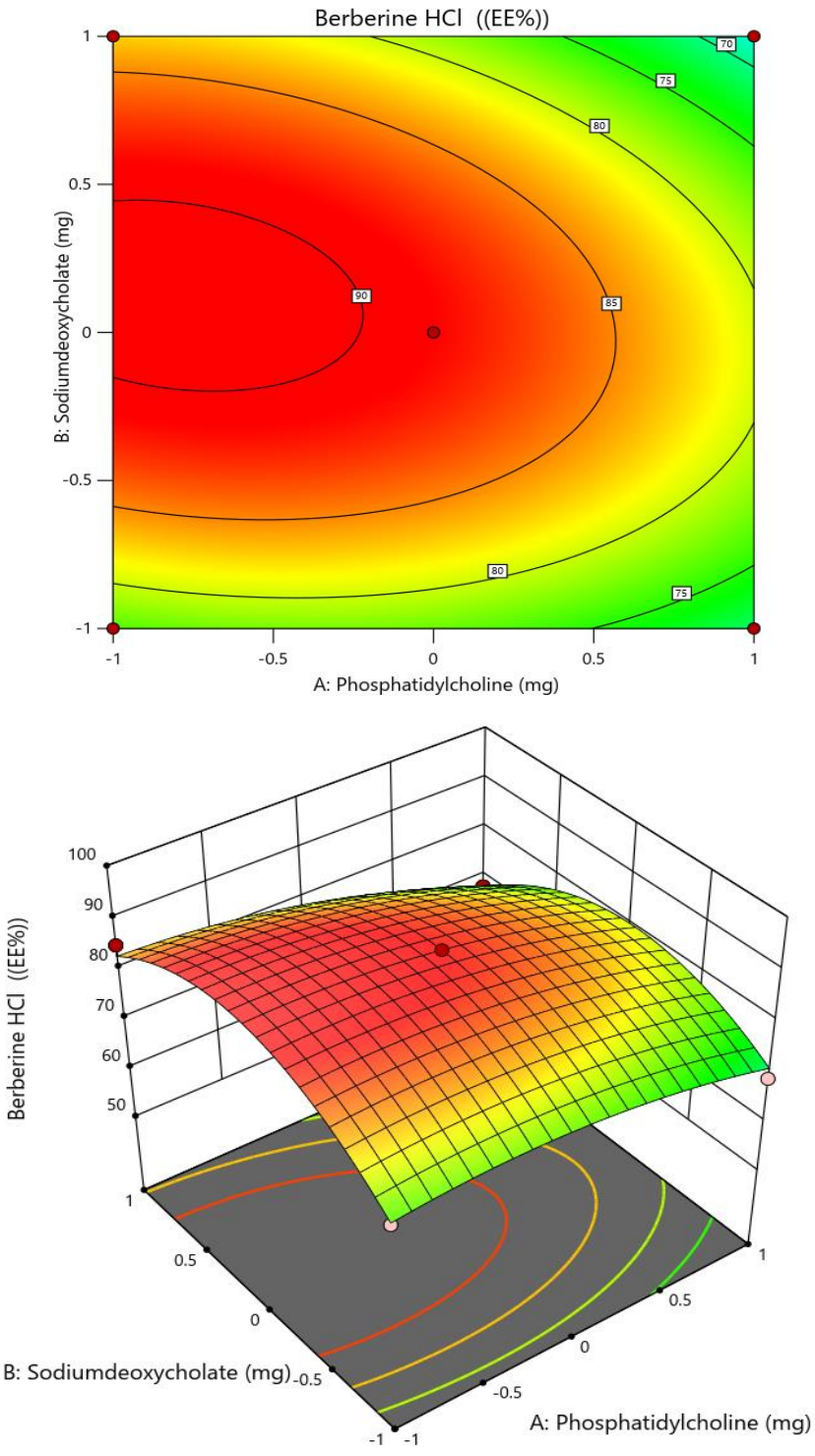

Figure 4.8. 3D response surface and contour plots illustrating the relationship between formulation variables (phosphatidylcholine concentration and sodium deoxycholate concentration) on percentage entrapment efficiency of berberine HCl.

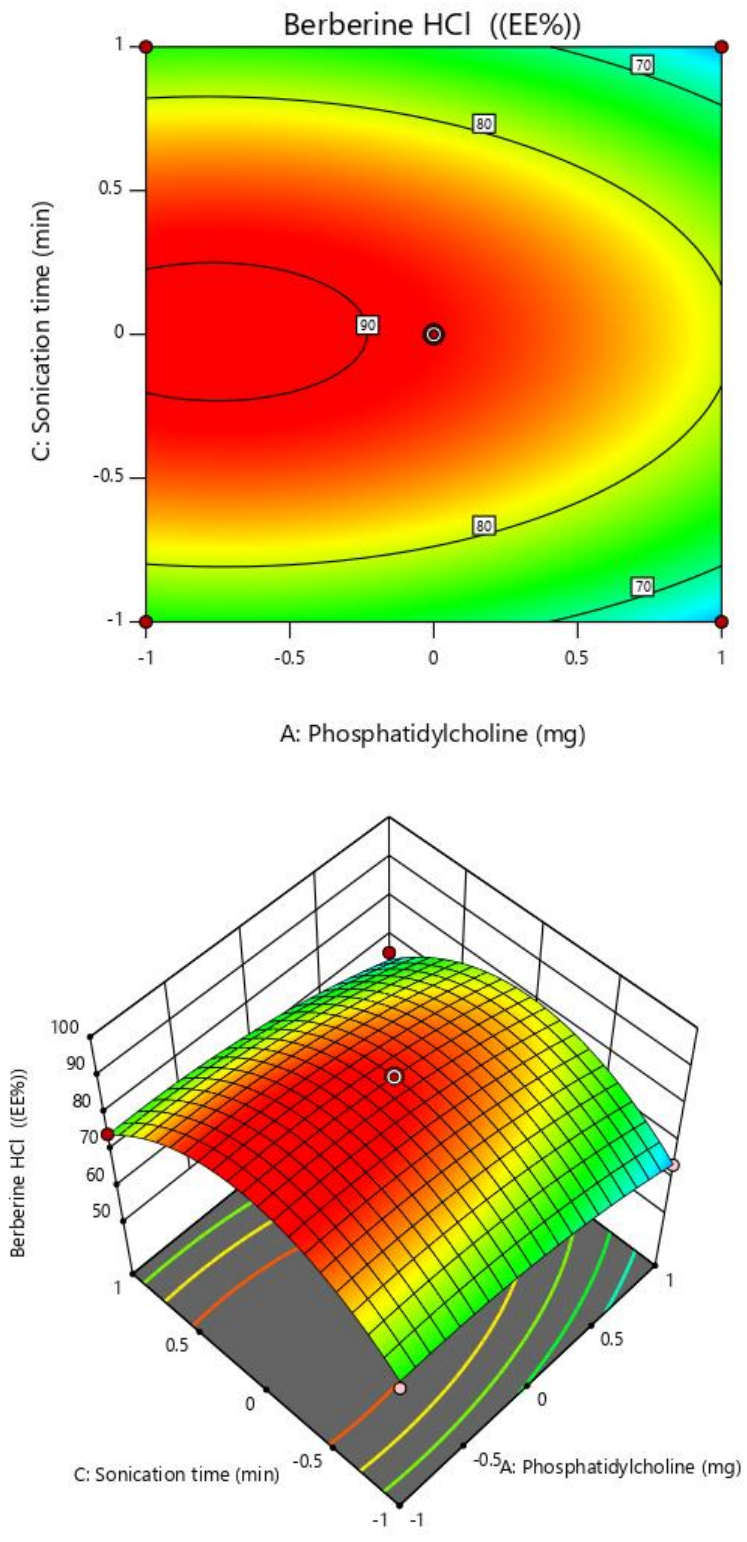

Figure 4.9. 3D response surface and contour plots illustrating the relationship between formulation variables (phosphatidylcholine concentration and sonication time) on percentage entrapment efficiency of berberine HCl.

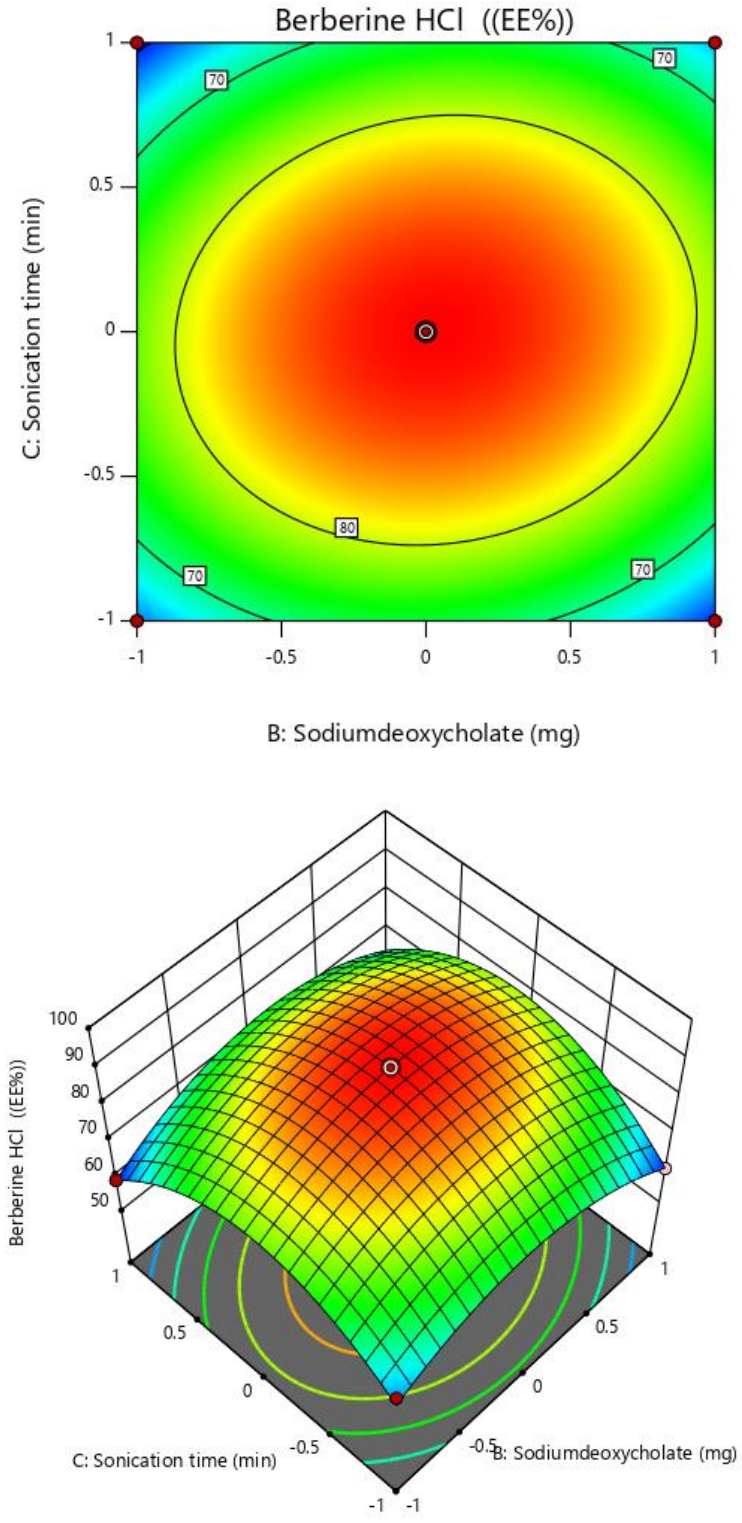

Figure 4.10. 3D response surface and contour plots illustrating the relationship between formulation variables (sonication cycles and sodium deoxycholate concentration) on percentage entrapment efficiency of berberine HCl.

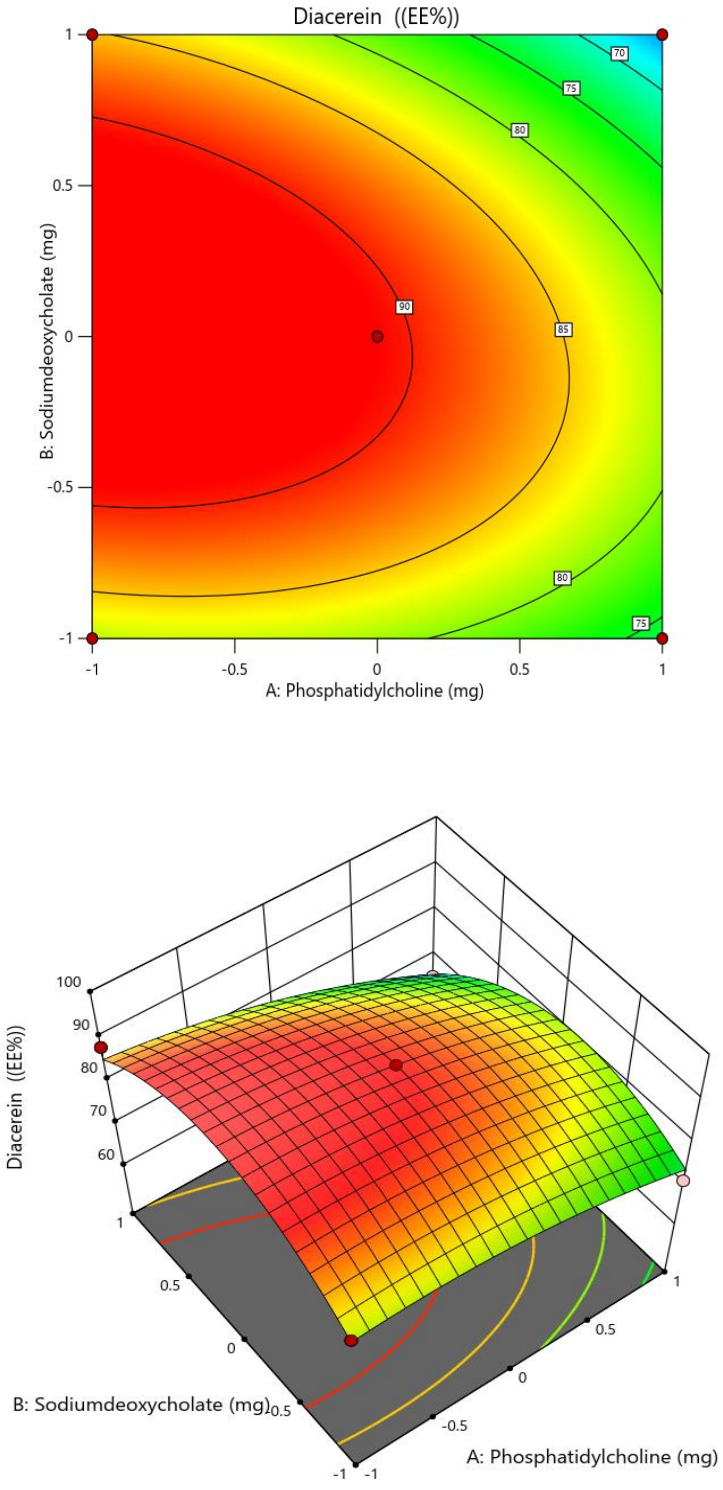

Figure 4.11. 3D response surface and contour plots illustrating the relationship between formulation variables (phosphatidylcholine concentration and sodium deoxycholate concentration) on percentage entrapment efficiency of diacerein.

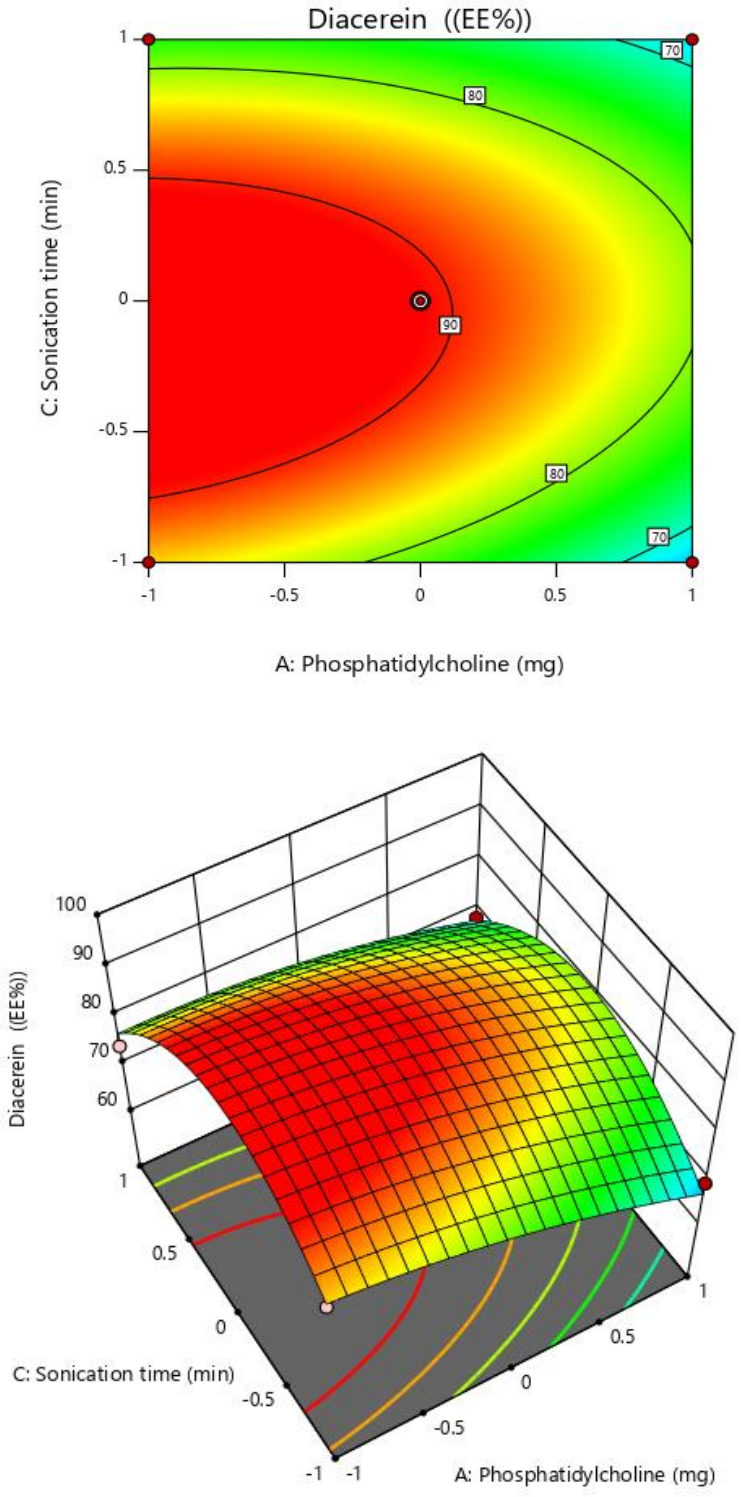

Figure 4.12. 3D response surface and contour plots illustrating the relationship between formulation variables (phosphatidylcholine concentration and sonication time) on percentage entrapment of diacerein.

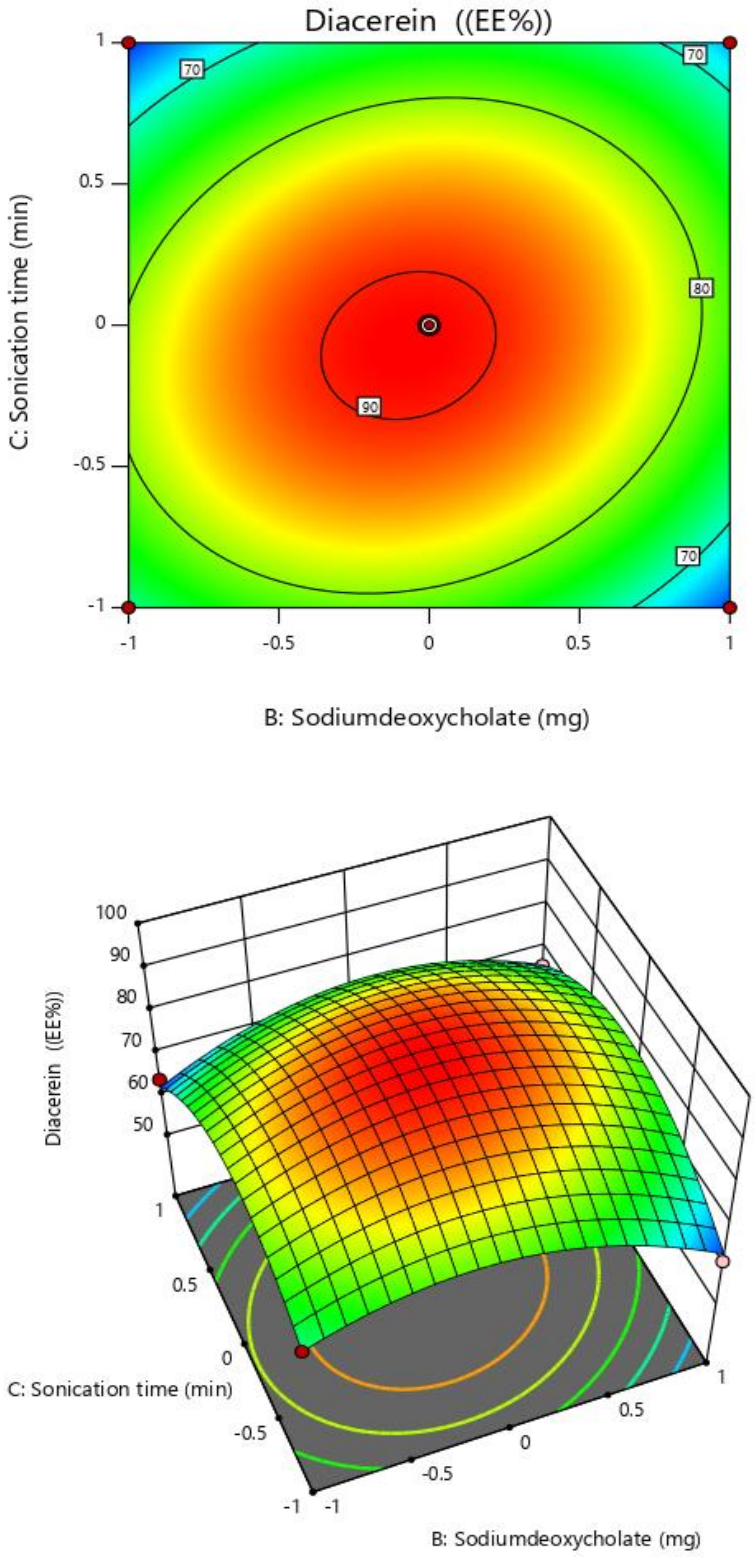

Figure 4.13. 3D response surface and contour plots illustrating the relationship between formulation variables (sonication cycles and sodium deoxycholate concentration) on percentage entrapment of diacerein.

Table 4.2. Predicted and actual values for all response variables.

Formulation code	Particle size (nm)		Encapsulation efficiency (%)			
			Berberine HCl		Diacerein	
	Predicted	Actual	Predicted	Actual	Predicted	Actual
BDT-1	95.08	95.93	71.12	69.00	73.75	71.00
BDT-2	119.46	118.45	62.62	65.00	71.87	72.00
BDT-3	101.98	103.00	64.37	62.00	66.12	66.00
BDT-4	113.32	114.60	58.87	59.00	61.87	64.00
BDT-5	105.35	104.50	82.87	85.00	85.25	88.00
BDT-6	89.67	90.80	67.62	68.00	65.50	65.00
BDT-7	99.74	99.90	64.25	64.00	66.37	69.00
BDT-8	116.86	119.00	74.00	72.00	84.62	84.00
BDT-9	108.18	106.90	60.12	60.00	63.12	61.00
BDT-10	110.9	110.90	89.00	89.00	90.85	90.85
BDT-11	115.15	115.00	74.75	75.00	76.62	74.00
BDT-12	89.11	86.98	64.00	66.00	67.37	68.00
BDT-13	122.57	121.45	76.37	76.00	81.50	82.00

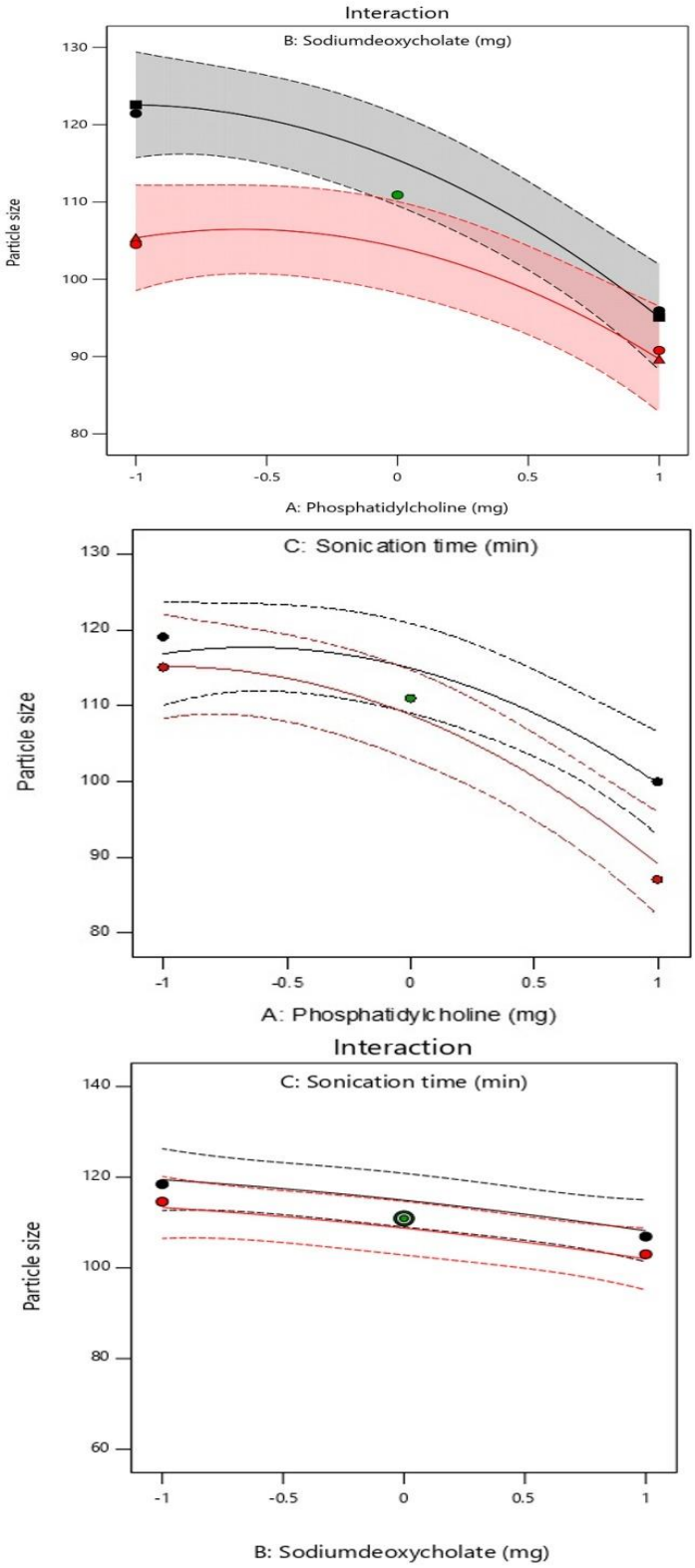

Figure 4.14. Interaction between the amount of edge activator (sodium deoxycholate) and phosphatidylcholine (phospholipid), amount of phospholipid and sonication time, and amount of edge activator and sonication time affecting particle size.

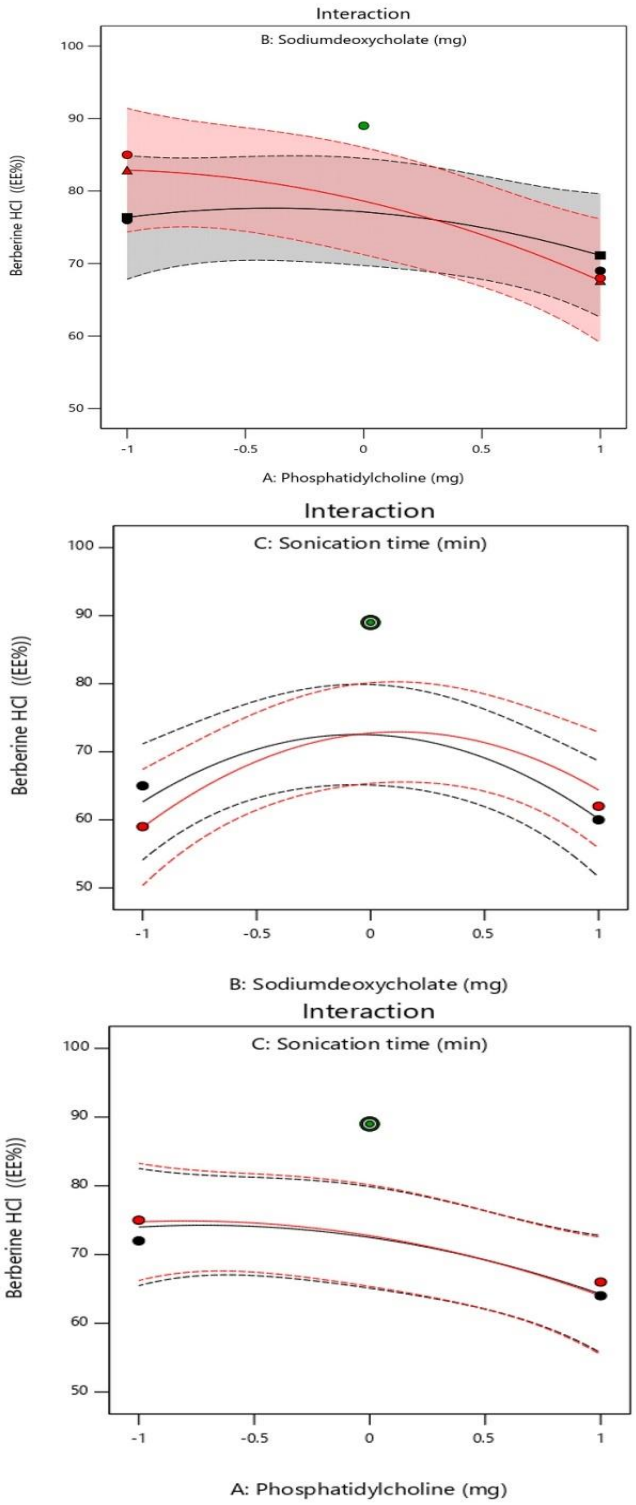

Figure 4.15. Interaction between the amount of edge activator (sodium deoxycholate) and phospholipid (phosphatidylcholine), amount of phospholipid and sonication time, and amount of edge activator and sonication time affecting entrapment of berberine HCl.

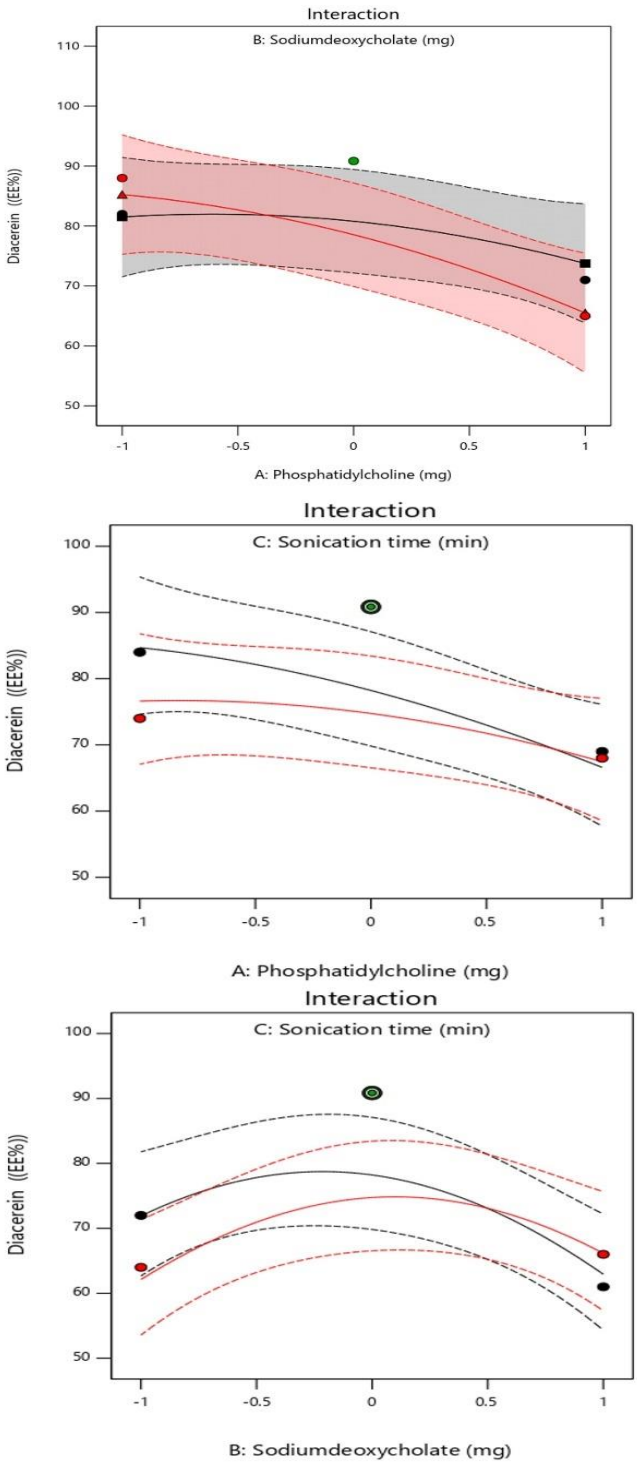

Figure 4.16. Interaction between phospholipid and edge activator, amount of phosphatidylcholine and sonication time, and amount of edge activator and sonication time affecting entrapment of diacerein.

Table 4.3. One Way ANOVA results for entrapment efficiency of diacerein and berberine HCl, and particle size.

Response	Source	Mean Square	Sum of Squares	F-value	p-value
Y_1: Particle size	Model	162.21	1459.88	26.37	0.0105*
	A	931.82	931.82	151.47	0.0012
	B	255.72	255.72	41.57	0.0076
	C	76.08	76.08	12.37	0.0390
	AB	34.93	34.93	5.68	0.0974
	AC	19.89	19.89	3.23	0.1700
	BC	0.0006	0.0006	0.0001	0.9926
	A^2	100.28	100.28	16.30	0.0273
	B^2	2.80	2.80	0.4547	0.5484
	C^2	2.04	2.04	0.3309	0.6054
	Residual	6.15	18.46		
	Cor total		1478.34		
Y_2: Entrapment efficiency of berberine HCl (%EE)	Model	109.92	989.25	11.47	0.0347*
	A	210.13	210.13	21.93	0.0184
	B	4.50	4.50	0.4696	0.5424
	C	0.1250	0.1250	0.0130	0.9163
	AB	25.00	25.00	2.61	0.2047
	AC	0.2500	0.2500	0.0261	0.8820
	BC	16.00	16.00	1.67	0.2868
	A^2	26.04	26.04	2.72	0.1979
	B^2	282.89	282.89	29.52	0.0122
	C^2	612.89	612.89	63.95	0.0041
	Residual	9.58	28.75		
	Cor total		1018.00		
Y_2: Entrapment efficiency of diacerein (%EE)	Model	120.97	1088.74	9.25	0.0468*
	A	378.13	378.13	28.90	0.0126
	B	10.13	10.13	0.7739	0.4438
	C	24.50	24.50	1.87	0.2646
	AB	36.00	36.00	2.75	0.1957
	AC	20.25	20.25	1.55	0.3018
	BC	42.25	42.25	3.23	0.1702
	A^2	23.04	23.04	1.76	0.2764
	B^2	285.44	285.44	21.82	0.0185
	C^2	443.21	443.21	33.88	0.0101
	Residual	13.08	39.25		
	Cor total		1127.99		

where A is the concentration of phosphatidylcholine, B is the concentration of sodium deoxycholate, C is the sonication time, and *represents significant

4.3. EVALUATION OF TRANSFEROSOMES

4.3.1. Fourier transformed infrared analysis

FTIR is useful technique for studying the behaviour of solid drugs and excipients. It is also beneficial in compatibility studies between drug-drug interaction and drug-excipient interactions. The drug-drug interaction can identify by analyzing alterations in vibrational frequencies of functional groups of drugs that involved in the interaction. The formation of new peaks, absorption peak disappearance, and peak intensity alleviation show incompatibility issues between drug-drug interaction and drug-excipient interaction due to the formation of hydrogen bonding and Vander Waals forces. (Segall *et al.*, 2019).

The FTIR analysis was performed by using KBr pellet method for pure drugs (berberine HCl and diacerein), drug-drug interaction, excipients (phosphatidylcholine and sodium deoxycholate) and optimized formulation BDT-10 reported in Figure 4.17. The functional group peak of berberine HCl and diacerein, phosphatidylcholine, and sodium deoxycholate was reported in Table 4.4. The physical mixture of berberine and diacerein did not showing any new peak formation in figure. that depicted compatibility of drugs among themselves.

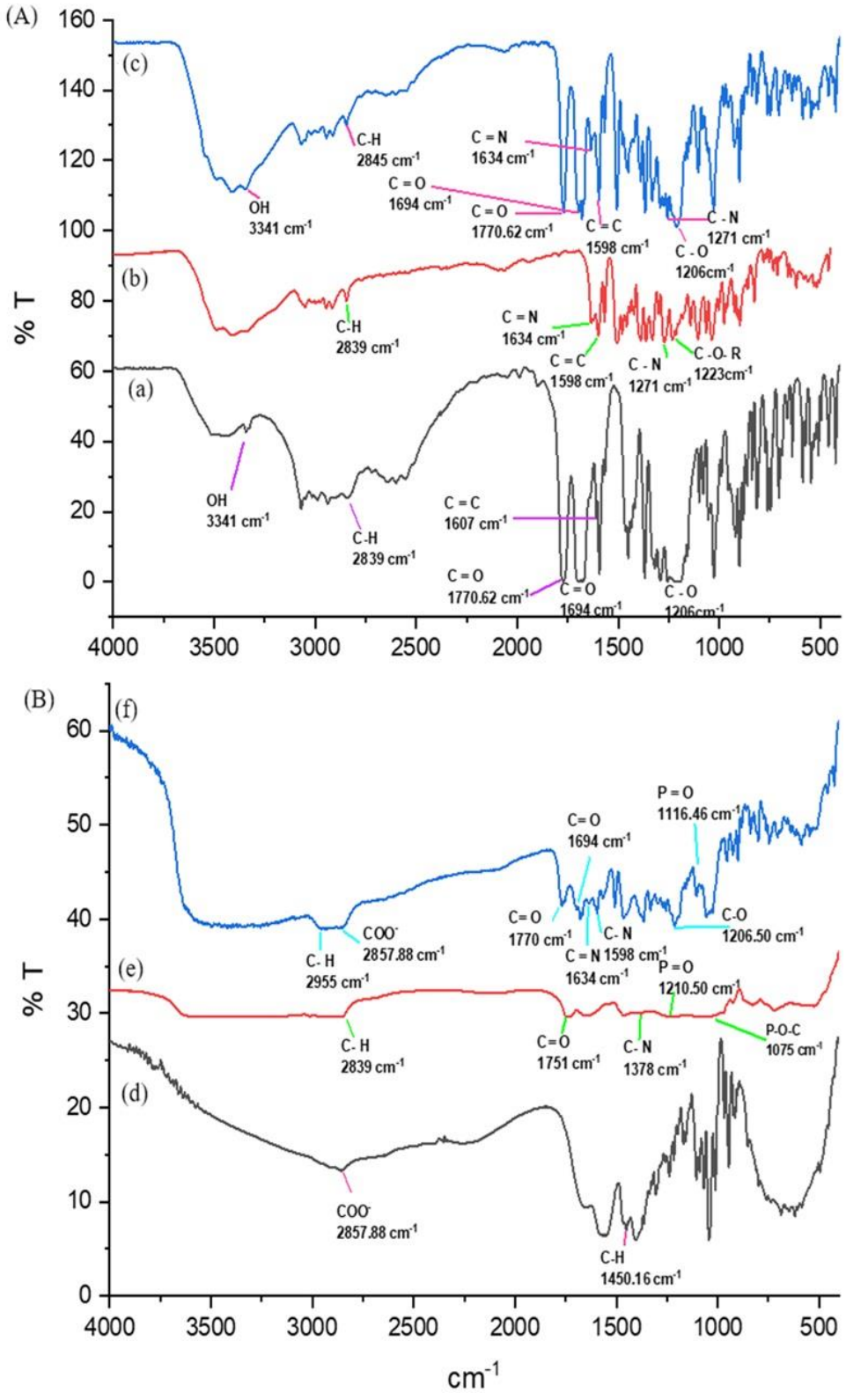

Figure 4.17: FTIR spectrum of diacerein (a), berberine HCl (b), physical mixture of berberine HCl and diacerein (c), sodium deoxycholate (d), phosphatidylcholine (e), and optimized formulation (formulation BDT-10) (f).

Table 4.4. Results of FTIR spectroscopy of diacerein, berberine HCl, physical mixture of berberine HCl and diacerein, phosphatidylcholine, sodium deoxycholate, and optimized formulation (formulation BDT-10).

Sample	Wavenumber (cm^{-1})	Remark	Ref.
Berberine HCl	2839	C-H stretching	(Choudury *et al.*, 2022; Sahibzada *et al.*, 2018; Battu *et al.*, 2010; Yan *et al.*, 2022)
	1634	Iminium $C=N^{+}$ double bond	
	1598	C=C stretching	
	1271	C-O-C stretching	
	1223	C-O stretching	
Diacerein	3341	O-H stretching band of -COOH	(Yan *et al.*, 2022; Eltobshi *et al.*, 2018; Khan *et al.*, 2017; Kesharwani *et al.*, 2023).
	2839	C-H stretching of an aliphatic symmetric group	
	1770	C=O stretching band of an ester group	
	1694	C=O stretching band of -COOH	
	1607	C=O stretching of an aromatic group	
	1206	C-O stretching	
Physical mixture of berberine HCl and diacerein	3341	O-H stretching	
	2845	C-H stretching	
	1770	C=O stretching band of an ester group	
	1694	C=O stretching band of -COOH	
	1634	Iminium C=N+ double bond	
	1598	C=C stretching	
	1271	C-O-C stretching	
	1206	C-O stretching	
Phosphatidylcholine	2839	C-H stretching	(Ghyadh *et al.*, 2023; Hsieh *et al.*, 2022)
	1751	C=O stretching	
	1210	P=O stretching	
	1075	P-O-C stretching	
Sodium deoxycholate	2857	C-H stretching	(Zhao et al., 2020; Sun *et al.*, 2011)
	1550	COO^{-} stretching	
Formulation BDT-10	2995	C-H stretching	
	1770	C=O stretching band of an ester group	
	1694	C=O stretching band of -COOH	
	1634	Iminium C=N+ double bond	
	1598	C=C stretching	
	1206	C-O stretching	
	1116	P=O stretching	

4.3.2. X-ray diffraction analysis

XRD technique is a valuable tool for identification of drug polymorphism form. These polymorphic forms play major role in drug solubility and stability. The sharp peaks of drugs molecules signify that molecules are crystalline in nature

while formation of diffuse halo indicated the amorphous nature of drug (Thakral *et al.*, 2018). An X-ray diffraction (XRD) examination was conducted on berberine HCl, diacerein, a physical mixture of berberine HCl and diacerein, and the optimized formulation (formulation BDT-10) to determine the physical state of the drugs in their pure form, physical mixture, and optimized formulation.

The berberine HCl diffractogram (Figure 4.18) showed diffraction angles and sharp peaks at 6.8, 7.5, 8.6, 12.9, 16.3, 20.4 and 25.5° (Sahibzada *et al.*, 2018; Choudhury *et al.*, 2022). The diacerein diffractogram (Figure 4.19) depicted sharp peaks at 5.2, 10.5, 17.4, 21.9, 25.1 and 27.8°. From the sharp peaks, it was found crystalline in nature and poor aqueous solubility. A similar diacerein diffractogram peaks has been documented previously (Naseef *et al.*, 2018). The berberine HCl and diacerein mixture diffractogram (Figure 4.20) showed peaks at 5.4, 10.3, 12.4, 17.39, and 27.25° that signifies there was no physical change appear in the drugs mixture. The diffractogram (Figure 4.21) of phosphatidylcholine showed a peak at 21.02° and sodium deoxycholate (Figure 4.22) showed a peak at 15.43°. The optimized formulation showed (Figure 4.23) peaks at 5.56, 10.88, 13.99, 15.92, 17.7 and 28.23° with less intensity. This less intensity showed the partial conversion of drug molecules into the amorphous phase.

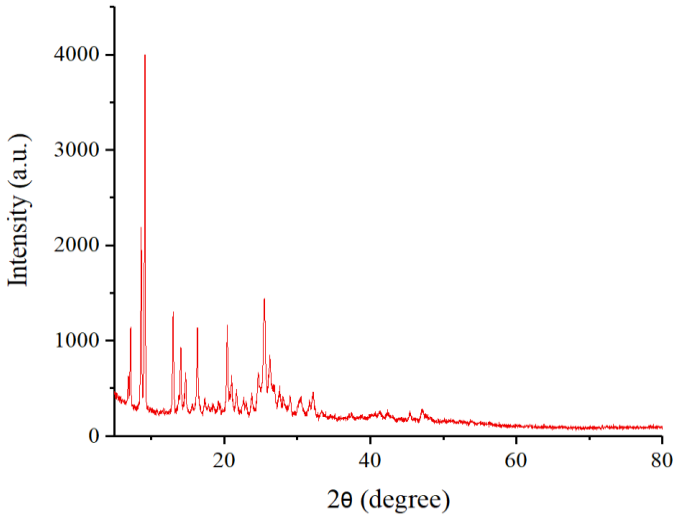

Figure 4.18: X-ray diffraction spectrum of berberine HCl.

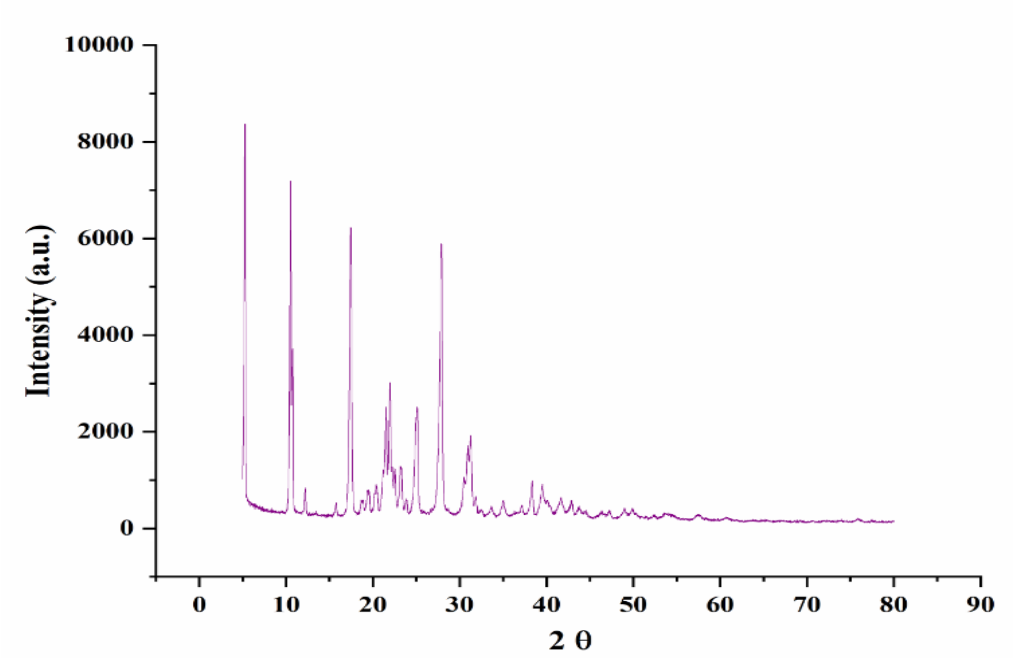

Figure 4.19: X-ray diffraction spectrum of diacerein.

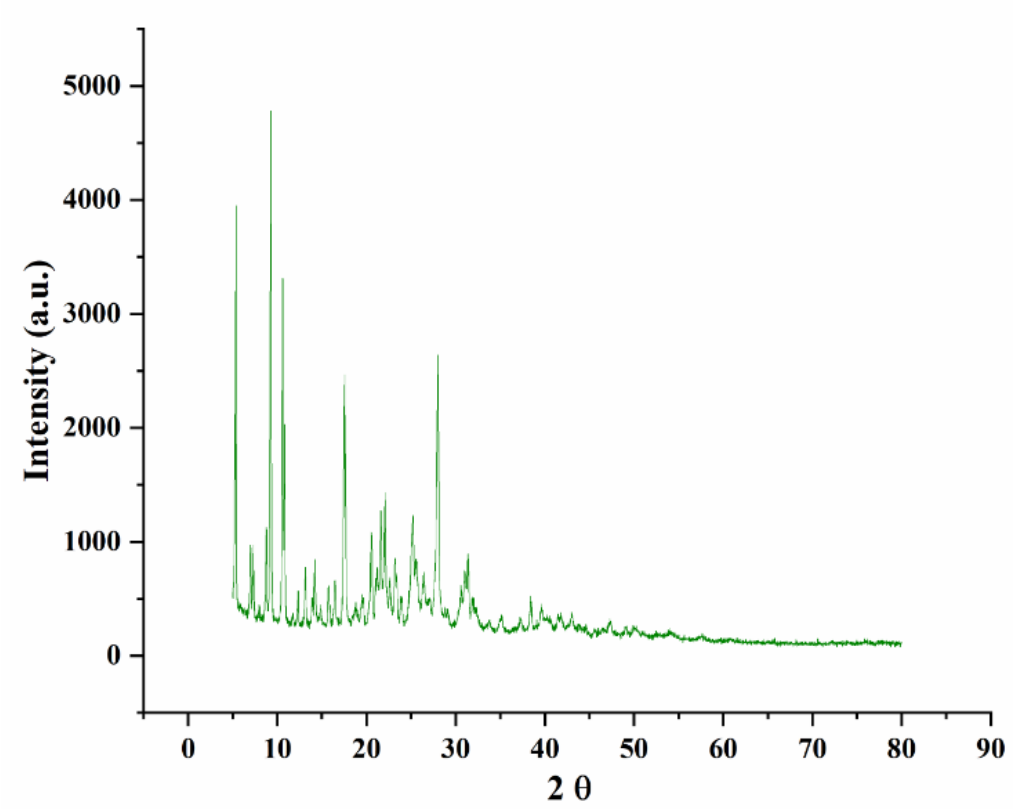

Figure 4.20: X-ray diffraction spectrum of physical mixture of berberine HCl and diacerein.

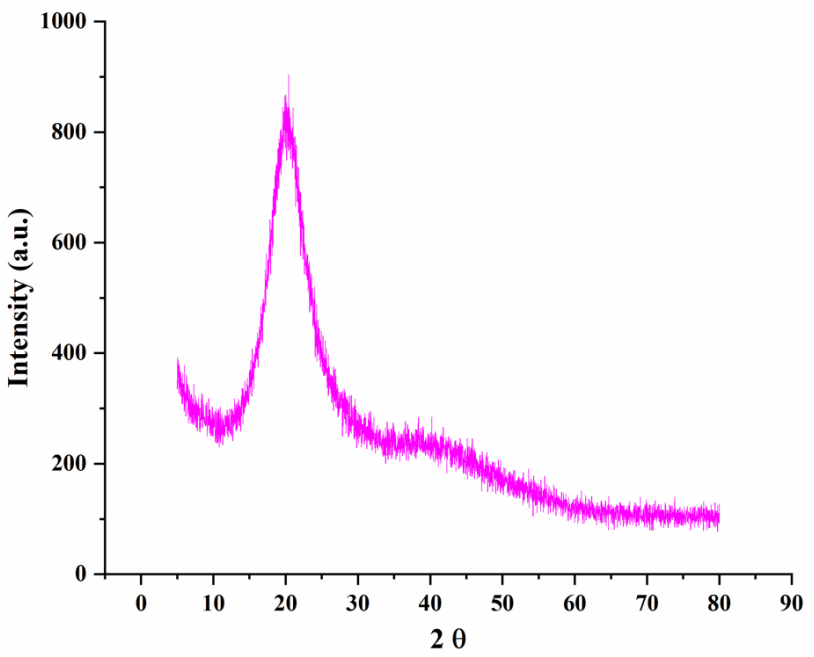

Figure 4.21: X-ray diffraction spectrum of phosphatidylcholine.

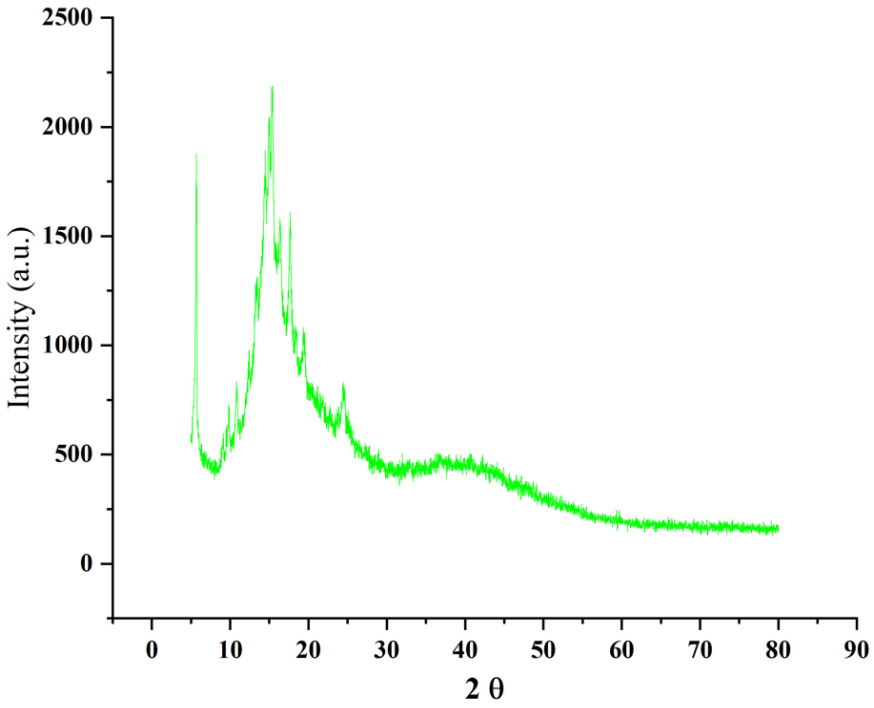

Figure 4.22: X-ray diffraction spectrum of sodium deoxycholate.

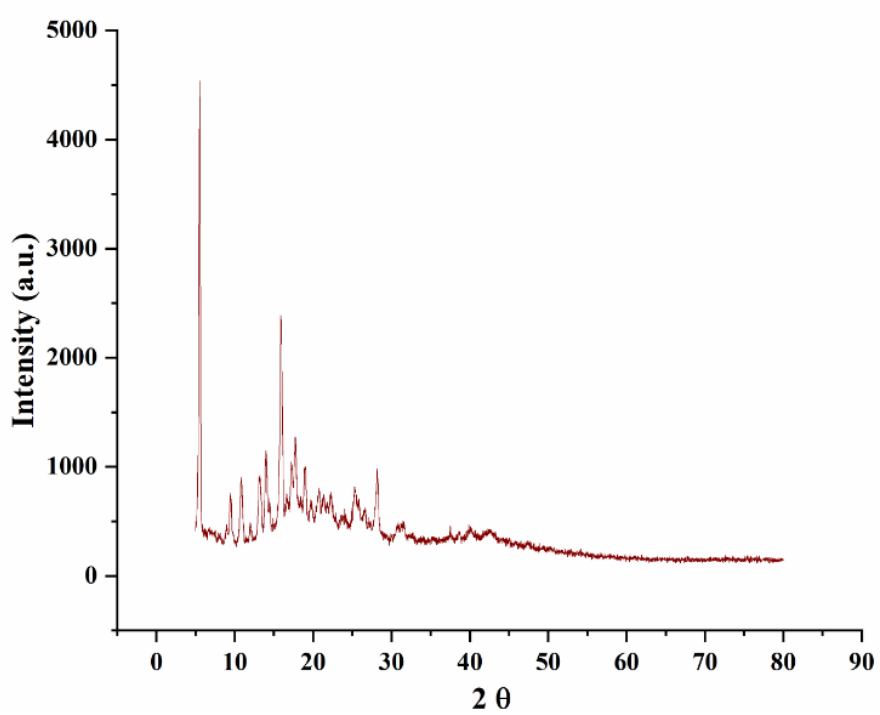

Figure 4.23: X-ray diffraction spectrum of optimized formulation (formulation BDT-10) (f).

4.3.3. Thermogravimetric analysis

Thermogravimetric analysis (TGA) is a method used to measure the change in mass of a sample because of temperature or time. The delta Y is used as a representation of weight loss. The berberine HCl drug showed weight loss because of the water decomposition at three stages near 100, 180, and above 280 °C (Figure 4.24) (Xiao *et al.,* 2020). The diacerein showed weight loss above at 250 °C because of the water decomposition (Figure 4.25). There was no peak development observed in phosphatidylcholine (Figure 4.26) while sodium deoxycholate showed a peak near 350°C (Figure 4.27). However, the berberine HCl and diacerein physical mixture depicted no temperature change but showed weight loss near 100 and above 200 °C, respectively. This weight loss occurred because of the methoxy group slow elimination (Figure 4.28) (Guan *et al.,* 2020). The optimized dual drug-loaded formulation showed weight loss because of berberine HCl and diacerein entrapment in phospholipid layers and water loss (Figure 4.29) (Mishra *et al.,* 2022).

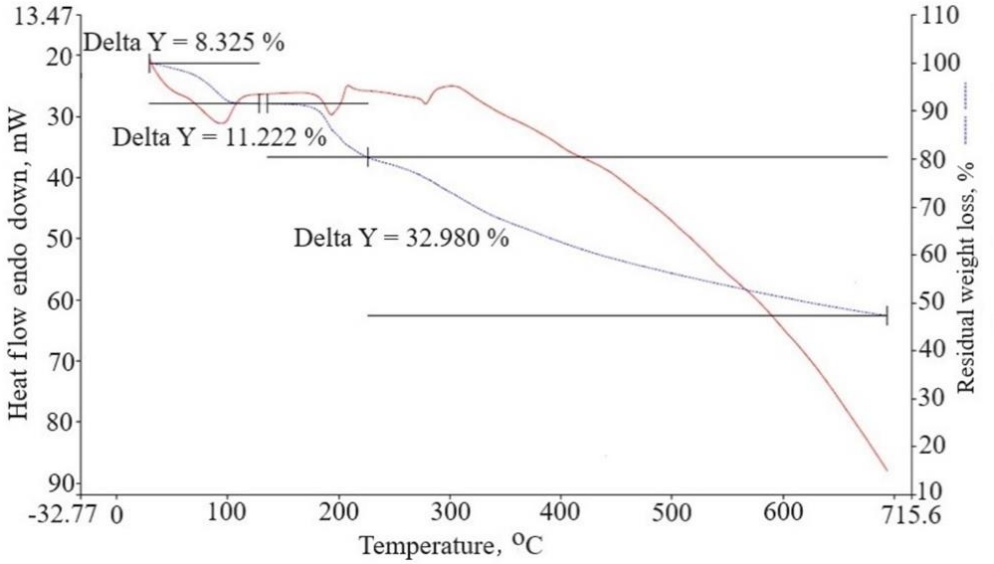

Figure 4.24: Thermogravimetric spectrum of berberine HCl. The curve representing Delta Y indicates residual weight loss.

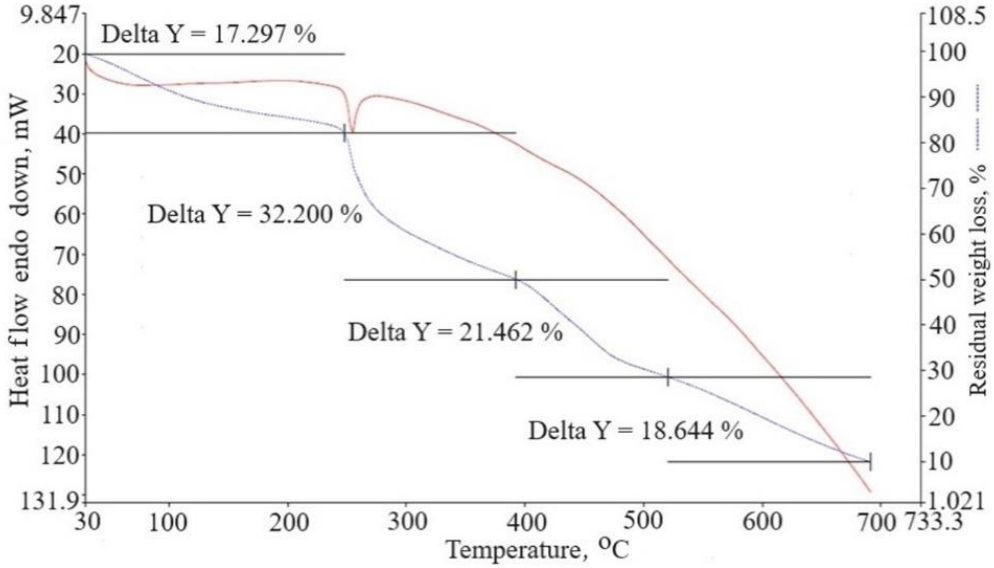

Figure 4.25: Thermogravimetric spectrum of diacerein. The curve representing Delta Y indicates residual weight loss.

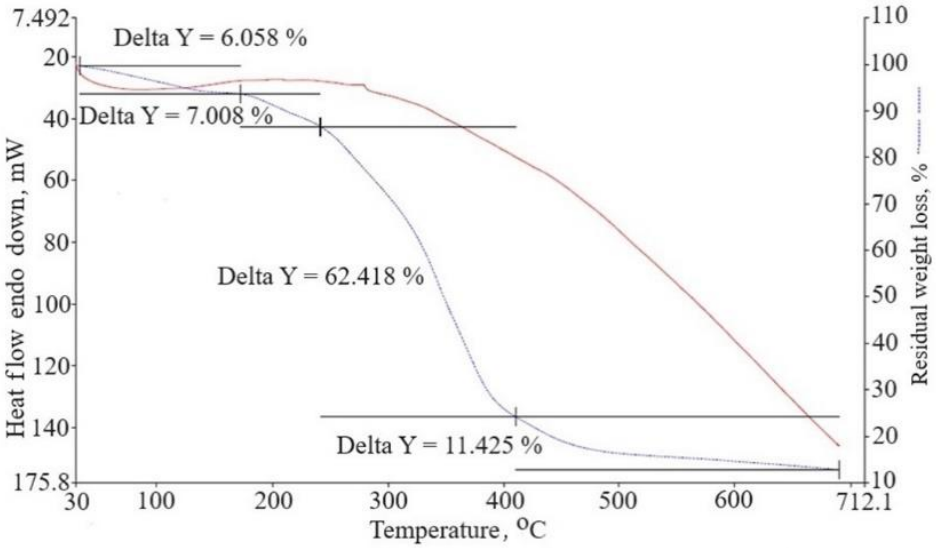

Figure 4.26: Thermogravimetric spectrum of phosphatidylcholine. The curve representing Delta Y indicates residual weight loss.

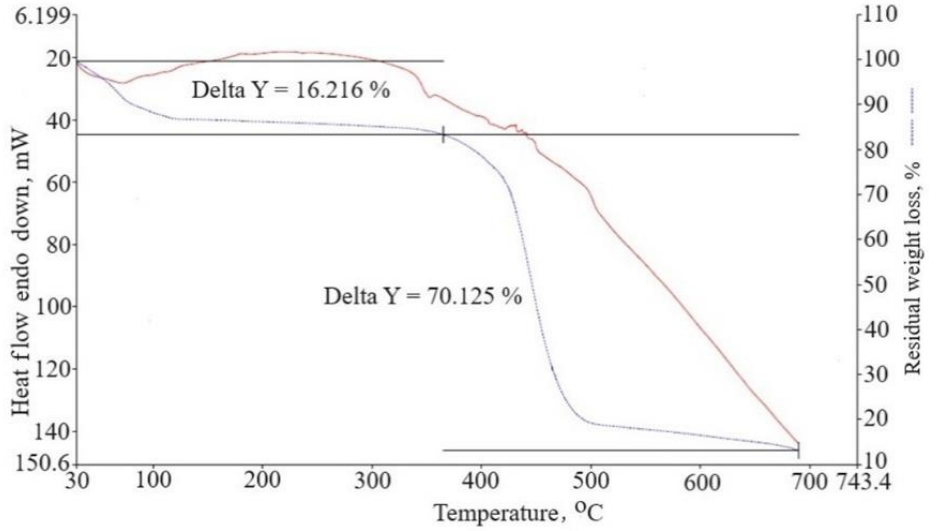

Figure 4.27: Thermogravimetric spectrum of sodium deoxycholate. The curve representing Delta Y indicates residual weight loss.

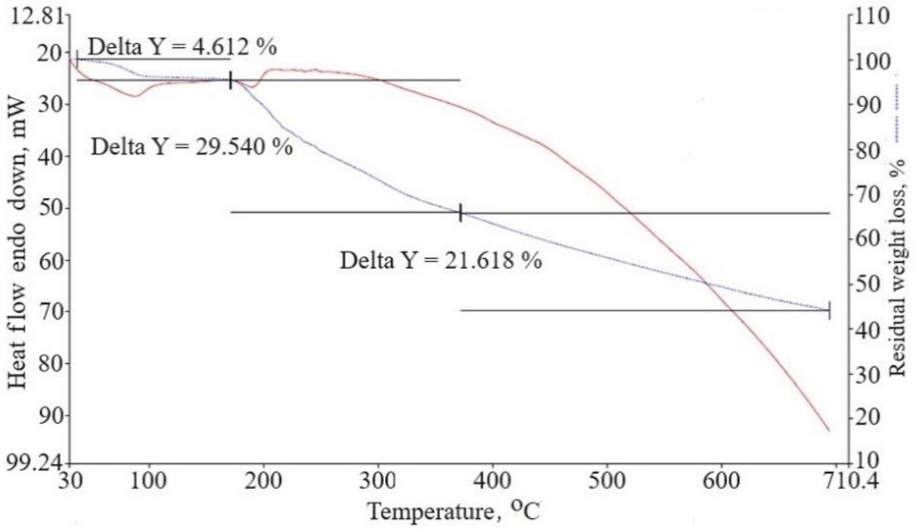

Figure 4.28: Thermogravimetric spectrum of physical mixture of berberine HCl and diacerein. The curve representing Delta Y indicates residual weight loss.

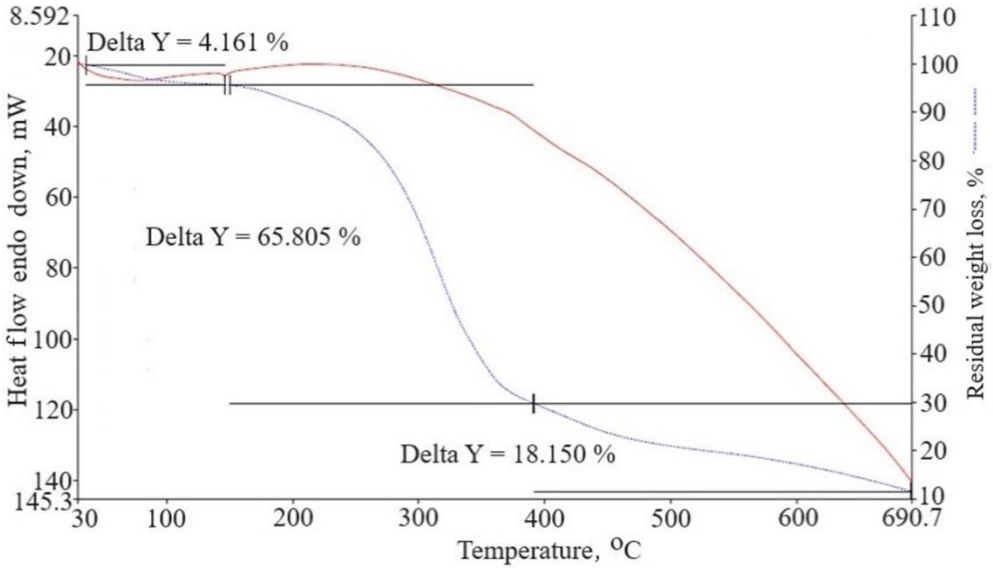

Figure 4.29: Thermogravimetric spectrum of optimized formulation (formulation BDT-10). The curve representing Delta Y indicates residual weight loss.

4.3.4. Vesicle size, polydispersity index, and zeta potential

A total of 13 transferosome formulations loaded with diacerein and berberine HCl were developed and optimized using Box-Behnken design. The developed transferosomes had PDI ranged from 0.244 ± 0.014 to 0.452 ± 0.008 and particle size ranged from 86.98 ± 2.4 to 121.45 ± 9.22 nm. The optimized formulation

showed a zeta potential of -13.3±0.6 mV (Figure 4.30), a PDI of 0.296, and a particle size of 110.9 ± 2.8 nm (Figure 4.31). The particle size directly affects the colloidal stability and cellular absorption, while the PDI controls the size distribution. Particles of a size of less than 300 nm can be easily deposited into the epidermis and dermis layers of the skin, and they may even be able to reach the sub-dermis layer in transdermal delivery. The particles within the 10-210 nm size range can pass via the transfollicular route, and those less than 7 nm can pass through the lipid transepidermal route. When the PDI value is greater than 0.7, it signifies that the system has an unacceptable variety of particle sizes that are more widespread. Because the PDI values for vesicular nanoparticles are lower than 0.3, this indicates that the system is homogeneous with less aggregation (Danaei *et al.,* 2018; Liu *et al.,* 2018; Dhavale *et al.,* 2021).

Transferosomes have deformable and flexible features because of the presence of an edge activator. The edge activator destabilizes lipid bilayers and provides transferosomes with squeezing properties. The reduction in particle size observed when sodium deoxycholate interacts with lipid layers can be attributed to its negative charge. By measuring the zeta potential of a nanoparticle system, the stability of the system can be identified. The repulsive energy between particles causes the electrostatic repulsion, and this potential provides information on the surface charge. The increase in colloidal electrostatic repulsion occurs because of the dominance of Van der Waals forces that lead to system stability. There are several factors, such as flocculation, particle distribution, and accumulation, that affect the zeta potential. The presence of electrostatic repulsion in vesicular structures made up of anionic surfactants shows less particle aggregation. The zeta potential displayed by transferosomes is constant within the range of +30 to -30 mV (Dhavale *et al.,* 2021; Ansari *et al.,* 2022). Our findings revealed that the optimized formulation (formulation BDT-10) demonstrated a uniform size distribution, favorable stability, and no aggregation, suggesting its potential to enhance skin permeability.

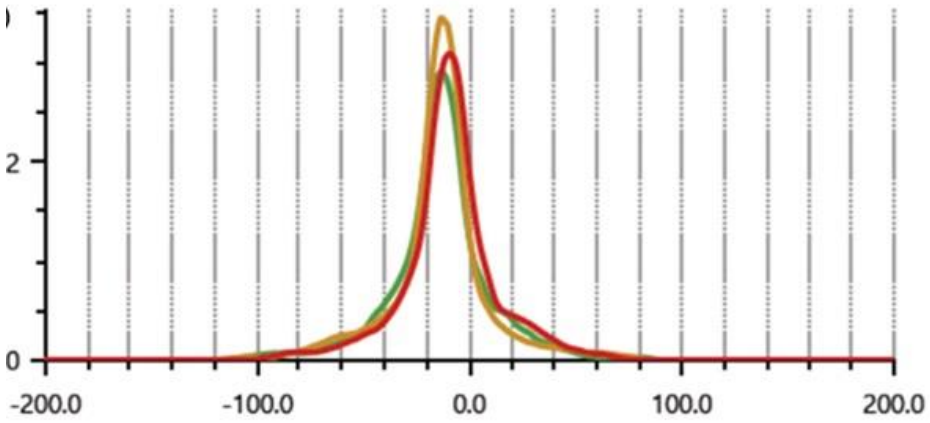

Figure 4.30. Zeta potential analysis of optimized formulation (formulation BDT-10).

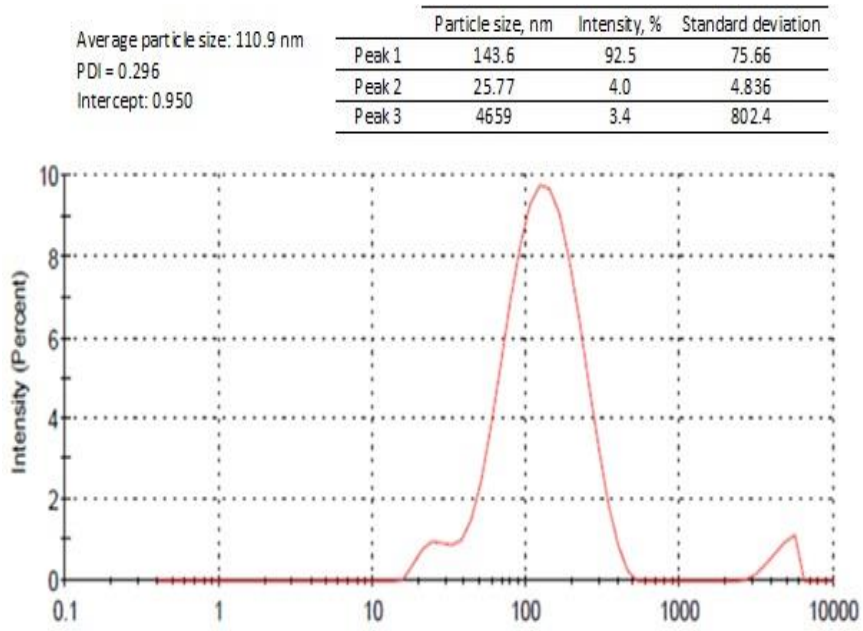

Figure 4.31. Particle size distribution and PDI of optimized formulation (Formulation BDT-10).

4.3.5. Entrapment efficiency and drug loading

The entrapment efficiency and drug loading depend upon independent factors like phosphatidylcholine, sodium deoxycholate, and sonication time and dependent factors like particle size, morphology, particle aggregation, etc. The entrapment efficiency of berberine HCl was found between 59.24 ± 1.5 to 89.50 ± 1.5% and diacerein was found between 61.15 ± 1.4 to 91.23 ± 1.8 % in

transferosome formulations. The drug loading of berberine HCl was found between 12.04 ± 0.02 to 19.41 ± 0.47% and diacerein drug loading was found between 14.40 ± 0.07 to 21.91 ± 0.05% in transferosome formulations. The optimized formulation BDT-10 exhibited berberine HCl and diacerein encapsulation efficiency of 89.50 ± 1.5 and 91.23 ± 1.8, respectively, and percentage drug loading of berberine HCl and diacerein was found to be 19.41 ± 0.47 and 21.91 ± 0.05, respectively. It has been reported that higher concentrations of phospholipids lead to less encapsulation. The high concentration of sodium deoxycholate reduced the berberine HCl encapsulation efficiency and enhanced diacerein encapsulation efficiency. The berberine encapsulation efficiency was reduced due to an increment of vesicle membrane permeability while diacerein encapsulation efficiency was found high because increased surfactant concentration produced a large number of vesicles that developed more hydrophobic bilayer region for hydrophobic drugs accommodation (Ahad *et al.,* 2012; Shaji *et al.,* 2014; Bnyan *et al.,* 2018; Opatha *et al.,* 2020).

4.3.6. Determination of deformability

The deformability of the transferosomes depends upon the edge activator that destabilizes phospholipids bilayers. This deformability feature of transferosomes allows them to pass through the stratum corneum by squeezing process. After squeezing, they can even reform themselves and deliver the drugs to the disease site. Moreover, surfactant charge also affects the transferosome features. The transferosome formulations exhibited deformability between 7.43 ± 0.04 to 14.51 ± 0.12% (Table 2). The optimized transferosome formulation BDT-10 showed 12.44 ± 0.39% deformability. It is clearly indicated that sodium deoxycholate amount affect the lipid bilayers and provides flexibility and squeezing properties to transferosomes without any rupturing in topical delivery (Shuwaili *et al.,* 2016).

4.3.7. Morphological characterization

The nanoparticle penetration and drug delivery to skin either topical or transdermal delivery depends upon its shape. Some factors like surface area, penetration depth, adhesion and retention of nanoparticles affect topical and transdermal delivery. The spherical and round-shaped nanoparticles can smoothly endocytose compared to other shape nanoparticles like nanorods. The cells cannot do endocytosis because of cell's inability to start actin-dependent membrane kinetics. It has been reported that clathrin-mediated endocytosis is highly susceptible in taken-up spherical shape nanoparticles (Yusuf *et al.*, 2023).

The optimized formulation BDT-10 depicted the spherical shape of the transferosomes in HRTEM images without any aggregation (Figure 4.32). The transferosomes particle size was found to be near the DLS result and can recommended for topical delivery. However, there is no strong relationship between the DLS results and HRTEM analysis. DLS is intensity intensity-dependent process and operates on the Brownian motion principle, whereas TEM is a number-dependent process in which image formation is a consequence of the electron flux passing through the sample. Moreover, DLS calculates the hydrodynamic diameter and due to hydrating layers formation around the particles, particle size depicts larger. But TEM discloses particles projected surface area.

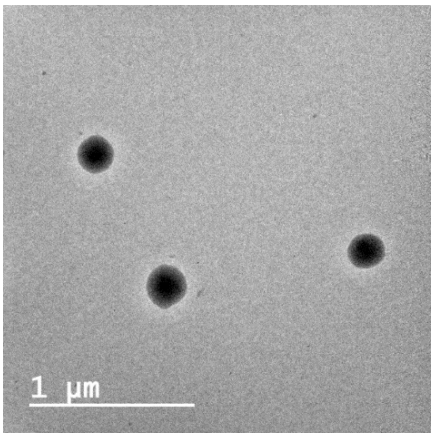

Figure 4.32: TEM image of diacerein and berberine HCl-loaded optimized transferosomes (formulation BDT-10).

The study of material structure is mostly done by using the SAED (selected area electron diffraction). SAED analysis discloses the crystallinity of drug molecules loaded in the nanoparticles. The formation of the diffused rings in SAED indicates that loaded molecule is crystalline. There were no diffused rings depicted by optimized formulation in the SAED pattern which confirms loaded drugs are not in crystalline form (not on a larger scale) (Figure 4.33).

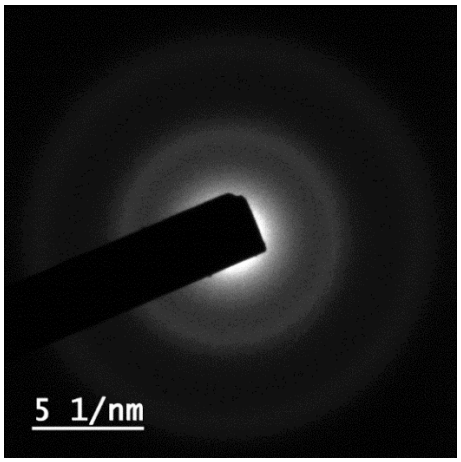

Figure 4.33: Selected area electron diffraction (SAED) image of diacerein and berberine HCl-loaded optimized transferosomes (formulation BDT-10).

Atomic force microscopy (AFM) has been used for the examination and interpretation of surface topography data obtained from both two-dimensional (2D) and three-dimensional (3D) views. The rough surface nanoparticles have high cellular uptake because rough surface offers a large surface area. This large surface area strongly interacts with cells due to more contact points. High rough surface also enhances cell adhesions that also improvise cellular uptake via endocytosis (Balata *et al.*, 2020; Kim *et al.*, 2021). The optimized formulation (formulation BDT-10) had average roughness (Ra) values of 5.43 nm and root mean square (Rq) values of 6.58 nm (Figure 4.34).

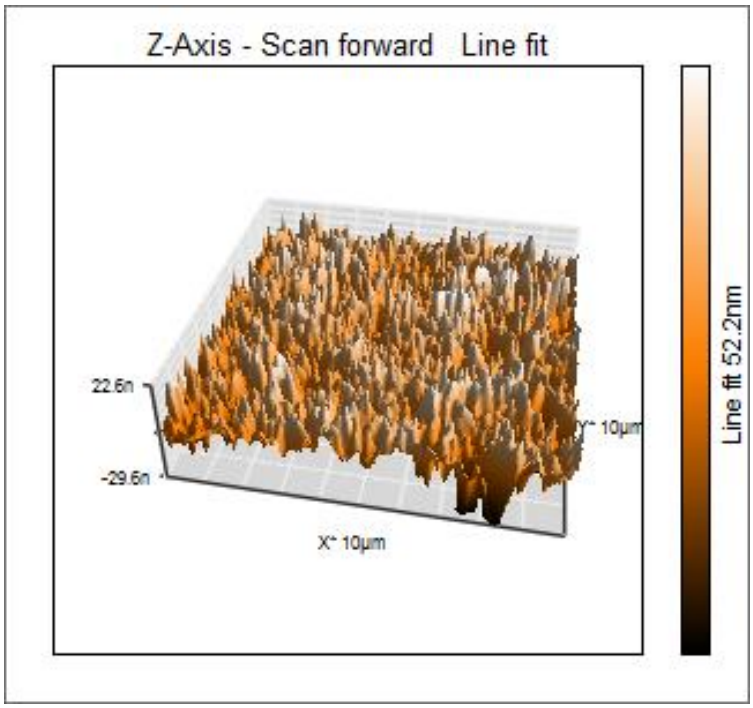

Figure 4.34: AFM image of diacerein and berberine HCl-loaded optimized transferosomes (formulation BDT-10).

4.3.8. *In vitro* release study and release kinetics

The optimized formulation (formulation BDT-10) was used to study the extended release of diacerein and berberine HCl in phosphate buffer (pH 7.4). The investigation was conducted by employing a dialysis membrane for a duration of 24 hours, which facilitated the comprehension of the mechanism of drug release. The optimized formulation exhibited a release (Figure 4.35) of 82.09 ± 0.81% of berberine HCl after 18 hours and 90.54 ± 0.21% after 24 hours. Additionally, diacerein shown a release of 85.02 ± 3.81% after 18 hours and 98.73 ± 3.21% after 24 hours. The study concluded that the optimized formulation exhibited a prolonged release of loaded bioactives, which can potentially improve the effectiveness of both the loaded drugs.

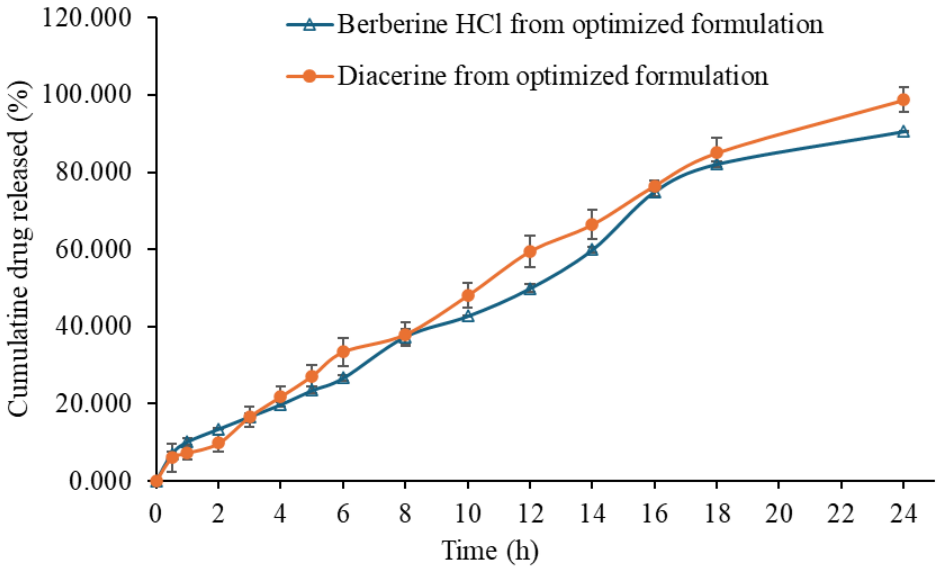

Figure 4.35: Release profile of diacerein and berberine HCl from the optimized transferosomes (formulation BDT-10) in phosphate buffer (pH 7.4). Data presents mean ± SD, n = 3.

The most suitable kinetic model was selected based on its superior goodness of fit, as evidenced by the highest r^2 value. Zero-order kinetics best described the release characteristics of diacerein and berberine HCl from optimized transferosomes, as demonstrated by the high r^2 values of 0.9901 and 0.9850, respectively. Higuchi's correlation and linearity coefficient findings indicate that the drug release profiles are diffusion controlled. Peppas' model shows that the optimized formulation had a strong correlation with both berberine HCl (r^2 0.9834) and diacerein (r^2 0.9893). This theory suggests that when the value of n is 0.43, the release of the drug is controlled by Fickian diffusion. Drug release is governed by non-Fickian (anomalous) diffusion when the value of n falls within the range of 0.43 to 0.85. In Case II transport mechanism is best described when the value of n is 0.85, indicating expansion of polymer matrix. Super-case II transport mechanism describes the release of drugs when the value of n exceeds 0.85. The investigation found berberine HCl (n value 0.6987) and diacerein (n value 0.8010), with n values ranging from 0.43 to 0.85. This indicates that the loaded drugs in the developed optimized transferosomes (formulation BDT-10) exhibited anomalous (non-Fickian) diffusion (Table 4.5).

Table 4.5: Results of kinetic modelling of diacerein and berberine HCl release data from optimized transferosomes (formulation BDT-10) in phosphate buffer (pH 7.4).

Kinetic model	Diacerein		Berberine HCl	
	R	k	R	K
Zero order	0.9901	0.0767	0.9850	0.0710
T-test	25.378	(Passes)	20.606	(Passes)
First order	0.8831	-0.0019	0.9591	-0.0014
T-test	6.786	(Passes)	12.224	(Passes)
Korsmeyer-Peppas' model*	0.9893	0.2890	0.9834	0.5171
T-test	24.400	(Passes)	19.559	(Passes)
Higuchi's model	0.9461	2.2013	0.9407	2.0391
T-test	10.530	(Passes)	10.002	(Passes)
Hixson Crowell model	0.9688	-0.0004	0.9825	-0.0004
T-test	14.094	(Passes)	19.034	(Passes)

*n value of diacerein berberine HCl and are 0.8010 and 0.6987, respectively.

4.3.9. Antioxidant activity

The imbalance among body oxidants and anti-oxidant molecules leads to the formation of oxidative stress. This oxidative stress is further responsible for ROS (reactive oxygen species) generation. These ROS play a major role in psoriasis pathogenesis due to their significant effect on autophagy, apoptosis, and regeneration process (Plenkowska *et al.*, 2020). It has been documented that berberine HCl and diacerein have anti-oxidant properties and can also scavenge the ROS (Abd-Ellatif *et al.*, 2019; Wang *et al.*, 2023). Even these therapeutic molecules have concentration-dependent manner property in suppression of ROS activity. Both berberine HCl and diacerein have high phenolic groups in their structure and can easily donate electrons that provide scavenging properties to them (Chukwuma *et al.*, 2023). Moreover, berberine HCl has

potential to elevate the level of natural anti-oxidants that form inside body like catalase, glutathione peroxidase, and superoxide dismutase, and also suppress the level of glutathione and malondialdehyde oxidative stress markers (Ghavipanje *et al.,* 2023). The optimized formulation showed an IC_{50} value of 36.42 μg mL^{-1} in reference to ascorbic acid which depicted IC_{50} value of 14.2 ± 0.1 μg mL^{-1}.

4.3.10. *Ex vivo* permeation studies

The pig ear skin was used for *ex vivo* permeation studies for a duration of 6 hours using the Franz diffusion assembly. According to the guidelines set by the OECD, pig skin is considered the most suitable substitute for human skin and is commonly used in *in vitro* studies for topical delivery (OECD EN/JM/MONO(2011)36). The optimized formulation demonstrated a cumulative drug permeation of 10.41 μg cm^{-2} for diacerein and 7.286 μg cm^{-2} for berberine HCl. The flux observed for diacerein and berberine HCl was 0.0462 μg cm^{-2} h^{-1} and 0.0224 μg cm^{-2} h^{-1}, respectively. Furthermore, the permeation coefficient (Kp) for diacerein and berberine HCl was determined to be 4.62 cm h^{-1} and 2.24 cm h^{-1}, respectively (Figure 4.36).

Results indicate that both the deformability characteristic and the driving force of the osmotic gradient play a significant role in facilitating the penetration of transferosomes through the skin (Guillot *et al.*, 2023). Transferosomes are required to traverse the stratum corneum, and drug partitioning occurs between the stratum corneum and the lipid portion of nanocarriers (Dhavale *et al.*, 2021). Intercellular lipid destabilization and the improvement of stratum corneum fluidity are additional factors contributing to elevated skin permeation (Zeb *et al.*, 2016).

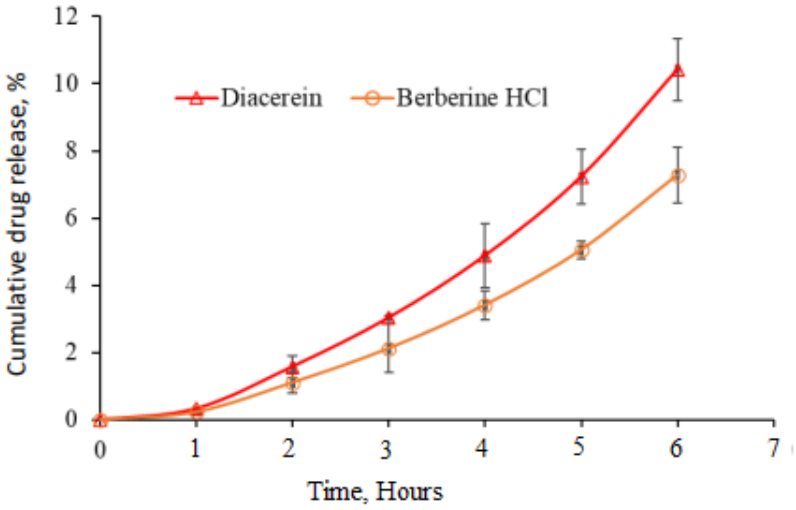

Figure 4.36: *Ex vivo* permeation study results in pig skin (n = 3, mean ± SD).

4.3.11. Raman analysis

Raman spectra were utilized to ascertain the vibrational modes that are active in the target species. This investigation involved acquiring and comparing the Raman spectra of untreated pig ear skin, the optimized formulation, and pig ear skin treated with the optimized formulation. Raman signal can overlap and interfere due to the presence of chemicals. These compounds can generate intense fluorescence signals. This phenomenon is especially evident in intricate surroundings, such as the skin, where melanin effectively absorbs visible light. Based on the aforementioned point, samples were subjected to the experimental investigation at a wavelength of 785 nm, which falls within the near infrared area. At this wavelength, the fluorescence intensity significantly drops, facilitating the precise identification of peaks corresponding to Raman-active vibrational modes (Gomez *et al.*, 2023). The optimized formulation showed a C=O peak at 1710 cm^{-1}, which was expanded and displaced due to the presence of hydrogen bonding. NH group exhibited a peak at 3152 cm^{-1}, while OH group showed a peak at 3318 cm^{-1}. Furthermore, the Raman spectra of optimized formulation treated pig skin indicated the presence of C=O functional group at 1714 cm^{-1}. This functional group exhibited broadening and shifting due to H-bonding, which was observed at 3154 cm^{-1} in the NH group and at 3326 cm^{-1} in the OH group, respectively (Figure 4.37). Optimized transferosome effectively

penetrated stratum corneum without causing any rupture due to its deformability. Raman spectroscopy analysis detected a reddish area in the pig skin, which can be attributed to the presence of erythrocytes and other blood components (Figure 4.38A). The optimized transferosomes successfully penetrated pig skin and were visually confirmed by their yellowish appearance (Figure 4.38B). Furthermore, the spectrum of the optimized formulation and pig skin treated with the optimized formulation exhibited G-band and D-band peaks at 1548 cm^{-1} and 1322 cm^{-1}, respectively.

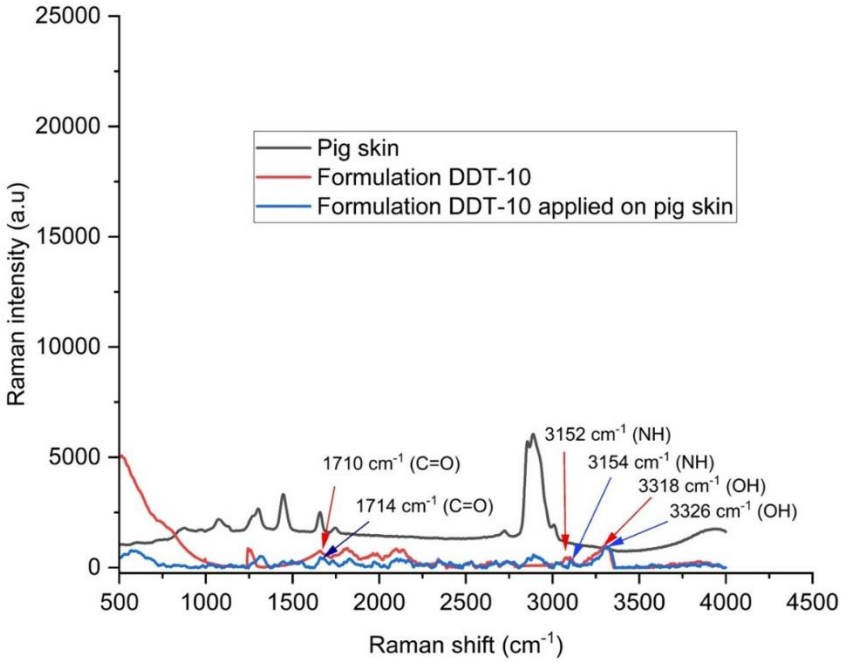

Figure 4.37: Raman spectra of treated pig skin with optimized formulation (formulation BDT-10).

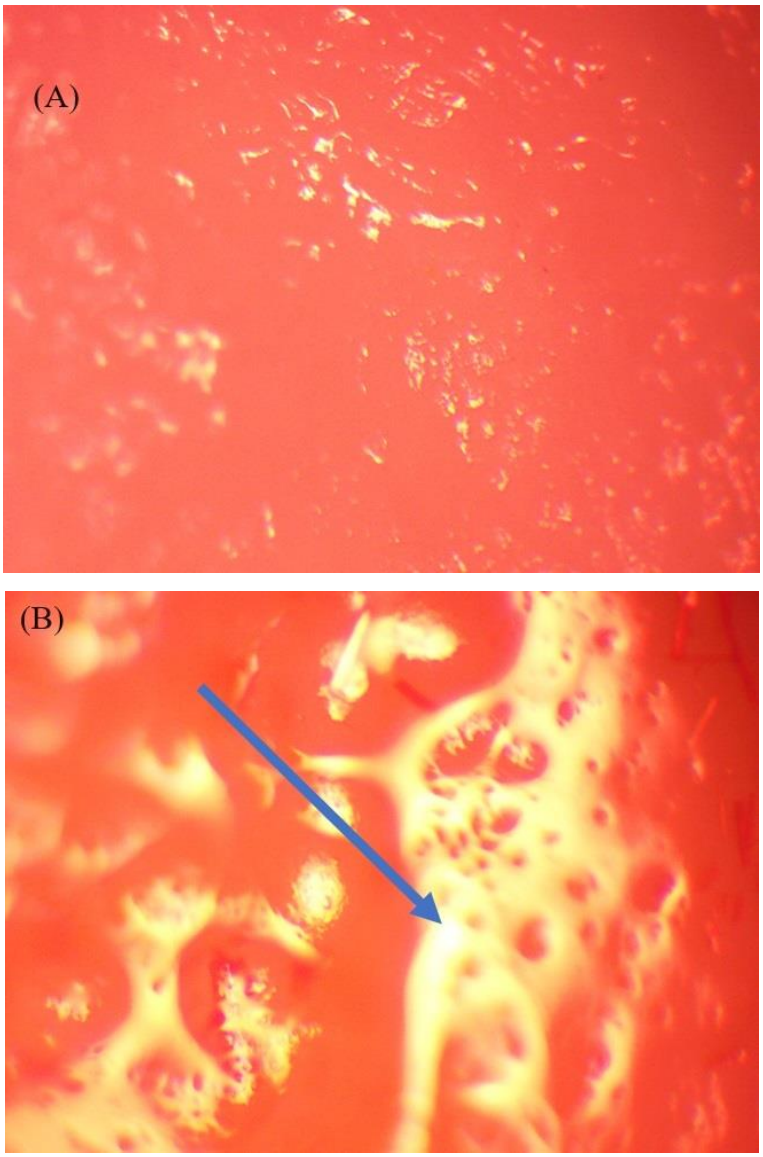

Figure 4.38: Results of Raman analysis: image of blank pig skin (A) and image of pig skin treated with optimized formulation (formulation BDT-10) (B).

4.3.12. Skin irritation test

Diacerein and berberine HCl-loaded optimized formulation (formulation BDT-10) did not exhibit any irritation in the skin of male BALB/c mice model (Figure 4.39) and no redness was observed in the erythema scores (Table 4.6). In summary, diacerein and berberine HCl-loaded optimized formulation was found safe and can be used for topical application.

Table 4.6. Results of erythema scores after application of normal saline and optimized transferosomes (formulation BDT-10) to the depilated dorsal skin of imiquimod-induced psoriatic BALB/c mice.

Day	Normal saline (Reference)	Formulation BDT-10 (Optimized formulation)
1	0	0
2	0	0
3	1	1
4	2	1
5	3	0
6	4	0
7	4	0

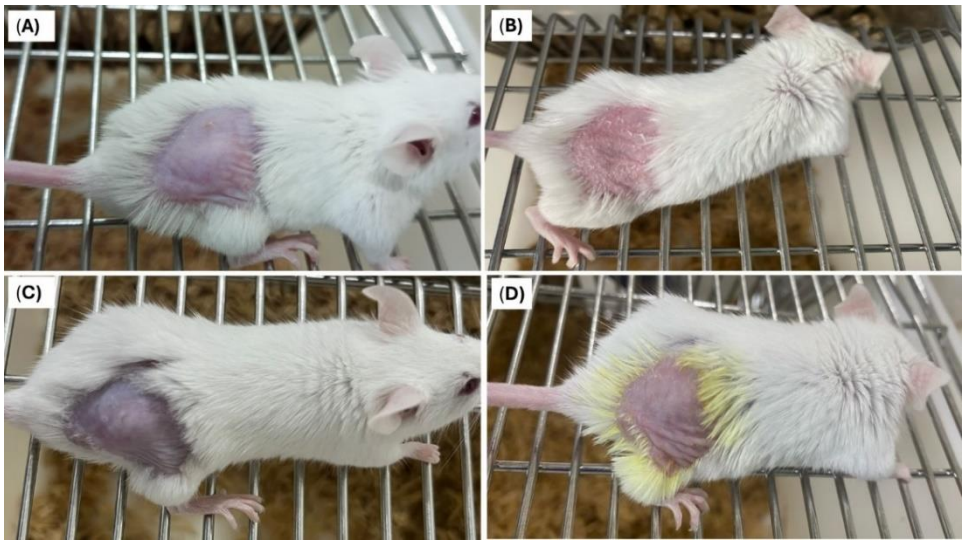

Figure 4.39: Results of skin irritation study in male BALB/c mice treated with Imiquad® cream. Image A and C depict mice treated with Imiquad® cream on day 0. Image B exhibits clear indications of change and redness in psoriatic mice that were treated with saline on the seventh day. Image D exhibits the absence of irritation or redness in psoriatic mice that were treated with optimized transferosomes on the seventh day.

4.3.13. Stability study

The optimized formulation (formulation BDT-10) did not exhibit any change in its physical appearance. No alteration in morphology (Figure 4.40 and Figure

4.41) was recorded at 4 °C and 25±2 °C. At the end of the 3-month stability study, the zeta potential values were within the acceptable range of ±30 mV (*i.e.*, -25.4±1.8 mV at 4 °C and -27.3±0.4 mV at 25±2 °C) (Figure 4.42 and Figure 4.43). No significant change in particle size was recorded at 4 °C (111.9 nm with 0.295 PDI) and 25±2 °C (114.1 with 0.292 PDI) (Figure 4.42 and Figure 4.43). This confirmed that there was no aggregation in the developed colloidal system. In the case of formulation stored at 4 °C, the entrapment efficiency of diacerein and berberine HCl was found to be 89.89±1.2% and 88.86±1.3%, respectively. In case of the formulation stored at 25±2 °C, the entrapment efficiency of diacerein and berberine HCl was found to be 89.06±0.6% and 88.11±1.4%, respectively. These entrapment efficiency results confirmed no drug leaching under both storage conditions.

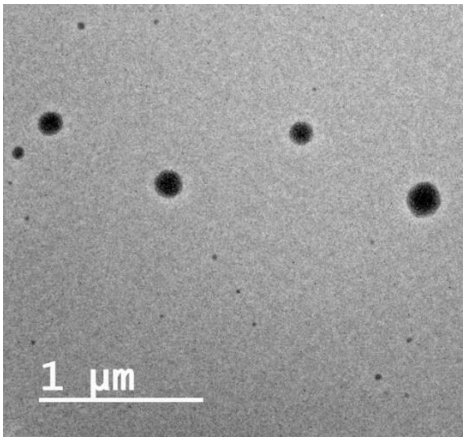

Figure 4.40: TEM image of optimized transferosomes (formulation BDT-10) stored at 4±1 °C for 3 months.

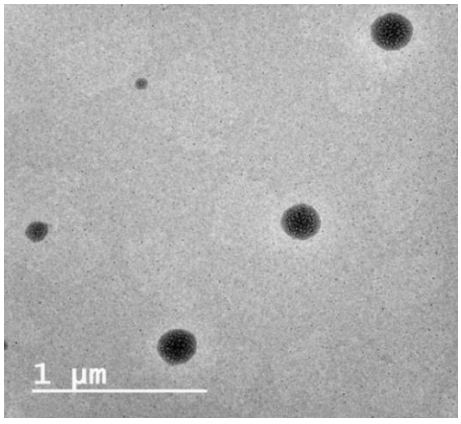

Figure 4.41: TEM image of the optimized transferosomes (formulation BDT-10) stored at 25±2 °C/ 60±5 % RH stored for 3 months.

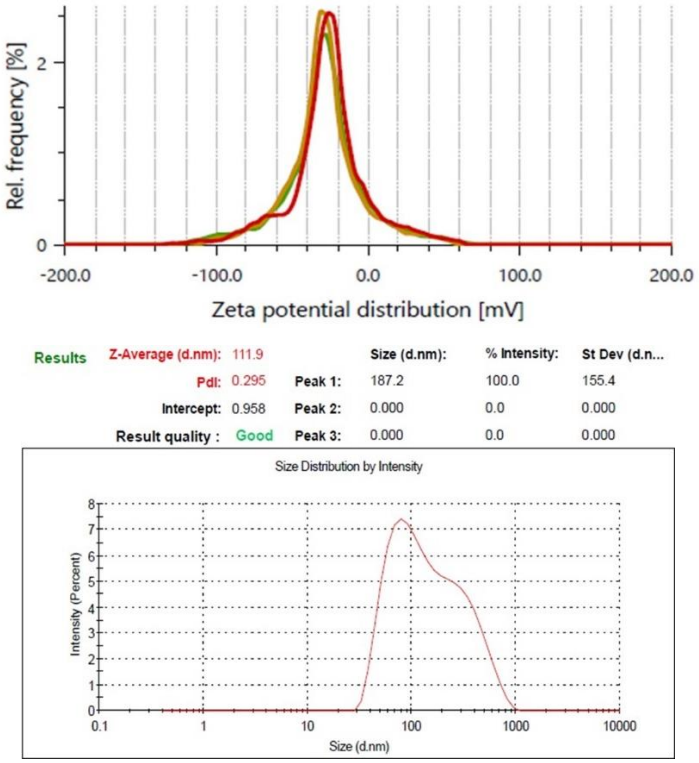

Figure 4.42: Zeta potential and particle size distribution results of optimized transferosomes (formulation BDT-10) stored for 3 months at 4±1 °C.

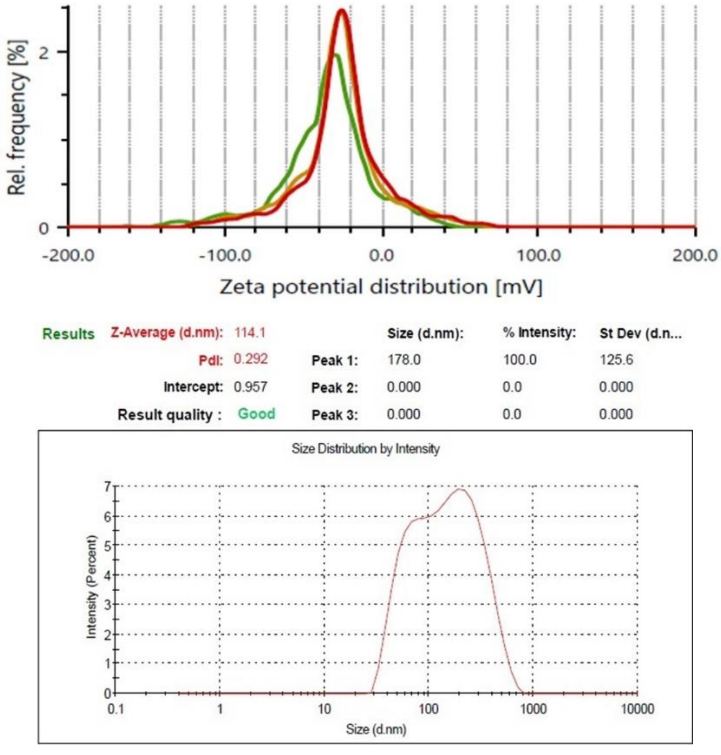

Figure 4.43: Zeta potential and particle size distribution results of optimized transferosomes (formulation BDT-10) stored at 25±2 °C/ 60±5 % RH for 3 months.

4.3.14. *In vitro* cytotoxicity of transferosomes

HaCaT cell lines are immortalized keratinocytes derived from human skin. The cytotoxic effect of optimized formulation was examined on HaCaT cell line via an MTT assay method. This assay determines cell viability by detecting mitochondrial enzymes in live cells. This enzyme reduces MTT dye into formazan crystals (purple color). The formation of formazan crystals is directly proportional to the viability of the cells, which is measured by an ELISA plate reader. Different concentrations (0.78, 1.56, 3.125, 6.25, 12.5, 25, and 50 µL/mL) of the optimized formulation were subjected to HaCaT cell lines for 24 hours for cytotoxicity analysis. The transferosomal formulation depicted an IC_{50} value that did not converge even at the highest treated concentration (50 µL/mL). Moreover, it was found that all tested concentrations did not significantly decrease cell viability (Figure 4.44).

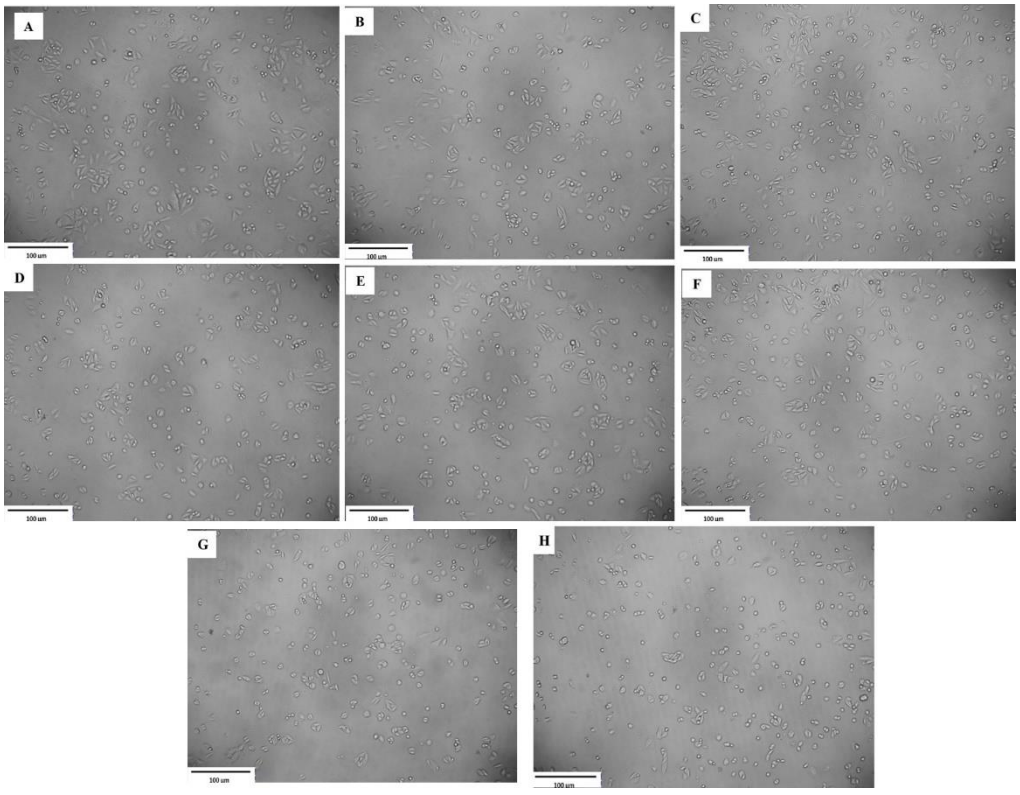

Figure 4.44: Results of cytotoxicity studies treated with optimized formulations at different concentrations: control (A), 0.78 µL/mL (B), 1.56 µL/mL (C), 3.125 µL/mL (D), 6.25 µL/mL (E), 12.5 µL/mL (F), 25 µL/mL (G), and 50 (H).

4.4. *IN VITRO* EVALUATION OF OPTIMIZED TRANSFEROSOMES LOADED GEL

4.4.1. Determination of optimized transferosomes loaded gel pH

The pH range of normal skin lies between 4 to 6 (Tsegay *et al.*, 2023). Dual delivery transferosomal gel formulation (BDTG) exhibited a pH of around 5.4±0.4 with a homogenous appearance. Formulation BTG and DTG exhibited a pH value of 5.5±1.2 and 5.5±1.8, respectively, with a homogenous appearance. Thus, the pH of hydrogel formulations (formulation BDTG, BTG, and DTG) are acceptable for topical delivery.

4.4.2. Rheological study

Rheological studies of transferosomes-loaded hydrogel formulations (formulation BDTG, BTG, and DTG) were carried to explore the rheological behavior of topical gel. Rheological behaviour of topical hydrogel formulations is associated with its spreadability and its contact time with the skin surface. In the present study, all the hydrogel formulations exhibited non-Newtonian properties, which was confirmed from a plot between shear rate (s-1) against shear pressure (Pa). The hydrogel formulation exhibited a pseudoplastic tendency, which is suitable for use in dermatological therapy since the limitation of formulation flow must be kept to a minimum when the gels are delivered under conditions of moderate to high shear (Figure 4.45).

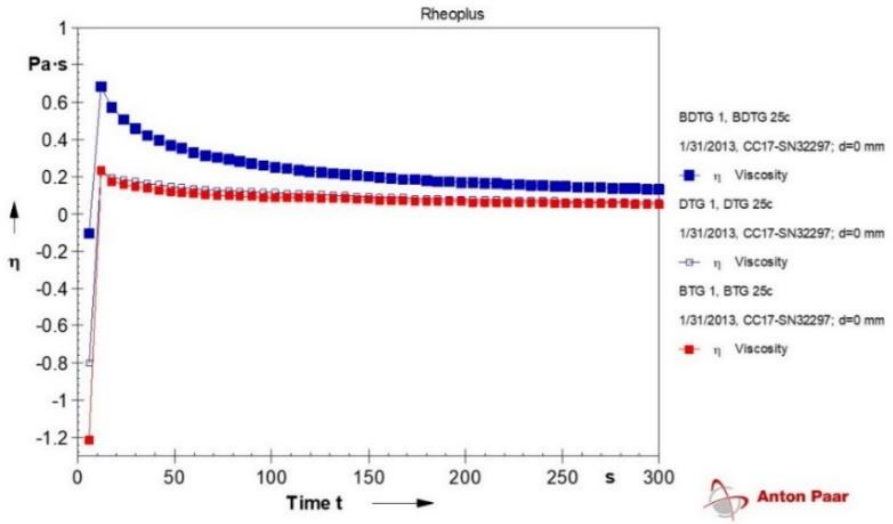

Figure 4.45. Shear stress *versus* shear rate results of optimized transferosomal hydrogels formulation.

Viscosity of the transferosomal hydrogel formulation decreased with an increase in shear rate (Figure 4.46). This means that hydrogel formulations (formulation BTG, DTG, and BDTG) demonstrated the shear-thinning process. The topical gel should exhibit this pseudoplastic behavior because it facilitates gel application to the skin's surface. This enables even distribution of gels with reduced force, leading to enhanced application (Jain *et al.,* 2022).

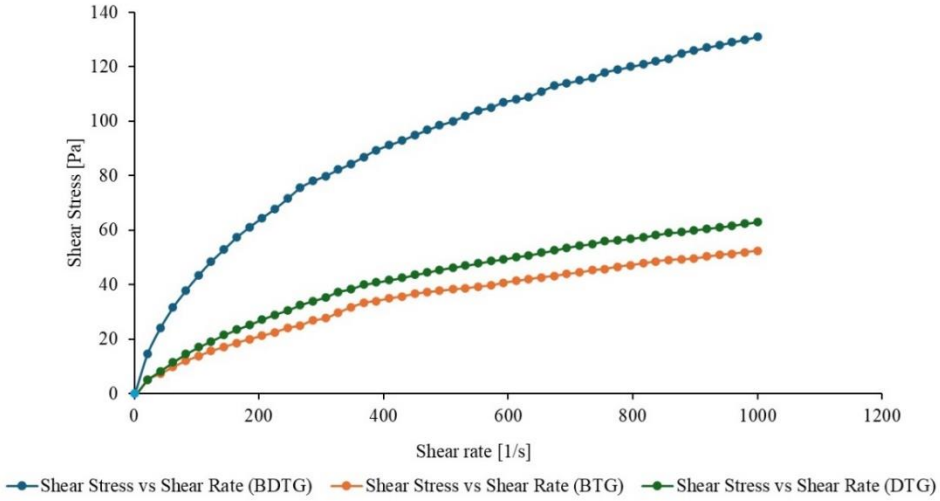

Figure 4.46. Results of rheological characterization of optimized transferosomal hydrogel formulation.

4.4.3. Spreadability

Spreadability experiment was conducted for transferosomal hydrogel formulations due to its significance in semisolid formulation. The spreadability values of transferosomal hydrogel formulations (formulation BTG, DTG, and BDTG) were determined to be 11.9 g cm sec^{-1}, 11.1 g cm sec^{-1}, and 9.8 g cm sec^{-1}, respectively. These values indicate that these formulations are suitable for topical application even under minimal stress (Figure 4.47). Furthermore, all the gel formulations can effortlessly disperse throughout the skin in a small amount. Gels possess a significant ability to spread, enabling them to adhere to and permeate the skin effortlessly. Additionally, this property makes gels suitable for the sustained release of drugs (Bonacucina *et al.,* 2004).

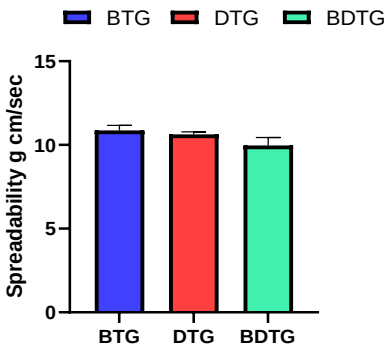

Figure 4.47: Spreadability profile of optimized transferosomal hydrogel (formulation BTG, DTG, and BDTG). n = 3, mean ± SD.

4.4.4. *In vitro* release study and release kinetics

The release profile of diacerein and berberine HCl from the transferosome-loaded hydrogel formulation (formulation BDTG) was investigated in phosphate buffer (pH 7.4) using a dialysis bag. The formulation showed 79.12±0.21 and 81.56±0.11% of berberine HCl released after 18 h and 24 h, respectively. Additionally, 82.45±2.41% and 88.44±2.11% of diacerein was released after 18 h and 24 h, respectively. The release data revealed that the transferosome-loaded hydrogel formulation demonstrated a sustained drug release profile for both the loaded bioactives, which can potentially enhance drug efficacy (Figure 4.48).

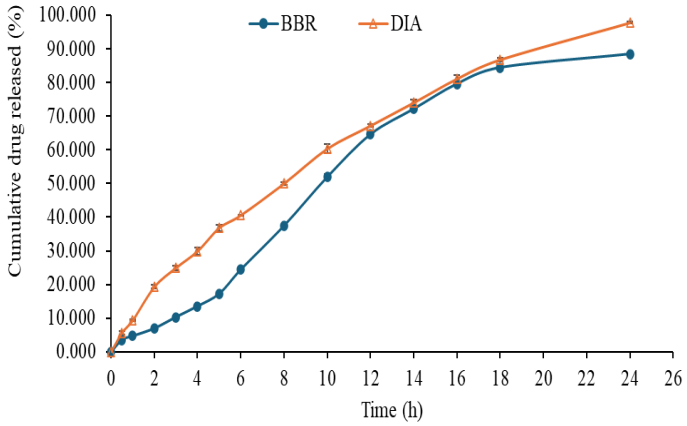

Figure 4.48: Release profile of diacerein and berberine HCl from the optimized transferosome-loaded hydrogel formulation (formulation BDTG) in phosphate buffer (pH 7.4). n = 3, Mean ± SD.

In this study, zero-order kinetics best explained the release features of diacerein and berberine HCl from transferosomal hydrogel formulation, with r^2 values of 0.9743 and 0.9496, respectively. Higuchi's plot indicated diffusion-controlled drug release profiles. In case of Peppas' model, transferosomes-loaded gel (formulation BDTG) exhibited linearity for both diacerein (r^2 = 0.9968, n = 0.7497) and berberine HCl (r^2 = 0.9810, n = 0.9766). The n values of $0.43 < n < 0.85$ shows anomalous (non-Fickian) diffusion of payloads (Table 4.7).

Table 4.7. Results of kinetic modelling of diacerein and berberine HCl release data from optimized transferosomes loaded hydrogel (formulation BDTG) in phosphate buffer (pH 7.4).

Kinetic model	**Diacerein**		**Berberine HCl**	
	R	**k**	**R**	**k**
Zero order	0.9496	0.0830	0.9743	0.0748
T-test	10.922	(Passes)	15.608	(Passes)
First order	0.9492	-0.0020	0.9737	-0.0015
T-test	10.872	(Passes)	15.409	(Passes)
Higuchi's model	0.9806	2.4448	0.9129	2.1264
T-test	18.053	(Passes)	8.065	(Passes)
Korsmeyer-Peppas' model*	0.9968	0.4783	0.9810	0.0846
T-test	45.126	(Passes)	18.225	(Passes)
Hixson Crowell model	0.9952	-0.0005	0.9809	-0.0004
T-test	36.766	(Passes)	18.229	(Passes)

*n value of diacerein and berberine HCl are 0.7497 and 0.9766, respectively.

4.5 *IN VIVO* STUDIES

4.5.1. Anti-psoriatic activity in mice model

The psoriasis mouse model was developed using imiquimod, and the efficacy of the transferosomal gel was evaluated. IMQ causes hyperproliferation of keratinocyte and dendritic cells, develop psoriasis and other symptoms such as redness, swelling, and flaking skin. IMQ cream was applied for 6 days to the mice skin as part of this study. The induction of symptoms was observed on day three and continued to the sixth day. In addition, when psoriasis began to develop, the epidermal thickness gradually increased and showed erythema. The negative group and vehicle group showed significant scaling and inflammation. Additionally, the positive treated group (betamethasone) and the BDTG treatment group effectively reduced the scaling and erythema. These results indicated that dual delivery of diacerein berberine HCl reduces inflammation and erythema in psoriatic skin (Figure 4.49).

4.5.2. Psoriasis area and severity index

Psoriasis Assessment Scale (PASI) is a useful tool for assessing the efficacy of treatment and evaluating the progression of the disease at an early stage. The essential parameters, such as erythema and scaling, were graded on a scale of 0 to 4. After the second day of disease induction, mice skin showed changes in its morphology by indicating erythema and fine scaling. On the 6th day, the negative control group displayed intense erythema and scaling. Vehicle treated group displayed similar erythema and high PASI scores. All the treatment groups showed disease improvement in comparison to the negative group. Body mass was decreased in all groups except control group, with a stronger effect in the negative control group and vehicle group (Figure 4.50).

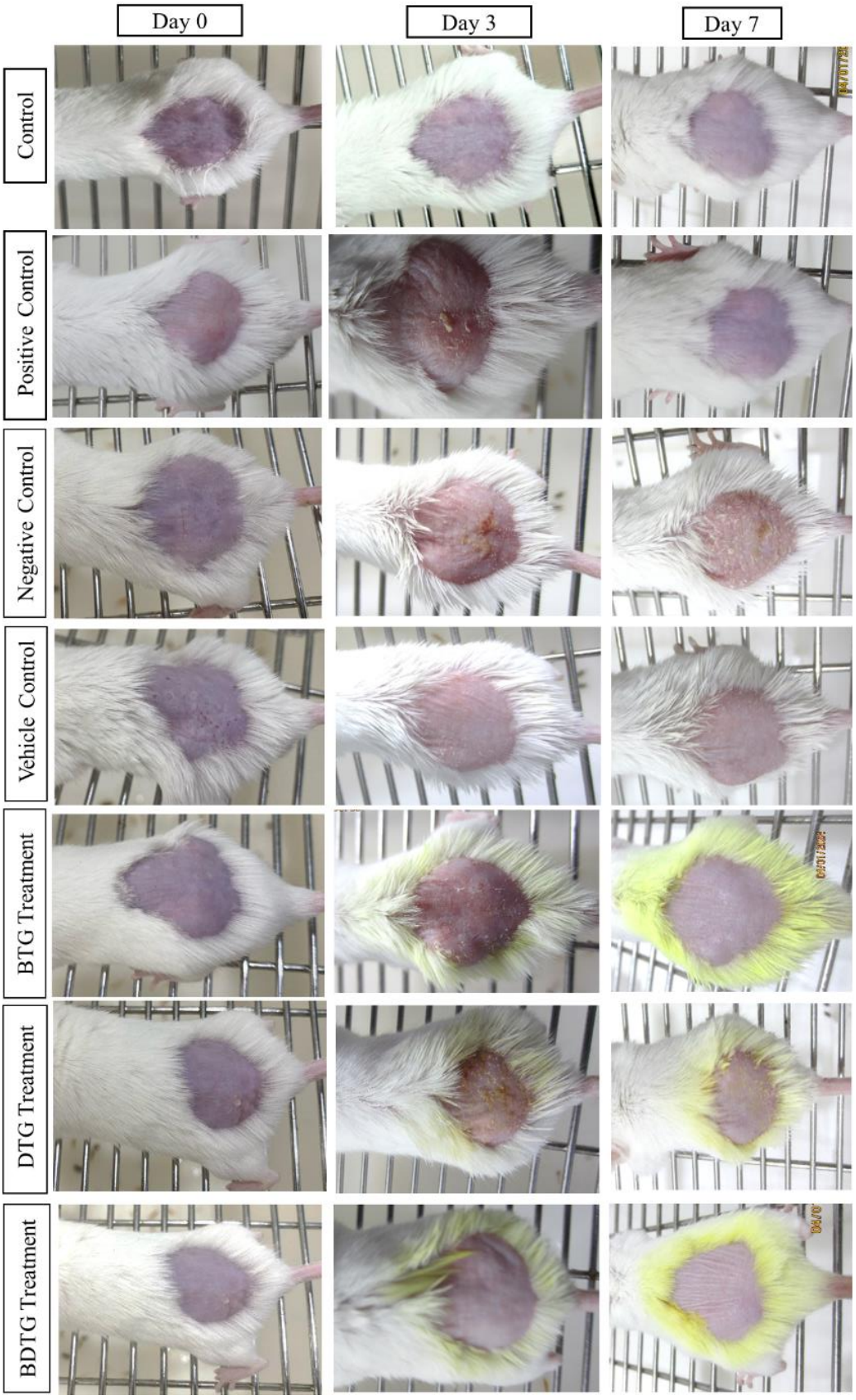

Figure 4.49. Phenotypic changes in the BALB/c mice during the experimental period and therapeutic effect of optimized transferosomal hydrogel formulation.

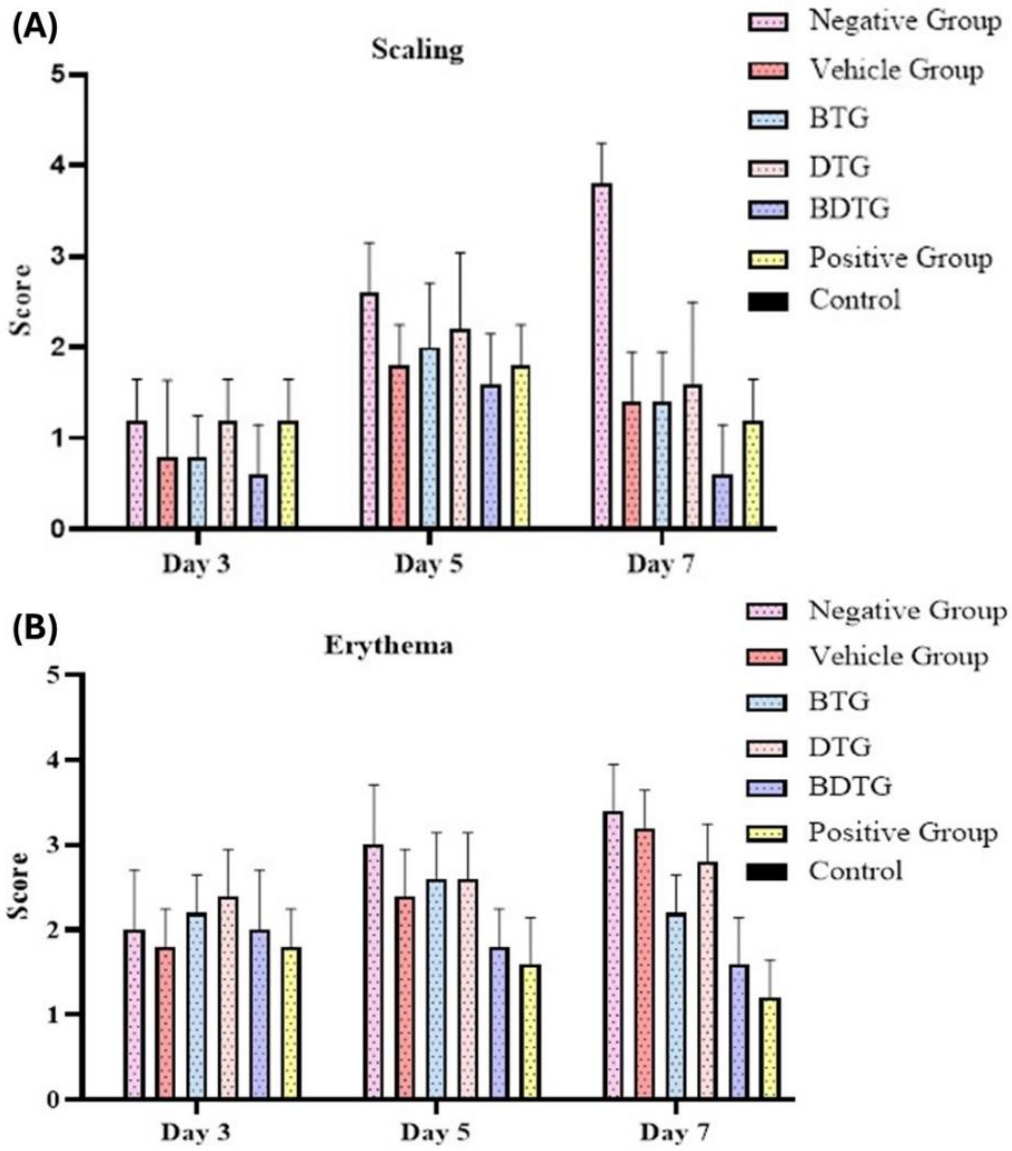

Figure 4.50. Results of Psoriasis Area and Severity Index: scaling (A) and erythema (B). n = 5, mean ± SD.

The body weight was measured in all groups during the study (Figure 4.51). The body weight was constantly increased in the control group from 0 to 6 days. Initially, the weight was slightly decreased in all groups except control group. From 4th to 6th day, the weight reduction was constantly observed in negative group and vehicle treated group. However, the weight was found increased in positive group (betamethasone treated), BTG, DTG, and BDTG treatment

groups from 4th to 6th day. Hence, the transferosomal loaded hydrogel formulation improved mice weight and depicted their therapeutic effectiveness.

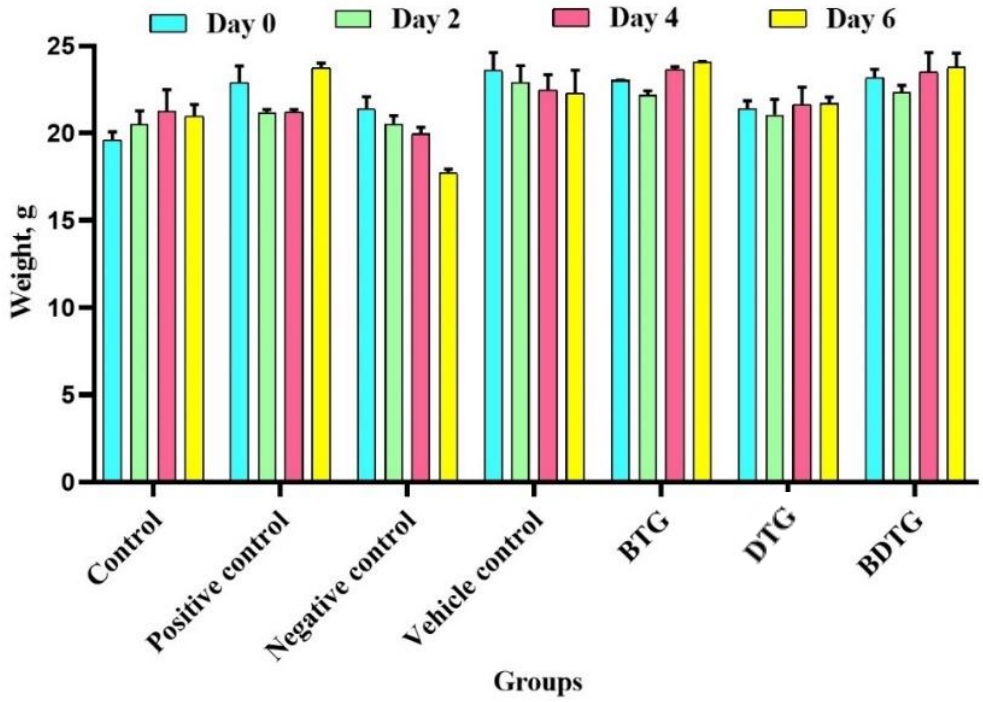

Figure 4.51. Effect of treatments on body weight of imiquimod induced psoriasis mice model. n = 5, mean ± SD.

The spleen is the primary immunological organ of the human body and plays an important role in iron recycling and blood cell homeostasis. The normal average size of a human spleen is 10 cm in length and 150 g in weight, but immune disease alters the size and weight of the spleen. This enlargement of the spleen is also known as splenomegaly. It has been reported that splenectomy is responsible for the IL-17A mRNA increment in the IMQ-treated mice skin. Moreover, several body cells, such as neutrophils, macrophages, B cells, dendritic cells, and pro-erythroblast increase, leading to a higher spleen weight (McKenzie *et al.*, 2018; Shinno-Hashimoto *et al.*, 2022). In our study, the spleen/body weight ratio was calculated by dividing the spleen weight (dry weight)/ body weight to assess the dynamic body changes. In comparison to the control group, the negative group showed a significant increase in the

spleen/body weight ratio (p = 0.0061). The vehicle treated group showed no significant difference in spleen/body weight ratio in comparison to the negative group (p = 0.9080). In both BTG and DTG formulation treatment, there was a reduction in the spleen/body weight ratio in the negative group, and the changes were non-significant (for the BTG treatment group, p = 0.1105; for the DTG treatment group, p = 0.0710). While formulation BDTG treated and positive control groups showed a significant reduction in spleen/body weight ratio in comparison to the negative group (formulation BDTG treatment group p = 0.0372 and positive group p = 0.0113) (Figure 4.52).

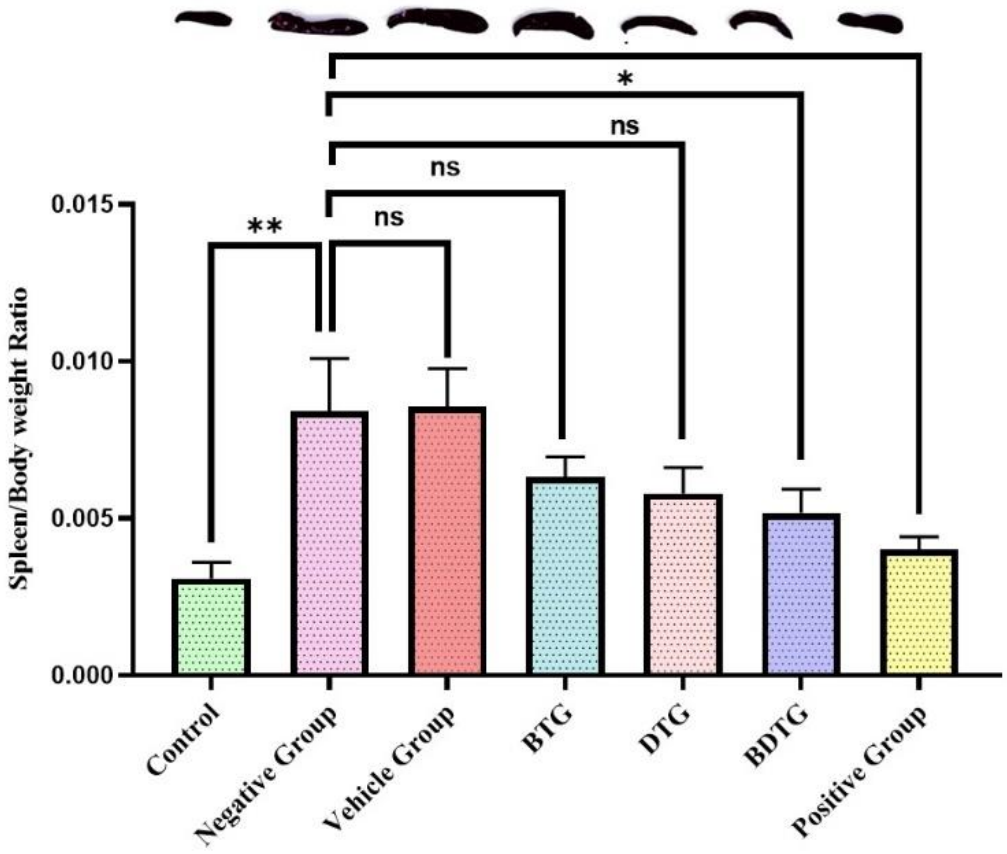

Figure 4.52. Results of spleen weight to body weight ratio in BALB/c mice model. n = 5, mean ± SD.

4.5.3. Histopathology of dorsal skin lesions and spleen

We carried out histopathological investigations in the dorsal section of skin samples to further confirm the anti-psoriatic effect of the optimized transferosomal formulation. The observations were done for architectural changes in the skin samples in various classified groups. The control group represented the normal skin epidermis and dermis. The negative control group represented psoriatic skin features such as hyperkeratosis (red arrow), acanthosis (yellow arrow), and inflammatory infiltrates (black arrow) (Figure 4.53), while the vehicle groups also displayed similar psoriatic skin features (Figure 4.54). In comparison to a negative group, the positive group depicted a reduction in epidermal thickness (Figure 4.53). In addition, the BTG and DTG also showed a reduction in epidermis thickness and acanthosis, respectively (Figure 4.54). The optimized formulation showed a better reduction of epidermal thickness in comparison to BTG and DTG (Figure 4.55).

These findings suggest that the developed formulation can effectively alleviate psoriatic symptoms in the IMQ-induced psoriatic animal model. The histology of the control spleen revealed white and red pulp, followed by a germinal center (Figure 4.56), indicating the effect on the spleen. The positive-treated group displayed a normal architecture (Figure 4.57). We observed white pulp hyperplasia and loss of germinal center in both the negative group (Figure 4.58) and the vehicle group (Figure 4.59). While the treatment groups BTG (Figure 4.60), DTG (Figure 4.61), and BDTG (Figure 4.62) demonstrated a reduction of pathological features as mentioned earlier (Abdel-Maged *et al.*, 2020).

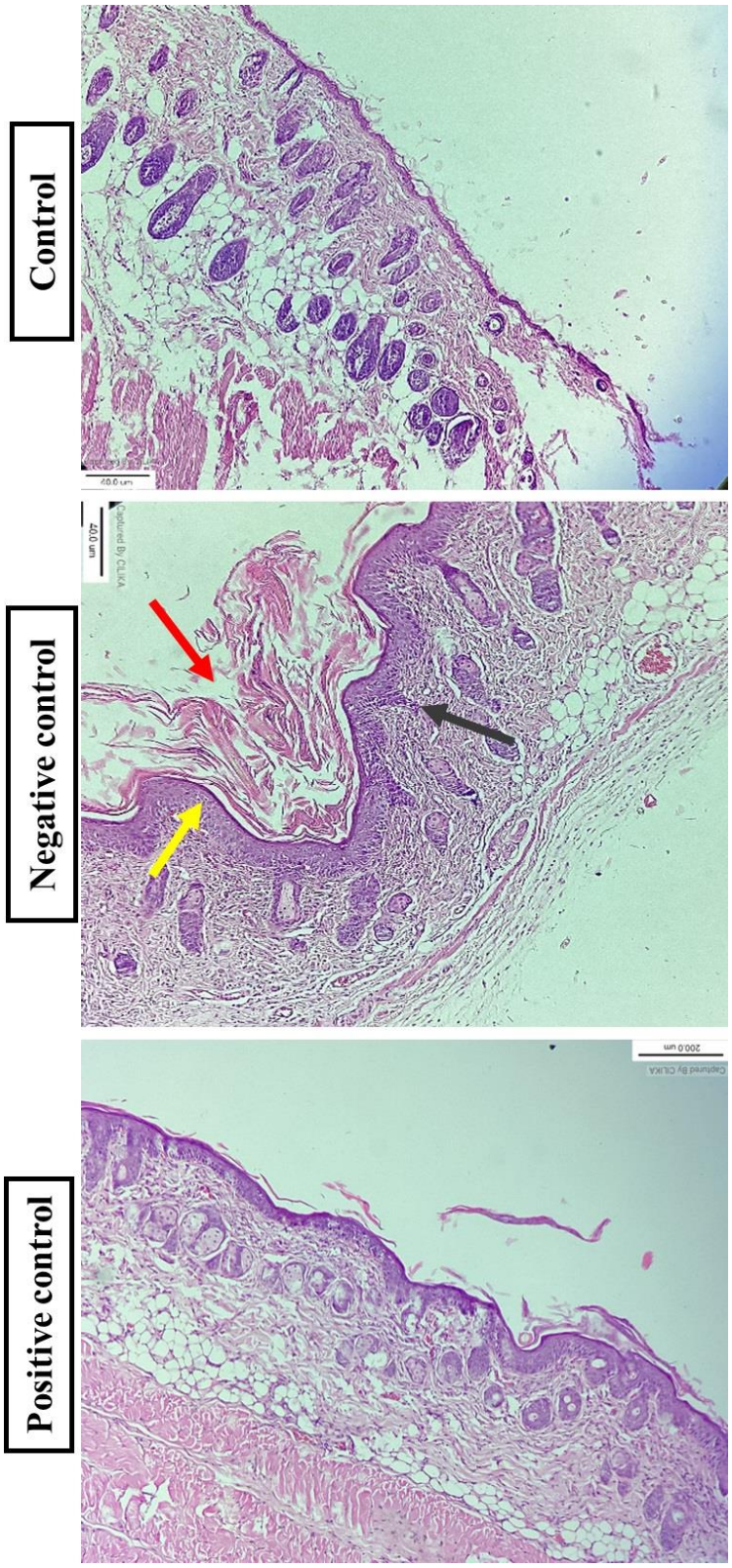

Figure 4.53. Histopathological features of hematoxylin and eosin stained IMQ-induced skin samples of psoriatic plaque BALB/c mice model (control, negative control, and positive control groups) (magnification 100X).

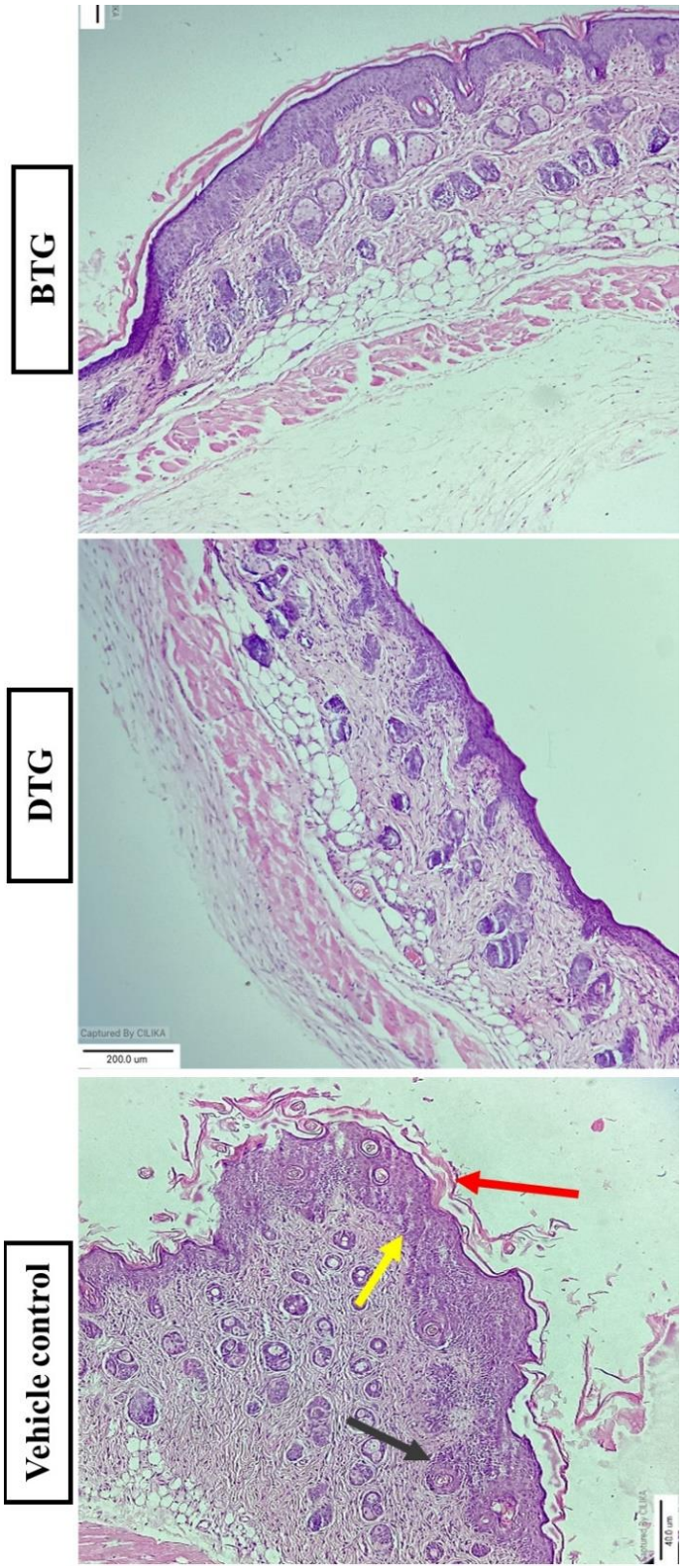

Figure 4.54. Histopathological features of hematoxylin and eosin stained IMQ-induced skin samples of psoriatic plaque BALB/c mice model (BTG treated, DTG treated, and vehicle control groups (magnification 100X).

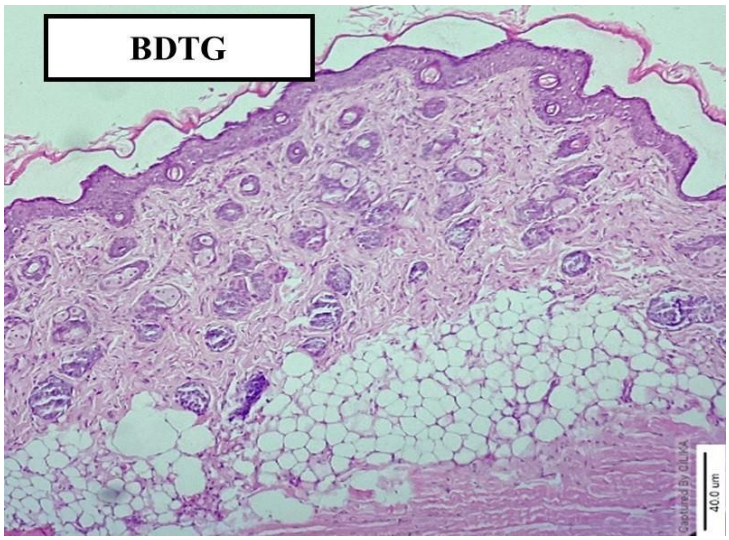

Figure 4.55. Histopathological features of hematoxylin and eosin stained IMQ-induced skin samples of psoriatic plaque BALB/c mice model (BDTG treated group) (magnification 100X).

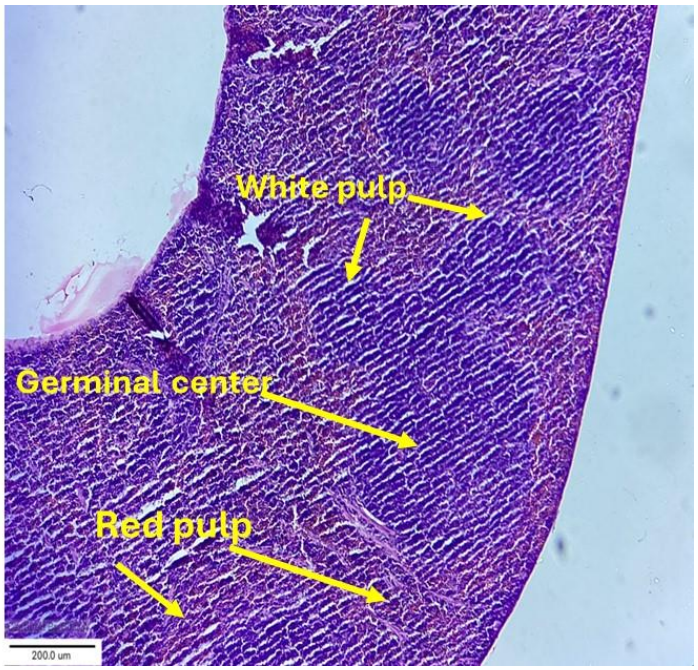

Figure 4.56. Histopathological features of hematoxylin and eosin stained IMQ-induced spleen of psoriatic plaque BALB/c mice model (control group) (magnification 100X).

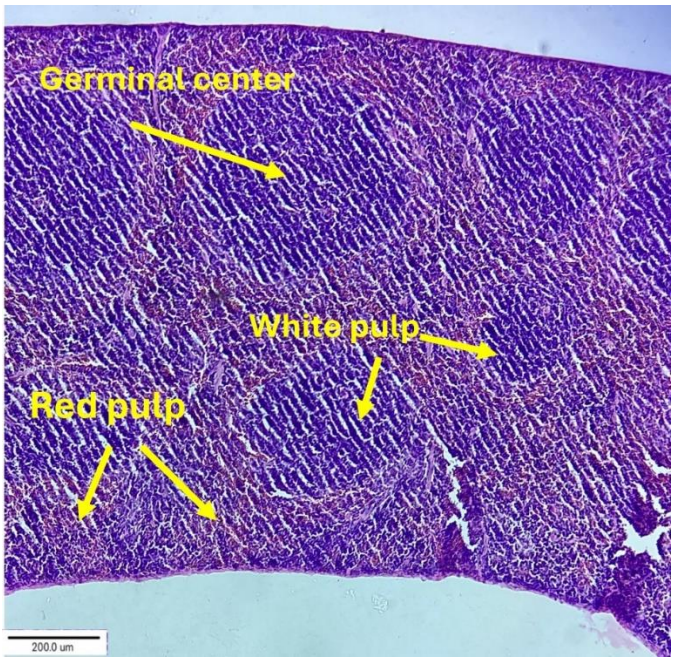

Figure 4.57. Histopathological features of hematoxylin and eosin stained IMQ-induced spleen of psoriatic plaque BALB/c mice model (positive control group) (magnification 100X).

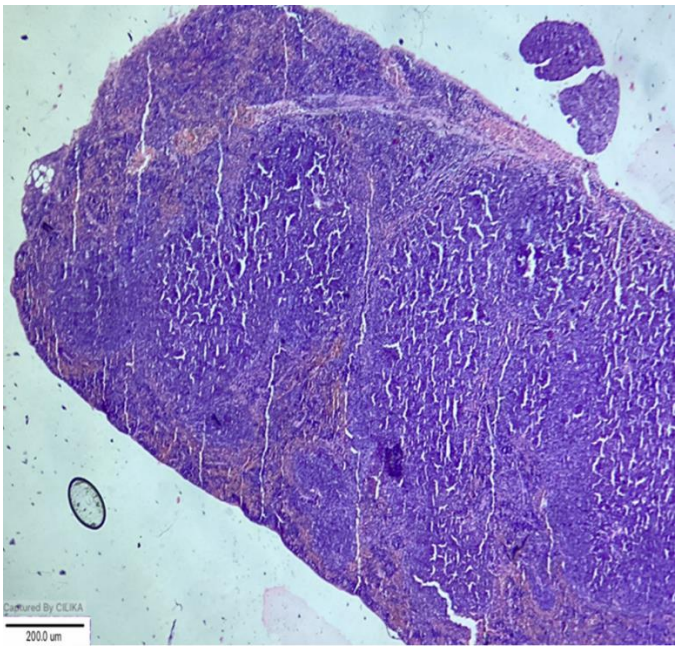

Figure 4.58. Histopathological features of hematoxylin and eosin stained IMQ-induced spleen of psoriatic plaque BALB/c mice model (negative control group) (magnification 100X).

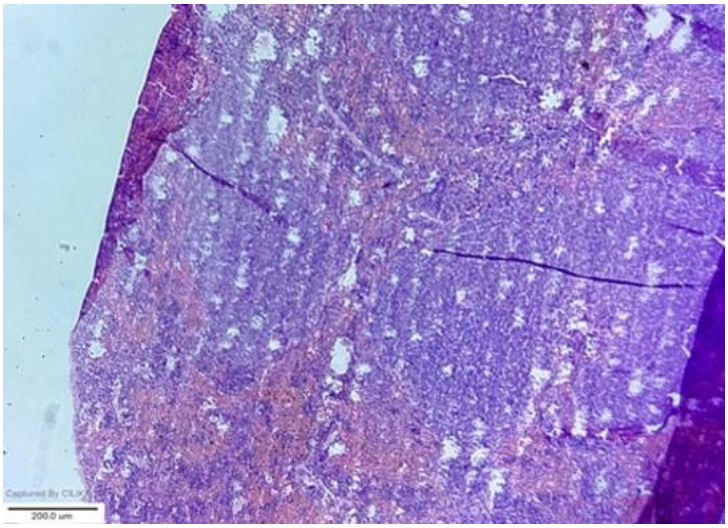

Figure 4.59. Histopathological features of hematoxylin and eosin stained IMQ-induced spleen of psoriatic plaque BALB/c mice model (vehicle control group) (magnification 100X).

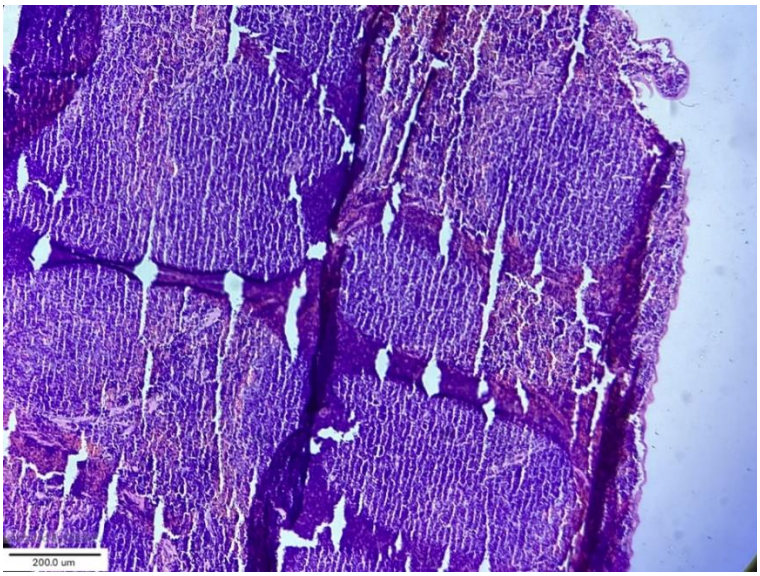

Figure 4.60. Histopathological features of hematoxylin and eosin stained IMQ-induced spleen of psoriatic plaque BALB/c mice model (formulation BTG treated group) (magnification 100X).

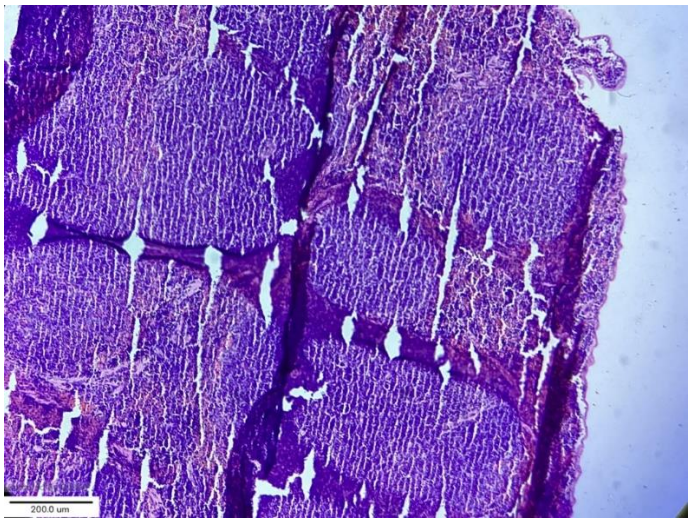

Figure 4.61. Histopathological features of hematoxylin and eosin stained IMQ-induced spleen of psoriatic plaque BALB/c mice model (formulation DTG treated group) (magnification 100X).

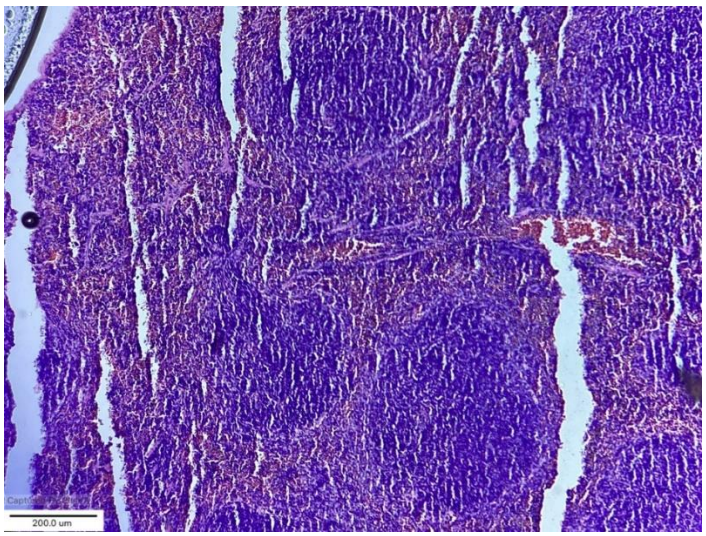

Figure 4.62. Histopathological features of hematoxylin and eosin stained IMQ-induced spleen of psoriatic plaque BALB/c mice model (formulation BDTG treated group) (magnification 100X).

4.5.4. Determination of cytokines using ELISA

Psoriasis is a multifactorial disease in which Th1 and Th17 cells play a major role and lead to the inflammation. These Th1 and Th17 cells are responsible for the release of the inflammatory cytokines IL-17, IL-22, IL-23, TNF-α, and IL-2. These cytokines stimulate keratinocyte hyperproliferation and inflammation.

Moreover, psoriasis is a complex process; apart from Th1 and Th17 cells, some other factors such as NF-kB, STAT, dendritic cells, neutrophils, mast cells, and endothelial cells contribute directly and indirectly to psoriatic inflammation. Macrophage has a powerful role in psoriasis because it is directly associated with TNF-α and regulates IL-17A secretion during disease progression. These macrophages accumulate in the psoriatic skin and release various cytokines.

Dendritic cells release cytokines and cause inflammation due to Toll-like receptor upregulation on their membrane. Imiquimod is a well-known drug that has been used for the treatment of solar keratosis, perianal warts, and genital warts. It has strong immune-stimulating properties. It is TLR7 and TLR8 agonist, and its topical delivery in mice develops psoriasis via the IL-23 and IL-17 cytokine axis, which is similar to human psoriasis.

TNF-α and IL-17A play a major role in the pathophysiology of psoriasis. TNF-α and IL-17A act synergistically in the hyperproliferation of keratinocytes, immune cell activation, and migration at the psoriatic lesions site, resulting in sustained chronic inflammation. Researchers have shown that targeting TNF-α and IL-17A subsides the psoriatic symptoms. Therefore, measuring TNF-α and IL-17A levels helps understand inflammatory conditions in psoriatic skin and determine the formulation's efficacy. A reduction in levels of these cytokines strongly shows that the formulated transferosomal gel was found effective in modulating the underlying immunopathogenesis of the psoriatic skin (Mosca *et al*., 2021, Leonardi *et al*., 2003).

The negative group exhibited a 4.74-fold higher TNF-α level in comparison to the control group. However, no significant difference was observed between the vehicle group and the negative group. Formulation BTG and DTG-treated groups alleviated TNF-α levels by 1.6 and 1.5 folds, respectively, in comparison to the negative group. Formulation BDTG treated group showed remarkable alleviation of TNF-α by 2.1 folds. The positive group (bethamethasonate)

reduced TNF-α by 2.3 folds in comparison to the negative control group. Result clearly signifies that diacerein and berberine HCl dual delivery transferosomes effectively reduced TNF-α levels in psoriatic mice (Figure 4.63).

Expression of IL-17A cytokine was not observed in the skin of the normal control mice. However, the negative control group showed a 6.0-fold increase in IL-17A levels compared to the control group. No significant difference was observed between the vehicle group and the negative control group. Formulation BTG and DTG treated groups reduced IL-17A levels by 2.9 and 2.0 times, respectively, relative to the negative group. Formulation BDTG treatment group exhibited a 5.45-fold decrease in IL-17A levels. Similarly, the positive treated group (betamethasone) showed a 6.6-fold decrease in IL-17A level compared to the negative group (Figure 4.63).

Statistical analysis revealed that the levels of TNF-α and IL-17A were much higher in the negative control group compared to the control group (p-value = 0.0075 less than 0.01 for TNF-α and 0.0007 less than 0.005 for IL-17A). There was no significant difference in levels of TNF-α and IL-17A between the negative group and the vehicle group (for TNF-α, p-value = 0.1306 more than 0.05, and for IL-17A, p-value = 0.0540 more than 0.005). Formulation BTG treatment showed a significant difference in TNF-α level (P-value 0.0296 less than 0.05) and IL-17A level (P-value 0.0017 less than 0.01) in comparison to the negative group. Similarly, animals treated with formulation DTG showed a significant difference in TNF-α level (P-value 0.0456 less than 0.05) and IL-17A level (P-value 0.0031 less than 0.01) in comparison to the negative group. In addition, BDTG treatment group also showed a significant difference in TNF-α level (P-value 0.0191 less than 0.05) and IL-17A level (P-value 0.0013 less than 0.01) in comparison to the negative group. Also, betamethasone treated group showed a big difference in TNF-α levels (P-value 0.0158 less than 0.05) and IL-17A levels (P-value 0.0009 less than 0.005) compared to the negative group.

Freag *et al.*, reported that berberine-loaded liquid crystalline hydrogel effectively permeated and retained the drug in the mouse skin, reducing psoriatic symptoms by alleviating IL-17 and IL-23 cytokine levels in the animal model (Freag *et al.*, 2019). Diacerein reduces the effects of IL-1α and IL-1β in keratinocytes, suppressing the expression of pro-inflammatory genes. Additionally, it has the potential to alleviate skin inflammation and splenomegaly associated with psoriasis by reducing the number of CD11c+ dendritic cells in the skin. Our study shows that diacerein and berberine HCl-loaded dual delivery transferosomal hydrogel has powerful anti-inflammatory effects on psoriasis. These effects include reducing the size of psoriatic lesions and erythema, and reduction of inflammatory cytokine levels.

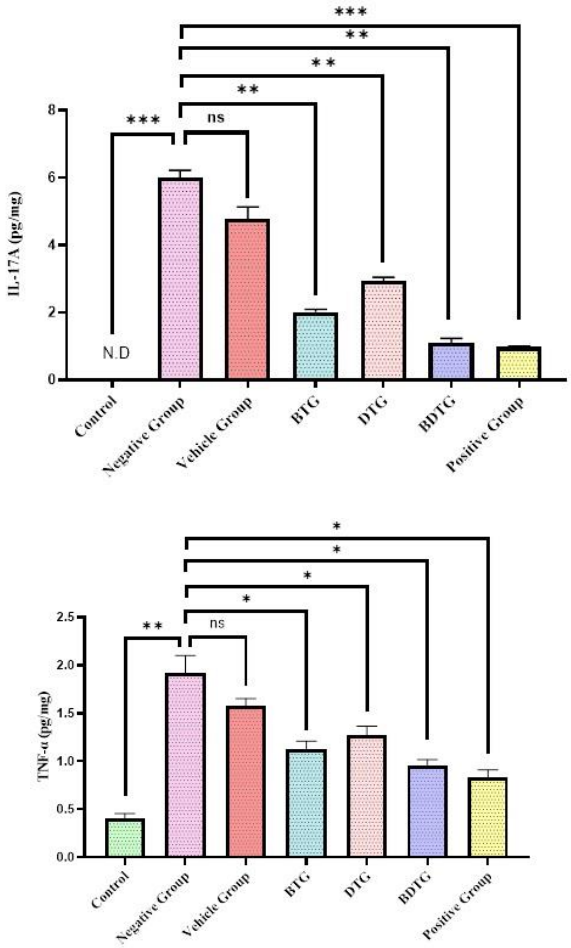

Figure 4.63. Results of ELISA assay to determine cytokine levels in in psoriatic BALB/c mice treated with developed formulations (BTG: berberine HCl loaded transferosomal hydrogel, DTG: diacerein loaded dual delivery transferosomal hydrogel, BDTG: diacerein-berberine HCl loaded transferosomal hydrogel). n = 3, mean ± SD.

CHAPTER 5
CONCLUSION

CONCLUSION

Psoriasis is an autoimmune and multifactorial disease characterized by hyperkeratosis, lesion formation, and inflammation of the skin. It affects almost 2-3% of the total world population. Topical therapy offers better therapeutic outcomes for psoriasis management in comparison to oral and systemic therapy. The thesis aimed to develop dual delivery transferosomes loaded with diacerein and berberine HCl for topical delivery, which would provide sustained-release therapeutic outcomes for psoriasis management. Transferosomes were incorporated into a hydrogel system for topical application. Berberine can show anti-inflammatory properties by reducing pro-inflammatory and inflammatory cytokine levels. Diacerein also has anti-inflammatory properties and can reduce psoriasis-associated splenomegaly.

Box-Behnken design was used to optimize the effect of various independent variables (amount of edge activator, amount of phosphatidylcholine, and sonication cycles) on the dependent variables (entrapment efficiency and particle size). The formulation was optimized with a desirable particle size (minimum) and entrapment efficiency (maximum) acceptable for topical drug delivery. The optimized formulation had high encapsulation efficiency and exhibited the desired deformability properties. TEM analysis showed spherical shape of optimized transferosomes. AFM confirmed surface roughness of the particles, which offers a high surface area. This would be helpful in the endocytosis process for cellular uptake. *In vitro* analysis revealed that the optimized formulation depicted sustained release delivery of drugs, which may be advantageous in dosage regimen (minimum dose with reduced dosing frequency). The optimized formulation enhanced skin penetration of drugs due to its deformable property in *ex vivo* permeation studies that were performed using pig ear skin. Raman analysis confirmed the permeation of loaded drugs in pig ear skin. DPPH assay confirmed antioxidant activity of the formulation. HaCaT cell line cytotoxicity analysis performed using MTT revealed formulation safety and non-toxicity.

The optimized transferosome-loaded hydrogel formulation showed no skin irritation and was found stable. In the psoriatic BALB/c mice model, the hydrogel formulation demonstrated a reduction in erythema and scaling. The histology of the skin samples revealed a reduction in acanthosis and a decrease in epidermis thickness. As shown by the enzyme-linked immunosorbent assay (ELISA), the hydrogel formulation effectively reduced inflammation by lowering the amounts of IL-17A and TNF-α. Thus, co-delivery of diacerein and berberine HCl *via* transferosomes containing hydrogel formulation had excellent therapeutic potential in the psoriatic BALB/c mice model due to enhanced epidermal penetration and prolonged local residence time.

Future research necessitates clinical investigations of the developed nanocarrier to validate its anti-psoriatic efficacy. The developed transferosomal gel warrants further investigation in human subjects to validate its clinical application in the management of psoriasis. This will facilitate the comparison of preliminary results from animal studies with the anti-inflammatory effects observed in human subjects. Furthermore, clinical studies will assess the efficacy of the developed formulation across various skin types in diverse populations. This will be helpful in comprehending potential side effects and tolerance of therapeutic molecules in formulations designed for extended use in psoriatic patients.

The anti-inflammatory properties of these transferosomes may be useful to other dermatological conditions, including eczema, dermatitis, and acne. Optimized transferosomes may act as template carriers for the delivery of various synthetic and natural molecules targeting multiple diseases. Transferosomes exhibit deformability, allowing them to effectively permeate the blood-brain barrier and facilitate drug delivery to targeted disease sites. Diacerein and berberine HCl-loaded transferosomes necessitate further investigation for their potential in brain delivery aimed at treating neurodegenerative diseases. The formulated transferosome exhibited anti-inflammatory properties. Therefore, it may be utilized to address neuroinflammation. This represents a significant research

gap that warrants exploration of the combinational therapy of berberine HCl and diacerein for brain disorders. This would facilitate the expansion of clinical application horizons. This research scheme indicated that the combination of berberine HCl and diacerein improved the anti-psoriatic effect in the psoriatic BALB/c mice model compared to the use of a single drug. The findings of this study will assist the pharmaceutical industry in developing novel formulations of berberine HCl and diacerein for psoriasis treatment.

CHAPTER 6

REFERENCES

REFERENCES

Abd-Allah, H., Ragaie, M. H., & Elmowafy, E. (2023). Unraveling the pharmaceutical and clinical relevance of the influence of syringic acid loaded linoleic acid transferosomes on acne. *International Journal of Pharmaceutics*, 639, 122940.

Abdelgawad, R., Nasr, M., Moftah, N. H., & Hamza, M. Y. (2017). Phospholipid membrane tubulation using ceramide doping "Cerosomes": Characterization and clinical application in psoriasis treatment. *European Journal of Pharmaceutical Sciences*, 101, 258–268.

Abdelkader, H., Alani, A. W., & Alany, R. G. (2014). Recent advances in non-ionic surfactant vesicles (niosomes): Self-assembly, fabrication, characterization, drug delivery applications, and limitations. *Drug Delivery*, 21(2), 87–100.

Abd-Ellatif, R. N., Hegab, I. I., Atef, M. M., Sadek, M. T., & Hafez, Y. M. (2019). Diacerein protects against glycerol-induced acute kidney injury: Modulating oxidative stress, inflammation, apoptosis and necroptosis. *Chemico-Biological Interactions*, 306, 47-53.

Abdel-Maged, A. E., Gad, A. M., Rashed, L. A., Azab, S. S., Mohamed, E. A., & Awad, A. S. (2020). Repurposing of secukinumab as neuroprotective in a cuprizone-induced multiple sclerosis experimental model via inhibition of oxidative, inflammatory, and neurodegenerative signaling. *Molecular Neurobiology*, 57(8), 3291-3306.

Abdulbaqi, I. M., Darwis, Y., Assi, R. A., & Khan, N. A. (2018). Transethosomal gels as carriers for the transdermal delivery of colchicine: Statistical optimization, characterization, and *ex vivo* evaluation. *Drug Design, Development and Therapy*, 12, 795–813.

Agrawal, M., Saraf, S., Saraf, S., Dubey, S. K., Puri, A., Patel, R. J., Ravichandiran, V., Murty, U. S., & Alexander, A. (2020). Recent strategies and

advances in the fabrication of nano lipid carriers and their application towards brain targeting. *Journal of Controlled Release*, 321, 372–415.

Agrawal, Y. O., Mahajan, U. B., Mahajan, H. S., Ojha, S., & Methotrexate-loaded, M. (2020). Nanostructured lipid carrier gel alleviates imiquimod-induced psoriasis by moderating inflammation: Formulation, optimization, characterization, *in vitro* and *in vivo* studies. *International Journal of Nanomedicine*, 15, 4763–4778.

Ahad, A., Aqil, M., Kohli, K., Sultana, Y., Mujeeb, M., & Ali, A. (2012). Formulation and optimization of nanotransfersomes using experimental design technique for accentuated transdermal delivery of valsartan. *Nanomedicine: Nanotechnology, Biology and Medicine*, 8(2), 237-249.

Ahmad, M. Z., Mohammed, A. A., Algahtani, M. S., Mishra, A., & Ahmad, J. (2022). Nanoscale topical pharmacotherapy in management of psoriasis: Contemporary research and scope. *Journal of Functional Biomaterials*, 14(1), 19.

Ai, X., Yu, P., Peng, L., Luo, L., Liu, J., Li, S., Lai, X., Luan, F., & Meng, X. (2021). Berberine: A review of its pharmacokinetics properties and therapeutic potentials in diverse vascular diseases. *Frontiers in Pharmacology*, 12, 762654.

Al Shuwaili, A. H., Rasool, B. K., & Abdulrasool, A. A. (2016). Optimization of elastic transfersomes formulations for transdermal delivery of pentoxifylline. *European Journal of Pharmaceutics and Biopharmaceutics*, 102, 101-114.

Aland, R., Ganesan, M., & Rao, P. R. (2019). *In vivo* evaluation of tazarotene solid lipid nanoparticles gel for topical delivery. *International Journal of Pharmaceutical Sciences and Drug Research*, 11(1), 45-50.

Albash, R., Abdelbary, A. A., Refai, H., & El-Nabarawi, M. A. (2019). Use of transethosomes for enhancing the transdermal delivery of olmesartan medoxomil: *In vitro, ex vivo,* and *in vivo* evaluation. *International Journal of Nanomedicine*, 14, 1953.

Al-Dhubaibi, M. S. (2018). Association between vitamin D deficiency and psoriasis: An exploratory study. *International Journal of Health Sciences*, 12(1), 33.

Aldredge, L. M., & Higham, R. C. (2018). Manifestations and management of difficult-to-treat psoriasis. *Journal of the Dermatology Nurses' Association*, 10(4), 189–197.

Alesci, S., Lauriano, E. R., Fumia, A., Irrera, N., Mastrantonio, E., Vaccaro, M., Gangemi, S., Santini, A., Cicero, N., & Pergolizzi, S. (2022). Relationship between immune cells, depression, stress, and psoriasis: Could the use of natural products be helpful? *Molecules*, 27(6), 1953.

Ali, A. U., Khallaf, I. S., Kamel, A. A., Badran, A. Y., Gomaa, A. S., & Mortagi, Y. I. (2022). Impact of quercetin spanlastics on livin and caspase-9 expression in the treatment of psoriasis vulgaris. *Journal of Drug Delivery Science and Technology*, 76, 103809.

Almezgagi, M., Zhang, Y., Hezam, K., Shamsan, E., Gamah, M., Al-Shaebi, F., Abbas, A. B., Shoaib, M., Saif, B., Han, Y., & Jia, R. (2020). Diacerein: Recent insight into pharmacological activities and molecular pathways. *Biomedicine & Pharmacotherapy*, 131, 110594.

Angelova-Fischer, I., Rippke, F., Richter, D., Filbry, A., Arrowitz, C., Weber, T. W., Fischer, T. W., & Zillikens, D. (2018). Stand-alone emollient treatment reduces flares after discontinuation of topical steroid treatment in atopic dermatitis: A double-blind, randomized, vehicle-controlled, left-right comparison study. *Acta Dermato-Venereologica*, 98(5), 517–523.

Ansari, M. D., Saifi, Z., Pandit, J., Khan, I., Solanki, P., Sultana, Y., & Aqil, M. (2022). Spanlastics: A novel nanovesicular carrier: Its potential application and emerging trends in therapeutic delivery. *AAPS PharmSciTech*, 23(1), 112.

Ardeleanu, V., Radaschin, D. S., & Tatu, A. L. (2020). Excimer laser for psoriasis treatment: a case report and short review. *Experimental and Therapeutic Medicine*, 20(1), 52–55.

Ariza, M. E., Williams, M. V., & Wong, H. K. (2013). Targeting IL-17 in psoriasis: From cutaneous immunobiology to clinical application. *Clinical Immunology*, 146(2), 131–139.

Armstrong, A. W., Gordon, K. B., & Wu, J. J. (2018). The evolving landscape of psoriasis treatment. *Seminars in Cutaneous Medicine and Surgery*, 37(2S), S39.

Arora, D., & Nanda, S. (2019). Quality by design driven development of resveratrol loaded ethosomal hydrogel for improved dermatological benefits via enhanced skin permeation and retention. *International Journal of Pharmaceutics*, 567, 118448.

Ávalos-Viveros, M., Esquivel-García, R., García-Pérez, M., Torres-García, E., Bartolomé-Camacho, M. C., Santes, V., & García-Pérez, M. E. (2022). Updated view of tars for psoriasis: What have we learned over the last decade? *International Journal of Dermatology*. *62*(3), 290–301.

Awasthi, R., Kumar, S., & Kulkarni, G. T. (2014). Frontier lipid-based carrier systems for drug targeting: A laconic review on niosomes. *Pharmaceutics & Nanotechnology*, 2(3), 116–128.

Bahramizadeh, M., Bahramizadeh, M., Kiafar, B., Jafarian, A. H., Nikpoor, A. R., Hatamipour, M., Esmaily, H., Rezaeemehr, Z., & Golmohammadzadeh, S. (2019). Development, characterization, and evaluation of topical methotrexate-entrapped deformable liposome on imiquimod-induced psoriasis in a mouse model. *International Journal of Pharmaceutics*, 569, 118623.

Bakshi, H., Nagpal, M., Singh, M., Dhingra, G. A., & Aggarwal, G. (2020). Treatment of psoriasis: a comprehensive review of entire therapies. *Current Drug Safety*, 15(2), 82–104.

Balata, G. F., Faisal, M. M., Elghamry, H. A., & Sabry, S. A. (2020). Preparation and characterization of ivabradine HCl transferosomes for enhanced transdermal delivery. *Journal of Drug Delivery Science and Technology*, 60, 101921.

Barani, M., Sangiovanni, M., Angarano, M., Rajizadeh, M. A., Mehrabani, M., Piazza, S., Gangadharappa, H. V., Pardakhty, A., Mehrbani, M., Dell'Agli, M., & Nematollahi, M. H. (2021). Phytosomes as innovative delivery systems for phytochemicals: A comprehensive review of literature. *International Journal of Nanomedicine*, 16, 6983.

Battu, S. K., Repka, M. A., Maddineni, S., Chittiboyina, A. G., Avery, M. A., & Majumdar, S. (2010). Physicochemical characterization of berberine chloride: A perspective in the development of a solution dosage form for oral delivery. *AAPS PharmSciTech*, 11(3), 1466-1475.

Baxi, K., Majmundar, D., Patel, A., Chandibhamar, V., Patel, N., & Majmundar, V. (2022). Diacerein in the treatment of chronic plaque psoriasis: A case report. *Indian Journal of Drugs in Dermatology*, 8(2), 79.

Ben Abdallah, H., Johansen, C., & Iversen, L. (2021). Key signaling pathways in psoriasis: Recent insights from antipsoriatic therapeutics. *Psoriasis: Targets and Therapy*, 11, 83–97.

Benezeder, T., Painsi, C., Patra, V., Dey, S., Holcmann, M., Lange-Asschenfeldt, B., Sibilia, M., & Wolf, P. (2020). Dithranol targets keratinocytes, their crosstalk with neutrophils and inhibits the IL-36 inflammatory loop in psoriasis. *eLife*, 9, e56991.

Bernardes, M. T., Agostini, S. B., Pereira, G. R., da Silva, L. P., da Silva, J. B., Bruschi, M. L., Novaes, R. D., & Carvalho, F. C. (2021). Preclinical study of methotrexate-based hydrogels versus surfactant-based liquid crystal systems on psoriasis treatment. *European Journal of Pharmaceutical Sciences*, 165, 105956.

Berna-Rico, E., Perez-Bootello, J., Abbad-Jaime de Aragon, C., & Gonzalez-Cantero, A. (2023). Genetic influence on treatment response in psoriasis: New insights into personalized medicine. *International Journal of Molecular Sciences*, 24(12), 9850.

Bewley, A., Burrage, D. M., Ersser, S. J., Hansen, M., & Ward, C. (2014). Identifying individual psychosocial and adherence support needs in patients with psoriasis: A multinational two-stage qualitative and quantitative study. *Journal of the European Academy of Dermatology and Venereology*, 28(6), 763–770.

Bhardwaj, P., Tripathi, P., Gupta, R., & Pandey, S. (2020). Niosomes, a review on niosomal research in the last decade. *Journal of Drug Delivery Science and Technology*, 56, 101581.

Bhardwaj, P., Tripathi, P., Pandey, S., Gupta, R., Khar, R. K., & Patil, P. R. (2022). Improved dermal delivery of pentoxifylline niosomes for the management of psoriasis: Development, optimization, and *in vivo* studies in imiquimod-induced psoriatic plaque model. *Journal of Drug Delivery Science and Technology*, 75, 103643.

Bhat, M., Pukale, S., Singh, S., Mittal, A., & Chitkara, D. (2021). Nano-enabled topical delivery of anti-psoriatic small molecules. *Journal of Drug Delivery Science and Technology*, 62, 102328.

Bikkad, M. L., Nathani, A. H., Mandlik, S. K., Shrotriya, S. N., & Ranpise, N. S. (2014). Halobetasol propionate-loaded solid lipid nanoparticles (SLN) for skin targeting by topical delivery. *Journal of Liposome Research*, 24(2), 113–123.

Bisoyi, H. K., & Li, Q. (2021). Liquid crystals: Versatile self-organized smart soft materials. *Chemical Reviews*, 122(5), 4887–4926.

Blanco-Fernandez, G., Blanco-Fernandez, B., Fernández-Ferreiro, A., & Otero-Espinar, F. J. (2023). Lipidic lyotropic liquid crystals: Insights on biomedical applications. *Advances in Colloid and Interface Science*, 102867.

Bnyan, R., Khan, I., Ehtezazi, T., Saleem, I., Gordon, S., O'Neill, F., & Roberts, M. (2018). Surfactant effects on lipid-based vesicles properties. *Journal of Pharmaceutical Sciences*, 107(5), 1237-1246.

Bonacucina, G., Martelli, S., & Palmieri, G. F. (2004). Rheological, mucoadhesive and release properties of Carbopol gels in hydrophilic cosolvents. *International Journal of Pharmaceutics*, 282(1-2), 115-130.

Borgia, F., Giuffrida, R., Caradonna, E., Vaccaro, M., Guarneri, F., & Cannavò, S. P. (2018). Early and late onset side effects of photodynamic therapy. *Biomedicines*, 6(1), 12.

Bragazzi, N. L., Sellami, M., Salem, I., Conic, R., Kimak, M., Pigatto, P. D., & Damiani, G. (2019). Fasting and its impact on skin anatomy, physiology, and physiopathology: A comprehensive review of the literature. *Nutrients*, 11(2), 249.

Brożyna, A. A., Żmijewski, M. A., Linowiecka, K., Kim, T. K., Slominski, R. M., & Slominski, A. T. (2022). Disturbed expression of vitamin D and retinoic acid-related orphan receptors α and γ and of megalin in inflammatory skin diseases. *Experimental Dermatology*, 31(5), 781–788.

Brunner, S. M., Ramspacher, A., Rieser, C., Leitner, J., Heil, H., Ablinger, M., Tevini, J., Wimmer, M., Koller, A., Piñón Hofbauer, J., & Felder, T. K. (2023). Topical diacerein decreases skin and splenic CD11c+ dendritic cells in psoriasis. *International Journal of Molecular Sciences*, 24(5), 4324.

Capon, F. (2017). The genetic basis of psoriasis. *International Journal of Molecular Sciences*, 18(12), 2526.

Case, A., & Deaton, A. (2015). Rising morbidity and mortality in midlife among white non-Hispanic Americans in the 21st century. *Proceedings of the National Academy of Sciences USA*, 112(49), 15078–15083.

Cestari, T. F., Pessato, S., & Corrêa, G. P. (2007). Fototerapia: Aplicações clínicas. *Anais Brasileiros de Dermatologia*, 82, 7–21.

Chacko, I. A., Ghate, V. M., Dsouza, L., & Lewis, S. A. (2020). Lipid vesicles: A versatile drug delivery platform for dermal and transdermal applications. *Colloids and Surfaces B: Biointerfaces*, 195, 111262.

Chandra, A., Aggarwal, G., Manchanda, S., & Narula, A. (2019). Development of topical gel of methotrexate incorporated ethosomes and salicylic acid for the treatment of psoriasis. *Pharmaceutical Nanotechnology*, 7(5), 362–374.

Chat, V. S., Kearns, D. G., Uppal, S. K., Han, G., & Wu, J. J. (2022). Management of psoriasis with topicals: applying the 2020 AAD-NPF guidelines of care to clinical practice. *Cutis*, 110(2 Suppl), 8–14.

Chauhan, N., Vasava, P., Khan, S. L., Siddiqui, F. A., Islam, F., Chopra, H., & Emran, T. B. (2022). Ethosomes: A novel drug carrier. *Annals of Medicine and Surgery*, 104595.

Chavda, V. P., Dawre, S., Pandya, A., Vora, L. K., Modh, D. H., Shah, V., Dave, D. J., & Patravale, V. (2022). Lyotropic liquid crystals for parenteral drug delivery. *Journal of Controlled Release*, 349, 533–549.

Chen, S., Hanning, S., Falconer, J., Locke, M., & Wen, J. (2019). Recent advances in non-ionic surfactant vesicles (niosomes): Fabrication, characterization, pharmaceutical and cosmetic applications. *European Journal of Pharmaceutics and Biopharmaceutics*, 144, 18–39.

Chiricozzi, A., Pimpinelli, N., Ricceri, F., Bagnoni, G., Bartoli, L., Bellini, M., Brandini, L., Caproni, M., Castelli, A., Fimiani, M., & Marsili, F. (2017).

Treatment of psoriasis with topical agents: Recommendations from a Tuscany consensus. *Dermatology Therapy*, 30(6), e12549.

Choudhury, D., Jala, A., Murty, U. S., Borkar, R. M., & Banerjee, S. (2022). *In vitro* and *ex vivo* evaluations of berberine-loaded microparticles filled in-house 3D printed hollow capsular device for improved oral bioavailability. *AAPS PharmSciTech*, 23(1), 89.

Chukwuma, I. F., Apeh, V. O., Nwora, F. N., Nkwocha, C. C., Mba, S. E., & Ossai, E. C. (2023). Phytochemical profiling and antioxidative potential of phenolic-rich extract of Cola acuminata nuts. *Biointerface Research in Applied Chemistry*, 13(1), 29.

Dahiya, M., Awasthi, R., Yadav, J. P., Sharma, S., Dua, K., & Dureja, H. (2023). Chitosan based sorafenib tosylate loaded magnetic nanoparticles: Formulation and *in-vitro* characterization. *International Journal of Biological Macromolecules*, 242, 124919.

Danaei, M., Dehghankhold, M., Ataei, S., Hasanzadeh Davarani, F., Javanmard, R., Dokhani, A., Khorasani, S., & Mozafari, M. R. (2018). Impact of particle size and polydispersity index on the clinical applications of lipidic nanocarrier systems. *Pharmaceutics*, 10(2), 57.

Dattola, A., Silvestri, M., Bennardo, L., Del Duca, E., Longo, C., Bianchi, L., & Nisticò, S. (2018). Update of calcineurin inhibitors to treat inverse psoriasis: A systematic review. *Dermatology Therapy*, 31(6), e12728.

Depieri, L. V., Borgheti-Cardoso, L. N., Campos, P. M., Otaguiri, K. K., de Carvalho Vicentini, F. T., Lopes, L. B., Fonseca, M. J., & Bentley, M. V. (2016). RNAi mediated IL-6 *in vitro* knockdown in psoriasis skin model with topical siRNA delivery system based on liquid crystalline phase. *European Journal of Pharmaceutics and Biopharmaceutics*, 105, 50–58.

Deshpande, P. K., Pathak, A. K., & Gothalwal, R. (2014). Phytosomes: A novel drug delivery system for phytoconstituents. *Journal of Nanobiotechnology Reports*, 3(3), 212–220.

Desmet, E., Bracke, S., Forier, K., Taevernier, L., Stuart, M. C., De Spiegeleer, B., Raemdonck, K., Van Gele, M., & Lambert, J. (2016). An elastic liposomal formulation for RNAi-based topical treatment of skin disorders: Proof-of-concept in the treatment of psoriasis. *International Journal of Pharmaceutics*, 500(1–2), 268–274.

Dhabale, A., & Nagpure, S. (2022). Types of psoriasis and their effects on the immune system. *Cureus*, 14(9), e29536.

Dhavale, R. P., Nadaf, S. J., & Bhatia, M. S. (2021). Quantitative structure property relationship assisted development of Fluocinolone acetonide loaded transfersomes for targeted delivery. *Journal of Drug Delivery Science and Technology*, 65, 102758.

Dhiman, N., Awasthi, R., Sharma, B., Kharkwal, H., & Kulkarni, G. T. (2021). Lipid nanoparticles as carriers for bioactive delivery. *Frontiers in Chemistry*, 9, 580118.

Dogra, S., Jain, A., & Kanwar, A. J. (2013). Efficacy and safety of acitretin in three fixed doses of 25, 35, and 50 mg in adult patients with severe plaque type psoriasis: A randomized, double-blind, parallel-group, dose-ranging study. *Journal of the European Academy of Dermatology and Venereology*, 27(3), e305–e311.

Doppalapudi, S., Jain, A., Chopra, D. K., & Khan, W. (2017). Psoralen loaded liposomal nanocarriers for improved skin penetration and efficacy of topical PUVA in psoriasis. *European Journal of Pharmaceutical Sciences*, 96, 515–529.

Dowlatshahi, E. A., Wakkee, M., Arends, L. R., & Nijsten, T. (2014). The prevalence and odds of depressive symptoms and clinical depression in

psoriasis patients: A systematic review and meta-analysis. *Journal of Investigative Dermatology*, 134(6), 1542–1551.

Dudhipala, N., Janga, K. Y., & Gorre, T. (2018). Comparative study of nisoldipine-loaded nanostructured lipid carriers and solid lipid nanoparticles for oral delivery: Preparation, characterization, permeation and pharmacokinetic evaluation. *Artificial Cells, Nanomedicine, and Biotechnology*, 46(sup2), 616–625.

Egeberg, A., Hansen, P. R., Gislason, G. H., Skov, L., & Mallbris, L. (2016). Risk of self-harm and nonfatal suicide attempts, and completed suicide in patients with psoriasis: A population-based cohort study. *British Journal of Dermatology*, 175(3), 493–500.

El-Esawy, F. M., Ahmed, I. A., El-Fallah, A. A., & Salem, R. M. (2022). Methotrexate mechanism of action in plaque psoriasis: Something new in the old view. *The Journal of Clinical and Aesthetic Dermatology*, 15(8), 42–46.

Elgewelly, M. A., Elmasry, S. M., El Sayed, N. S., & Abbas, H. (2022). Resveratrol-loaded vesicular elastic nanocarriers gel in imiquimod-induced psoriasis treatment: *In vitro* and *in vivo* evaluation. *Journal of Pharmaceutical Sciences*, 111(2), 417–431.

Elias, P. M. (2005). Stratum corneum defensive functions: An integrated view. *Journal of Investigative Dermatology*, 125(2), 183–200.

Elmowafy, E., El-Gogary, R. I., Ragai, M. H., & Nasr, M. (2019). Novel antipsoriatic fluidized spanlastic nanovesicles: In vitro physicochemical characterization, *ex vivo* cutaneous retention and exploratory clinical therapeutic efficacy. *International Journal of Pharmaceutics*, 568, 118556.

Eltobshi, A. A., Mohamed, E. A., Abdelghani, G. M., & Nouh, A. T. (2018). Self-nanoemulsifying drug-delivery systems for potentiated anti-inflammatory activity of diacerein. *International Journal of Nanomedicine*, 18, 6585-6602.

Engin, B., Tanakol, A., Bulut, H., Songür, A., Vehid, H. E., Gökalp, E., Kutlubay, Z., Özkoca, D., Tüzün, Y., & Serdaroğlu, S. (2020). Changes in serum TNF-like weak inducer of apoptosis (TWEAK) levels and Psoriasis Area Severity Index (PASI) scores in plaque psoriasis patients treated with conventional versus anti-TNF treatments. *International Journal of Dermatology*, 59(2), 207–215.

Environment Directorate Joint Meeting of the Chemicals Committee and the Working Party on Chemicals, Pesticides and Biotechnology. (2011). Organisation of the Environment Health and Safety Programme. Unclassified. ENV/JM/MONO(2011)36. Available from: https://www.oecd.org/env/ehs/organisationoftheenvironmenthealthandsafetyprogramme.htm (accessed on March 19, 2024).

Erol, I., Üstündağ Okur, N., Orak, D., Sipahi, H., Aydın, A., & Özer, Ö. (2020). Tazarotene-loaded in situ gels for potential management of psoriasis: Biocompatibility, anti-inflammatory, and analgesic effect. *Pharmaceutical Development and Technology*, 25(8), 909–918.

Fan, J., Zhang, K., Jin, Y., Li, B., Gao, S., Zhu, J., & Cui, R. (2019). Pharmacological effects of berberine on mood disorders. *Journal of Cellular and Molecular Medicine*, 23(1), 21-28.

Fernandez-García, R., Lalatsa, A., Statts, L., Bolás-Fernandez, F., Ballesteros, M. P., & Serrano, D. R. (2020). Transferosomes as nanocarriers for drugs across the skin: Quality by design from lab to industrial scale. *International Journal of Pharmaceutics,* 573, 118817.

Ferreira, M., Barreiros, L., Segundo, M. A., Torres, T., Selores, M., Lima, S. A. C., & Reis, S. (2017). Topical co-delivery of methotrexate and etanercept using lipid nanoparticles: A targeted approach for psoriasis management. *Colloids and Surfaces B: Biointerfaces*, 159, 23-29.

Filoni, A., Vestita, M., Congedo, M., Giudice, G., Tafuri, S., & Bonamonte, D. (2018). Association between psoriasis and vitamin D: Duration of disease

correlates with decreased vitamin D serum levels: An observational case-control study. *Medicine*, 97(25), e11185.

Freag, M. S., Torky, A. S., Nasra, M. M., Abdelmonsif, D. A., & Abdallah, O. Y. (2019). Liquid crystalline nanoreservoir releasing a highly skin-penetrating berberine oleate complex for psoriasis management. *Nanomedicine,* 14(8), 931–954.

Frusic-Zlotkin, M., Soroka, Y., Tivony, R., Larush, L., Verkhovsky, L., Brégégère, F. M., Neuman, R., Magdassi, S., & Milner, Y. (2012). Penetration and biological effects of topically applied cyclosporin A nanoparticles in a human skin organ culture inflammatory model. *Experimental Dermatology*, 21(12), 938–943.

Gabros, S., Nessel, T. A., & Zito, P. M. (2021). Sunscreens and photoprotection. StatPearls Publishing.

Gelfand, J. M., Wan, J., Duffin, K. C., Krueger, G. G., Kalb, R. E., Weisman, J. D., Sperber, B. R., Stierstorfer, M. B., Brod, B. A., Schleicher, S. M., & Bebo, B. F. (2012). Comparative effectiveness of commonly used systemic treatments or phototherapy for moderate to severe plaque psoriasis in the clinical practice setting. *Archives of Dermatology*, 148(4), 487–494.

Ghate, V. M., Kodoth, A. K., Shah, A., Vishalakshi, B., & Lewis, S. A. (2019). Colloidal nanostructured lipid carriers of pentoxifylline produced by microwave irradiation ameliorates imiquimod-induced psoriasis in mice. *Colloids and Surfaces B: Biointerfaces*, 181, 389–399.

Ghavipanje, N., Nasri, M. H. F., & Vargas-Bello-Pérez, E. (2023). An insight into the potential of berberine in animal nutrition: Current knowledge and future perspectives. *Journal of Animal Physiology and Animal Nutrition (Berl)*, 107(3), 808-829.

Ghyadh, B. K., & Al-Khedairy, E. (2023). Solubility and dissolution enhancement of atorvastatin calcium using phospholipid solid dispersion

technique. *Iraqi Journal of Pharmaceutical Sciences*, 32(Supplement), 244-253.

Gisondi, P., Altomare, G., Ayala, F., Bardazzi, F., Bianchi, L., Chiricozzi, A., Costanzo, A., Conti, A., Dapavo, P., De Simone, C., & Foti, C. (2017). Italian guidelines on the systemic treatments of moderate-to-severe plaque psoriasis. *Journal of the European Academy of Dermatology and Venereology*, 31(5), 774–790.

Gisondi, P., Del Giglio, M., & Girolomoni, G. (2017). Treatment approaches to moderate to severe psoriasis. *International Journal of Molecular Sciences*, 18(11), 2427.

Gómez, G. E., Calienni, M. N., Alonso, S. D. V., Alvira, F. C., & Montanari, J. (2023). Raman spectroscopy to monitor the delivery of a nano-formulation of vismodegib in the skin. *Applied Sciences*, 13(15), 7687.

Grän, F., Kerstan, A., Serfling, E., Goebeler, M., & Muhammad, K. (2020). Current developments in the immunology of psoriasis. *Yale Journal of Biology and Medicine*, 93(1), 97–110.

Gupta, P. K., Hubbard, M., Gurley, B., Hendrickson, HP. (2009). Validation of a liquid chromatography–tandem mass spectrometric assay for the quantitative determination of hydrastine and berberine in human serum. *Journal of pharmaceutical and biomedical analysis*, 49(4):1021-6.

Guan, X., Jiang, L., Cai, L., Zhang, L., & Hu, X. (2020). A new co-crystal of synthetic drug rosiglitazone with natural medicine berberine: Preparation, crystal structures, and dissolution. *Molecules*, 25(18), 4288.

Guillot, A. J., Martínez-Navarrete, M., Garrigues, T. M., & Melero, A. (2023). Skin drug delivery using lipid vesicles: A starting guideline for their development. *Journal of Controlled Release*, 355, 624-654.

Guo, T., Lu, J., Fan, Y., Zhang, Y., Yin, S., Sha, X., & Feng, N. (2021). TPGS assists the percutaneous administration of curcumin and glycyrrhetinic acid coloaded functionalized ethosomes for the synergistic treatment of psoriasis. *International Journal of Pharmaceutics*, 604, 120762.

Haghiralsadat, F., Amoabediny, G., Helder, M. N., Naderinezhad, S., Sheikhha, M. H., & Forouzanfar, T., Zandieh-Doulabi, B. (2018). A comprehensive mathematical model of drug release kinetics from nano-liposomes, derived from optimization studies of cationic PEGylated liposomal doxorubicin formulations for drug-gene delivery. *Artificial Cells, Nanomedicine, and Biotechnology*, 46(1), 169–177.

Hare, J. I., Lammers, T., Ashford, M. B., Puri, S., Storm, G., & Barry, S. T. (2017). Challenges and strategies in anti-cancer nanomedicine development: An industry perspective. *Advanced Drug Delivery Reviews*, 108, 25–38.

Hashim, II., El-Magd, N. F., El-Sheakh, A. R., Hamed, M. F., & Abd El, A. E. (2018). Pivotal role of Acitretin nanovesicular gel for effective treatment of psoriasis: *Ex vivo* and *in vivo* evaluation study. *International Journal of Nanomedicine*, 13, 1059.

Hawkes, J. E., Yan, B. Y., Chan, T. C., & Krueger, J. G. (2018). Discovery of the IL-23/IL-17 signaling pathway and the treatment of psoriasis. *Journal of Immunology*, 201(6), 1605–1613.

He, Y., Zhang, W., Xiao, Q., Fan, L., Huang, D., Chen, W., & He, W. (2022). Liposomes and liposome-like nanoparticles: From anti-fungal infection to the COVID-19 pandemic treatment. *Asian Journal of Pharmaceutical Sciences*, 17(6), 817–837.

Heath, M. S., Sahni, D. R., Curry, Z. A., & Feldman, S. R. (2018). Pharmacokinetics of tazarotene and acitretin in psoriasis. *Expert Opinion on Drug Metabolism & Toxicology*, 14(9), 919–927.

Heymann, W. R. (2019). “Tar smarts” may have a new meaning for atopic dermatitis and psoriasis. *Journal of the American Academy of Dermatology*, 80(1), 56–57.

Hoath, S. B., & Leahy, D. G. (2003). The organization of human epidermis: Functional epidermal units and phi proportionality. *Journal of Investigative Dermatology*, 121(6), 1440–1446.

Hollywood, K. A., Winder, C. L., Dunn, W. B., Xu, Y., Broadhurst, D., Griffiths, C. E., & Goodacre, R. (2015). Exploring the mode of action of dithranol therapy for psoriasis: A metabolomic analysis using HaCaT cells. *Molecular Biosystems*, 11(8), 2198–2209.

Hsieh, Y. S., Chen, Y. F., Cheng, Y. Y., Liu, W. Y., & Wu, Y. T. (2022). Self-emulsifying phospholipid preconcentrates for the enhanced photoprotection of luteolin. *Pharmaceutics*, 14(9), 1896.

Hu, P., Wang, M., Gao, H., Zheng, A., Li, J., Mu, D., & Tong, J. (2021). The role of helper T cells in psoriasis. *Frontiers in Immunology*, *12*, 788940.

Huang, C., Gou, K., Yue, X., Zhao, S., Zeng, R., Qu, Y., & Zhang, C. (2022). A novel hyaluronic acid-based dissolving microneedle patch loaded with ginsenoside Rg3 liposome for effectively alleviate psoriasis. *Materials Design*, 224, 111363.

Huang, K., Wu, X., Li, Y., Lv, C., Yan, Y., Wu, Z., Zhang, M., Huang, W., Jiang, Z., Hu, K., & Li, M. (2023). Artificial intelligence–based psoriasis severity assessment: Real-world study and application. *Journal of Medical Internet Research*, 25, e44932.

Ibaraki, H., Kanazawa, T., Oogi, C., Takashima, Y., & Seta, Y. (2019). Effects of surface charge and flexibility of liposomes on dermal drug delivery. *Journal of Drug Delivery Science and Technology*, 50, 155–162.

Jafari, A., Daneshamouz, S., Ghasemiyeh, P., & Mohammadi-Samani, S. (2022). Ethosomes as dermal/transdermal drug delivery systems: Applications, preparation, and characterization. *Journal of Liposome Research*, 1–9.

Jain, H., Devabattula, G., Bhat, A., Dalvi, H., Rangaraj, N., Godugu, C., & Srivastava, S. (2022). Topical delivery of Bruton's tyrosine kinase inhibitor and curcumin-loaded nanostructured lipid carrier gel: Repurposing strategy for the psoriasis management. *Pharmaceutical Development and Technology*, 27(9), 975–988.

Jain, H., Geetanjali, D., Dalvi, H., Bhat, A., Godugu, C., & Srivastava, S. (2022). Liposome mediated topical delivery of ibrutinib and curcumin as a synergistic approach to combat imiquimod induced psoriasis. *Journal of Drug Delivery Science and Technology*, 68, 103103.

Jain, S., Jain, P., Umamaheshwari, R. B., & Jain, N. K. (2003). Transfersomes: A novel vesicular carrier for enhanced transdermal delivery: Development, characterization, and performance evaluation. *Drug Development and Industrial Pharmacy*, 29(9), 1013-1026.

Jappe, U., Beckert, H., Bergmann, K. C., Gülsen, A., Klimek, L., Philipp, S., Pickert, J., Rauber-Ellinghaus, M. M., Renz, H., Taube, C., & Treudler, R. (2021). Biologics for atopic diseases: indication, side effect management, and new developments. *Allergologie Select*, 5, 1-25.

Javed Iqbal, M., Quispe, C., Javed, Z., Sadia, H., Qadri, Q. R., Raza, S., … & Sharifi-Rad, J. (2021). Nanotechnology-based strategies for berberine delivery system in cancer treatment: Pulling strings to keep berberine in power. *Frontiers in Molecular Biosciences*, 7, 624494.

Javia, A., Misra, A., & Thakkar, H. (2022). Liposomes encapsulating novel antimicrobial peptide Omiganan: Characterization and its pharmacodynamic evaluation in atopic dermatitis and psoriasis mice model. *International Journal of Pharmaceutics*, 624, 122045.

Jindal, S., Awasthi, R., Singare, D., & Kulkarni, G. T. (2021). Isolation, characterization and evaluation of anti-proliferative properties of andrographolide isolated from Andrographis paniculata on cultured HaCaT cells. *Herba Polonica*, 67(1), 35–45.

Jindal, S., Awasthi, R., Singhare, D., & Kulkarni, G. T. (2020). Topical delivery of Tacrolimus using liposome containing gel: An emerging and synergistic approach in management of psoriasis. *Medical Hypotheses*, 142, 109838.

Kadagothy, H., Nene, S., Amulya, E., Vambhurkar, G., Rajalakshmi, A. N., Khatri, D. K., Singh, S. B., & Srivastava, S. (2023). Perspective insights of small molecules, phytoconstituents and biologics in the management of psoriasis: A focus on targeting major inflammatory cytokine pathways. *European Journal of Pharmacology*, 947, 175668.

Kapoor, B., Gupta, R., Gulati, M., Singh, S. K., Khursheed, R., & Gupta, M. (2019). The why, where, who, how, and what of vesicular delivery systems. *Advances in Colloid and Interface Science*, 271, 101985.

Katopodi, A., & Detsi, A. (2021). Solid Lipid Nanoparticles and Nanostructured Lipid Carriers of natural products as promising systems for their bioactivity enhancement: The case of essential oils and flavonoids. *Colloids and Surfaces A: Physicochemical and Engineering Aspects*, 630, 127529.

Kaur, D., Kaur, J., & Kamal, S. S. (2019). Diacerein, its beneficial impact on chondrocytes and notable new clinical applications. *Brazilian Journal of Pharmaceutical Sciences*, 54, e17534.

Kaur, N., Sharma, K., & Bedi, N. (2018). Topical nanostructured lipid carrier-based hydrogel of mometasone furoate for the treatment of psoriasis. *Pharmaceutical Nanotechnology*, 6(2), 133–143.

Kawai, M., Ibaraki, H., Takashima, Y., Kanazawa, T., & Okada, H. (2021). Development of a liquid crystal formulation that can penetrate the stratum

corneum for intradermal delivery of small interfering RNA. *Molecular Pharmaceutics*, 18(3), 1038–1047.

Kesharwani, D., Paul, S. D., Paliwal, R., & Satapathy, T. (2023). Development, QbD based optimization, and *in vitro* characterization of diacerein-loaded nanostructured lipid carriers for topical applications. *Journal of Radiation Research and Applied Sciences*, 16(2), 100565.

Khampieng, T., Wongkittithavorn, S., Chaiarwut, S., Ekabutr, P., Pavasant, P., & Supaphol, P. (2018). Silver nanoparticles-based hydrogel: Characterization of material parameters for pressure ulcer dressing applications. *Journal of Drug Delivery Science and Technology*, 44, 91–100.

Khan, I., Saeed, K., & Khan, I. (2019). Nanoparticles: Properties, applications, and toxicities. *Arabian Journal of Chemistry*, 12(7), 908–931.

Khan, M. I., Madni, A., Hirvonen, J., & Peltonen, L. (2017). Ultrasonic processing technique as a green preparation approach for diacerein-loaded niosomes. *AAPS PharmSciTech*, 18(5), 1554-1563.

Khan, S., Hussain, A., Attar, F., Bloukh, S. H., Edis, Z., Sharifi, M., Balali, E., Nemati, F., Derakhshankhah, H., Zeinabad, H. A., & Nabi, F. (2022). A review of the berberine natural polysaccharide nanostructures as potential anticancer and antibacterial agents. *Biomedicine & Pharmacotherapy*, 146, 112531.

Khosa, A., Reddi, S., & Saha, R. N. (2018). Nanostructured lipid carriers for site-specific drug delivery. *Biomedicine & Pharmacotherapy*, 103, 598–613.

Kim, B. R., Yang, S., Doh, E. J., Choi, C. W., & Youn, S. W. (2018). Risk factors affecting adverse effects of cyclosporine A in a real-world psoriasis treatment. *Annals of Dermatology*, 30(2), 143–149.

Kim, H. J., Kim, S. H., Kim, H. M., Kim, Y. S., & Oh, J. M. (2021). Surface roughness effect on the cellular uptake of layered double hydroxide nanoparticles. *Applied Clay Science*, 202, 105992.

Kim, W. J., Koo, J. H., Cho, H. J., Lee, J. U., Kim, J. Y., Lee, H. G., Lee, S., Kim, J. H., Oh, M. S., Suh, M., & Shin, E. C. (2018). Protein tyrosine phosphatase conjugated with a novel transdermal delivery peptide, astrotactin 1–derived peptide recombinant protein tyrosine phosphatase (AP-rPTP), alleviates both atopic dermatitis–like and psoriasis-like dermatitis. *Journal of Allergy and Clinical Immunology*, 141(1), 137–151.

Koo, J., Ho, R. S., & Thibodeaux, Q. (2019). Depression and suicidality in psoriasis and clinical studies of brodalumab: A narrative review. *Cutis*, 104(6), 361–365.

Koo, J., Marangell, L. B., Nakamura, M., Armstrong, A., Jeon, C., Bhutani, T., & Wu, J. J. (2017). Depression and suicidality in psoriasis: Review of the literature including the cytokine theory of depression. *Journal of the European Academy of Dermatology and Venereology*, 31(12), 1999–2009.

Kopfnagel, V., Wagenknecht, S., Harder, J., Hofmann, K., Kleine, M., Buch, A., Sodeik, B., & Werfel, T. (2018). RNase 7 strongly promotes TLR9-mediated DNA sensing by human plasmacytoid dendritic cells. *Journal of Investigative Dermatology*, 138(4), 872–881.

Korkmaz, E., & Falo, L. D., Jr. (2020). Spherical nucleic acids as emerging topical therapeutics: A focus on psoriasis. *Journal of Investigative Dermatology*, 140(2), 278–281.

Kornhauser, S. G., & Coelho, S. G. (2010). Applications of hydroxy acids: Classification, mechanisms, and photoactivity. *Clinical, Cosmetic and Investigational Dermatology*, *3*, 135–142.

Kowalska, A., & Kalinowska-Lis, U. (2019). 18β-Glycyrrhetinic acid: Its core biological properties and dermatological applications. *International Journal of Cosmetic Science*, 41(4), 325–331.

Krueger, J. G., & Bowcock, A. M. (2005). Psoriasis pathophysiology: Current concepts of pathogenesis. *Annals of the Rheumatic Diseases*, 64(suppl 2), ii30–ii36.

Kui, R., Kovács, R., & Kemény, L. (2018). Topical therapies in psoriasis. *Borgyógyászati és Venerológiai Szemle*, 94(4), 194–197.

Kulkarni, C. V., Wachter, W., Iglesias-Salto, G., Engelskirchen, S., & Ahualli, S. (2011). Monoolein: A magic lipid? *Physical Chemistry Chemical Physics*, 13(8), 3004–3021.

Kumar, S., & Awasthi, R. (2015). Development of montelukast sodium loaded niosomal carriers by film hydration technique. *Anti-Inflammatory & Anti-Allergy Agents in Medicinal Chemistry*, 14(1), 63–78.

Lamb, R. C., Matcham, F., Turner, M. A., Rayner, L., Simpson, A., Hotopf, M., Barker, J. N., Jackson, K., & Smith, C. H. (2017). Screening for anxiety and depression in people with psoriasis: A cross-sectional study in a tertiary referral setting. *British Journal of Dermatology*, 176(4), 1028–1034.

Lauterbach, A., & Müller-Goymann, C. C. (2015). Applications and limitations of lipid nanoparticles in dermal and transdermal drug delivery via the follicular route. *European Journal of Pharmaceutical Sciences*, 97, 152–163.

Le Roux, E., & Frow, H. (2020). Diagnosis and management of mild to moderate psoriasis. *Prescriber*, 31(7–8), 9–17.

Lé, A. M., & Torres, T. (2022). New topical therapies for psoriasis. *American Journal of Clinical Dermatology*, 23(1), 13–24.

Leonardi, C. L., Powers, J. L., Matheson, R. T., Goffe, B. S., Zitnik, R., Wang, A., Gottlieb, A. B., & Etanercept Psoriasis Study Group (2003). Etanercept as monotherapy in patients with psoriasis. *The New England Journal of Medicine*, 349(21), 2014–2022.

Li, K., & Armstrong, A. W. (2012). A review of health outcomes in patients with psoriasis. *Dermatologic Clinics*, 30(1), 61–72.

Li, L., Liu, C., Fu, J., Wang, Y., Yang, D., Peng, B., Liu, X., Han, X., Meng, Y., Feng, F., & Hu, X. (2023). CD44 targeted indirubin nanocrystal-loaded hyaluronic acid hydrogel for the treatment of psoriasis. *International Journal of Biological Macromolecules*, 243, 125239.

Li, Q., Fang, H., Dang, E., & Wang, G. (2020). The role of ceramides in skin homeostasis and inflammatory skin diseases. *Journal of Dermatological Science*, 97(1), 2–8.

Liu, H., Kang, R. S., Bagnowski, K., Yu, J. M., Radecki, S., Daniel, W. L., Anderson, B. R., Nallagatla, S., Schook, A., Agarwal, R., & Giljohann, D. A. (2020). Targeting the IL-17 receptor using liposomal spherical nucleic acids as topical therapy for psoriasis. *Journal of Investigative Dermatology*, 140(2), 435–444.

Liu, P., Chen, G., & Zhang, J. (2022). A review of liposomes as a drug delivery system: Current status of approved products, regulatory environments, and future perspectives. *Molecules*, 27(5), 1372.

Liu, Y., Bravo, K. M., & Liu, J. (2021). Targeted liposomal drug delivery: A nanoscience and biophysical perspective. *Nanoscale Horizons*, 6(2), 78–94.

Lu, M., Qiu, Q., Luo, X., Liu, X., Sun, J., Wang, C., Lin, X., Deng, Y., & Song, Y. (2019). Phytophospholipid complexes (phytosomes): A novel strategy to improve the bioavailability of active constituents. *Asian Journal of Pharmaceutical Sciences*, 14(3), 265–274.

Mahajan, M., Kaur, M., Thakur, S., Singh, A., Shahtaghi, N. R., Shivgotra, R., Bhardwaj, N., Saini, S. K., & Jain, S. K. (2022). Solid lipid nanoparticles as carrier to increase local bioavailability of acitretin after topical administration in psoriasis treatment. *Journal of Pharmaceutical Innovation*. *18*(1), 220-237.

Mahmood, S., Mandal, U. K., & Chatterjee, B. (2018). Transdermal delivery of raloxifene HCl via ethosomal system: Formulation, advanced characterizations, and pharmacokinetic evaluation. *International Journal of Pharmaceutics*, 542(1–2), 36–46.

Makuch, S., Drożdż, A., Makarec, A., Ziółkowski, P., & Woźniak, M. (2022). An update on photodynamic therapy of psoriasis—current strategies and nanotechnology as a future perspective. *International Journal of Molecular Sciences*, 23(17), 9845.

Mala, R., Fida, M., Jorgaqi, E., & Vasili, E. (2019). Efficacy of biologic therapies in psoriasis vulgaris. *Dermatology Therapy*, 32(4), e12936.

Manconi, M., Caddeo, C., Nacher, A., Diez-Sales, O., Peris, J. E., Ferrer, E. E., Fadda, A. M., & Manca, M. L. (2019). Eco-scalable baicalin loaded vesicles developed by combining phospholipid with ethanol, glycerol, and propylene glycol to enhance skin permeation and protection. *Colloids and Surfaces B: Biointerfaces*, 184, 110504.

Mancuso, A., Cristiano, M. C., Fresta, M., Torella, D., & Paolino, D. (2021). Positively charged lipid as potential tool to influence the fate of ethosomes. *Applied Sciences*, 11(15), 7060.

Martínez-Ortega, J. M., Nogueras, P., Muñoz-Negro, J. E., Gutiérrez-Rojas, L., González-Domenech, P., & Gurpegui, M. (2019). Quality of life, anxiety and depressive symptoms in patients with psoriasis: A case-control study. *Journal of Psychosomatic Research*, 124, 109780.

Mascarenhas-Melo, F., Carvalho, A., Gonçalves, M. B., Paiva-Santos, A. C., & Veiga, F. (2022). Nanocarriers for the topical treatment of psoriasis—pathophysiology, conventional treatments, nanotechnology, regulatory and toxicology. *European Journal of Pharmaceutics and Biopharmaceutics*, 176, 95–107.

Mateu-Arrom, L., & Puig, L. (2023). Genetic and epigenetic mechanisms of psoriasis. *Genes*, 14(8), 1619.

McKenzie, C. V., Colonne, C. K., Yeo, J. H., & Fraser, S. T. (2018). Splenomegaly: Pathophysiological bases and therapeutic options. *The International Journal of Biochemistry & Cell Biology*, 94, 40-43.

McKnight, G., Shah, J., & Hargest, R. (2022). Physiology of the skin. *Surgery*, 40(1), 8–12.

Mendonça, C. O., & Burden, A. D. (2003). Current concepts in psoriasis and its treatment. *Pharmacology & Therapeutics*, 99(2), 133–147.

Meng, S., Lin, Z., Wang, Y., Wang, Z., Li, P., & Zheng, Y. (2018). Psoriasis therapy by Chinese medicine and modern agents. *Chinese Medicine*, 13, 16.

Meng, S., Sun, L., Wang, L., Lin, Z., Liu, Z., Xi, L., Wang, Z., & Zheng, Y. (2019). Loading of water-insoluble celastrol into niosome hydrogels for improved topical permeation and anti-psoriasis activity. *Colloids and Surfaces B: Biointerfaces*, 182, 110352.

Menter, A., Korman, N. J., Elmets, C. A., Feldman, S. R., Gelfand, J. M., Gordon, K. B., Gottlieb, A., Koo, J. Y., Lebwohl, M., Lim, H. W., & Van Voorhees, A. S. (2010). Guidelines of care for the management of psoriasis and psoriatic arthritis: Section 5. Guidelines of care for the treatment of psoriasis with phototherapy and photochemotherapy. *Journal of the American Academy of Dermatology*, 62(1), 114–135.

Menter, A., Korman, N. J., Elmets, C. A., Feldman, S. R., Gelfand, J. M., Gordon, K. B., Gottlieb, A. B., Koo, J. Y., Lebwohl, M., Lim, H. W., & Van Voorhees, A. S. (2009). Guidelines of care for the management of psoriasis and psoriatic arthritis: section 4. Guidelines of care for the management and

treatment of psoriasis with traditional systemic agents. *Journal of the American Academy of Dermatology*, 61(3), 451–485.

Menter, A., Strober, B. E., Kaplan, D. H., Kivelevitch, D., Prater, E. F., Stoff, B., Armstrong, A. W., Connor, C., Cordoro, K. M., Davis, D. M., & Elewski, B. E. (2019). Joint AAD-NPF guidelines of care for the management and treatment of psoriasis with biologics. *Journal of the American Academy of Dermatology*, 80(4), 1029–1072.

Mirchandani, Y., Patravale, V. B., & Brijesh, S. (2021). Solid lipid nanoparticles for hydrophilic drugs. *Journal of Controlled Release*, 335, 457–464.

Mishra, G., Awasthi, R., Singh, A. K., Singh, S., Mishra, S. K., Singh, S. K., & Nandi, M. K. (2022). Intranasally co-administered berberine and curcumin loaded in transfersomal vesicles improved inhibition of amyloid formation and BACE-1. *ACS Omega*, 7(47), 43290–43305.

Miyagaki, T., & Sugaya, M. (2015). Recent advances in atopic dermatitis and psoriasis: Genetic background, barrier function, and therapeutic targets. *Journal of Dermatological Science*, 78(2), 89–94.

Mohamed, S. A., & Hargest, R. (2021). Surgical anatomy of the skin. *Oxford University Press*.

Morita, A. (2018). Current developments in phototherapy for psoriasis. *Journal of Dermatology*, 45(3), 287–292.

Mosca, M., Hong, J., Hadeler, E., Hakimi, M., Liao, W., & Bhutani, T. (2021). The Role of IL-17 Cytokines in Psoriasis. *ImmunoTargets and Therapy*, 10, 409–418.

Myschik, J., Rades, T., & Hook, S. (2009). Advances in lipid-based subunit vaccine formulations. *Current Immunology Reviews*, 5(1), 42–48.

Nagadevi, B., Kumar, K. S., Venkanna, P., & Prabhakar, D. (2014). Formulation and characterization of tizanidine hydrochloride loaded ethosomes patch. *International Journal of Pharmacy and Pharmaceutical Sciences,* 6(4), 199–205.

Naseef, M. A., Ibrahim, H. K., & El-Nour, S. A. (2018). Solid form of lipid-based self-nanoemulsifying drug delivery systems for minimization of diacerein adverse effects: Development and bioequivalence evaluation in Albino rabbits. *AAPS PharmSciTech*, 19(7), 3097-3109.

Nel, J., Elkhoury, K., Velot, É., Bianchi, A., Acherar, S., Francius, G., Tamayol, A., Grandemange, S., & Arab-Tehrany, E. (2023). Functionalized liposomes for targeted breast cancer drug delivery. *Bioactive Materials*, 24, 401–437.

Nordin, U. U., Ahmad, N., Salim, N., & Yusof, N. S. (2021). Lipid-based nanoparticles for psoriasis treatment: A review on conventional treatments, recent works, and future prospects. *RSC Advances*, 11(46), 29080–29101.

Nsairat, H., Khater, D., Sayed, U., Odeh, F., Al Bawab, A., & Alshaer, W. (2022). Liposomes: Structure, composition, types, and clinical applications. *Heliyon*, 8(5), e09394.

Olejnik-Wojciechowska, J., Boboryko, D., Bratborska, A. W., Rusińska, K., Ostrowski, P., Baranowska, M., & Pawlik, A. (2024). The role of epigenetic factors in the pathogenesis of psoriasis. *International Journal of Molecular Sciences*, 25(7), 3831.

Olivier, C., Robert, P. D., Daihung, D. O., Urbà, G., Catalin, M. P., Hywel, W., Kurd, S. K., Troxel, A. B., Crits-Christoph, P., & Gelfand, J. M. (2010). The risk of depression, anxiety, and suicidality in patients with psoriasis: A population-based cohort study. *Archives of Dermatology,* 146(8), 891–895.

Opatha, S. A., Titapiwatanakun, V., & Chutoprapat, S. (2020). Transfersomes: A promising nanoencapsulation technique for transdermal drug delivery. *Pharmaceutics*, 12(9), 855.

Pandey, P., Satija, S., Wadhwa, R., Mehta, M., Purohit, D., Gupta, G., Prasher, P., Chellappan, D. K., Awasthi, R., Dureja, H., & Dua, K. (2020). Emerging trends in nanomedicine for topical delivery in skin disorders: Current and translational approaches. *Dermatology Therapy*, 33(3), e13292.

Parisi, R., Iskandar, I. Y., Kontopantelis, E., Augustin, M., Griffiths, C. E., & Ashcroft, D. M. (2020). National, regional, and worldwide epidemiology of psoriasis: Systematic analysis and modelling study. *BMJ*, 369, m1590.

Parkash, V., Maan, S., Chaudhary, V., Jogpal, V., Mittal, G., & Jain, V. (2018). Implementation of design of experiments in development and optimization of transfersomal carrier system of tacrolimus for the dermal management of psoriasis in albino wistar rat. *Journal of Bioequivalence & Bioavailability*, 10, 98–105.

Patel, N. S., Nandurbarkar, V.P., Patel, A. J., Patel, S. G. (2014). Simultaneous spectrophotometric determination of celecoxib and diacerein in bulk and capsule by absorption correction method and chemometric methods. *Spectrochimica Acta Part A: Molecular and Biomolecular Spectroscopy*, 125, 46-52.

Patel, R. D., Raval, M. K., & Sheth, N. R. (2020). Formation of Diacerein−fumaric acid eutectic as a multi-component system for the functionality enhancement. *Journal of Drug Delivery Science and Technology*, 58, 101562.

Patel, R., Singh, S. K., Singh, S., Sheth, N. R., & Gendle, R. (2009). Development and characterization of curcumin-loaded transfersome for transdermal delivery. *Journal of Pharmaceutical Sciences and Research*, 1(4), 71-80.

Patil, T. S., Gujarathi, N. A., Aher, A. A., Pachpande, H. E., Sharma, C., Ojha, S., Goyal, S. N., & Agrawal, Y. O. (2023). Recent advancements in topical anti-psoriatic nanostructured lipid carrier-based drug delivery. *International Journal of Molecular Sciences*, 24(3), 2978.

Paus, R., Klein, J., Permana, P. A., Owecki, M., Chaldakov, G. N., Böhm, M., Hausman, G., Lapière, C. M., Atanassova, P., Sowiński, J., Fasshauer, M. (2007). What are subcutaneous adipocytes really good for? *Experimental Dermatology*, 16(1), 45–47.

Pleguezuelos-Villa, M., Diez-Sales, O., Manca, M. L., Manconi, M., Sauri, A. R., Escribano-Ferrer, E., & Nàcher, A. (2020). Mangiferin glycethosomes as a new potential adjuvant for the treatment of psoriasis. *International Journal of Pharmaceutics*, 573, 118844.

Pleńkowska, J., Gabig-Cimińska, M., & Mozolewski, P. (2020). Oxidative stress as an important contributor to the pathogenesis of psoriasis. *International Journal of Molecular Sciences*, 21(17), 6206.

Pradhan, M., Alexander, A., Singh, M. R., Singh, D., Saraf, S., & Saraf, S. (2018). Understanding the prospective of nano-formulations towards the treatment of psoriasis. *Biomedicine & Pharmacotherapy*, 107, 447-463.

Pradhan, M., Sahu, K. K., Singh, D., S., R. M., & Yadav, K. (2021). A method of preparation of triamcinolone acetonide encapsulated nanostructured lipid carriers for psoriasis treatment. AU2021106678A4, 18.

Pradhan, M., Singh, D., & Singh, M. R. (2015). Development characterization and skin permeating potential of lipid based novel delivery system for topical treatment of psoriasis. *Chemistry and Physics of Lipids*, 186, 9–16.

Pradhan, M., Yadav, K., Singh, D., & Singh, M. R. (2021). Topical delivery of fluocinolone acetonide integrated NLCs and salicylic acid enriched gel: A potential and synergistic approach in the management of psoriasis. *Journal of Drug Delivery Science and Technology*, 61, 102282.

Prado, A. H., Duarte, J. L., Di Filippo, L. D., Victorelli, F. D., de Abreu Fantini, M. C., Peccinini, R. G., & Chorilli, M. (2022). Bioadhesive liquid crystal systems for octyl methoxycinnamate skin delivery. *Journal of Molecular Liquids*, 345, 117450.

Purohit, S. J., Tharmavaram, M., Rawtani, D., Prajapati, P., Pandya, H., & Dey, A. (2022). Niosomes as cutting edge nanocarrier for controlled and targeted delivery of essential oils and biomolecules. *Journal of Drug Delivery Science and Technology*, 103438.

Qushawy, M., Nasr, A., Abd-Alhaseeb, M., & Swidan, S. (2018). Design, optimization, and characterization of a transfersomal gel using miconazole nitrate for the treatment of Candida skin infections. *Pharmaceutics*, 10(1), 26.

Rahangdale, M., & Pandey, P. (2021). Development and characterization of apremilast transethosomal gel for transdermal delivery. *International Journal of Pharmaceutical Sciences and Nanotechnology (IJPSN)*, 14(3), 5508–5518.

Rai, S., Pandey, V., & Rai, G. (2017). Transfersomes as versatile and flexible nano-vesicular carriers in skin cancer therapy: The state of the art. *Nano Reviews & Experiments*, 8(1), 1325708.

Rapalli, V. K., Singhvi, G., Dubey, S. K., Gupta, G., Chellappan, D. K., & Dua, K. (2018). Emerging landscape in psoriasis management: From topical application to targeting biomolecules. *Biomedicine & Pharmacotherapy*, 106, 707–713.

Rapalli, V. K., Tomar, Y., Sharma, S., Roy, A., & Singhvi, G. (2023). Apremilast loaded lyotropic liquid crystalline nanoparticles embedded hydrogel for improved permeation and skin retention: An effective approach for psoriasis treatment. *Biomedicine & Pharmacotherapy*, 162, 114634.

Raza, H., Shah, S. U., Ali, Z., Khan, A. U., Rajput, I. B., Farid, A., Mohaini, M. A., Alsalman, A. J., Al Hawaj, M. A., Mahmood, S., & Hussain, A. (2022). *In vitro* and *ex vivo* evaluation of fluocinolone acetonide–acitretin-coloaded nanostructured lipid carriers for topical treatment of psoriasis. *Gels*, 8(11), 746.

Raza, K., Singh, B., Lohan, S., Sharma, G., Negi, P., Yachha, Y., & Katare, O. P. (2013). Nano-lipoidal carriers of tretinoin with enhanced percutaneous

absorption, photostability, biocompatibility and anti-psoriatic activity. *International Journal of Pharmaceutics*, 456(1), 65–72.

Ren, Y., Song, X., Tan, L., Guo, C., Wang, M., Liu, H., Cao, Z., Li, Y., & Peng, C. (2020). A review of the pharmacological properties of psoralen. *Frontiers in Pharmacology*, 11, 571535.

Rendon, A., & Schäkel, K. (2019). Psoriasis pathogenesis and treatment. *International Journal of Molecular Sciences*, 20(6), 1475.

Ring, L., Kettis-Lindblad, Å., Kjellgren, K. I., Kindell, Y., Maroti, M., & Serup, J. (2007). Living with skin diseases and topical treatment: Patients' and providers' perspectives and priorities. *Journal of Dermatological Treatment*, 18(4), 209–218.

Rodríguez-Luna, A., Talero, E., Avila-Román, J. M., Romero, A. M., Rabasco, A. M., Motilva, V., & Gonzalez-Rodríguez, M. L. (2021). Preparation and *in vivo* evaluation of rosmarinic acid-loaded transethosomes after percutaneous application on a psoriasis animal model. *AAPS PharmSciTech*, 22, 1–8.

Rozenblit, M., & Lebwohl, M. (2009). New biologics for psoriasis and psoriatic arthritis. *Dermatology Therapy*, 22(1), 56–60.

Ryan, C., Korman, N. J., Gelfand, J. M., Lim, H. W., Elmets, C. A., Feldman, S. R., Gottlieb, A. B., Koo, J. Y., Lebwohl, M., Leonardi, C. L., & Van Voorhees, A. S. (2014). Research gaps in psoriasis: Opportunities for future studies. *Journal of the American Academy of Dermatology*, 70(1), 146–167.

Sahibzada, M. U. K., Sadiq, A., Faidah, H. S., Khurram, M., Amin, M. U., Haseeb, A., & Kakar, M. (2018). Berberine nanoparticles with enhanced in vitro bioavailability: Characterization and antimicrobial activity. *Drug Design, Development and Therapy*, 12, 303-312.

Saka, R., Jain, H., Kommineni, N., Chella, N., & Khan, W. (2020). Enhanced penetration and improved therapeutic efficacy of bexarotene via topical

liposomal gel in imiquimod induced psoriatic plaque model in BALB/c mice. *Journal of Drug Delivery Science and Technology*, 58, 101691.

Sala, M., Elaissari, A., & Fessi, H. (2016). Advances in psoriasis physiopathology and treatments: Up to date of mechanistic insights and perspectives of novel therapies based on innovative skin drug delivery systems (ISDDS). *Journal of Controlled Release*, 239, 182–202.

Sathe, P., Saka, R., Kommineni, N., Raza, K., & Khan, W. (2019). Dithranol-loaded nanostructured lipid carrier-based gel ameliorate psoriasis in imiquimod-induced mice psoriatic plaque model. *Drug Development and Industrial Pharmacy*, 45(5), 826–838.

Scognamiglio, I., De Stefano, D., Campani, V., Mayol, L., Carnuccio, R., Fabbrocini, G., Ayala, F., La Rotonda, M. I., & De Rosa, G. (2013). Nanocarriers for topical administration of resveratrol: A comparative study. *International Journal of Pharmaceutics*, 440(2), 179–187.

Segall, A. I. (2019). Preformulation: The use of FTIR in compatibility studies.

Sekhon, S., Jeon, C., Nakamura, M., Afifi, L., Yan, D., Wu, J. J., Liao, W., & Bhutani, T. (2018). Review of the mechanism of action of coal tar in psoriasis. *Journal of Dermatological Treatment*, 29(3), 230–232.

Shaji, J. E., & Lal, M. A. (2014). Preparation, optimization, and evaluation of transferosomal formulation for enhanced transdermal delivery of a COX-2 inhibitor. *International Journal of Pharmacy and Pharmaceutical Sciences*, 6(1), 467-477.

Shams, G., Abd Allah, S., & Ezzat, R. (2024). Pharmacological activities and medicinal uses of berberine: A review. *Journal of Advanced Veterinary Research*, 14(2), 330–334.

Sharma, A., Pahwa, S., Bhati, S., & Kudeshia, P. (2020). Spanlastics: A modern approach for nanovesicular drug delivery system. *International Journal of Pharma Sciences and Research*, 11, 1057–1065.

Sheoran, S., Arora, S., & Pilli, G. (2022). Lipid based nanoparticles for treatment of cancer. *Heliyon*, e09403.

Shinno-Hashimoto, H., Eguchi, A., Sakamoto, A., Wan, X., Hashimoto, Y., Fujita, Y., Mori, C., Hatano, M., Matsue, H., & Hashimoto, K. (2022). Effects of splenectomy on skin inflammation and psoriasis-like phenotype of imiquimod-treated mice. *Scientific Reports*, 12(1), 14738.

Singh, A. K., Awasthi, R., & Malviya, R. (2023). Bioinspired microrobots: Opportunities and challenges in targeted cancer therapy. *Journal of Controlled Release*, 354, 439–452.

Singh, A. K., Singh, S. S., Rathore, A. S., Singh, S. P., Mishra, G., Awasthi, R., Mishra, S. K., Gautam, V., & Singh, S. K. (2021). Lipid-coated MCM-41 mesoporous silica nanoparticles loaded with berberine improved inhibition of acetylcholine esterase and amyloid formation. *ACS Biomaterials Science & Engineering*, 7(11), 3737–3753.

Singh, N., & Sharma, B. (2018). Toxicological effects of berberine and sanguinarine. *Frontiers in Molecular Biosciences*, 5, 21.

Singh, S., Taylor, C., Kornmehl, H., & Armstrong, A. W. (2017). Psoriasis and suicidality: A systematic review and meta-analysis. *Journal of the American Academy of Dermatology*, 77(3), 425–440.

Singh, T. G., & Sharma, N. (2016). Nanobiomaterials in cosmetics: Current status and future prospects. In *Nanobiomaterials in Galenic Formulations and Cosmetics*, 149–174.

Slominski, A. T., Zmijewski, M. A., Skobowiat, C., Zbytek, B., Slominski, R. M., & Steketee, J. D. (2012). Sensing the environment: Regulation of local and

global homeostasis by the skin's neuroendocrine system. *Advances in Anatomy, Embryology and Cell Biology*, 212, 115.

Slominski, A., & Wortsman, J. (2000). Neuroendocrinology of the skin. *Endocrine Reviews*, 21(5), 457–487.

Stenn, K. S., Nixon, A. J., Jahoda, C. A., McKay, I. A., & Paus, R. (1999). What controls hair follicle cycling? *Experimental Dermatology*, 8(4), 229–236.

Strober, B., Gooderham, M., de Jong, E. M., Kimball, A. B., Langley, R. G., Lakdawala, N., Goyal, K., Lawson, F., Langholff, W., Hopkins, L., & Fakharzadeh, S. (2018). Depressive symptoms, depression, and the effect of biologic therapy among patients in Psoriasis Longitudinal Assessment and Registry (PSOLAR). *Journal of the American Academy of Dermatology*, 78(1), 70–80.

Suadoni, M. T., & Atherton, I. (2021). Berberine for the treatment of hypertension: A systematic review. *Complementary Therapies in Clinical Practice*, 42, 101287.

Sun, S., Liang, N. A., Kawashima, Y., Xia, D., & Cui, F. (2011). Hydrophobic ion pairing of an insulin-sodium deoxycholate complex for oral delivery of insulin. *International Journal of Nanomedicine*, 28(1), 3049-3056.

Sun, S., Zhang, X., Xu, M., Zhang, F., Tian, F., Cui, J., Xia, Y., Liang, C., Zhou, S., Wei, H., & Zhao, H. (2019). Berberine downregulates CDC6 and inhibits proliferation via targeting JAK-STAT3 signaling in keratinocytes. *Cell Death & Disease*, 10(4), 274.

Sunoqrot, S., Niazi, M., Al-Natour, M., Jaber, M., & Abu-Qatouseh, L. (2022). Loading of coal tar in polymeric nanoparticles as a potential therapeutic modality for psoriasis. *ACS Omega*, 7(8), 7333–7340.

Tambe, VS., Nautiyal, A., Wairkar, S. (2021). Topical lipid nanocarriers for management of psoriasis-an overview. Journal of Drug Delivery Science and Technology, 64, 102671.

Taléns-Visconti, R., Perra, M., Ruiz-Saurí, A., & Nàcher, A. (2022). New vehiculation systems of mometasone furoate for the treatment of inflammatory skin diseases. *Pharmaceutics,* 14(12), 2558.

Thaçi, D., Augustin, M., Krutmann, J., & Luger, T. (2015). Importance of basic therapy in psoriasis. *Journal of the German Society of Dermatology*, 13(5), 415–418.

Thakral, N. K., Zanon, R. L., Kelly, R. C., & Thakral, S. (2018). Applications of powder X-ray diffraction in small molecule pharmaceuticals: Achievements and aspirations. *Journal of Pharmaceutical Sciences*, 107(12), 2969-2982.

Thapa, R. K., & Yoo, B. K. (2014). Evaluation of the effect of tacrolimus-loaded liquid crystalline nanoparticles on psoriasis-like skin inflammation. *Journal of Dermatological Treatment*, 25(1), 22–25.

Thomas, A. H., Catalá, A., & Vignoni, M. (2016). Soybean phosphatidylcholine liposomes as model membranes to study lipid peroxidation photoinduced by pterin. *Biochimica et Biophysica Acta - Biomembranes*, 1858(1), 139–145.

Thomas, J., Kumar, P., Balaji, S. R., & Devraj, D. K. (2016). *Textbook of psoriasis*. JP Medical Ltd.

Togni, S., Maramaldi, G., Di Pierro, F., & Biondi, M. (2014). A cosmeceutical formulation based on boswellic acids for the treatment of erythematous eczema and psoriasis. *Clinical, Cosmetic and Investigational Dermatology*, 321–327.

Torsekar, R., & Gautam, M. M. (2017). Topical therapies in psoriasis. *Indian Dermatology Online Journal*, 8(4), 235.

Trémezaygues, L., & Reichrath, J. (2011). Vitamin D analogs in the treatment of psoriasis: Where are we standing and where will we be going? *Dermatology Endocrinology*, 3(3), 180–186.

Tripathi, P., Kumar, A., Jain, P. K., & Patel, J. R. (2018). Carbomer gel bearing methotrexate loaded lipid nanocontainers shows improved topical delivery intended for effective management of psoriasis. *International Journal of Biological Macromolecules*, 120, 1322–1334.

Trombino, S., Russo, R., Mellace, S., Varano, G. P., Laganà, A. S., Marcucci, F., & Cassano, R. (2019). Solid lipid nanoparticles made of trehalose monooleate for cyclosporin-A topic release. *Journal of Drug Delivery Science and Technology*, 49, 563–569.

Tsegay, F., Hisham, M., Elsherif, M., Schiffer, A., & Butt, H. (2023). 3D printing of pH indicator auxetic hydrogel skin wound dressing. *Molecules*, 28(3), 1339.

Van, N. H., Vy, N. T., Toi, V. V., Dao, A. H., & Lee, B. J. (2022). Nanostructured lipid carriers and their potential applications for versatile drug delivery via oral administration. *Open*, 8, 100064.

Varia, U., Joshi, D., Jadeja, M., Katariya, H., Detholia, K., & Soni, V. (2022). Development and evaluation of ultradeformable vesicles loaded transdermal film of boswellic acid. *Future Journal of Pharmaceutical Sciences*, 8(1), 1-16.

Vasanth, S., Dubey, A., G S, R., Lewis, S. A., Ghate, V. M., El-Zahaby, S. A., & Hebbar, S. (2020). Development and investigation of vitamin C-enriched adapalene-loaded transfersome gel: A collegial approach for the treatment of Acne vulgaris. *AAPS PharmSciTech*, 21(1), 61.

Verma, S., & Utreja, P. (2019). Vesicular nanocarrier based treatment of skin fungal infections: Potential and emerging trends in nanoscale pharmacotherapy. *Asian Journal of Pharmaceutical Sciences*, 14(2), 117–129.

Viegas, J. S., Praca, F. G., Caron, A. L., Suzuki, I., Silvestrini, A. V., Medina, W. S., Del Ciampo, J. O., Kravicz, M., & Bentley, M. V. (2020). Nanostructured lipid carrier co-delivering tacrolimus and TNF-α siRNA as an innovative approach to psoriasis. *Drug Delivery and Translational Research*, 10, 646–660.

Volarić, I., Vičić, M., & Prpic-Massari, L. (2019). The role of CD8+ T-cells and their cytokines in the pathogenesis of psoriasis. *Acta Dermatovenerologica Croatica*, 27(3), 159.

Volc, S., & Ghoreschi, K. (2016). Pathophysiological basis of systemic treatments in psoriasis. *Journal der Deutschen Dermatologischen Gesellschaft*, 14(6), 557–572.

Vovesná, A., Zhigunov, A., Balouch, M., & Zbytovská, J. (2021). Ceramide liposomes for skin barrier recovery: A novel formulation based on natural skin lipids. *International Journal of Pharmaceutics*, 596, 120264.

Wadhwa, S., Garg, V., Gulati, M., Kapoor, B., Singh, S. K., & Mittal, N. (2019). Nanovesicles for nanomedicine: Theory and practices. *Pharmaceutical Nanotechnology: Basic Protocols*, 2000, 1–17.

Walunj, M., Doppalapudi, S., Bulbake, U., & Khan, W. (2020). Preparation, characterization, and in vivo evaluation of cyclosporine cationic liposomes for the treatment of psoriasis. *Journal of Liposome Research*, 30(1), 68–79.

Wang, M., Xia, H., Yang, X., Zhang, Q., Li, Y., Wang, Y., Xia, Y., & Xie, Z. (2023). Berberine hydrochloride-loaded liposomes gel: Preparation, characterization and antioxidant activity. *Indian Journal of Pharmaceutical Education and Research*, 57(1), 74-82.

Wang, W., Shu, G. F., Lu, K. J., Xu, X. L., Sun, M. C., Qi, J., Huang, Q. L., Tan, W. Q., & Du, Y. Z. (2020). Flexible liposomal gel dual-loaded with all-trans retinoic acid and betamethasone for enhanced therapeutic efficiency of psoriasis. *Journal of Nanobiotechnology*, 18(1), 1–4.

Wollina, U. (2007). The role of topical calcineurin inhibitors for skin diseases other than atopic dermatitis. *American Journal of Clinical Dermatology*, 8(3), 157–173.

Wu, J. J., Penfold, R. B., Primatesta, P., Fox, T. K., Stewart, C., Reddy, S. P., Egeberg, A., Liu, J., & Simon, G. (2017). The risk of depression, suicidal ideation and suicide attempt in patients with psoriasis, psoriatic arthritis or ankylosing spondylitis. *Journal of the European Academy of Dermatology and Venereology*, 31(7), 1168–1175.

Wu, S., Zhao, M., Sun, Y., Xie, M., Le, K., Xu, M., & Huang, C. (2020). The potential of Diosgenin in treating psoriasis: Studies from HaCaT keratinocytes and imiquimod-induced murine model. *Life Sciences*, 241, 117115.

Xi, L., Lin, Z., Qiu, F., Chen, S., Li, P., Chen, X., Wang, Z., & Zheng, Y. (2022). Enhanced uptake and anti-maturation effect of celastrol-loaded mannosylated liposomes on dendritic cells for psoriasis treatment. *Acta Pharmaceutica Sinica B*, 12(1), 339–352.

Xiao, L., Poudel, A. J., Huang, L., Wang, Y., Abdalla, A. M. E., & Yang, G. (2020). Nanocellulose hyperfine network achieves sustained release of berberine hydrochloride solubilized with β-cyclodextrin for potential anti-infection oral administration. *International Journal of Biological Macromolecules*, 153, 633-640.

Xie, J., Huang, S., Huang, H., Deng, X., Yue, P., Lin, J., Yang, M., Han, L., & Zhang, D. K. (2021). Advances in the application of natural products and the novel drug delivery systems for psoriasis. *Frontiers in Pharmacology*, 12, 644952.

Yadav, K., Singh, D., & Singh, M. R. (2021). Nanovesicles delivery approach for targeting steroid mediated mechanism of antipsoriatic therapeutics. *Journal of Drug Delivery Science and Technology*, 65, 102688.

Yaghmur, A., & Mu, H. (2021). Recent advances in drug delivery applications of cubosomes, hexosomes, and solid lipid nanoparticles. *Acta Pharmaceutica Sinica B*, 11(4), 871–885.

Yan, B. X., Chen, X. Y., Ye, L. R., Chen, J. Q., Zheng, M., & Man, X. Y. (2021). Cutaneous and systemic psoriasis: Classifications and classification for the distinction. *Frontiers in Medicine*, 8, 649408.

Yan, Z., Sun, M., & Lv, Y. (2022). Novel berberine-based pharmaceutical salts with fatty acid anions: Synthesis, characterization, physicochemical properties. *Journal of Molecular Liquids*, 360, 119397.

Yang, L., Wu, L., Wu, D., Shi, D., Wang, T., & Zhu, X. (2017). Mechanism of transdermal permeation promotion of lipophilic drugs by ethosomes. *International Journal of Nanomedicine*, 12, 3357.

Yang, X., Tang, Y., Wang, M., Wang, Y., Wang, W., Pang, M., & Xu, Y. (2021). Co-delivery of methotrexate and nicotinamide by cerosomes for topical psoriasis treatment with enhanced efficacy. *International Journal of Pharmaceutics*, 605, 120826.

Yao, Q., Zhai, Y., He, Z., Wang, Q., Sun, L., Sun, T., Lv, L., Li, Y., Yang, J., Lv, D., & Chen, R. (2023). Water-responsive gel extends drug retention and facilitates skin penetration for curcumin topical delivery against psoriasis. *Asian Journal of Pharmaceutical Sciences*, 18(2), 100782.

Yousef, H., Alhajj, M., & Sharma, S. (n.d.). Anatomy, skin (integument), epidermis. StatPearls Publishing.

Yu, F., Zhang, Y., Yang, C., Li, F., Qiu, B., & Ding, W. (2021). Enhanced transdermal efficiency of curcumin-loaded peptide-modified liposomes for highly effective antipsoriatic therapy. *Journal of Materials Chemistry B*, 9(24), 4846–4856.

Yusuf, A., Almotairy, A. R., Henidi, H., Alshehri, O. Y., & Aldughaim, M. S. (2023). Nanoparticles as drug delivery systems: A review of the implication of nanoparticles' physicochemical properties on responses in biological systems. *Polymers*, 15(7), 1596.

Zeb, A., Qureshi, O. S., Kim, H. S., Cha, J. H., Kim, H. S., & Kim, J. K. (2016). Improved skin permeation of methotrexate via nanosized ultradeformable liposomes. *International Journal of Nanomedicine*, 11, 3813-3824.

Zhang, L., Gu, C., Huang, S., Rong, R., & Zhu, T. (2015). Calcineurin inhibitor—A necessary evil: Pharmacogenetical approach to a promising future. *SM Journal of Urology*, 1(2), 1008.

Zhang, Y. T., Shen, L. N., Wu, Z. H., Zhao, J. H., & Feng, N. P. (2014). Comparison of ethosomes and liposomes for skin delivery of psoralen for psoriasis therapy. *International Journal of Pharmaceutics*, 471(1–2), 449–452.

Zhang, Y., Liang, R., Liu, C., & Yang, C. (2022). Improved stability and skin penetration through glycethosomes loaded with glycyrrhetinic acid. *International Journal of Cosmetic Science*, 44(2), 249–261.

Zhang, Y., Xia, Q., Li, Y., He, Z., Li, Z., Guo, T., Wu, Z., & Feng, N. (2019). CD44 assists the topical anti-psoriatic efficacy of curcumin-loaded hyaluronan-modified ethosomes: A new strategy for clustering drug in inflammatory skin. *Theranostics*, 9(1), 48-64.

Zhao, Q., Liu, X., Veldhuis, S., & Zhitomirsky, I. (2020). Sodium deoxycholate as a versatile dispersing and coating-forming agent: A new facet of electrophoretic deposition technology. *Colloids and Surfaces A: Physicochemical and Engineering Aspects*, 588, 124382.

Zhao, Z., Chen, Y., & Shi, Y. (2020). Microneedles: A potential strategy in transdermal delivery and application in the management of psoriasis. *RSC Advances*, 10(24), 14040–14049.

Zheng, H., Gu, L., Wang, Z., Zhou, H., Zhang, C., Teng, X., Hu, Z., Wei, X., Liu, X., Zeng, F., & Zhao, Q. (2021). Establishing transcription profile of psoriasiform cutaneous *in vitro* using HaCaT cells stimulated with combination of cytokines. *Journal of Visualized Experiments*, 169, e61537.

LIST OF PUBLICATIONS

1. Singh, S., & Awasthi, R. (2024). Berberine HCl and diacerein loaded dual delivery transferosomes: Formulation and optimization using Box-Behnken design. *ADMET and DMPK*.

2. Singh, S., & Awasthi, R. (2023). Breakthroughs and bottlenecks of psoriasis therapy: Emerging trends and advances in lipid based nano-drug delivery platforms for dermal and transdermal drug delivery. *Journal of Drug Delivery Science and Technology*, 104548.

3. Singh, S., Malviya, R., & Awasthi, R. (2024). STAR particles as potential game-changer in drug delivery and biological processes: Moving beyond conventional nanoparticles. *Journal of Drug Delivery Science and Technology*, 105413.

4. Singh S. Awasthi R†. Topical transferosomal gel of berberine HCl and diacerein reduced TNF-α and IL-17A levels and reduced epidermal thickness in imiquimod-induced psoriatic BALB/c mice. Journal of Drug Delivery Science and Technology. (Under Review).

ANNEXURE

IAEC Letter

UPES
UNIVERSITY OF TOMORROW

Great Place To Work. Certified MAR 2022 - MAR 2023 INDIA

Certificate

This is to certify that the project proposal no **UPES/ IAEC/2023/3/07 Development of nano delivery system for topical therapy of psoriasis** submitted by **Dr. Rajendra Awasthi** has been approved by the IAEC of **UPES, Dehradun** in its meeting held on **20th December 2023** and **45 BALB/c Mice** have been sanctioned under this proposal for a duration of next 8 months.

Authorized by	Name	Signature	Date
Chairman:	Dr. Kuldeep Kumar Roy	Kuldeep Kumar Roy	20/12/23
Member Secretary:	Dr. Shubham Dwivedi	Dwivedi	20-12-23
Main Nominee of CPCSEA:	Dr. Amandeep Baghla		20.12.23

Plagiarism Certificate

Development of nano delivery system for topical therapy of psoriasis (Siddharth Singh: 500090012) _ Supervisor _ Dr. Rajendra Awasthi

ORIGINALITY REPORT

6%	3%	8%	0%
SIMILARITY INDEX	INTERNET SOURCES	PUBLICATIONS	STUDENT PAPERS

PRIMARY SOURCES

1	www.wvj.science-line.com Internet Source	1%
2	Aldeen, Taha Hassan. ""Have Patients with Chronic Skin Diseases Needs Been Met?":A Thesis on Psoriasis and Eczema Patient Care in Dermatology Service", Lancaster University (United Kingdom), 2023 Publication	1%
3	Atanu Bhattacharjee, Akula Ramakrishna, Magisetty Obulesu. "Phytomedicine and Alzheimer's Disease", CRC Press, 2020 Publication	1%
4	Gerald Weinstein, Alice Gottlieb. "Therapy of Moderate-to-Severe-Psoriasis", CRC Press, 2019 Publication	<1%

List of chemicals and their sources

Chemicals	Source
Berberine HCl	Yarrow Chem Products, Mumbai, India
Diacerein	Yarrow Chem Products, Mumbai, India
Methanol	Sigma Aldrich, MA, United States
Chloroform	Sigma Aldrich, MA, United States
Sodium deoxycholate	SD Fine Chemicals, Mumbai, India
Phosphatidylcholine	SRL Chemicals, Mumbai, India
Sodium hydroxide	SRL Chemicals, Mumbai, India
Potassium dihydrogen phosphate	SRL Chemicals, Mumbai, India
Dialysis membrane (MWCO 12000 Da)	Hi-Media Laboratory, Mumbai, India
Ethanol (EtOH)	Sigma-Aldrich, MA, United States
Hematoxylin	Sigma-Aldrich, MA, United States
DPPH	Sigma Aldrich, MA, United States
Imiquimod cream	Imiquad® cream, Glenmark Pharmaceuticals, Mumbai, India
Betnovate cream 0.01%	Glaxo SmithKline Pharmaceutical Limited, Bangalore, India
Formalin	SRL Chemicals, Mumbai, India
ELISA kit	R&D Systems, Minneapolis, United States
Streptavidin-HRP solution	Hi-Media Laboratory, Mumbai, India
Tetramethylbenzidine solution	Hi-Media Laboratory, Mumbai, India
HaCaT cell line	NCCS, Pune, Maharashtra, India
Dimethylsulfoxide (DMSO)	Sigma-Aldrich, MA, United States
DMEM medium	Himedia, Mumbai, India
Penicillin	Sigma-Aldrich, MA, United States
Streptomycin	Himedia, Mumbai, India
Trypan blue solution	Himedia, Mumbai, India
Trypsin-EDTA solution	Himedia, Mumbai, India
Fetal bovine serum (FBS)	Thermofischer Scientific, MA, United States
Amphotericin B	Himedia, Mumbai, India

List of instruments and their sources

Instrument	Source
Sonicator	Hielscher, Germany
Lyophilizer	Christ, Germany
Centrifuge	REMI C-24 PLUS, Mumbai, India
UV Spectrophotometer	UV-1900 Shimadzu, Japan
Zetasizer	Litesizer 500, AntonPaar, Austria
Malvern Particle Size Analyzer	Malvern Instruments, United Kingdom
Frontier FT-IR/FIR	Norwalk, United States
X-ray Powder Diffractometer	Bruker, United States
Thermal Gravimetric Analysis	Shimadzu, Japan
HR-TEM	JOEL, Japan
Atomic Force Microscopy (AFM)	Liestal, Switzerland
Raman Spectrometer	Rinztech Nz Ltd., New Zealand
Rheometer	Anton Paar Pvt. Ltd., Germany
Digital Microscope	BT-E Cilika microscope by Medprime Technologies Pvt Ltd, Maharashtra, India
Rotatory Evaporator	DLAB-RE Pro 100, Thermo Life Sciences, Mumbai, India
-20 °C Deep Freezer	ULT-185, REMI, Mumbai, India
USP Type II Dissolution Apparatus	Electro Lab, Mumbai, India
CO_2 Incubator	REMI, Mumbai, India
Tissue Homogenizer	REMI Electro Kinetic Ltd., Mumbai, India

List of software and their sources

Software	**Source**
Design Expert Software	StatEase®, Minneapolis, Minnesota, USA
PCP Disso V3 Software	PCP, BVDU, Pune, India
Origin Pro	OriginLab, Northampton, Massachusetts, USA
GraphPad Prism 8.0.2 Software	GraphPad Software, San Diego, California, USA